TRANSFORMATIONS IN SOME AIR COOLED Fe-Mn-Cr-Cu CORROSION RESISTANT WHITE IRONS

A THESIS

submitted in fulfilment of the
requirements for the award of the degree
of
DOCTOR OF PHILOSOPHY
in
METALLURGICAL ENGINEERING

By

VINOD KUMAR

DEPARTMENT OF METALLURGICAL ENGINEERING
UNIVERSITY OF ROORKEE
ROORKEE-247 667 (INDIA)

November, 1990

TO

THE REVERED MEMORY

OF

MY FATHER

CANDIDATE'S DECLARATION

I hereby certify that the work which is being presented in the thesis entitled **TRANSFORMATIONS IN SOME AIR COOLED Fe-Mn-Cr-Cu CORROSION RESISTANT WHITE IRONS** in fulfilment of the requirement for the award of the Degree of Doctor of Philosophy, submitted in the **Department of Metallurgical Engineering** of the University is an authentic record of my own work carried out during a period from August 1985 to November 1990 under the supervision of Prof. A. K. Patwardhan.

The matter embodied in this thesis has not been submitted by me for the award of any other degree.

Vinod Kumar

(VINOD KUMAR)

This is to certify that the above statement made by the candidate is correct to the best of my knowledge.

Signature of Supervisor

A. K. Patwardhan

(Dr. A.K.PATWARDHAN) 28/11/90
Professor
Metallurgical Engineering Department
University of Roorkee
Roorkee-247 667 (INDIA)

Date: 28th Nov., 1990

The Ph.D. viva-voce examination of **Sri VINOD KUMAR, Research Scholar** has been held on .....

Signature of Guide

Signature of External Examiners

(Prof. A.K. PATWARDHAN)

ACKNOWLEDGEMENT

The author wishes to record his indebtedness with sincere and heartfelt gratitude to Prof. A.K.Patwardhan, Metallurgical Engineering Department, University of Roorkee, Roorkee for suggesting the problem, inspiration and active supervision, thought provoking discussions, criticism and suggestions given by him during the entire period of this investigation. Without his timely and untiring help it would not have been possible to present the thesis in its present form.

I am highly thankful to Dr. V.K. Tewari, Dept. of Metallurgical Engg. for extending financial support in the form of Research Associate fellowship under his Oil Industry Development Board, New Delhi Research project which greatly helped me in pursuing my research work uninterrupted.

The author is also thankful to Prof. M.L. Kapoor, Head and Prof. D.B.Goel, Ex-Head and all O.C.'s of the concerned laboratories Metallurgical Engineering Department, University of Roorkee for extending the laboratories and other facilities which enabled me to present the thesis in time.

I am sincerely thankful to Dr. N.C. Jain, presently Technical Officer, Indian Lead Zinc Information Centre, New Delhi for providing initial data for modelling and other studies and for the encouragement, support extended to me during the entire period of my work.

I am grateful to Dr. R.P. Ram for the continuous help, support and for his useful discussion and suggestions extended to me.

The author is greatly thankful to Prof. B.S. Varshney, Head, Chemical Engineering Department for kind help and constant encouragement and for providing departmental facilities during the entire period of my research work. The constant and continuous help, encouragement, support and critical criticism, discussions and suggestions rendered by Dr. B. Mohanty is greatly acknowledged. I am also thankful to Dr. Surendra Kumar of the same department for useful discussion, criticism and suggestions on the modelling part of the thesis.

I am extremely thankful to Dr. S.R. Mediratta, Dr. R.Mukharjee and Dr. D.Mukharjee, Research Managers, Product Development Group, R & D Centre for Iron and Steel, SAIL, Ranchi for providing the laboratories facilities to do EPMA, quantitative metallography, microhardness measurement, and DTA. I am very grateful to Mr.B.Singh, Research Engineer, R & D Centre, SAIL, Ranchi for extending continuous help and encouragement during the entire period of work. I am also thankful to Dr. Ashok Kumar, Mr. B.K.Jha, Research Engineers and Sri U.N.Jha and Sri Mahapatro, Laboratory Technicians of TAS and EPMA labs. for their co-operation and help.

I am greatly thankful to Dr. K.C.Mittal, Prof. and Director, USIC, University of Roorkee for providing facilities for X-ray diffractometry, scanning electron microscopy. I am also thankful to Mr. Chandrashekhar, Mr. Brahm Pal, Mr. Anil Kumar, Mrs. Rekha Sharma and Mr. K.N.R.Jual for the help rendered.

I am also thankful to Dr. P.C.Gupta, Prof. & Co-ordinator, Welding Research Laboratory, University of Roorkee for providing

testing.

I am also grateful to Dr. A.K. Ray, Reader for the constant encouragement and to Dr.A.K.Singh, Reader and Mr. B.Gaur, Institute of Paper Technology, Saharanpur for providing corrosion testing facilities. The help rendered by Dr. S.K. Bhatanagar, Fire Research Division, CBRI is also greatfully acknowledged.

I would like to express my thanks to many friends and colleagues, too numerous to mention individually, who have helped me during the preparation of this thesis. I am very thankful to Miss Shalini Joshi, Research Assistant for extending her help in proof reading and corrections done at the final stage of the work. In addition, I am also thankful to all those who have helped me directly or indirectly during the course of my research work. Help extended by Mr. A.K. Kakkar is also acknowledged.

The help rendered by Shri S.P.Kush, Madhu Singh, R.M. Mangal, S.C.Kaushik, S.N. Kaushik, J.P.Sharma, S.P.Anand, Karan Singh, Vidya Prakash, Kailash and Hari Chand(Retd.) is greatly acknowledged. I am also thankful to Sri S.K. Seth for the quality printing of micrographs and Sri Rakesh for the high quality xeroxing of my thesis.

I will like to remember my mother who inspired and encouraged me all along my life to achieve this goal. Finally, I wish to thank my wife Asha and son Rajul who exhibited great understanding and supported me all along in many ways. I am thankful to Mrs. Patwardhan, Mammi and daughters for their kind support and help.

Vinod Kumar

Date: 28 Nov,1990 (VINOD KUMAR)

ABBREVIATIONS

A	Austenite
AC	Air cooled
AVE	Average
B	Bainite
BHN	Brinell hardness number
B1, B2, B3, B4	Alloy designation
C	Carbon
Cb	Carbide
CE	Carbon equivalent
CI	Coarsening Index
COND	Condition
COP	Cross over point
CR	Corrosion rate
CS	Compressive strength, MN/m^2
DC	Dispersed carbide(s)
DF	Distribution factor
DTA	Differential Thermal Analysis
EPMA	Electron probe micro analysis
GB	Grain boundary
Gms	Grams
H	Hardness
HRS,h,hr,hrs	Hours; austenizing period; test duration
HT, H/T, h/t	Heat-treatment
HV_{30}	Vickers hardness at 30 kg load
IPY, ipy	Inch penetration per year
M	Martensite

mA	Milliampere
mV	Millivolt
Max	Maximum
MC	Massive carbide
M3	M3C (orthorhombic)
M5	M5C2 (monoclinic)
M7	M7C3 (hexagonal)
M23	M23C6 (cubic)
MDD, mdd	Milligram per decimeter^2/ day
MN/M^2, MN/m^2	Mega newton per square meter
MPa	Mega Pascal
mpy	mils per year
Min	Minimum
NOP	Number of particles
NP	New phase
OQ	Oil quenched
P	Pearlite
PC	Platy carbide
RA	Retained austenite
SP	Soaking period/austenitizing period
ST	Soaking temperature
SA, S. AREA	Surface area
Sq.cm	Square centimeter
SD	Standard deviation
SG	Spheroidal graphite
SCC	Stress corrosion cracking
S.S.	Stainless steel

SFE	Stacking fault energy
TD	Test duration
T, Temp	Temperature
TSI, tsi	Tonnes per square inch
Sq.	Square
t	Time
μ	Micron
μA	Micron-ampere
VF, vf	Volume fraction
VPN	Vickers pyramid number
Wt.%	Weight percent
α	*Ferrite*
α'	Martensite/ shear transformation product
r	Austenite
r"	Austenite (low stability)

Note : (i) All spellings conformed to (a) Chamber's dictionary and (b) a *word-processing software SOFTWORD*'s dictionary (commonly employed in U.S.).

(ii) Tables, figures, sections and equations start with capital letters wherever table, figure, section and equation numbers are mentioned.

ABSTRACT

Of the three varieties of corrosion resistant alloy cast irons in use, the high Si irons have useful applications only in strongly oxidizing conditions. They however, suffer from poor mechanical strength and shock resistance. The high nickel irons, although extensively used in a number of aqueous environments, have a low strength, suffer from graphitic corrosion and are unsuitable at operating temperatures ≥800°C. The high chromium irons exhibit relatively higher strength and can be employed upto higher service temperatures. Their shock resistance is improved by lowering carbon content.

A critical analysis revealed that little information is available on the structure-property interrelations in alloy cast irons in general. Furthermore, there is a lack of systematic information on the electro-chemical and on the deformation behaviour of microstructures commonly encountered in alloy white irons namely, 'martensite + carbide'(M + C), 'austenite + carbide'(A + C), and their allied counterparts.

Detailed information on these aspects is likely to prove useful in ascertaining whether microstructures exhibiting good resistance to aqueous corrosion and useful mechanical properties could be attained through the 'white iron' route. A major advantage foreseen is that the limitations encountered in alloyed gray irons would stand eliminated. It would be equally pertinent to investigate whether these microstructures could be generated by utilizing low cost alloying elements (Mn, Cu etc.) in preference to the conventionally employed costlier alloying elements Ni and Mo.

The present investigation, therefore, essentially comprised investigating in detail, certain newly designed Fe-Mn-Cr-Cu white iron compositions, in the air cooled condition. Investigations were mainly devoted to assessing their heat-treatment response aimed at establishing interrelations between structure and properties. A study of this kind would require a detailed insight into the transformation characteristics of the alloys. This aspect has received maximum attention in the present study.

The alloys which were air induction melted and sand cast (25mm round and 120x20x8mm rectangular strips), were investigated for the transformation behaviour by employing hardness measurements, optical and scanning metallography, quantitative metallography, X-ray diffractometry, electron probe micro analysis and differential thermal analysis. The electro-chemical characterization of the alloys was carried out by employing the potentiostatic method. Compression testing was also carried out to a limited extent to assess the deformation behaviour of the experimental alloys. Computational techniques were extensively employed for data analysis using DEC-2050 and IBM compatible PC-XT and PC-AT systems. Necessary software packages were also developed in FORTRAN IV as and when required.

The experimental work involved subjecting disc specimens of the four alloys, containing ≈6% and ≈8% Mn, ≈4% Cr and ≈1.5 and ≈3% Cu, to heat-treatments comprising holding for 2, 4, 6, 8, and 10 hours at 800, 850, 900, 950, 1000 and 1050°C followed by air cooling. This treatment was preferred over oil quenching because

---

B1:4Cr-6Mn-1.5Cu; B2:4Cr-8Mn-1.5Cu; B3:4Cr-6Mn-3Cu; B4:4Cr-8Mn-3Cu

it can be directly utilized for industrial applications. Optical metallography was extensively used to assess how the alloy content and heat-treating schedule influenced the microstructure which comprised :

(i) P/B + M + MC with and without RA in the as-cast state,

(ii) M + MC + DC with and without retained austenite(RA) on heat-treating from upto 900°C,

(iii) A + MC + DC or A + MC with and without M (in traces) on heat-treating from upto 1000°C, and

(iv) A + MC + New phase (eutectic of austenite + carbide called 'anomalous eutectic') on heat-treating from upto 1050°C; volume fraction of the eutectic reaching very low levels at higher soaking periods.

The volume fraction of massive carbides(MC) decreased with temperature or with soaking period at a given heat-treating temperature, the effect being marked at temperatures ≥950°C. Simultaneously, massive carbides were rendered discontinuous from the 'early' stages of heat-treatment. The 'rounding-off' tendency set in at 1000°C.

Dispersed carbides(DC) formed at 800°C, 10 hrs. heat-treatment directly from austenite. They underwent coarsening with an increase in temperature and or soaking period. The extent of coarsening which was marked at 900°C and 950°C, has been represented by the 'coarsening index'(CI). The dispersed carbides dissolved on heat-treating from 1000°C.

Hardness measurements provided a quick yet reliable indication of the mechanical properties. A mathematical model was developed based on the effect of heat-treating temperature and

time on hardness. This can be represented as:

$$H = C1\ e^{C2/T} + (C3 + C4.T).t$$

where, H = hardness, VHN_{30}

T = temperature, °K

t = time in seconds

C1, C2, C3 and C4 are constants and are different for different alloys.

Through intensive calculations it has been possible to demonstrate that the first term of this model represents the matrix related transformations and the second term represents the 'carbide' transformations. The model is thus physically consistent. The predicted hardness values are within ±5% of the experimentally determined values.

3D plots amongst the hardness-heat treating temperature & time were also constructed to study the overall transformation behaviour at a glance. The plots revealed that the abovesaid relationship can be represented by a surface with opposite slopes on the two sides of the temperature axis.

X-ray diffractometry proved extremely helpful in identifying the different microconstituents observed in the experimental alloys (both in the as-cast and in the heat-treated conditions). It proved helpful in identifying the matrix microstructure in 'marginal' cases e.g. in confirming the presence of P/B & M in the as-cast condition and of martensite even upto ≈950°C heat-treated condition. It also established that M_3C, $M_{23}C_6$, M_5C_2 and M_7C_3 carbides formed in differently identified temperature regimes. Additionally, presence of Cu in the elemental form and of

Fe-Si-carbide(Fe_8Si_2C) was also established. Even after such a detailed analysis, carried out with the help of developed software packages, certain reflections remained unidentified whose indexing was possible based on the likely formation of $CrMn_3$ and Cu_2S. This aspect needs further investigation.

EPMA studies (point, line and area analysis) carried out on specimens heat-treated at 950°C,(10 hrs.,AC) and 1050°C, (4hrs., AC), besides confirming the deductions arrived at on the basis of X-ray diffractometry and optical metallography, helped in establishing the partitioning behaviour of the different alloying elements e.g. Mn, Cr and Cu into the matrix and carbide phases. Chemical compositions of the carbides were also determined.

Differential thermal analysis (DTA) of the experimental alloys in the as-cast condition revealed that all the alloys underwent transformations at ≈720-735°C (matrix transformation) and ≈890-955°C (carbide transformation). Additionally, the alloys B2 and B4 underwent a third transformation at ≈1050-1075°C representing another carbide transformation.

The same study also proved useful in predicting the suitability of the experimental alloys for high temperature applications through an analysis of thermogravimetric (weight gain) data. The as-cast microstructures were found to be suitable upto a service temperature of 600°C only. However, on giving the 950°C, 10 hrs., AC heat-treatment, the usefulness of the alloys was extended upto <800°C. Similarly, on imparting the 1050°C, 10 hrs., AC heat-treatment, the temperature upto which the alloys are useful was further extended at least upto 800°C. This beneficially reflects upon attaining a microstructure, normally

observed at high temperatures, down to room temperature for improving the high temperature performance of the alloys. A further analysis also explains the relative merits of different microstructures which are a function of the composition and heat-treatment employed for high temperature applications.

A mathematical model, developed to interrelate the weight gain with temperature, is of the form

$$TG = A1.e^{(-A2/T)}$$

where, TG = weight gain

T = temperature

A1 and A2 are constants.

Potentiostatic studies, carried out in the Tafel region in 5% NaCl solution, were helpful in characterizing the alloys/ selected microstructures to assess their suitability in resisting corrosion. Two Ni-resist compositions were also studied under similar conditions for the purpose of a comparison. The study showed that in most instances single step polarization curves were obtained signifying corrosion to be a unitary process. In some instances two-step polarization curves, revealing corrosion to occur in two stages, have been obtained. Factors leading to these differences have been identified and the reasons for the occurrence explained.

The effect of heat-treatment on the E_{corr} & I_{corr} values, via the medium of the microstructure, revealed that the larger the stability and volume fraction of the austenite matrix the more noble (less -ve) the E_{corr} and smaller the I_{corr}. The effect of the second phase(MC + DC) was a function of the morphology and

volume fraction of the MC and the size, shape and distribution of the DC. Microstructure, formed on heat-treating at 1050°C (4 hrs., AC), illustrates the adverse effect of plate like morphology and a large volume fraction of the MC in spite of the austenite matrix being favourably disposed (in improving corrosion resistance). Similarly the microstructure at 950°C (10 hrs., AC) clearly brings out that the corrosion resistance is adversely affected by the coarsened DC. An analysis of the data obtained has proved extremely useful in interrelating the test parameters E_{corr} & I_{corr} with the microstructure and the electro-chemical events constituting corrosion. This has enabled laying down of guide lines for developing corrosion resistant microstructures in terms of E_{corr}, I_{corr} and I_c.

In the study involving modelling of the corrosion behaviour (interrelating corrosion rate with the microstructure), the models developed in a recent study were critically examined. The first model interrelating corrosion rate with the total volume fraction of MC+DC and the number of particles (NOP) was of the form :

$$CR = [C1 + C2\ (VCb) + C3\ (VCb)^2]\ (NOP)^{C4}$$

where, VCb = volume of carbides (MC+DC)

CR = corrosion rate in mdd

$\rightarrow$ NOP =

C1, C2, C3 and C4 are constants which were different for different alloys.

The above model did not predict the corrosion rates very satisfactorily as the contribution of the DC was included in the VCb as well as NOP. Therefore, the volume fraction of DC was excluded from the VCb (only the volume fraction of MC was

included) and DC represented by the NOP. The resulting expression is represented as :

$$CR = [C1' + C2' (VMC) + C3' (VMC)^2] (NOP)^{C4'}$$

This was justified on the basis that the mean diameter (or the surface area) of a DC particle is much smaller as compared to the surface area of massive carbide and since DC were expected to enhance corrosion through the formation of a number of electro-chemical cells, NOP was a more representative measure of this tendency rather than the surface area.

This model although superior and more representative none the less did not make a true representation of the actual state of the DC. This difficulty was overcome in the earlier study by defining DC on the basis of a newly evolved parameter termed as distribution factor(DF). The modified model was of the form

$$CR = [C1'' + C2'' (VMC) + C3'' (VMC)^2] (DF)^{C4''}$$

The actual models although mathematically valid, were not physically consistent. This was because the absolute values of corrosion rate, VMC and DF differed greatly and they had not been normalized before computing the constants. After the necessary modifications had been carried out in the present study, the final models arrived at were not only physically consistent but predicted corrosion rates within ±10% of the experimentally determined values.

On comparing the predictions based on the various models, it appeared that inconsistencies still persisted. 3D-plots between C_R, VMC & NOP and CR, VMC & DF showed that the inconsistencies perhaps arose because it was difficult to keep VMC a constant and

vary NOP/DF or vice-a-versa. None the less, the 3D-plots proved extremely useful in arriving at the minimal optimals of VMC/DF or VMC/NOP to obtain the best in terms of corrosion resistance in each of the experimental alloys. The data thus generated proved extremely helpful in developing a unified model (a single model) describing the corrosion behaviour of all the experimental alloys. Barring few instances, the deviation between the predicted and the experimentally determined corrosion behaviour does not exceed ±10-12%.

From the point of view of mechanical properties the martensite bearing microstructures were brittle and were characterized by low compressive strength(CS) and %strain. The austenite based microstructures gave high values of compressive strength and %strain. The key parameter in influencing the deformation behaviour was the amount and stability of austenite. The effect of massive carbides on the deformation behaviour was a function of the compatibility, volume fraction and morphology while the effect of DC was governed by their size, shape and distribution. The new phase (anomalous eutectic) formed at 1050°C, 4 hrs., AC heat-treatment adversely affected the deformation behaviour.

Mathematical models were developed interrelating (i) CS with hardness and (ii) %strain with hardness. Mechanical properties (CS, %strain) reported in an earlier study on similar alloys but in the oil quenched condition were used for these computations.

The relation which comprised a second order polynomial is :

$$R = A1 + A2\,(H) + A3\,(H)^2$$

where R = CS/H or %strain/H

H = hardness

A1, A2 and A3 are constants.

This correlation proved useful in characterizing some of the microstructures in the present study whose mechanical properties were not assessed.

Based on a detailed analysis of the results it is recommended that the future alloy design should incorporate useful features of the alloy B2 and strive to attain the beneficial microstructure with a minimum of heat-treatment / processing.

PREFACE

The thesis comprises a total of seven chapters. The first chapter has been divided into two sections. The first section deals with a discussion on the composition, properties and applications of the three types of corrosion resistant alloy cast irons currently in use. The second section, devoted to fundamental considerations in the design of corrosion resistant microstructures, critically examines the factors affecting corrosion and the effect of metallurgical parameters (crystal structure, microstructure and the defect structure) in influencing corrosion. Major deductions arising from an appraisal of the aforesaid information lead to the design of the experimental alloys. This aspect along with a phase-wise planning of experiments have been included in the chapter II.

Chapter III deals with the experimental techniques and procedures employed with major emphasis on the X-ray diffractometry, EPMA, DTA, corrosion testing and compression testing.

Results and discussion have been divided into three chapters. Chapter IV includes the effect of heat-treatment schedule(s) on the hardness, and microstructure characterized qualitatively and quantitatively.

Chapter V deals with the (i) structural investigations by X-ray diffractometry and EPM analysis to carry out a detailed phase (anomalous eutectic) analysis and for assessing the partitioning behaviour of Mn, Cr, Si, and Cu into the matrix, massive carbide and the new phase formed on heat- treating from

1050°C and (ii) study of the transformation behaviour of the four alloys by DTA primarily to assess the suitability of selected microstructures for high temperature applications.

Chapter VI is devoted to the electro-chemical characterization of selected microstructures by potentiostatic method, a study of the corroded specimens by scanning electron microscopy and to the assessment of the deformation behaviour of selected microstructures in the as-cast and in the heat-treated conditions by compression testing. A salient feature of the present study has been the development of a number of mathematical models interrelating the

(i) heat-treating parameters with the hardness,

(ii) microstructure (especially the effect of second phase corresponding MC & DC) with the the corrosion rate,

(iii) temperature with the oxidation behaviour (characterized by weight gain) in air,

(iv) hardness with the compression strength,

(v) hardness with the %strain,

(vi) compressive strength with the corrosion behaviour, and

(vii) %strain with the corrosion behaviour.

Based on the above findings, conclusions have been drawn with regard to the transformation behaviour of the alloys under various heat treating conditions and the suitability of different microstructures from the point of view of corrosion resistance, mechanical properties and high temperature oxidation behaviour. Such a study is expected to prove very useful in optimizing the microstructure with regard to the above mentioned properties.

They (conclusions) are enumerated in the chapter VII.

A key feature of the present investigation has been the extensive use of computational techniques and the development of application software, of immense use for materials development/ characterization, for the DEC-2050 and IBM compatible PC-XT and AT systems.

CONTENTS

LIST OF TABLES

LIST OF FIGURES

CHAPTER 1

LITERATURE REVIEW

1.1 Corrosion Resistant Alloy Cast Irons

Cast irons are extensively employed for diverse applications, including those where resistance to corrosion is an essential requirement. Both gray and white irons are in use. Additions of alloying elements in smaller proportions have a limited effect on the corrosion resistance of cast irons. Therefore, larger additions have been made to develop cast irons with improved corrosion resistance and mechanical properties. They include (i) the high Si irons containing upto 18% Si, (ii) the high chromium irons with 12 to 35% Cr and (iii) the austenitic irons of the Ni-resist type essentially containing 14 to 36% Ni (1)..

1.1.1 High Silicon Irons

The matrix microstructure of the high silicon irons containing less than 15.2% Si consists of α-silico-ferrite along with distribution of fine graphite flakes (2) and some η-phase is also present when silicon is more than 15.2% (3). Since the low strength is due to the brittle matrix rather than the graphite form, the nodular graphite silicon irons have not proved very popular. The high silicon irons show high hardness and low impact strength. Their excellent corrosion resistance is due to an inert SiO_2 surface film which forms during exposure to the environment. The maximum advantage of the protective film is achieved at Si contents ≥ 14.25% (3,4). Additions of Mo in small amounts prevents the formation of graphite by forming stable complex

carbides, thus resulting in improved corrosion resistance (2). Chromium also gives a similar beneficial effect.

These alloys are commonly employed as castings for pumps, valves and other process equipments. They have also found extensive use as anode for impressed current protection. They are used for making mixing nozzles, tanks, outlets and steam jets and for handling severe corrodents like chromic acid, sulphuric acid, slurries etc. Compositions and mechanical properties of the high silicon irons are given in Tables 1.1 and 1.2 respectively (4).

1.1.2 High Chromium Irons

The microstructure consists of a uniform dispersion of chromium-iron complex carbides in a matrix of chromium containing ferrite. The true nature of the matrix microstructure would depend upon the Cr/C ratio and may vary from α-ferrite to martensite and austenite. The carbides are probably mixtures of the types Cr_7C_3 and $Cr_{23}C_6$ in which some of the Cr has been replaced by Fe (5). The high chromium irons are hard but not unmachinable like the high silicon irons (Table 1.2). Lowering the carbon content to ≈1.2%C improves their shock resistance. The excellent corrosion resistance is achieved by the formation of an impervious and highly tenacious surface film probably consisting of a complex chromium iron oxide. An improvement in the corrosion resistance is attained by Si and Mo additions through refining of carbides (3,6). Molybdenum may alternatively enhance corrosion resistance by displacing some of the Cr by combining with the carbon and thereby increasing the Cr content of ferrite (3). Kuttner has reported that an increase in the Cr content according to the formula %Cr = (%C X 5) + 36 may prove effective in inducing

resistance to aqua-regia (6). These irons are completely resistant to other acids at room temperature, although corrosion rate can at times increase at elevated temperatures. Like the high silicon irons, the high chromium irons are no better than the unalloyed gray irons in resisting alkalies (3). However, they prove good against oxidizing acids.

High chromium irons are most usefully employed in environment containing a plentiful supply of oxygen or oxidizing agents. `Low carbon' versions are useful for annealing pots, Pb, Zn, or Al melting pots, conveyer links and other parts exposed to corrosion at high temperature (i.e. ≥1000°C) (4).

1.1.3 High Nickel or Ni-Resist Irons

These irons contain 1.6 to 6% Cr and 1% Mo along with high Ni. Occasionally Cu may also be present (Table 1.3a) (4,7). The microstructure consists of graphite flakes in a matrix of austenite and some carbide if Cr and/or Mo are present. These irons do not exhibit high strength and machinability is satisfactory due to the presence of graphite. Toughness/shock resistance is the best amongst all the alloyed cast irons due to austenitic matrix (Table 1.4a) (7). Ni-resist irons can withstand a wide range of corrosive media and give highly economical service in marine environment (Table 1.5) (7). They can resist sulphuric acid at room temperature, and HCl & H_3PO_4 even at elevated temperatures. Resistance to organic acids such as acetic, oleic, and stearic and to HNO_3 is similar to that of unalloyed irons. Ni-resist irons are also immune to strong and weak alkalies, although they are subjected to stress corrosion

cracking (SCC) at stress over 70 MPa in boiling alkali solutions (4). The overall excellent corrosion resistance is mainly due to the austenitic matrix (4,7).

The difference in the electrochemical-potential between the graphite and the matrix in Ni-resist irons is less than in the ordinary grey irons. Therefore, in environment in which graphitic corrosion is a problem, Ni-resist irons will perform much better than the ordinary or low alloyed cast irons (7).

1.1.3.1 Spheroidal Graphite Ni-Resist Irons

These are commonly produced by adding Mg (Table 1.3b) to liquid iron in sufficient quantity to enable graphite to separate as spheroids rather than as flakes. Mechanical properties of these irons are given in Table 1.4b (7). To distinguish them from the flake ones, the prefix 'D' has been added. The composition ranges are listed in Table 1.3b (7). It is well established that the corrosion resistance of any S.G. grade is similar to that of the corresponding flake graphite irons. They have been successfully used in all environments and also at elevated temperatures (700-800°C). They are mostly used in marine conditions, and also where cyclically varying loads are experienced (4,7).

1.2 Fundamental Considerations In The Design And Development Of Corrosion Resistant Alloys

Section 1.1 dealt with corrosion resistant alloy cast irons presently in use. In order to arrive at a rationalized understanding of the physical metallurgical considerations involved in designing, a critical review of the literature was made. The information thus collated has been condensed into section 1.2.

The term `metallic corrosion' includes all interactions of a metal or an alloy (solid/liquid), with its environment (liquid/gas), at any temperature, irrespective of whether this is deliberate and beneficial or advantageous and deleterious(8-10). In a way corrosion is a spontaneous process, electro-chemical in nature where electricity is generated. Although, the term corrosion has been defined in different ways by different workers(11-16), this in its simplest form occurs by the formation of anode(s) and cathode(s). The manner in which these are formed give rise to different forms/types of corrosion. The extent to which it may occur is governed by, (i) the process related parameters, (ii) the materials(metallurgical) related parameters and, (iii) the design related parameters.

The important forms of corrosion, their appearance, causes and possible methods of prevention and the different process related parameters along with their effects on corrosion have been summarized in detail by Jain(17). This aspect is being excluded from the present report. Accordingly the following sections are devoted to a critical analysis of the metallurgical parameters only. The discussion has been essentially confined to aqueous corrosion. Wherever, the data on the corrosion behaviour of cast irons is not available, data on corrosion aspects of plain carbon and alloy steels have been appropriately included to make the discussion more meaningful.

1.2.1 Metallurgical factors

This section deals with the effect of microstructure, crystal structure and the defect structure in controlling corrosion.

Whereas, the crystal structure is a fundamental entity, microstructure depends upon the (i) composition (presence/absence of alloying elements, inhomogeneity), (ii) the heat treatment employed, and (iii) whether or not a deformation (cold/hot) component is employed while treating.

The following sections contain an account of how a combination of the above mentioned parameters may give rise to conditions responsible for inducing one or more of the different forms of corrosion. It has also been mentioned how the problems thus created could be overcome by a skillful manipulation of alloying and heat treatment.

1.2.1.1 Microstructure

Microstructure has a marked effect on the corrosion rate. It has been established by Uhlig that the corrosion rate of any microstructure may not depend on the total amount of second phase. However, its distribution may have an important bearing on the corrosion behaviour(18). Thus, a microstructure exposes a very complex front to a corroding environment and an analysis of the possible interactions that may occur is of utmost importance in predicting the final outcome. Different parameters related with microstructure have been discussed below :

1.2.1.1.1 Single Phase Microstructures

A single phase, preferably either fcc or hcp (c/a ratio closest to ideal value) with a high packing factor is most useful in resisting corrosion. However, in the presence of a passive film, crystal structures with lower packing factors (bcc) would prove equally effective (austenitic and ferritic stainless steels). Since single phase microstructures exhibit limited strength,

therefore, either a two-phase or multi-phase microstructures are preferred in actual practice. This has been discussed in the following sections.

1.2.1.1.2 Two phase microstructures

A large number of options arise and only the more relevant ones have been discussed.

1.2.1.1.2.1 Soft matrix containing a soft phase

Such instances are not common and are likely to be adopted under special circumstances for a specific beneficial effect of the second phase e.g. utilization of controlled quantities of δ-ferrite in an austenitic matrix which is produced in 18-8 steel by cold rolling (deformation induced transformation to the more stable phase) or by prolonged soaking at high temperatures, for improving susceptibility of the matrix to SCC (19). However, if the amount of δ-ferrite exceeds a critical value, the notch toughness and formability are adversely affected.

A more common example is the presence of graphite in a ferrite matrix. This combination is most unfavourable from the corrosion resistance point of view as the two constituents are farthest apart in the electro-chemical series (starting from the most noble graphite and followed by Fe_3C, Fe_3P, MnS, FeS to ferrite) (20). For optimum conditions graphite should be in the flake form(20). Corrosion resistance can be further improved by replacing ferrite matrix by pearlite or austenite, the latter being a costlier option (Ni-resist irons) to make the matrix more noble.

1.2.1.1.2.2 Soft phase containing a phase mixture

The most common example is the presence of pearlite in a ferrite matrix. This combination is favourable from the point of view of corrosion particularly when the matrix phase is predominant e.g. the usefulness of mild steel in different environments. The relative proportion of ferrite and pearlite, the fineness of the microstructure, and the morphology of cementite and the difference in electro-chemical potentials between ferrite and cementite have an equally important bearing on the corrosion resistance. Ferrite and carbide are less farther apart compared with ferrite and graphite and therefore, more useful (1)

1.2.1.1.2.3 Second phase as dispersoid in a soft matrix

Two possibilities arise: the second phase being (i) a soft constituent or (ii) a hard constituent. Presence of graphite nodules or the spheroidal dispersed carbides in a ferritic/austenitic matrix are examples representing the two instances.

For a microstructure of this type, the parameters controlling the corrosion behaviour are (i) the difference in electro-chemical potential between the second phase and the matrix, (ii) size, shape, and distribution of the second phase, and (iii) the nature of the matrix-particle interface.

The first parameter has already been discussed in section 1.2.1.1.2.1. As regards the second parameter, an optimum corrosion resistance would correspond to (i) a critical size and shape (spherical being most preferred) and (ii) a uniform dispersion. It would not be desirable to have a very fine/coarse particles present as their effect, based on interfacial surface

area considerations alone, may be similar (18,21). However, the attack may tend to get localized in the presence of a fine dispersion e.g. as in pitting(22) but not so with the coarse (oversized) particles. It is in fact suggested that the second phase particles may be graded based on their effect on corrosion behaviour, on similar lines as the flake/spheroidal graphite classification in cast irons as proposed by AFS-ASTM (4).

The nature of the matrix-particle interface would depend upon whether the second phase particles are coherent, semi-coherent or incoherent. Coherent shearable particles have a soft interface and should, therefore, be regarded as useful(23). To what extent they may improve corrosion resistance would, however, be governed by the size, shape, distribution and the heat-treatment (effect of stress relieving on the interface). If the difference in hardness between the localized regions and the matrix is large, locally formed cells may accelerate corrosion. Under these conditions, the extent of acceleration/stifling would be decided by the crystal structure of the matrix.

Incoherent/semi-coherent particles are by themselves hard and are not sheared(23). However, partial coherency is associated with strains and this in turn may set up local cells of the type mentioned above. This state may be altered by the heat-treatment (stress-relieving) employed.

The discussion so far has been confined to the spherical shapes of the second phase. However, other morphologies such as platelets/plates or a massive form (with/without sharp edges) are also possible. Their presence would give rise to a higher rate of

corrosion in comparison to a spherical or polygonal morphology because of a larger interfacial contact/surface area (21) and an unfavourable morphology from the point of view of crack propagation behaviour.

1.2.1.1.2.4 Single phase with high hardness

This includes martensite and bainite formed wholly or partly by shear transformation. Their effect on the corrosion behaviour would depend upon (i) the nature of the environment and its ability or otherwise in inducing SCC, (ii) possibility of gas assisted cracking *e.g.* susceptibility of twinned martensites to hydrogen embrittlement (24-26), (iii) the possible effect of surface stresses induced during transformation, (iv) the possible role of defect structure, (v) other features (if any) and (vi) a high hardness.

Based on the literature (19-27), it was suggested that martensite may not prove useful in imparting good corrosion resistance. However, far from being so, the formation of martensite with a distorted tetragonal lattice results in 1/5 the corrosion rate of the same steel subsequently tempered at 300-400°C (producing a second phase of finely dispersed iron carbides)(22). This observation clearly implies that the higher corrosion resistance of homogeneous single phase alloys holds even if the alloys are thermodynamically unstable and which can subsequently transform into an equilibrium multiphase microstructure(22). In fact, inspite of its brittleness the high hardness associated with martensite may lead to lesser rates of dissolution and hence to an improvement in corrosion resistance(27). Based on the above considerations, bainites

(particularly lower bainite) may also prove useful due to (i) their high hardness and (ii) a crack resistant microstructure.

1.2.1.1.2.5 Second phase with a high hardness in a hard matrix

Second phases with a high hardness are usually compounds (carbides, nitrides, borides etc.) which are inert and stable at high temperatures. Their stability both in the as-cast and in the heat-treated conditions may be further improved by adding elements which primarily partition to them (e.g. partitioning of Cr, Mo, V, Ti etc. to the carbides) thereby making them more inert. The overall corrosion behaviour of the combination M + a compound would depend upon the potential difference between the two, the state of stress and the crack propagation behaviour. Data on the behaviour of `martensite + a hard phase' couple, vis-a-vis their corrosion behaviour, is not readily available. However, based on fundamental considerations, the `couple' is likely to perform satisfactorily, the high hardness/britlleness of the matrix not withstanding.

1.2.1.1.3 Multi-phase microstructures

They include the presence of a third phase which may improve the corrosion resistance indirectly by resisting crack propagation if it is ductile and tough e.g. the presence of austenite around carbides along with martensite, wherein a favourable carbide morphology would be an added advantage (28).

1.2.1.2 Unintended microconstituents

They are formed while heat treating. Their location, electro-chemical behaviour and structural changes accompanying their formation will greatly influence the final microstructure.

1.2.1.2.1 Grain boundary precipitation/segregation

This may occur either during soaking or during cooling while heat treating. Grain boundary precipitation of $Cr_{23}C_6$ type carbide in austenitic stainless steels while cooling in the temperature range of 550-950°C is one of the examples. The possible mechanism of the precipitation of $Cr_{23}C_6$ and the adverse microstructural changes it produces are now well understood(15,22). This problem may be overcome by heat-treatments involving elevated temperature soaking which disperses carbon uniformly throughout the alloy, followed by fast cooling. Grain boundary corrosion can also be avoided by stabilization (adding Ti or Nb to the alloy). Their carbides have a lower free energy of formation i.e. are more stable than chromium carbides (3,22). Another useful option is to keep the carbon content low i.e. < 0.03% (3).

1.2.1.2.2 Formation of sigma and chi phases

These are topologically closed packed phases and are usually formed in alloys with high alloy content e.g. stainless steels (22,29), and 28Cr-4Mo (30), 28Cr-4Mo-4Ni and 48%Cr (atomic) iron based alloys (31) during heat-treatment.

There are conflicting opinions on the effect of sigma and chi phases on corrosion resistance and mechanical properties. An important observation is that the phases themselves exert no detrimental effect but the concentration gradient set up in the proximity of the adjoining phases may cause a reduction in the corrosion resistance (29).

1.2.1.3 Minor factors

1.2.1.3.1 Effect of grain structure

One such example is the severe localized attack on the faces perpendicular to the working direction and proceeding into the metal in the working direction, while the surfaces parallel to the working direction remain relatively unattacked. Such end-grain attack, which is basically the result of the grain structure being elongated in the working direction, has been observed in austenitic stainless steels, Ti alloys and mild steels (3).

1.2.1.3.2 Effect of grain orientation

Grain orientation is of minor importance when aqueous corrosion is under consideration. This is because polycrystalline metals corrode more or less uniformly. However, there is a fundamental difference in the tendency for one crystal face to corrode more readily compared to another leaving behind a residual face. For example the residual faces for iron in nitric acid and copper in copper sulphate are (100) and (111) respectively. This variable attack leads to the roughening of the surface, depending upon the grain orientation, as has been shown by Gwathmey (22) in the measurements of friction and wear.

1.2.1.3.3 Inhomogeneity

This refers to a variation in chemical composition within a grain e.g. as encountered during coring. This type of microstructure can be considered as comprising an in-built electrochemical cell. Hence, corrosion resistance will be adversely affected. Homogenization annealing is recommended to overcome this problem (31).

1.2.1.4 Impurities

Impurities are detrimental to corrosion resistance of metals/alloys. For example the presence of S and P increases the corrosion rate by forming a compound of low H_2 over-voltage (22). Therefore, they have to be maintained at a low level. The level of impurities that can be tolerated in a material is a function of the strength level (3).

Inclusions are also detrimental. It has been observed that a relatively pure iron but containing sulphide inclusions has a marked tendency to react even in mildly corrosive environment (31). Their size, shape, distribution and volume fraction will have an important bearing on the corrosion behaviour (32). Inclusions enhance corrosion by initiating pitting and in some instances crevice corrosion too (33). Corrosion attack is further enhanced if the material is in the deformed state due to directionality imparted to inclusions (31).

The adverse effect of impurities can be minimized by restricting them to a desired low level. Use of suitable melting and refining techniques e.g. vacuum melting and casting ...ld greatly help in achieving this objective. The

o resort to alloying. It has been shown

mium is useful in altering the electro-

he sulphide inclusions by combining to

the resistance to pitting and crevice

line and surface defects are faulted

ociated with a high energy and, therefore,

will have a definite bearing on the corrosion behaviour. These areas act as anodic sites in comparison with the surrounding matrix (3) resulting in the pit formation at the intersection of dislocations with a surface. Triangular etch pits around a dislocation are caused by selective chemical attack due to stress field around it (dislocation). The shape of the etch pit is related with the orientation of the grain to the etched surface (31).

1.2.2.1 Effect of cold work

Cold working and heat treatment involving high rate of cooling produce higher density of dislocations and therefore, their effect needs to be discussed in more detail. Cold working increases the corrosion rate probably because of an increase in the dislocation density per sq.cm. possibly as a result of an increase in the number of kink sites on the surface thereby increasing the anodic exchange current density. On the other hand Foroulis and Uhlig (34) suggested that the increased corrosion rate is due to the segregation of carbon and nitrogen atoms to dislocations, and that the cathodic (hydrogen evolution) reaction is kinetically easier at these sites. This was supported by their observation that cold work does not increase the corrosion rate of high purity iron.

In addition to an increase in the dislocation density, grains get aligned in the direction of working and the boundaries may be fragmented as a consequence of cold working. Such areas are subjected to pitting (31). Impurities or alloying element atoms migrate to these imperfections thereby causing an even

greater change in the electro-chemical character of these defects(31).

Another aspect of cold working is that it may create anodic and cathodic sites due to differential stress distribution from the periphery to the centre of a bar e.g. as in `tor' steel (reinforcing material made by controlled cold torsion twisting mild steel bars). The increase in the corrosion rate is not so much a consequence of an increase in the dislocation density as much to a difference in stress distribution leading to galvanic action.

To overcome the problem associated with cold working, stored energy of cold work has to be effectively released. Heat-treatment helps in doing so (31).

1.2.3 Heat-treatment

Functionally, heat-treatments are employed to bring about one or more of the following effects (i) strengthening, (ii) homogenizing, (iii) softening, (iv) stress relieving, (v) removal of extraneous phases, and (vi) other than those listed before.

Strengthening through heat-treatment may involve either producing meta-stable microstructures by inducing shear transformation or by affecting precipitation. Both the transformations are affected in the solid state. The effect of the resultant transformation products in influencing corrosion behaviour has already been discussed (Section 1.2.1.1).

Homogenizing is employed to bring about uniformity in composition and will therefore improve corrosion resistance.

Softening, which is brought about by annealing, leads to the attainment of microstructures with low energy. Hence, an

improvement in corrosion resistance is expected provided no adverse microstructural changes are taking place either during soaking or while cooling.

Stress relieving is useful in relieving residual stresses and is expected to bring about an improvement in corrosion and stress corrosion resistance provided no structural changes occur during this treatment.

An important function of a heat-treating schedule is to help eliminate/counteract the formation of extraneous phases/micro-constituents. Their effect on the corrosion behaviour has already been discussed in detail. Through carefully designed heat-treating cycles, it would be possible to overcome conditions leading to the formation of extraneous micro-constituents, e.g. cooling rapidly to suppress grain boundary precipitation or avoiding excessive soaking at high temperatures to prevent δ- ferrite or sigma phase formation in stainless steels.

Lastly, heat-treatment may prove useful in improving corrosion resistance by altering the surface characteristics e.g. heat-treatment of a surface to increase its hardness is useful in improving fretting and erosion-corrosion resistance (3,11-13).

1.2.4 Alloying

Alloying elements form the basis of microstructure control through heat-treatment. Accordingly, it is useful in controlling the corrosion behaviour. Alloy additions may also influence corrosion behaviour by forming solid solutions, by forming passive films (applicable when Cr, Si and Al are added in requisite amounts) and by altering the electro-chemical behaviour

of the phases and the impurities present.

The effect of alloying elements, generally added to cast irons, has been summarized in the Table 1.6 (3,34-36).

1.3 Conclusion

A critical survey of the different alloy cast irons currently in use has been presented. The physical metallurgical considerations summarized in section 1.2 not only give us a basis for understanding the development of alloy cast irons already in use but also provide a broad frame work for designing new/alternative compositions effective in resisting corrosion.

CHAPTER II

FORMULATION OF THE PROBLEM

2.1 Introduction

Certain factors of design interest emerge from a critical appraisal of the previous chapter :

(i) Corrosion control essentially centres around three parameters, the material of construction, process/design parameters, and forms of corrosion. Not much flexibility exists with regard to latter two since they are primarily dictated by service conditions which can not be altered. The design would incorporate features so as to minimize corrosion damage. Thus the primary factor is the optimal selection of the material of construction.

(ii) A single phase microstructure although exhibiting low strength is most useful in resisting corrosion. A more close packed structure(e.g. fcc) is preferred. Its effectiveness is enhanced in the presence of a passive film.

(iii) The effectiveness of a two phase/microconstituent microstructure in resisting corrosion depends upon (a) morphology, size, location and distribution of the second phase, (b) its volume fraction and (c) difference in the electro-chemical potentials of the two constituents(e.g. between the matrix and the second phase).

(iv) Presence of a hard meta-stable constituent(martensite) may prove helpful in reducing dissolution/corrosion rate.

(v) Alloying elements prove helpful in resisting corrosion firstly by being in the dissolved state, secondly by bringing about a change in the matrix microstructure(e.g. by converting pearlite into bainite, martensite or austenite) and thirdly by forming a passive film.

(vi) Impurities(inclusions) enhance corrosion rates by providing small anodic areas surrounded by large cathodic areas. Alloying is also effective in altering the behaviour of inclusions by altering their electro-chemical character.

(vii) Compositional/concentration gradients are more effective than microstructural variations in enhancing the attack.

(viii) Topologically close packed phases(e.g. sigma and chi-phases), formed during prolonged soaking(while heat treating), may either favourably or adversely affect corrosion behaviour. Another opinion is that the 'sigma phase' effect is more related with the concentration gradient it sets up.

(ix) Thermal(heat - treating) and processing(e.g. cold working vs hot working) histories and defect structure influence the corrosion rate.

(x) Corrosion resistant alloy cast irons have been based on austenitic(high Ni), ferritic(high Si) and martensitic/austenitic (high Cr + Mo) matrices. Second phase is graphite(both flake and nodular morphology) in the first two types and carbide in the third. Presence of a passive film resists corrosion in the ferritic and also in the martensitic/austenitic grades but not in the austenitic irons. Bulk of the literature on corrosion resistant cast

irons is confined to austenitic Ni-resist cast irons.

(xi) Most graphite bearing corrosion resistant cast irons suffer from graphitic corrosion- a phenomenon considered as undesirable.

2.2 The approach and alloy design

Of the two possible approaches for developing corrosion resistant cast irons, the microstructures developed through the gray iron route suffer from certain intrinsic disadvantages, namely (i) limited mechanical strength due to the presence of graphite, (ii) flake graphite morphology, although useful from the corrosion resistance point of view, creating further impediments in the attainment of requisite mechanical strength, and (iii) graphitic corrosion giving rise to a deterioration in corrosion resistance over prolonged use.

To overcome these problems, it was suggested by Patwardhan(37) that there are definite merits in pursuing the white iron route for developing corrosion resistant microstructures. For it to be effective, information was required on the electro-chemical and on the deformation behaviour of different microstructures encountered in the white irons. There is a paucity of such an information. It was also suggested that the proposed study would be additionally meaningful if it were possible to attain the said microstructures at a minimum of cost i.e. by employing low cost indigenously available alloying elements.

A study(38) was accordingly initiated in which certain low cost compositions were designed incorporating Mn, Cr, and Cu as

the principal alloying elements. The compositions were so designed that the microstructure(s) of interest were attained with a minimum of alloying either in the as-cast state or through simple heat treatments. Mn, Cr, and Cu were selected on the basis of the following :

(i) Mn improves hardenability significantly at a low cost, helps in retaining austenite, stabilizes carbides, and does not adversely affect fluidity.

(ii) Cu is a useful graphitizer(helpful in rendering carbides discontinuous and in altering carbide morphology during heat treatment), solution hardens and improves resistance to corrosion in the presence of dilute acids(acetic, hydrochloric, sulphuric) and acid mine water(39,40).

(iii)Cr stabilizes carbides (not as strongly as Mo, V, W or Nb), is helpful in attaining a uniform microstructure(i.e. with a minimum of segregation) and may prove useful in attaining martensite/austenite even if present singly in large proportions.

A detailed analysis involving the design of alloys is discussed elsewhere(41). Its essential features are summarized below :

(i) C content was kept around 3.0% and Si around 1.5-2.0% (normally acceptable limits in cast irons).

(ii) Cr content was adjusted around 4-5% to ensure that a desired composition is cast white over a range of section sizes even on sand casting.

(iii)Two Mn levels namely, around 6 and around 8% were selected. The former ensured that austenite could be

attained at room temperature on heat treating from ≥900°C(42). The latter would ensure that austenite based microstructures are attained with a greater ease on heat - treating.

(iv) Cu was added in two distinct amounts namely, 1.5 and 3.0% for aiding the formation of austenite and for imparting higher resistance to corrosion. Evidently, it would prove useful in attaining discontinuous carbides on heat treating.

The alloys were initially investigated in the oil quenched condition and emphasis was laid on studying the behaviour of M + C, M + A + C, and A + C microstructures with or without dispersed carbides.

Although certain major findings of design interest emerged(41), an important drawback of the aforesaid study is that the heat treatments employed involved oil quenching. Although there is no restriction to using oil quenching while heat treating cast irons, it is always appropriate to use a simple heat treatment to attain the desired microstructure(s) and therefore the properties. It was therefore felt that the findings of the aforesaid study would have greater relevance if it were possible to get the desired microstructures through air cooling(37).

Accordingly, the present investigation is predominantly confined to a study of the different microstructures attained on air cooling the 6% Mn and the 8% Mn alloys, whose detailed compositions have already been indicated above. The main emphasis has been on the study of the phase transformation behaviour

involving phase identification and quantitative estimations. In the final analysis qualitative and quantitative interrelations have been developed between composition, heat treatment, microstructure and properties.

2.3 Planning of experiments

The experiments have been phased out as follows:

Phase I

A study of the structure-property relation by subjecting the alloys to different heat treatments, assessing their hardness and conducting structural investigations by optical metallography.

Phase II

A further detailed structural examination by x-ray diffractometry, differential thermal analysis, quantitative metallography and electron probe micro analysis techniques.

Phase III

Electro-chemical characterization of the alloys by the potentiostatic method and deformation behaviour of the selected microstructures by compression testing.

CHAPTER III

EXPERIMENTAL TECHNIQUES AND PROCEDURE

3.1 Alloy preparation

Raw materials used for preparing different alloys were pig iron, low carbon ferro-alloys (ferro-chromium, ferro-manganese and ferro-silicon), graphite powder, electrolytic copper and mild steel scrap. Compositions of the pig iron and the ferro-alloys are reported in the Table 3.1.

The charge consisted of the aforesaid raw materials in the requisite proportions so as to ensure that the desired compositions are attained. Due consideration was given to the metal content of the ferro-alloys and to the melt losses while making charge calculations. Alloys were air melted in clay bonded graphite crucibles in a medium frequency induction furnace.

Initially two base alloys, each weighing 65 kgs. and containing ≈4-5% Cr and 1.5% & 3.0% Cu respectively, were prepared by first melting requisite proportions of pig iron, mild steel scrap and graphite to a super-heat followed by deslagging and subsequent addition of ferro-chromium, ferro-silicon and copper. After ensuring complete dissolution of the alloy additions, small samples were taken out of the melt for estimation of carbon by the LECO analyser. In the intervening period the melt temperature was lowered to reduce losses. After ensuring that the carbon content had reached the desired level, the liquid metal temperature was raised to about 1400°C and slag removed. Each of the molten alloy was then cast into two cylindrical blocks of approximately equal weight at the two

copper levels. Thus in all four castings were poured.

Finally, the Mn content was adjusted to the desired level (i.e. ≈6% and 8%) by adding requisite amount of ferro-manganese to each of the four base alloy castings in the molten condition. Carbon content was rechecked even at this stage to ensure that it was maintained at the desired level. After deslagging, temperature of the molten metal was measured with an optical pyrometer. The alloys were poured at about 1425°C into ≈25 mm diameter X 250 mm long cylindrical ingots and 8 x 22x 120 mm rectangular strips in sand moulds.

Alloys were analysed for C, S, P and Si on a vacuum quantometer and for Mn, Cr, Cu, P and Si on x-ray fluorescence spectrometer. Detailed chemical analysis is reported in Table 3.2(43).

3.2 Specimen preparation

Alloys were very hard and could not be cut either with a power saw or with high speed steel tools. Disc samples(height 14 to 18 mm) were sliced off from the cylindrical ingots by making a 2 to 3 mm deep cut all along the circumference on a silicon carbide cut-off wheel followed by hammering. Heating of the specimens during slitting was kept to a minimum through water cooling. Specimens thus obtained were ground to have parallel faces and paper polished in the usual manner.

3.3 Heat-treatment

Heat-treatments primarily comprised soaking at 800, 850, 900, 950, 1000 and 1050°C for 2, 4, 6, 8 and 10 hours followed by air cooling. They were carried out in muffle furnaces whose

temperature was measured with a Pt-Pt/13% Rh thermocouples and controlled to an accuracy of ±5°.

3.4 Hardness measurement

Hardness testing was extensively employed because it provides a quick yet reliable indication of the effect of heat-treatment on properties.

Heat treated specimens were initially ground to a uniform depth of about 1 mm to remove any decarburized layer. Thereafter, they were paper polished upto 3/0 stage in the usual manner. Hardness measurements were carried out on both the faces of a specimen on a Vickers hardness testing machine employing a 30 kg load. A minimum of 20 impressions were taken on each specimen. The permissible scatter in the hardness values was ±17 VPN(44). In the event of the variation exceeding this limit, the hardness has been represented as a band denoting both the maximum and the minimum values.

As the alloy system under investigation is heterogeneous in character, both the representative hardness readings as well as the average values have been reported.

3.5 Metallography

3.5.1 Optical metallography

This has been extensively employed to study how heat-treatment influenced microstructure. Specimens were paper polished in the usual manner (section 3.2). The final (wheel) polishing was carried out using 1.0 and 0.1 micron alumina as the abrasive. After proper cleaning, specimen surfaces were etched in freshly prepared 2% nital. Metallographic examination was carried out on a REICHERT METAVERT-368 microscope.

3.5.2 Quantitative metallography

It was carried out on LEITZ image analyser (auto-scan) at a magnification of 2500X. Specimen size was the same as that employed during optical metallography. Ten different fields of view were examined on each specimen. Quantitative estimations including plotting of histograms were carried out with the help of computational techniques.

3.6 X-ray diffractometry

As-cast and the heat-treated bulk specimens of the different alloys were subjected to structural investigations on a PHILLIPS X-ray diffractometer PW 1140/90, employing an iron target and a manganese filter, at an accelerating voltage of 35 kV and a current of 12mA.

Specimens, which were polished and lightly etched, were scanned from 35 to 130°. In most instances time constant and scanning speed were kept at 2 seconds and 1° per minute respectively. Diffractograms were analysed/indexed by adopting the following procedures.

Indexing of x-ray diffractogram

Indexing of the diffractograms and the detailed analysis of the probable microconstituents present was done with the help of a computer software package 'XRAY'(45) as follows:

1. Based on the chemical composition of the alloy and the heat-treatment employed, a list of probable micro-constituents was made. It comprised 16 micro-constituents which was enlarged to 30 microconstituents (Table 4.61) when some of the reflections could not be

indexed. However, some peak-angles were still unidentified. Therefore, all the possible combinations of elements to form any type of micro-constituents like carbides, sulphides, phosphides, oxides, silicides, and their combinations along with the possible presence of metals in an elemental form were also considered. This enlarged the number of micro-constituents considered to 196. Carrying out a detailed analysis of this type would not have been possible without employing computational techniques.

2. 'd'-values and corresponding relative intensities and their miller indices of planes of diffraction of the above microconstituents were collected from different sources(46-49). The lattice parameters were also noted down to use them as a reference to study the variation in the lattice parameter through alloying and/or by heat-treatment.

3. The data sets at 1 & 2 above were fed into a computer as input data to carry out a detailed analysis of diffractograms.

4. The experimental error limit for 2θ- matching was taken as ± 0.2° (the minimum value of 2θ- which can be measured accurately at a chart speed of 1° per cm). The experimental error limit for d-matching was calculated from the above values.

5. The identification was done by a computer software which performs the following functions :

   a. The experimental error determination for d-

matching.

b. Calculation of d-values from 2θ- values and vice-versa whenever required.

c. Matching of the d-values or the 2θ- values which ever is required.

d. Prediction of the confidence limit of peak angle-matching considering all the possible(i.e. 196) microconstituents as well as the confidence limit of the possible presence of a micro-constituent. It also calculates standard deviation of matching of d or 2θ values.

e. Reporting of the result of matching in the form of a 2-D matrix.

f. Reporting of the miller indicies of the diffraction planes of micro-constituents that might be present.

g. Indicating the possible peak-angles corresponding to the Kβ- radiation.

The software output is shown in Tables 4.62-4.101.

3.7 Electron probe micro-analysis

This study was extensively carried out for assessing the partitioning behaviour of different alloying elements as influenced by heat-treatment, particularly Mn, Cr, Cu, C, Si, and Fe in the experimental alloys in the as-cast as well as in the heat-treated conditions. This was carried out on a JEOL Electron probe micro-analyser (EPMA) at an accelerating voltage of 15 kV and beam current of 60 μA.

The three different modes of analysis usually available are the fixed-probe technique, the line-scan technique and the area-scan technique. All the three methods were employed in the present investigation. Details concerning them have been discussed elsewhere(50).

The specimens used for the microprobe analysis were similar to those used for optical metallography except that they were etched just enough to reveal the microstructure. This way it was ensured that the composition of different phase(s)/ microconstituent(s) was practically unaltered.

3.8 DTA Studies

This was carried out on NETZSCH Simultaneous Thermal Analyzer STA 409 using KEOLINE as reference material. The powder sample of the alloy weighing nearly 45 mg. was taken in a alumina crucible and heated at a rate of 10°C per minute in air. The emerg. reset temperature and the end temperature were 1250°C and 1175°C respectively. The sampling time, the acquisition rate, and the total time taken for the experiment were 3.0 seconds, 2.0 points/K, and 1.56 hh.mm respectively. The start temperatures for the four alloys were 23.8, 19.9, 20.7, and 19.4°C respectively, and the TG offset were 18.5, 28.1, 28.5, and 28.1 mg. respectively. Ranges for DTA, TG, and DDTA were fixed at 200.00 uV, 125.00mg, and 200uV respectively. The experimental data were analysed and plotted by NETZSCH DATA ACQUISITION SYSTEM.

3. 9 Potentiostatic studies

This technique is useful in determining whether the alloy under investigation exhibits the active-passive transition.

The experimental set-up consisted of a corrosion cell which

was connected to a microprocessor based potentiostat(PRINCTON). An auto voltage scan generator was in-built in the potentiostat.

The corrosion cell consisted of a flask which was modified by the addition of various necks to introduce the test and the counter electrodes, and a reference electrode. This cell and its components have been described in detail by Greene(51).

The test electrode, also known as the working electrode, was made of the test material of approximately 2.0 cm^2 cross-sectional area. It was hot mounted in a manner that it was leak proof. The surface of the test electrode was prepared just before the experimental measurements in accordance with the recommended practice(52-53).

The reference electrode was a saturated calomel electrode(SCE) and was throughout dipped in solution. The potential of the reference electrode was checked frequently to ensure the stability.

The tests were carried out in a potential range of -1200 to -300 mV(-100 mV in few cases) to obtain tafel plots. The scan rate was kept constant at 5 mV/sec. The polarization curves were automatically plotted by a chart recorder.

3.10 Compression testing

Deformation behaviour of the different microstructures was assessed by carrying out compression tests on selected specimens. They were carried out on cylindrical specimens (size approx. 10 mm dia X 10 mm height) on a 60 ton capacity microprocessor based MFL universal testing machine, at a cross-head speed of 1.0 mm/min. Compressive strength and the percent deformation (height

strain) were calculated from the stress-strain curves in the usual manner.

3.11 Data analysis

Analysis of the data obtained was carried out with the help of computational techniques(54-55) using DEC-2050 main frame computer and PC-XT & PC-AT systems. Programmes were developed for analysing hardness, quantitative metallography data, and for indexing of the x-ray diffractograms. Programmes were also developed for establishing structure-properties correlations.

CHAPTER IV

EFFECT OF HEAT-TREATMENT ON HARDNESS AND MICROSTRUCTURE

The present investigation was primarily carried out to assess the heat-treatment response of the four alloys namely B1, B2, B3, and B4 with the help of hardness measurements, optical metallography, and quantitative metallography.

The results thus obtained have been summarized in the following sections.

4.1 Results

4.1.1 Effect of heat-treatment on hardness

Transformation behaviour of the alloys was investigated in the first instance (i) to ascertain the different microstructures that can be generated, (ii) to determine how the heat-treating schedule influenced the as-cast hardness, (iii) to assess the effect of composition and heat-treatment on hardness and (iv) to characterise the microstructures initially on the basis of hardness. This was achieved by heat treating disc specimens (25mm dia X 18mm height) of the four alloys by air cooling from 800, 850, 900, 950, 1000, and 1050°C after holding for periods ranging from 2 to 10 hours.

Effect of time and temperature on the hardness is summarized in the Tables 4.1 to 4.45 (Table 4.45 summarizes data contained in the Tables 4.1 to 4.44) and in the Figures 4.1a to 4.1d (the base curves). The data contained in the figures represents the experimentally determined values whereas the actual plots conform to the best fit data. A perusal of the tables and the figures revealed that :

1. The overall transformation behaviour of the alloys could be classified as follows :

   (a) A general increase in the hardness with soaking period on air cooling from 800°C (valid for all the alloys)

   (b) A general increase in the hardness with soaking period on air cooling from 850°C (valid for B1 and B3).

   (c) Hardness remaining independent of the soaking period on air cooling from 850°C (valid for B2 & B4).

   (d) Hardness remaining independent of the soaking period on heat treating from 900°C (valid for all alloys).

   (e) A general slight decrease in hardness with soaking period on heat treating from 950°C (valid for B1 and B3).

   (f) Hardness remaining independent of the soaking period on heat treating from 950°C (valid for B2 and B4).

   (g) Hardness decreasing with soaking period on heat treating from 1000 and 1050°C (valid for all the alloys).

   (h) The hardness, in general, decreasing with the soaking temperature in the order

$$H_{1050} < H_{1000} < H_{950} < H_{900} < H_{850} < H_{800}$$

2. On heat treating from 800°C, the hardness of the four

alloys was higher than their corresponding as-cast hardness(Figs. 4.1a to 4.1d).

3. However, on heat treating from temperatures between 850 to 1050°C hardness in general was lower than that in as-cast state except when B1 was air cooled from 850°C (Figs. 4.1a to 4.1d).

The aforesaid data (Figs. 4.1a to 4.1d) although providing very useful information did not provide a comprehensive understanding of the transformation behaviour. The additional information required was obtained by replotting the data contained in the Tables 4.1 to 4.44 in the following manner:

(i) Effect of time on the hardness as influenced by the heat treating temperatures (Figs. 4.2a to 4.2f).

(ii) Effect of temperature on the hardness as influenced by the holding period for each alloy (Figs. 4.3a to 4.3d)

(iii) Effect of temperature on the hardness at each of the five soaking periods for all the alloys (Figs. 4.4a to 4.4e).

(iv) Effect of alloy composition on the hardness as influenced by the heat treating parameters [for each alloy] (Figs. 4.5a to 4.5e and 4.6a to 4.6f which are in the form of bar diagrams)

The following deductions would reveal the usefulness of the Figures 4.2 to 4.6 along with the Figures 4.1a to 4.1d, in providing further useful information on the (a) individual and (b) comparative behaviour of the alloy(s).

4. The comparative hardness vs time plots, as influenced by temperature, further confirmed the similarity between B1

and B3 and that between B2 and B4 upon heat treating from upto 850°C (Figs. 4.2a & 4.2b).

5. On air cooling from 900 and 950°C, hardness was independent of time for all the alloys. B1, by attaining a higher level of hardness, revealed an ability to sustain it to higher levels compared with the rest (Fig. 4.2c & 4.2d).

6. On air cooling from 1000°C, once again the alloy B1 had the maximum overall hardness followed by B3, B2 and B4 except that the overall hardness of B4 was now lower than that of B1, B2 and B3 (Fig. 4.2e).

7. On air cooling from 1050°C, the differences in the hardness levels of the four alloys evened out and for all practical purposes their overall behaviour might be regarded as similar. However, the alloy B4 showed the lowest overall hardness level (Fig. 4.2f). In fact, the maximum decrease in hardness with time occurred at this temperature (Fig. 4.2f).

8.(a) The hardness vs temperature plots as influenced by time (Figs. 4.3a to 4.3d) represented how effectively each alloy sustained its hardness on heat treating.

(b) These curves had a horizontal S-shape.

(c) The slope of the curve altered around a threshold temperature or over a narrow range of temperature. This was termed as the 'cross over point'(COP).

(d) To its left, the higher the time the higher was the level of hardness. To its right the situation was

just the reverse. This is valid for all the alloys.

9. The profile of the hardness vs temperature plots was steeper for the alloys B1 & B3 and flatter for the alloys B2 & B4 (Figs. 4.3a to 4.3d). Further, the hardness band (variation in the hardness as influenced by time) at 1050°C was the maximum for the alloy B1 followed by B4, B2 and B3 in that order.

   Based on these observations the similarity in the behaviour of the alloys B1 & B3 and that between B2 & B4 was reaffirmed. Thus B1 & B3 and B2 & B4 could thus be grouped together.

10. The COP of the alloys B1 and B3 was around 915°C (Figs. 4.3a and 4.3c) whereas, that of B2 and B4 was approximately in the range of 875-885°C (Figs. 4.3b and 4.3d).

11. A comparison of the hardness vs temperature plots as influenced by time (Figs. 4.4a to 4.4e), further reveals broad similarities in behaviour between B1 and B3 and that between B2 and B4.

12. At the lowest soaking period (2 hours) the plots tended to be flat (Fig. 4.4a) and their slope became steeper with an increase in the soaking period (Figs. 4.4b to 4.4e).

13. The aforesaid plots (Figs. 4.4a to 4.4e) may also be interpreted as indicating the relative hardness sustaining ability of the different alloys on heat treating.

14. An important inference from the data summarized in the

Figures 4.1 to 4.4 is that it is possible to deduce (a) the temperature(s) at which the hardness is independent of the soaking period or (b) the different temperature and time combinations to arrive at any desired value of hardness for the alloys (also refer Figures 4.42-4.45).

15. The deductions (a) to (h) and (1) to (14) are further reaffirmed through the bar diagrams shown in Figures 4.5 & 4.6.

4.1.2 Microstructure

Effect of heat-treatment on the hardness was substantiated by carrying out micro-structural studies. Initially the experiments were confined to assessing qualitative changes in the microstructure and these are summarized in the Figures 4.7 to 4.32. Subsequently, quantitative estimations involving massive and dispersed carbides were also carried out. These data have been dealt with separately.

Considering the former to start with, the microstructure of the four alloys in the as-cast condition consisted of :

1. (a) P/B + M + carbide (B1) Fig. 4.7 a&b
   (b) B/M + carbide + RA (B2) Fig. 4.7 c&d
   (c) B/M + carbide + RA(?) (B3) Fig. 4.8 a&b
   (d) B/M + carbide + RA (B4) Fig. 4.8 c&d
2. On heat-treating from 800°C, the as-cast microstructure transformed to one comprising massive carbides in a matrix of martensite (Figs. 4.9, 4.15, 4.21 & 4.27). Dispersed carbides were clearly observed corresponding

to the 10 hrs. heat-treatment. Massive carbides have been rendered discontinuous (Figs. 4.9, 4.15, 4.21 & 4.27).

3. On heat-treating from 850°C, austenite was retained in the micro-structure at 2 hrs. soaking period although its amount varied from alloy to alloy (Figs. 4.10a, 4.16a, 4.22a, and 4.28a). On raising the soaking period to 10 hrs., the amount of retained austenite decreased and the volume fraction of martensite and DC increased (Figs. 4.10e, 4.16c, 4.22c, 4.28c). Massive carbides were mostly discontinuous and their volume fraction was comparable with that observed on heat-treating from 800°C (Figs. 4.9 & 4.10, 4.15 & 4.16, 4.21 & 4.22, and 4.27 & 4.28). Needle-like structure, associated with dispersed carbides was observed in B2 and B4 (Figs. 4.16c and 4.28c).

4. On heat-treating from 900°, the matrix microstructure comprised martensite and austenite in B1 & B3 (Figs. 4.11 & 4.23) and predominantly austenite in B2 & B4 (Figs. 4.17 & 4.29). On increasing the soaking period from 2 to 10 hours, the matrix microstructure was not much altered. The second phase as before comprised massive as well as dispersed carbides (Figs. 4.11, 4.17, 4.23 and 4.29). The size and the volume fraction of the dispersed carbides, which is a maximum in B4, increased with soaking period (Figs. 4.11a-e, 4.17a-e, 4.23a-e and 4.29a-e). Further, the volume fraction of the massive carbides also decreased

somewhat with the soaking period (Figs. 4.11, 4.17, 4.23 and 4.29). Needle type structure was observed in all the four alloys (Figs. 4.11c, 4.17a&c, 4.23a&c and 4.29a,c&e), it being the maximum in alloy B4 (Fig. 4.29). It was further observed that the needle type structure was surrounded by dispersed carbides; the regions containing needle type structure were free from dispersed carbides (Figs. 4.11, 4.17, 4.23 and 4.29).

5. On heat-treating from 950°C, a similar situation as above existed (Figs. 4.12, 4.18, 4.24 and 4.30). The needle type structure, sometimes in the form of obtuse plates, was still observed (Figs. 4.12c, 4.18c&e, 4.24c and 4.30a&c), it being the maximum in B4. Its presence is not fully understood but it might either indicate the possible presence of an intermetallic compound/ some other form of carbide.

6. On heat-treating from 1000°C, the matrix was plain and completely austenitic (Figs. 4.13, 4.19, 4.25 and 4.31). Volume fraction of the dispersed carbides has considerably reduced. It was only observed for the 2 hrs. treatments and in some of the 4 hrs. treatments. Stray carbide particles occasionally observed were very coarse in nature. Similarly, the amount of massive carbides decreased markedly with time(Figs. 4.13, 4.19, 4.25 and 4.31). Inter-linking or bridging together amongst different massive carbide regions was observed

at 4 hours soaking period indicating the possible onset of another transformation (Figs. 4.13c, 4.19a, 4.25c and 4.31c). Hardly any dispersed carbides were observed corresponding to the 10 hours heat-treatment. Simultaneously, the massive carbides tended to 'round off'.

7. On heat-treating from 1050°C, the matrix is austenitic (Figs. 4.14, 4.20, 4.26 and 4.32). A new phase formed which resembles the 'sigma phase' when observed at low magnification (Figs. 4.14d, 4.20d, 4,26d and 4.42b&d). Higher magnification observations revealed that it resembled plate like carbides (4.14c, 4.20c, 4.26c and 4.32c). A close examination revealed that the microstructure may be described as comprising austenite + an eutectic of austenite + carbide (anomalous eutectic). The volume fraction of the eutectic initially increased upto 4-6 hrs. soaking period and decreased thereafter (Figs. 4.14, 4.20, 4.26 and 4.32). At 10 hrs. soaking period perforations were observed in the carbides present (Figs. 4.14e, 4.20e, 4.26e and 4.32e).

4.1.3 Quantitative Metallography

4.1.3.1 Massive Carbides

Effect of heat-treatment on the volume fraction of massive carbides was investigated with the help of a LEITZ image analyser. The data thus obtained have been summarized in Table 4.46 and in Figure 4.33.

A perusal of this table and figure revealed that :

1. Volume fraction of the massive carbides in the as-cast

condition ranged from 22-27%, it being higher in B1 & B3 in comparison to that in B2 & B4.

2. An increase in the temperature/time, in general, led to a decrease in the amount of massive carbides (Figs. 4.33a-d).
3. Upto 950°C, the aforesaid decrease was gradual.
4. Raising the temperature to 1000°C led to a steep fall in the volume fraction with time except in B4. A similar response was qualitatively observed on heat-treating from 1050°C (Figs. 4.14, 4.20, 4.26 and 4.32). The 1050°C,10hrs. heat-treatment resulted in the formation of lowest volume fractions of massive carbides (Figs. 4.14e, 4.20e, 4.26e, and 4.32e).
5. The decrease in massive carbides on heat treating was found to be lower in B2 and B4 in comparison to that observed in B1 and B3. Further, amongst B1 and B3, the volume fraction of MC was higher in the former and so also the decrease in it on heat treating.

4.1.3.2Dispersed carbides

Dispersed carbides(particles) were characterized on the basis of the following parameters :

(i) Average particle size,
(ii) Total number of particles,
(iii) Their volume fraction,
(iv) Their percent number in different classes, and
(v) Percent area occupied by them in different classes.

In the present study the particles were characterized on the

basis of six classes separated from one another by ≈0.58 micron.

The data thus generated are summarized in the Tables 4.47-4.55 and in the Figures 4.34-4.37 (histograms). Each histogram is a composite of five histograms representing five different fields of observation for a given heat treatment. The aforesaid data were analysed in two ways, (a) by assessing whether any general trend existed and (b) by laying down a detailed account of how the heat treating variables affected the parameters employed to characterize dispersed carbides.

Considering to start with the former, the following general trends were observed for all the alloys:

(i) Dispersed carbides predominantly belonged to class I and II i.e. size upto ≈1.16 microns (Tables 4.47-4.55 and Figs. 4.34-4.37).

(ii) The number of particles was a maximum for heat treatments carried out at 800°C & 850°C (Table 4.52).

(iii) On increasing the heat-treating temperature upto 950°C, the average particle diameter increased (Table 4.51) whereas the carbide volume fraction decreased or remained unaltered (Table 4.53).

(iv) For a given time, increasing the temperature upto 900°C resulted in a decrease in the volume fraction followed by an increase on raising the temperature further to 950°C.

(v) For a given heat treating temperature, the volume fraction increased with an increase in the heat treating time in a majority of instances (Table 4.53). A similar trend was observed for the average particle size (Table 4.51).

(vi) By and large the number of particles decreased on

increasing the temperature at a given heat-treating time or by increasing the heat treating time at a given heat treating temperature (Table 4.52).

(vii) In a general way, it can be stated that for a given time, the number of particles and the percent area occupied by the particles in classes I & II decreased with an increase in temperature. A similar trend was observed on increasing the heat treating time at a given heat treating temperature (Tables 4.47-4.50 and Figs. 4.34-4.37).

(viii) The changes described in (vii) above were simultaneously supplemented by changes in the number of particles in classes III to VI, the nature of changes being just the opposite of those described in (vi) above (Tables 4.47-4.50).

(ix) The histograms summarized in Figs.4.34-4.37 proved extremely helpful in understanding how the distribution of the particles varied with temperature and time.

4.2 Discussion

The main aim of the present investigation was to establish the transformation behaviour of the alloys. This was achieved by heat-treating the alloys from different temperatures and by assessing the microstructural changes by hardness measurements. Subsequently, the microstructures were quantitatively characterized by studying the variation in (i) the volume fraction of massive carbide and (ii) the size and distribution of dispersed carbides as influenced by heat-treating parameters. The data thus generated proved helpful in establishing mathematical

models of (i) the transformation behaviour and (ii) the coarsening behaviour of dispersed carbides.

4.2.1 Structural changes during heating

Based on earlier studies (42) it has been established that (a) nearly 45% of the Mn added partitions to austenite and the balance to the carbide phase, (b) bulk of the chromium partitions to the carbide phase, and (c) bulk of the Cu partitions to austenite. This enables an understanding of the structural changes that will occur which comprise (i) a reduction in the volume fraction of the massive carbides due to the presence of Si and Cu (attributed to their graphitizing tendency), (ii) an increase in the stability of austenite due to the dissolution of additional alloying elements made available as a consequence of (i), and (iii) a possible 'rounding off' of the massive carbides and their being rendered discontinuous due to (i), (iv) occurrence of a carbide transformation which would be governed by the nature of the phase diagrams, and (v) possible precipitation of carbides from austenite on prolonged soaking as represented by the reaction

austenite --> austenite + DC ...(4.1)

The likely structural changes therefore, can be summarized with the help of the following equations :

austenite --> austenite (lesser alloy content) + DC ...(4.2)

MC --> MC (discontinuous with reduced VF)

+ interstitial and substitutional solutes ...(4.3)

MC --> other types of carbides ...(4.4)

Interstitial + substitutional solutes + austenite ->

austenite (with increased stability) ...(4.5)

austenite (with higher stability) increase in SP/ST—>

austenite (lower stability) + DC ...(4.6)

$$\text{DC increase in } \frac{\text{ST at given SP}}{\text{SP at given ST}} \rightarrow \text{DC (coarse) or possible dissolution at higher temperature(s)} \quad \ldots(4.7)$$

4.2.2 Changes during cooling to room temperature

They will be governed by the cooling rate and the alloy content and would primarily be confined to austenite. Some changes may also occur in the massive carbides and the DC that have formed. The possible changes in austenite would depend upon the temperature and time as they govern the relative stability of austenite in accordance with the Equations (4.2), (4.5) and (4.6). If air cooling is done, austenite may reject excess solute in the form of dispersed carbides and would subsequently transform to either B/M and or remain untransformed. Since the minimum Mn content in the alloys(6%) ensures that martensite can form on air cooling from 800 and 850°C and austenite is partly retained on air cooling from 900°C(56), it is evident that the transformation product of austenite would essentially be martensite on air cooling from upto 850°C, a combination of martensite + austenite on air cooling from upto 950°C and predominantly austenitic on raising the temperature further. The relative proportions of austenite/martensite will be governed by the extent to which the reactions(4.2) and (4.6) proceed.

Carbide precipitation during cooling mainly occurs because of a decrease in the solid solubility of carbon with temperature in the austenite. If austenite is supersaturated after heat treatment, it would reject out excess solute as carbides and

these would be inherited by the transformation product of austenite on cooling. However, if the austenite is not supersaturated and is in a state wherein the solutes are fully dissolved (requiring a higher heat-treating temperature), it will be retained as such on cooling.

Taking an overall view, the possible structural changes on cooling can be summarized with the help of the following equations :

Slow cooling (as during casting)

austenite --> P/B + M ...(4.8)

(relative proportion of the P/B & M depending on alloy content)

Carbide --> unchanged or otherwise depending upon carbide transformation ...(4.9)

Retention of austenite --> [depends upon austenite stabilising tendency of Mn & Cu)] ...(4.10)

Final likely structure : **P/B + M + MC + RA (?)**

Heat treated condition

(a) Lower temperatures 800 and 850°C

austenite --> austenite" + DC ...(4.11)

austenite" --> M ...(4.12)

(extent of M depends upon soaking period i.e. less at lower soaking period and more at higher soaking period)

austenite" --> austenite (depending upon alloy content) ...(4.13)

Massive carbide --> M_3C + other variants ...(4.14)

DC --> DC (coarse) ...(4.7)

Final likely structure : **M + austenite + MC + DC**

(b) Temperatures 900 & 950°C

austenite" --> austenite (most probable at higher temperature and soaking periods) ...(4.15)

austenite" --> austenite + M (VF small which will further decrease with temperature and time) ...(4.16)

DC --> DC (coarse) ...(4.7)

MC --> M_3C + other variants (VF reduced) ...(4.14)

Likely final structure : **austenite + DC + MC + some M(?)**

(c) 1000 and 1050°C

austenite" --> austenite (matrix completely austenitic) ...(4.17)

DC --> DC (coarse) and possible dissolution at higher soaking period(s) and temperature(s) ...(4.7)

MC --> M_3C + other variants (VF low, possible rounding off may be observed) ...(4.14)

Final likely structure : **austenite + MC + some DC**
or austenite + MC

4.2.3 Strengthening response of different transformations

Before analysing the structure-property relations it would be appropriate to consider the strengthening associated with different transformations.

The austenite to martensite transformation leads to hardening and to simultaneous embrittlement. The attainment of austenitic matrices would lead to an improvement in the ease of deformation. In such instances, the stacking fault energy (SFE) of the matrix would determine the strength-ductility interrelation as it (SFE) controls the extent of work hardening. It is relevant to record here that Mn-austenites have a low SFE and hence exhibit a high rate of work hardening (57).

Massive carbides have a higher hardness and the strengthening response would be directly related to their volume fraction. Its morphology and compatibility with the matrix are

also equally important. The latter is governed by the crystal structure. The effect of dispersed carbides would be governed by the volume fraction, compatibility with the matrix, size, shape and distribution (58,59).

4.2.4 Interrelation between microstructure and hardness

The general microstructural changes that may occur in the experimental alloys, highlighted in the earlier sections, facilitate interpretation of the structural changes that would occur in B1, B2, B3, and B4. As hardness is governed by the microstructure, the two have been discussed together.

4.2.4.1 As-cast state

The microstructure of the alloys in the as cast condition namely, P/B + M + MC, B/M + RA + MC, B/M + RA (?) + MC and B/M + RA + MC respectively (Figs. 4.7 and 4.8), is consistent with the analysis outlined in the Section 4.2.1 to 4.2.3 (Equations 4.8-4.10). Mn alone is controlling the matrix microstructure because Cu separates out on slow cooling due to its limited solubility in austenite and ferrite and to a further decrease in it (solubility) with temperature in ferrite (60-63). Accordingly, the matrices of the alloys B2 and B4 are not likely to be fully martensitic (Figs. 4.7c and 4.8c). Although this is clearly reflected in the microstructure of B1 (Figs. 4.8a&b), the same is not clearly evident from the microstructure of B3 (Figs. 4.8a&b).

The higher Mn alloys B2 and B4 would attain a higher proportion of martensite (Figs. 4.7 and 4.8) with some austenite retention being a distinct possibility at least in B4 (Fig.

4.8c&d). Accordingly, the hardness values of B1 and B3 and that of B2 and B4 are expected to be nearly similar. Furthermore, B4 is likely to be less harder than B2 due to possible retention of austenite. However, B3 is harder than B1 and B4 is harder than B2. This may be attributed to a higher P content in B3 and B4 (Table 3.2).

4.2.4.2 Heat-treated condition

The alloys are so designed that they readily transform to martensite at the lower of the two Mn contents and that the retention of austenite is not ruled out on air cooling from 900°C. This tendency would be further enhanced in the higher Mn/Cu alloys. When this is considered along with the general structural changes that have been outlined in the Sections 4.2.1 to 4.2.3, it becomes easy to rationalize how microstructure would vary on heat-treating.

4.2.4.3 Alloy B1

The changes can be easily explained based on Equations 4.1 to 4.17.

(a) 800°C :

High hardness (Fig. 4.1a) at 2 hours soaking period is due to the formation of a martensitic matrix (Fig. 4.9a&b). Hardness increased marginally with time(Fig. 4.1a) due to the formation of some dispersed carbides (DC) at higher soaking periods (Fig. 4.9c).

(b) 850°C :

The lower hardness at 2 hrs. soaking period (Fig. 4.1a) is due to the retention of austenite (equations 4.5 & 4.12) (Fig. 4.10a&b). Increase in the hardness with soaking period

(Fig. 4.1a) is due to the formation of martensite and to the formation of a larger volume fraction of dispersed carbides (Fig. 4.10) as per equations 4.6 and 4.12. The lower overall hardness values attained on heat treating at 850°C, in comparison to that observed on heat treating from 800°C, are due to an increase in the austenite stabilizing tendency and hence to the formation of a relatively smaller volume fraction of martensite.

(c) 900°C :

The lower hardness (Fig. 4.1a) at 2/4 hrs. soaking period is due to a further increase in the austenite stabilizing tendency (Fig. 4.11 a&b). Increasing the soaking period has practically no effect on the hardness because the microstructure is practically unaltered except for a limited coarsening of the dispersed carbides and some reduction in the volume fraction of the massive carbides (Fig. 4.11 and Table 4.46). The lower overall hardness at 900°C in comparison to that observed on heat treating from 850°C is largely due to an increase in the proportion of retained austenite. This effect is marked at the highest soaking period(Fig. 4.11e).

(d) 950°C :

The basic structural changes on heat treating at 950°C are similar to those occurring on heat treating at 900°C except that the coarsening of dispersed carbides is enhanced and reduction in the volume fraction of massive carbides is larger(Fig. 4.12 a-f; Table 4.46). These changes, which promote the retention of relatively larger volume fraction of stable austenite, not only

result in a lower overall hardness compared with that observed on heat treating from 900°C but are also responsible for a slight decrease in hardness with soaking period (Fig. 4.1a). Volume fraction of massive carbides has decreased to a level so as to contribute to the decreasing hardness trend.

(e) 1000°C :

The lower hardness at 2 hrs. soaking is due to (i) a predominantly austenitic matrix rendered even more stable and (ii) a further decrease in the amount of massive and dispersed carbides (Fig. 4.13a&b; Table 4.46). The decrease in hardness with soaking period (Fig. 4.1a) is due to a marked decrease in volume fraction of massive carbides and to a near complete dissolution of the dispersed carbides(Fig. 4.13c&d). Presence of dark jagged regions at 2 hours soaking period in an otherwise plain austenitic matrix reveals the formation of a new phase (Fig. 4.13a). Its presence is more clearly visible at higher soaking periods where it is seen to 'bridge' massive carbide regions (Figs. 4.13c&d).

(f) 1050°C :

Structural changes are similar to those observed at 1000°C but are still further accelerated as the temperature is higher. This leads to a decrease in hardness with the soaking period. This decrease would have been steeper but for the formation of austenite + carbide eutectic (perhaps with a high hardness) whose formation was initiated at 1000°C and which has now resolved itself into an eutectic like morphology. Its volume fraction initially increased with soaking period (4-6 hours) and decreased thereafter on increasing the soaking period to 10 hrs. (Fig. 4.14

a-f). At the end of 10 hrs. soaking period this phase is still present as a thin network along with massive carbides whose volume fraction is very small and which have by now attained a globular morphology having perforations (Figs. 4.14e&f). The lowest overall hardness at 1050°C is due to the presence of a predominantly high stability austenitic matrix containing very small amounts of massive carbide and the eutectic.

4.2.4.4 Alloys B2, B3, B4

The analysis put forth in the previous Section (4.2.4.3) satisfactorily explains the interrelation between hardness and microstructure. Transformations in B2, B3 and B4 would proceed on similar lines. It would be reasonable to suggest that the changes taking place in these alloys may be classified as common with and different from those occurring in B1. The former shall comprise transformations in which the final microstructure is predominantly austenitic i.e. the structural changes occurring on heat treating from temperatures ≥950°C. Under these conditions, B2, B3 and B4 may differ from B1 in terms of the (a) the relative stability of austenite which is governed by the alloy content, (b) volume fractions of massive carbides (Table 4.46), dispersed carbides (Tables 4.47-4.55), and the eutectic (Figs. 4.14, 4.20, 4.26 and 4.32), and (c)coarsening behaviour of dispersed carbides (Tables 4.47-4.55). All these parameters are a function of the alloy content and the heat treating schedule.

The aforesaid differences in the microstructure would not only lead to differences in the overall hardness between B1 and B2, B3, B4 but also amongst B2, B3 and B4. The micro-structure

and hardness on heat treating B2 (Figs. 4.1b and 4.15-4.20), B3(Figs. 4.1c and 4.21-4.26) and B4 (Figs. 4.1d and 4.27-4.32) at temperatures ranging from 950-1050°C are consistent with the above reasoning.

B2, B3 and B4 would differ from B1 based on the transformations occurring on air cooling from 800-950°C. At 800°C, the transformation behaviour of B3 would be similar to B1 in view of their similar Mn contents. The effect of a higher Cu content in B3 is not experienced at 800°C due to the temperature being lower. However, it is manifested at 850°C leading to increased austenite stabilization. This does not permit reactions represented by 4.12 & 4.13 to go completion i.e., these occur only partly. In view of this, the overall level of hardness and the rate of increase in hardness in B3 is lower than that in B1 on heat treating from 850°C. The microstructural and hardness changes in B3 on air cooling from 800°C (Figs. 4.1c and 4.21 a-d) and 850°C (Figs. 4.1c and 4.22 a-d) are consistent with this reasoning.

In view of a higher Mn content (a higher austenite stabilizing tendency), the nature of the microstructural and hardness changes in B2 on heat treating from 800°C (Figs. 4.1b and 4.15 a-d) would be broadly similar to those observed in B1 on heat treating from 850°C. A similar situation would exist in B4 on heat treating from 800°C (Figs. 4.1d and 4.27 a-d). On heat treating from 850°C, however, the aforesaid changes in B2 (Figs. 4.1b and 4.16 a-d) and B4 (Figs. 4.1d and 4.28 a-d) would be similar to those generally observed on heat treating B1 from a temperature higher than 850°C. In fact the situation is

comparable with that observed on heat treating B1 from 950°C. This is attributed to an increased austenite stabilizing tendency due to higher Mn and Cu contents. The overall hardness level in B4 is expected to be slightly lower than that in B2 due to a higher Cu content. However, this has not been observed due to a higher 'P' content in B4 and the fact that air cooling has been employed. However, as already discussed, the effect of a higher Cu content in B4 is clearly manifested on heat treating from higher temperatures. On heat-treating at 900°C, the difference in the austenite stabilizing tendency between the B1 and the rest of the alloys is further reduced. The overall transformation behaviour could justifiably be represented on the basis of the hardness values as $H_{B1} > H_{B3} > H_{B2} > H_{B4}$; the hardness of the alloys being B3, B2 and B4 is not much different from one another. On raising the temperature further, the difference in hardness between B1 and the rest is further reduced and would be only marginal at the 1050°C, 10 hrs. heat-treatment. A similar deduction is not being made for the lower soaking periods at the highest heat-treating temperature (at 1050°C) because of the formation of an eutectic whose magnitude varies from alloy to alloy.

4.2.4.5 Relative hardness vs time plots

It would now be pertinent to compare the hardness levels in different alloys as influenced by time at different heat treating temperatures. The derived plots (Figs. 4.2 a-f) were obtained from the base curves (Figs. 4.1 a-d) to elicit this information unambiguously. The data contained in the Figures 4.2a-f can be

interpreted on a similar basis as the base curves and reveal that:

(i) At 800°C the behaviour of B1 and B3 and that of the higher Mn alloys B2 and B4 are similar. As already discussed, the transformation behaviour is controlled by the Mn content alone. The former combination attains a higher overall level of hardness (Fig. 4.2a) due to a lower austenite stabilizing tendency attributable to a lower Mn content (≈6%). Thus, the reaction corresponding to equation 4.12 goes to completion.

(ii) On heat treating from 850°C, the Cu effect comes into play. Its magnitude in terms of austenite stabilizing tendency would depend upon the Mn content of the alloys. B1 and B3 show an increase in hardness with soaking period (equations 4.5, 4.6 and 4.12), the overall level in B1 being higher than that in B3 due to a lower austenite stabilizing tendency. The hardness in B2 and B4 is unaltered/shows a marginally decreasing trend with soaking period, because the reaction corresponding to equation 4.12 does not go to completion leading to some austenite retention. The overall level of hardness is higher in the former group of alloys (B1 and B3) for reasons already stated. Thus, from the overall hardness point of view B1>B3>B2,B4 (Fig. 4.2b).

(iii) At 900°C, the bunching together of the H vs t curves is due to a similarity in the microstructure (Fig. 4.2c). All the same, observation at (ii) regarding the relative hardness levels, is still valid as it is intrinsically related with the alloy content.

(iv) The situation at 950°C is nearly identical with that observed on heat treating from 900°C due to a similarity in the microstructure. However, the slight decrease in hardness with soaking period is because the transformations inducing a reduction in the volume fraction of massive carbides and a coarsening of dispersed carbides are accelerated. This can be attributed to a higher heat treating temperature further aided by the presence of a higher Mn and Cu contents (Fig. 4.2d).

(v) **1000°C** : Reasons for a decrease in the hardness with soaking period have already been explained. The hardness levels associated with the alloys are (a) directly related to the Vf of MC and (b) inversely proportional to the overall alloy content (Fig. 4.2e). Hence the hardness sequence is B1>B3>B2>B4.

(vi) **1050°C** : A situation similar to that observed on air cooling from 1000°C exists, and the comparative hardness data can be explained essentially on a similar basis as in (v) (Fig. 4.2f).

4.2.5 Hardness - time interrelation

In order to arrive at such a correlation, the data contained in the Tables 4.1-4.24 were analysed with the help of a computer programme. Constants for the first, second and third order variations were calculated using the least square techniques (54,55) and are also reported at the bottom of each of the Tables 4.1-4.24. Although the variance decreased as the order of equations increased, plotting of the data revealed that the

variation in hardness with time and its subsequent interpretation based on microstructural changes can be best explained on the basis of a first order equation. The theoretical values of hardness calculated on this basis (also indicated in the Tables) are in excellent agreement with the experimental values. Thus, hardness H can be expressed by an equation :

$$H = C_1 + C_2 t \text{ (at a constant temperature)} \quad ...(4.18)$$

The values of C_1 and C_2 for each of the alloys at different heat-treating temperatures are indicated in the Tables 4.1-4.24.

4.2.6 Hardness-temperature interrelation

4.2.6.1 Nature of variation

In order to arrive at the aforesaid correlation, the hardness vs temperature data for each of the alloys (summarized in the Tables 4.25-4.44) were analysed and the constants for the first to fourth order variations were calculated (Tables 4.25 to 4.44). It is not reasonable to assume that hardness varies linearly with temperature especially so when changes in the microstructure are being brought about by three different transformations. A fourth degree variation is also ruled out. Of the available options a third order variation represents the microstructural changes most appropriately (Figs. 4.1 a-d) which comprise (i) a hardness plateau around 900 to 950°C, (ii) a decrease in hardness beyond 950°C and (iii) an increase in hardness on heat-treating at <900°C. Hence the variation in hardness with temperature at each of the soaking periods can most appropriately be represented by a third order polynomial :

$$H = C_1 + C_2 T + C_3 T^2 + C_4 T^3 \quad ...(4.19)$$

The values of the constants C_1, C_2, C_3, and C_4 have been

indicated in the Tables 4.25-4.44. This analysis forms the basis of arriving at the hardness vs temperature plots (Figs. 4.3 & 4.4) which are in the form of a horizontal 'S'- shape.

4.2.6.2 Effect of temperature on hardness and microstructure

The data summarised in the Figs. 4.3 and 4.4 can essentially be interpreted on a basis similar to the one employed for interpreting the data contained in the Figs. 4.1a-d. However, in the present context, it is the shape of the hardness vs temperature plots that needs analysing. As already stated (Section 4.2.6.1), the hardness vs temperature plots should have an 'S' shaped configuration. The plateau region indicates constancy of hardness over a range of temperature. At temperatures lower than this range, the hardness increases because of an increase in the tendency to form martensite which is directly proportional to the soaking period and inversely related to the Mn and Cu contents (Sections 4.2.1-4.2.3, 4.2.4.1 and 4.2.4.2). At temperatures higher than the aforesaid constant temperature range, the hardness decreases because of (i) an increase in the volume fraction and stability of austenite, (ii) the microstructures being predominantly austenitic and (iii) a steep decrease in the Vf of both MC and DC. These changes are directly related with the Mn and Cu contents (Sections 4.2.1-4.2.3). This analysis satisfactorily explains the general features of the hardness vs temperature plots (Figs. 4.3a-d).

The higher Mn alloys B2 and B4 exhibit a flatter profile in comparison to the lower Mn alloys B1 and B3 due to a higher austenite stabilising tendency leading to an early (at relatively

lower temperatures) formation of the austenite based microstructures (Figs. 4.3b,d). The steeper profiles associated with B1 and B3, signifying a marked decrease in hardness with temperature in a unit of time, can be similarly explained based on a reduced austenite stabilizing tendency (on heat-treating from 'lower' temperatures) thereby implying an enhanced tendency to form martensite/ partly martensitic structures (Figs. 4.3a,c). On the basis of a similar reasoning it is easy to deduce that the COP signifying the plateau region of the hardness vs temperature plots would set in early (i.e. at lower temperatures) in B2 and B4 (Fig. 4.3b,d). The maximum decrease in the hardness (hardness band) in the four alloys has occurred at 1050°C firstly because this is the highest heat treating temperature employed and secondly because at this temperature the different structural changes leading to a decrease in hardness occur the fastest and to the maximum extent. At 1050°C, the higher the soaking period, the smaller would be the volume fraction of massive carbide and larger the volume fraction of austenite and therefore, the lower would be the hardness (Figs. 4.3a-d). This explains the existence of a 'hardness band' (signifying hardness variation at 1050°C with soaking period) for each of the alloys. All other factors being identical, the width of the band would be mainly related to austenite stabilizing tendency (i.e. the soaking period and Mn+Cu content) and to the volume fraction of the massive carbides. Ideally the width would be a maximum for B1, i.e. for the composition with the least alloy content to be followed by B2, B3, and B4. However, experimentally, the order is found to be B1>B4>B2>B3. The deviation from the expected

behaviour may be attributed to the differing volume fractions of the eutectic.

4.2.6.3 Comparative hardness vs temperature data

The comparative plots indicating the effect of temperature on hardness (Figs. 4.4a-e), essentially derived from the data summarized in the Figures 4.3a-d, indicate the effect of soaking period and can essentially be interpreted on a basis similar to the one employed for interpreting the Figures 4.3a-d. The usefulness of the Figures 4.4a-e is that they give the comparative data for the experimental alloys at a glance. The same is further evident from the bar diagrams depicted in Figures 4.5 and 4.6.

4.2.7 Effect of temperature and time on the morphology and volume fraction of massive carbides

Although the effect of massive carbides in controlling the overall hardness has been discussed at length in Section 4.2.6.2, it would be appropriate to comment upon the effect of heat-treating parameters on their morphology and volume fraction. Massive carbides present in the as-cast structure (Figs. 4.7 and 4.8) are partly discontinuous and have been so rendered due to the graphitizing action of Cu and Si (Sections 4.2.1-4.2.3). It will increase with Cu content and heat treating temperature and time and also brings about a reduction in the volume fraction of massive carbides on heat-treating.

Based on physical metallurgical considerations associated with malleabilizing in so far as carbide decomposition/ disintegration is concerned(64), it is expected that the tendency towards attaining (a) a discontinuous morphology and (b) a

reduced volume fraction would become marked only at temperature ≥ 950°C. Another reason why volume fraction of massive carbides may not significantly decrease until 950°C is that other transformations (highlighted earlier) take precedence over the carbide transformation presently under consideration. This is because they require lesser activation in terms of temperature.

However, unlike in malleable irons, the carbide phase in the experimental alloys has been rendered stable by Cr additions (Section 2.2). Additionally a fair proportion of Mn also partitions to it, thereby enhancing its stability(42). Therefore, as the heat-treating temperature and time are increased the massive carbides instead of decomposing into graphite, will acquire a low energy configuration/morphology namely either near spherical or hexagonal. The precise nature would be governed by the crystal structure of the massive carbides as influenced by heat-treating temperature and time. This analysis explains the 'rounding off' observed in massive carbides on heat-treating from higher temperatures (Figs. 4.12 & 4.13, 4.18 & 4.19, 4.24 & 4.25 and 4.30 & 4.31).

Considering the decrease in the Vf of massive carbides, the Cr containing carbides, as already stated, are further rendered stable because Mn partitions to them (45). Therefore, taking an overall view, the decrease in the volume fraction of massive carbides will be faster only at temperatures around 950°C or higher (i.e. ≈1000°C) as has been observed in the present investigation (Fig.4.33). This process (involving a reduction in the volume fraction of massive carbides) will be further aided by the presence of a fully austenitic matrix and this occurs

only at temperatures around 950°C. The data summarized in Table 4.46 and in Figure 4.33 thus stand appropriately explained. The least volume fraction of massive carbides will accordingly be observed at the highest soaking temperature and time (Table 4.46).

4.2.8 Effect of time and temperature on the distribution of dispersed carbides

Sections 4.2.1 & 4.2.2 highlight the mechanism of formation of dispersed carbides from austenite. The results summarized in the Tables 4.47 to 4.55 and in the Figures 4.34-4.37 prove helpful in characterizing them fully. As can be seen, particles constituting the dispersed carbides have a size upto ≈1.16 μ because they exclusively fall into classes I and II at the formation stage. This is valid for all the alloys. On heat-treating, their distribution is altered in a manner consistent with the attributes of nucleation and growth type of transformations. Simultaneously, coarsening would also set in. This would involve a reduction in the number of particles in the first two classes and a simultaneous increase in their number in the classes III-VI. Additionally, the mean diameter would also increase. This is what has been observed in a majority of the instances(Tables 4.47-4.55). The comparative data given in the Tables 4.47 to 4.55 reveal that it would be difficult to arrive at a general interrelation correlating the effect of alloy content and heat-treating schedule on the extent of coarsening. This would be of interest as it (the coarsening behaviour) would govern the overall properties of the alloys.

Mathematically, the coarsening behaviour of second phase

particles is studied with the help of the Ostwald's equation(65) which can be represented as :

$$r_1^3 - r_o^3 = k(t_1 - t_o) \qquad ...(4.20)$$

where r_1 = particle radius at time t_1, and

r_o = particle radius at time t_o

A major limitation of this equation is that a large number of data are required to ascertain its validity/ to ensure its application under a given set of experimental conditions. Moreover the equation merely correlates the arithmetical mean of particle radius with time but in no way reflects upon how the particle distribution is influenced by temperature/time. Further, finding out the arithmetical average of particle radius does not represent the true picture since the particle size distribution is statistical in nature. In the present investigation for a given heat treating temperature, the data related with the second phase are available only at 3 or more soaking periods. Generally, this should have sufficed for any further analysis of the data but not so with the Ostwald's equation. Difficulties arising out of the incapabilities/ inadequacies were resolved by evolving a new parameter called the 'coarsening index'(CI)(43).

In order to calculate coarsening index, it is necessary to first evolve a parameter which can represent particle size distribution for a given heat-treating schedule. Development of such a parameter was greatly facilitated by the data generated while conducting quantitative metallographic work namely (a) categorization of particles into different classes, (b) assessment of the number of particles in different classes, (c) calculation of percent area occupied by particles in different

classes, and (d) measurement of the average particle diameter. The new parameter termed 'distribution factor'(DF) which incorporated the variables (a) to (d) is defined as

$$DF = \frac{\sum_{i=1}^{n} X_i N_i}{\sum_{i=1}^{n} N_i} \qquad \ldots(4.21)$$

where, n = the number of classes,

N_i = the number of particles in i^{th} class,

X_i = volume fraction in the i^{th} class /VDC,

and, VDC = total volume fraction of dispersed carbides.

Effect of heat-treatment on the distribution factor

h/t schedule	B1	B2	B3	B4
800°C, 2 hrs.	0.378	0.395	0.410	0.393
800°C, 10 hrs.	0.370	0.380	0.322	0.384
850°C, 2 hrs.	0.368	0.374	0.362	0.303
850 °C, 4 hrs.	0.344	0.310	0.329	0.399
850°C, 6 hrs.	0.364	0.380	0.352	0.331
850°C, 10 hrs.	0.353	0.399	0.388	0.316
900°C, 2 hrs.	0.344	0.369	0.344	0.335
900°C, 4 hrs.	0.335	0.360	0.337	0.344
900°C, 6 hrs.	0.297	0.382	0.344	0.367
900°C, 10 hrs.	0.259	0.301	0.339	0.337
950°C, 2 hrs.	0.233	0.339	0.355	0.329
950°C, 4 hrs.	0.249	0.211	0.261	0.249
950°C, 6 hrs.	0.267	0.213	0.257	0.275
950°C, 10 hrs.	0.199	0.143	0.163	0.181

Distribution factors, calculated on the basis of the aforesaid formula, are summarized in the above table.

Having defined this parameter(DF), coarsening index can now be calculated with respect to a specified reference base - a concept also implicitly in-built into the Ostwald's formula. In the present instance, this reference base was taken to be the heat-treating schedule at which the dispersed carbide particles just about formed namely the heat-treating schedule corresponding to which dispersed carbides were present in classes I and II only.

The coarsening index(CI) is thus defined as

$$CI = \frac{\text{DF for a given heat treatment}}{\text{DF for the h/t with particles in classes I \& II}} \qquad (4.22)$$

Based on the above formulation, the coarsening index for the different alloys was calculated and is summarized in the following table.

As already discussed above, the aforesaid table proves extremely useful in assessing the relative coarsening tendency of different alloys, and this is duly reflected in the 'remarks' column of the aforesaid table. No comment is being made on the possible effect of Mn and Cu on the extent of coarsening because both the higher Cu alloys B3 and B4 have a higher P content compared with that in B1 and B2 (Table 3.2); furthermore added complications arise because DC are forming directly from austenite and also during air cooling. thereby making any comparison untenable.

Relative coarsening behaviour of the alloys

h/t schedule	Coarsening index B1	B2	B3	B4	Remarks
800°C, 2 hrs.	1.000	1.000	1.000	1.000	----
800°C, 10 hrs.	0.979	0.962	0.785	0.977	B1>B4>B2>B3
850°C, 2 hrs.	0.973	0.947	0.883	0.771	B1>B2>B3>B4
850°C, 4 hrs.	0.910	0.785	0.802	1.015	B4>B1>B3>B2
850°C, 6 hrs.	0.963	0.962	0.858	0.842	B1>B2>b3>B4
850°C, 10 hrs.	0.934	1.010	0.946	0.804	B4=B1>B3>B2
900°C, 2 hrs.	0.910	0.934	0.839	0.852	B2>B1>B4>B3
900°C, 4 hrs.	0.886	0.911	0.822	0.875	B2>B1>B4>B3
900°C, 6 hrs.	0.785	0.992	0.839	0.934	B2>B4>B3>B1
900°C, 10 hrs.	0.685	0.762	0.827	0.857	B4>B3>B2>B1
950°C, 2 hrs.	0.616	0.858	0.866	0.837	B3>B2>B4>B1
950°C, 4 hrs.	0.659	0.534	0.637	0.634	B1>B3>B4>B2
950°C, 6 hrs.	0.706	0.539	0.627	0.700	B1>B4>B3>B2
950°C, 10 hrs.	0.526	0.362	0.398	0.461	B1>B4>B3>B2

The data on the relative coarsening behaviour of the alloys is relevant to an understanding of the deformation and the corrosion behaviour of the alloys as would be evident from an analysis put forth in Chapter VI.

4.2.9 Mathematical modelling of the transformation behaviour

Figures 4.1a-4.1d reveal how time and temperature control the transformation behaviour and therefore, the hardness of the experimental alloys. It was concluded that hardness, H varies linearly with time, t and can be represented by Eq.4.18

$$H = C_1 + C_2 t$$

The values of C_1 and C_2 were found to be different for

different temperatures, T and therefore, can be expressed as a function of temperature in the form of equations

$$C_1 = f(T) \qquad \ldots(4.23)$$

$$C_2 = f(T) \qquad \ldots(4.24)$$

The plots of C_1 vs T and C_2 vs T revealed that the C_2 vs T is linear and gives a relationship $C_2 = A_3 + A_4T$. However, the $\ln C_1$ vs 1/T plots indicated a linear behaviour and hence, the relation between C_1 and T can be expressed as :

$$\ln C_1 = \ln A_1 + A_2.1/T \qquad \ldots(4.25)$$

$$C_1 = A_1\, e^{A2/T} \qquad \ldots(4.26)$$

Substituting for C_1 and C_2 in the equation 4.25, the final relationship is

$$H = A_1.e^{A2/T} + (A_3+A_4T)t \qquad \ldots(4.27)$$

The constants A_1, A_2, A_3, A_4 were calculated for different alloys using the multivariable nonlinear constraint optimization technique (54,55). The final equations along with the overall standard deviations are reported below :

B_1 : $H = 168.213\, e^{1471.47/T} + (0.043-0.374\times10^{-4}T)t$

Overall SD = 27.05 ...(4.28)

B_2 : $H = 100.779\, e^{1889.66/T} + (0.026-0.223\times10^{-4}T)t$

Overall SD = 18.45 ...(4.29)

B_3 : $H = 98.285\, e^{2021.33/T} + (0.037-0.316\times10^{-4}T)t$

Overall SD = 29.87 ...(4.30)

B_4 : $H = 78.357\, e^{2205.77/T} + (0.027-0.244\times10^{-4}T)t$

Overall SD = 25.45 ...(4.31)

Where T = temperature in °K

t = time in seconds

H = hardness, HV_{30}

The theoretical hardness values calculated from the above equations were plotted against the corresponding experimental values and are shown in Figure 4.38. It reveals that barring a few instances, the calculated values are well within ±5%.

Contribution of the second factor

Heat-treatment	Contribution of the second factor			
	B1	B2	B3	B4
800 2 AC	23	12	21	9
800 4 AC	47	24	42	18
800 6 AC	70	36	63	28
800 8 AC	96	49	84	37
800 10 AC	117	61	101	47
850 2 AC	10	4	10	0
850 4 AC	20	8	21	1
850 6 AC	30	12	32	2
850 8 AC	40	16	42	2
850 10 AC	50	21	53	3
900 2 AC	-3	-3	0	-8
900 4 AC	-6	-7	0	-16
900 6 AC	-10	-11	0	-24
900 8 AC	-13	-15	0	-32
900 10 AC	-16	-19	1	-40
950 2 AC	-16	-11	-10	-16
950 4 AC	-33	-23	-20	-33
950 6 AC	-50	-35	-30	-50
950 8 AC	-67	-47	-40	-67
950 10 AC	-84	-59	-50	-83
1000 2 AC	-30	-20	-20	-25
1000 4 AC	-60	-40	-41	-51
1000 6 AC	-90	-60	-61	-76
1000 8 AC	-121	-80	-82	-102
1000 10 AC	-151	-100	-103	-127
1050 2 AC	-43	-28	-31	-34
1050 4 AC	-87	-56	-62	-68
1050 6 AC	-131	-84	-93	-102
1050 8 AC	-175	-112	-124	-136
1050 10 AC	-218	-140	-155	-171

It is observed that the constants A_1, A_2, and A_3 are positive for all the alloys. Hence their effect would be similar and additive. The constant A_4 is negative and therefore, its

effect needs to be analysed. This calls for assessing the contribution of second factor of the equation 4.27. Its values, as influenced by the heat-treating temperature and time are given below. As will be evident, the contribution of the factor becomes negative at temperatures higher than ≥900°C.

It will be seen that the contribution of this factor to the overall hardness varies linearly with time for a given h/t temperature.

The above discussion reveals that the term (A3 + A4.T)t has a significant impact on the overall hardness especially so when the alloys are heat-treated from 'higher' temperatures.

Because of a difference in the nature of the contribution of the second factor, as influenced by temperature, further calculations were made to find out the temperature at which the contribution of the aforesaid factor became negative. The change over occurred at 888, 877, 901 and 858°C in B1, B2, B3 and B4 respectively, which is in fact, the temperature representing the cross-over point (Section 4.2.6.2). This deduction is valid for all the alloys, duly remembering that the value of the COP would differ from alloy to alloy.

A further calculation revealed that the temperature corresponding to COP is a function of time as is evident from the following table.

In fact, in a strict sense, varying the soaking period will alter the profile of the hardness vs temperature plot as is evident from Figs. 4.1a to 4.1d. However, in spite of this happening, the COP (representing the point of inflexion) should

Effect of time on COP

Alloy	H/T time, hrs.	COP
B1	2	912
	4	924
	6	922
	8	908
	10	---
B2	2	---
	4	962
	6	955
	8	937
	10	930
B3	2	948
	4	950
	6	988
	8	948
	10	952
B4	2	958
	4	962
	6	960
	8	950
	10	914

have occurred at or over a narrow range of temperature, preferably the latter, because in heterogeneous alloys such as the present ones it is extremely difficult to visualize structural changes to occur at sharply delineated temperatures. The data summarized in the above table is thus consistent with this reasoning. It may be further observed that barring one or two instances the overall variation in COP with time for each of the alloy can be considered to be within ±2%.

When the values of COP summarized in the above table are compared with those observed on the basis of the model (their magnitude being 888, 877, 901, and 858°C respectively for B1, B2, B3, and B4), the apparent difference can be explained by stating that the discrepanceis may have arisen due to the assumptions/

simplifications made while developing the model. A more likely possibility is that whereas the equations represent transformations without reflecting upon their complexities, the actual situation is to the contrary due to heterogeneity of the system and also because a large number of phases are participating in the transformations.The lag between the 'ideal' and 'actual' situations can not be represented mathematically.

4.2.9.1 Physical interpretation of the proposed model

The data summarized in the four tables over-leaf, when viewed in the context of the structural changes already discussed, leads to certain important inferences. Firstly, the hardness is essentially controlled by the parameter $A_1e^{A2/T}$. This is independent of the matrix microstructure, i.e, independent of whether the matrix is martensitic, martensitic/austenitic, or simply austenite. As the amount of MC does not exceed 25%, the aforesaid factor can be considered as controlling the matrix microstructure. Recalling the basis on which the alloys are designed, it is easy to visualise why the matrix microstructure should be controlled by the temperature alone.

The contribution from the second factor, although less significant to start with, assumes prominence at higher temperatures and soaking periods. The parameter $(A_3 + A_4T)t$ can therefore, be said to represent the carbide transformation. At lower temperatures (≈800°C), its contribution is positive and increases with time (Vf of DC) because the particle size and distribution is appropriate in contributing to the strength. The correctness of this analysis is proved by the data obtained on heat-treating from 850°C, wherein the contribution has decreased

Relative contribution of the factors constituting the model

Alloy : B1

Heat-treatment		Overall hardness HV30	First factor Value	First factor %	Second factor Value	Second factor %
800	2 AC	685	662	96.6	23	3.4
800	4 AC	709	662	93.4	47	6.6
800	6 AC	732	662	90.4	70	9.6
800	8 AC	756	662	87.6	94	12.4
800	10 AC	779	662	85.0	117	15.0
850	2 AC	633	623	98.4	10	1.6
850	4 AC	643	623	96.9	20	3.1
850	6 AC	653	623	95.4	30	4.6
850	8 AC	663	623	94.0	40	6.0
850	10 AC	673	623	92.6	50	7.4
900	2 AC	586	589	99.5	-3	0.5
900	4 AC	583	589	99.0	-6	1.0
900	6 AC	579	589	98.3	-10	1.7
900	8 AC	576	589	97.7	-13	2.3
900	10 AC	573	589	97.2	-16	2.8
950	2 AC	544	560	97.1	-16	2.9
950	4 AC	527	560	93.7	-33	6.3
950	6 AC	510	560	90.2	-50	9.8
950	8 AC	493	560	86.4	-67	13.6
950	10 AC	476	560	82.4	-84	17.6
1000	2 AC	504	534	94.0	-30	6.0
1000	4 AC	474	534	87.3	-60	12.7
1000	6 AC	444	534	79.7	-90	20.3
1000	8 AC	413	534	70.7	-121	29.3
1000	10 AC	383	534	60.6	-151	39.4
1050	2 AC	468	511	90.8	-43	9.2
1050	4 AC	424	511	79.5	-87	20.5
1050	6 AC	380	511	65.5	-131	34.5
1050	8 AC	336	511	47.9	-175	52.1
1050	10 AC	293	511	25.6	-218	74.4

Relative contribution of the factors constituting the model

Alloy : B2

Heat-treatment		Overall hardness HV30	First factor Value	First factor %	Second factor Value	Second factor %
800	2 AC	598	586	98.0	12	2.0
800	4 AC	610	586	96.1	24	3.9
800	6 AC	622	586	94.2	36	5.8
800	8 AC	635	586	92.3	49	7.7
800	10 AC	647	586	90.6	61	9.4
850	2 AC	546	542	99.3	4	0.7
850	4 AC	550	542	98.5	8	1.5
850	6 AC	554	542	97.8	12	2.2
850	8 AC	558	542	97.1	16	2.9
850	10 AC	563	542	96.3	21	3.7
900	2 AC	502	505	99.4	-3	0.6
900	4 AC	498	505	98.6	-7	1.4
900	6 AC	494	505	97.8	-11	2.2
900	8 AC	490	505	96.9	-15	3.1
900	10 AC	486	505	96.1	-19	3.9
950	2 AC	462	473	97.6	-11	2.4
950	4 AC	450	473	94.9	-23	5.1
950	6 AC	438	473	92.0	-35	8.0
950	8 AC	426	473	89.0	-47	11.0
950	10 AC	414	473	85.7	-59	14.3
1000	2 AC	425	445	95.3	-20	4.7
1000	4 AC	405	445	90.1	-40	9.9
1000	6 AC	385	445	84.4	-60	15.6
1000	8 AC	365	445	78.1	-80	21.9
1000	10 AC	345	445	71.0	-100	29.0
1050	2 AC	393	421	92.9	-28	7.1
1050	4 AC	365	421	84.7	-56	15.3
1050	6 AC	337	421	75.1	-84	24.9
1050	8 AC	309	421	63.8	-112	36.2
1050	10 AC	281	421	50.2	-140	49.8

Relative contribution of the factors constituting the model

Alloy : B3

Heat-treatment		Overall hardness HV30	First factor Value	First factor %	Second factor Value	Second factor %
800	2 AC	664	643	96.8	21	3.2
800	4 AC	685	643	93.9	42	6.1
800	6 AC	706	643	91.1	63	8.9
800	8 AC	727	643	88.4	84	11.6
800	10 AC	748	643	86.0	105	14.0
850	2 AC	595	585	98.3	10	1.7
850	4 AC	606	585	96.5	21	3.5
850	6 AC	617	585	94.8	32	5.2
850	8 AC	627	585	93.3	42	6.7
850	10 AC	638	585	91.7	53	8.3
900	2 AC	537	537	100.0	0	0.0
900	4 AC	537	537	100.0	0	0.0
900	6 AC	537	537	100.0	0	0.0
900	8 AC	537	537	100.0	0	0.0
900	10 AC	538	537	99.8	1	0.2
950	2 AC	486	496	97.9	-10	2.1
950	4 AC	476	496	95.8	-20	4.2
950	6 AC	466	496	93.6	-30	6.4
950	8 AC	456	496	91.2	-40	8.8
950	10 AC	446	496	88.8	-50	11.2
1000	2 AC	441	461	95.5	-20	4.5
1000	4 AC	420	461	90.2	-41	9.8
1000	6 AC	400	461	84.8	-61	15.3
1000	8 AC	379	461	78.4	-82	21.6
1000	10 AC	358	461	71.2	-103	28.8
1050	2 AC	400	431	92.3	-31	7.8
1050	4 AC	369	431	83.2	-62	16.8
1050	6 AC	338	431	72.5	-93	27.5
1050	8 AC	307	431	59.6	-124	40.4
1050	10 AC	276	431	43.8	-155	56.2

Relative contribution of the factors constituting the model

Alloy : B4

Heat-treatment		Overall hardness HV30	First factor Value	First factor %	Second factor Value	Second factor %
800	2 AC	619	610	98.5	9	1.5
800	4 AC	628	610	97.1	18	2.9
800	6 AC	638	610	95.6	28	4.4
800	8 AC	647	610	94.3	37	5.7
800	10 AC	657	610	92.8	47	7.2
850	2 AC	557	557	100.0	0	0.0
850	4 AC	558	557	99.8	1	0.2
850	6 AC	559	557	99.6	2	0.4
850	8 AC	559	557	99.6	2	0.4
850	10 AC	560	557	99.5	3	0.5
900	2 AC	505	513	98.4	-8	1.6
900	4 AC	497	513	96.8	-16	3.2
900	6 AC	489	513	95.1	-24	4.9
900	8 AC	481	513	93.3	-32	6.7
900	10 AC	473	513	91.5	-40	8.5
950	2 AC	459	475	96.5	-16	3.5
950	4 AC	442	475	92.5	-33	7.5
950	6 AC	425	475	88.2	-50	11.8
950	8 AC	408	475	83.6	-67	16.4
950	10 AC	392	475	78.8	-83	21.2
1000	2 AC	417	442	94.0	-25	6.0
1000	4 AC	391	442	87.0	-51	13.0
1000	6 AC	366	442	79.2	-76	20.8
1000	8 AC	340	442	70.0	-102	30.0
1000	10 AC	315	442	59.7	-127	40.3
1050	2 AC	380	414	91.1	-34	8.9
1050	4 AC	346	414	80.3	-68	19.7
1050	6 AC	312	414	67.3	-102	32.7
1050	8 AC	278	414	51.1	-136	48.9
1050	10 AC	243	414	29.6	-171	70.4

with respect to what it was on heat-treating from 800°C due to coarsening. Its contribution, on heat-treating from 900°C is either negligible or marginally negative thereby signifying that the DC are virtually ineffective in influencing the hardness.

The negative contribution is seen to have a sizable effect only on heat-treating from upwards of 950°C, a temperature at which hardness begins to decrease with time. It is thus noteworthy that the negative contribution is assuming reasonable proportions just when the Vf of MC is beginning to decrease and the dispersed carbides are present in a state such that they cease to have an effect on the overall hardness. Therefore its magnitude will increase steeply (i) as the temperature is raised beyond 950°C and (ii) at higher soaking periods at a given temperature. The reasons for the negative contribution from this parameter, with an increase in temperature, have already been analysed in the Section 4.2.7. Therefore, the two parameters constituting the model are physically consistent with the attendant microstructural changes; the first term representing the matrix transformation and the second term the carbide transformation.

4.2.10 Mathematical modelling of the distribution factor

A critical analysis reveals that the DF can be mathematically represented with the help of the following equations :

$$B1: \quad 0.071\, e^{1377.542/T} + (0.047 - 0.591 \times 10^{-4}T)t \qquad ...(4.32)$$

$$B2: \quad 0.266\, e^{290.260/T} + (0.136 - 0.163 \times 10^{-3}T)t \qquad ...(4.33)$$

$$B3: \quad 0.224\, e^{444.033/T} + (0.073 - 0.917 \times 10^{-4}T)t \qquad ...(4.34)$$

$$B4: \quad 0.208\, e^{474.813/T} + (0.079 - 0.957 \times 10^{-4}T)t \qquad ...(4.35)$$

The basis of arriving at these equations is the same as the

one on which the mathematical modelling of the transformation behaviour of the alloys was carried out (Section 4.2.9). The theoretically calculated values of the DF agree well with the experimentally determined values, the maximum difference in a majority of the values being within ±5%.

4.2.11.1 3D plots representing interrelation amongst temperature, time and hardness

Till now the effect of heat-treatment on the hardness has been analysed on the basis of varying one of the parameters while keeping the other a constant. This has been represented in Figs. 4.1 to 4.6. Although, these plots provided useful and necessary explanations of the transformation behaviour, they failed to provide the overall effect of heat-treatment at a glance.

This difficulty was resolved by constructing 3-dimensional plots (Figs. 4.39-4.42) using the equations 4.28 to 4.31, at rotation angles 45° and 225° around the Z-axis and at a tilt angle of 30°. For each of the alloy Fig (a) represents the gradual change in the slope of the hardness vs time plots as influenced by temperature which are represented over a surface.

The Fig (b) clearly reveals that the so called COP is not a sharply delineated temperature but that the change over is occurring over a narrow dark region represented by a surface.

A comparison of the Figs (a) for the experimental alloys further brings out that the change in slope between hardness vs temperature/time is generating a common surface which has been depicted in Figs (b). The 3-D plots reaffirm the similarity between B1 & B3 (having marked darkened surface region due to a steep profile of the hardness vs temperature plots) and that

between B2 & B4 (not exhibiting a marked surface region due to the flatter profile of the hardness vs temperature plots).

4.2.11.2 Iso-hardness plots

Iso-hardness plots were made by plotting out hardness (as influenced by temperature and time) as contours (Figs.4.43-4.46). Evdently, the hardness is a constant along a contour and as such it would be possible to determine the different temperature and time combinations (from the plot) to get a desired hardness. The variation in hardness is marked in the alloy B1 and gradual in the alloy B2. This behaviour is in accordance with the expected behaviour of the alloy B2 which can sustain hardness over a longer range of h/t time and temperature. The existence of more widely spaced contours in alloy B2 indicates that there is a greater flexibility, in terms of temperature & time, in attaining a desired level of hardness i.e. to say that a given hardness will be attained comfortably even if an inadvertent error were to be committed in controlling temperature & time.

4.3 Conclusion

This chapter has dealt at length with the transformation behaviour of the experimental alloys characterized on the basis of hardness measurements and the attendant microstructural changes. A detailed analysis of the latter proved extremely helpful in arriving at a qualitative understanding of the interrelation between microstructure and properties. The behaviour of the second phase particles as influenced by heat treating schedule has been mathematically represented by evolving a parameter called the 'distribution factor'. This enables

calculation of the coarsening behaviour of the second phase particles on the basis of a parameter called as the 'coarsening index'. The evolution of these parameters has proved extremely helpful in overcoming the limitations of the Ostwald's ripening formula which is regarded as the sole basis for characterizing the coarsening behaviour of the second phase particles. The development of these models has proved useful in establishing models interrelating properties with the microstructure. This has been discussed in Chapter VI.

Finally mathematical models have been developed interrelating hardness with the heat-treating temperature and time (microstructures). It has been established that the parameters constituting the model are physically consistent with the structural changes occurring on heat treating.

Although much has been said about the characterization of different phases, the presence of martensite could not be unequivocally established in marginal cases. Similarly, the nature and types of carbides remained unidentified. Therefore, a detailed study comprising X-ray diffractometry and EPMA was carried out. The data thus obtained have been discussed in the next chapter.

CHAPTER V

TRANSFORMATION BEHAVIOUR OF THE ALLOYS

5.1 Structural analysis by X-ray diffractometry

The as-cast, as well as the heat-treated (900°C upwards) specimens of the four alloys were extensively examined by X-ray diffractometry to identify/confirm (i) the nature of matrix microstructure, and (ii) the nature of different carbides that formed during heat treatment. The analysis of the X-ray diffractograms has been summarized in the Tables 5.1 to 5.41 and Figures 5.1 & 5.2. A summary table (Table 5.42) has also been prepared to make the discussion more concise. With the help of diffraction data, it was possible to interpret the structures more or less fully as would be evident from the ensuing data and its analysis.

5.1.1 Results

5.1.1.1 As-cast condition

The microconstituents commonly observed in the four alloys consisted of P/B + M_3C (isomorphous with Fe_3C) + M_7C_3 (isomorphous with Cr_7C_3). Some M_5C_2 was also present. Additionally, Fe_8Si_2C was also indexed in alloys B2, B3, and B4. Lower angle peaks corresponding to α/M were observed in all the alloys. However, the higher angle peaks characterizing martensite were present only in B3.

5.1.1.2 Heat-treated condition

On heat-treating, there was a general shift in the diffraction angles of different micro-constituents present, compared with their standard 2θ-values, obtained from the diffraction data

cards (Tables 5.2- 5.41). The effect of heat-treating temperature and time on the possible transformations occurring within the matrix and the carbides, along with any additional features that were observed, have been discussed below.

5.1.1.2.1 Effect of heat-treatment on the matrix microstructure

On heat-treating (temperatures ≥900°C), the following changes were observed in the matrix microstructures :

(i) The matrix essentially comprised austenite. Lower angle peaks corresponding to ferrite/martensite were also present (Since there is no possibility of free ferrite being present, they can be considered as representing the possible presence of martensite).

(ii) Possible presence of martensite was indicated in B1, B3 & B4 corresponding to the 900°C heat-treatment. However, its presence was not clearly established in B2.

(iii) On heat-treating from 950°C, some martensite still persisted in B1, but not in B2, B3, & B4.

(iv) On heat-treating from higher temperatures the matrix in all the alloys was austenitic.

(v) An important observation is that the 2θ-values for austenite were shifted with respect to the standard 2θ-values. This shift was minimum in B1, slightly higher in B2 and marked in B3 and B4.

5.1.1.2.2 Effect of heat-treatment on the nature of carbides

On heat-treating, a clear cut carbide transformation sequence was observed. However, the main difference was with regard to their stability as influenced by heat-treating temperature and the alloy content.

(i) On heat-treating from 900°C, in addition to M_3C, the formation of $M_{23}C_6$ type of carbide was indicated in all the alloys at both the soaking periods.

(ii) Simultaneously, formation of M_5C_2 was also indicated, whose indexing in B3 and B4 was more distinct in comparison to that observed in B1 and B2. A similar situation persisted even on altering the soaking period.

(iii) On heat-treating from 950°C, the indexing of $M_{23}C_6$ became less marked but that of M_3C more distinct. On raising the soaking period to 10 hours, $M_{23}C_6$ was present in only small yet comparable proportions in B1 and B3, in still lesser proportions in B4 and in traces in B2. As in (ii) above, M_5C_2 was also present on heat-treating from 950°C.

(iv) On raising the heat-treating temperature to 1000°C, the presence of $M_{23}C_6$ was not detected in B2 and B3, whereas it was present in traces in B1 and B4 only at the lower soaking periods. Indexing of M_3C revealed its presence only in small amounts which was reduced to traces at higher soaking periods. The M_5C_2 carbide was present only in traces but persisted even at the higher soaking periods.

The additional carbide to form at 1000°C is M_7C_3 whose indexing was confirmed at 10 hours soaking period. It was more distinctly indexed in B3 and B4 in comparison to that in B1 and B2. Thus the overall position of carbides at 1000°C is

B1 : M_3C

B2 : $M_3C + M_5C_2$

B3 : $M_3C + M_7C_3 + M_5C_2$(traces)

B4 : $M_7C_3 + M_3C$(some) $+ M_5C_2$(traces)

(v) On heat-treating from 1050°C, M_7C_3 was the dominant carbide present, with M_5C_2 present only in traces. The latter carbide was not observed at higher soaking periods.

Thus the carbide transformation sequence observed is

M_3C	present upto 1000°C, 4 hours
$M_{23}C_6$	present upto 950°C, 4 hours & at best in traces upto 950°C, 10 hours
M_5C_2	present upto 1000°C,10 hours/ 1050°C, 4 hours
M_7C_3	present from 1000°C, 10 hours to 1050°C, 10 hours

5.1.1.2.3 Other features

(a) Elemental copper :

Copper was indexed in the as-cast condition and corresponding to the high temperature treatments(1000 & 1050°C) at both the soaking periods especially in B3 and B4.

(b) Fe_8Si_2C:

It was invariably indexed at all the heat-treatments.

(c) $CrMn_3$:

It was present on heat-treating from lower temperatures (900 and 950°C) [The needle like feature observed through optical metallography may be due to the presence of this constituent since inter-metallics are known to have a needle like appearance.

5.1.2 Discussion

5.1.2.1 Matrix microstructure

A summary of the findings concerning the matrix microstructure

has been presented in the Section 5.1. In the present study, the alloys were primarily designed to attain martensitic microstructure on air cooling from low temperatures (upto 850°C) and austenitic microstructure on heat-treating from higher temperatures. This has been explained in detail on the basis of the equations 4.8 to 4.16 which duly support this contention. This is further borne out by the optical metallographic studies on the as-cast as well as on the heat treated specimens (Section 4.1.2). The x-ray observations duly confirm these findings in a majority of instances. There are certain deviations, however, which need a closer examination. For example, on heat-treating from 900°C, there was a suspicion that some martensite may be present at least in alloys B1 & B3 at all soaking periods on the basis of optical metallography. The x-ray observations duly confirm this to be so. Additionally, they also indicate the possible presence of martensite in B4 but not in B2. This is not clearly understood. Since, the Mn content of both B2 & B4 is the same and B4 in addition contains a higher proportion of Cu, this alloy(B4) was not expected to attain martensitic structures especially so since its counterpart with reduced Cu content does not attain martensite.

On heat-treating from 950°C, 4 hours soaking period, the possibility of some martensite forming is once again indicated in alloys B1 & B3 based on optical metallographic observation. The X-ray results, while confirming this to be so in B1 clearly indicate its absence in the other three alloys. Thus the x-ray findings while satisfactorily reaffirming some of the findings

based on optical metallography have also resolved some of the ambiguities. No comment is being made regarding the possible deductions on heat-treating from 1000 & 1050°C because there was no ambiguity based on optical metallographic observations. In fact the observations based on X-ray diffraction and optical metallographic studies are in complete agreement.

X-ray studies have not proved conclusive in establishing the possible presence of martensite in alloys B1 & B2 and in confirming austenite retention at least in B2 & B4 in the as-cast condition. Whereas hardness values and optical metallography do indicate the possible presence of martensite in all the alloys, the reason why x-ray analysis is not helpful on this score is that the ferrite peaks, constituting P/B, may have coincided with the intensity peaks resulting from the presence of martensite. A somewhat similar analysis may point to the inadequacy of the technique in clearly detecting retained austenite as the carbide peaks may have merged with the austenite peaks.

When the above analysis is considered along with the various inferences arrived at based on optical metallographic studies, it can now be stated that the present set of alloys have fully responded to the generation of different microstructures on heat treating based on the possible utilization of a minimum yet optimum amount of alloying elements - a key feature of alloy design as formulated in Chapter II in Section 2.1. This would be evident from the summary tables given on the next page.

Summary table of the matrix microstructure as influenced by the heat treatments analysed through optical metallography

h/t schedule	Alloy B1	B2	B3	B4
As-cast	P/B + M	B/M + RA	B/M + RA?	B/M + RA
900°C, 4 hrs.	A + M?	A	A + M?	A
900°C, 10 hrs.	A + M?	A	A + M?	A
950°C, 4 hrs.	A + M?	A	A + M?	A
950°C, 10 hrs.	A + M?	A	A + M?	A
1000°C, 4 hrs.	A	A	A	A
1000°C, 10 hrs.	A	A	A	A
1050°C, 4 hrs.	A	A	A	A
1050°C, 6 hrs.	A	A	A	A
1050°C, 10 hrs.	A	A	A	A

Summary table of the matrix microstructure as influenced by the heat treatments analysed through x-ray

h/t schedule	Alloy B1	B2	B3	B4
As-cast	P/B	P/B	P/B + M	B/M
900°C, 4 hrs.	A + M?	A	A + M?	A + M?
900°C, 10 hrs.	A + M?	A	A + M?	A + M?
950°C, 4 hrs.	A + M?	A	A	A
950°C, 10 hrs.	A	A	A	A
1000°C, 4 hrs.	A	A	A	A
1000°C, 10 hrs.	A	A	A	A
1050°C, 4 hrs.	A	A	A	A
1050°C, 6 hrs.	A	A	A	A
1050°C, 10 hrs.	A	A	A	A

5.1.2.2 Carbide transformation

Based on an analysis of the observations contained in Section 5.1.1.2 (Table 5.2-5.41 and summary Table 5.42), it is evident that the general carbide transformation sequence in the present study is as follows:

Carbide transformation	Stability range
M_3C + some $M_{23}C_6$ + (M_5C_2? + M_7C_3?)	(As-cast state)
↓	
M_3C + larger amount of $M_{23}C_6$ + (some M_5C_2 + M_7C_3?)	(upto 950°C)
↓	
M_3C (reduced content) + M_5C_2 + $M_{23}C_6$ (reduced content) + (M_7C_3?)	(upto 1000°C; lower SP)
↓	
M_5C_2 + M_7C_3 + M_3C (at best in traces)	(upto 1000°C; higher SP)
↓	
M_5C_2 + M_7C_3 (some amount)	(upto 1050°C;lower SP)
↓	
M_7C_3	(upto 1050°C ; higher SP)

A study of the Fe-Mn-C and Fe-Cr-C ternary diagrams reveals that M_7C_3, M_5C_2 and $M_{23}C_6$ are essentially high temperature carbides with the last mentioned having a relatively lower dissolution temperature/thermal stability as compared with the first two(66). Further, the predominant carbide would be M_3C. Accordingly, the carbide expected to be present in the as-cast

state should be M_3C as this is the stable form at room temperature. The possible presence of higher temperature forms of carbides can be explained by stating that because of the complexity of the alloy system under study, the different high temperature carbides have not fully transformed successively to their lower temperature forms due to the reactions being sluggish resulting in the former being retained in smaller amounts even in the as-cast condition.

This contention is borne out by the fact that on heat-treating from 900°C, the predominant carbides are only M_3C & $M_{23}C_6$, whereas the detection level of the other two carbides is either negligible (as for example M_7C_3) or in traces (as for example M_5C_2). Thus, whatever M_7C_3 carbide was present in the as-cast state has participated in the carbide transformation. Only traces of M_5C_2 remain primarily because M_5C_2 is a more stable carbide (i.e. sluggish in transforming, perhaps, because of its monoclinic crystal structure). Therefore, the effective transformation sequence under review is M_3C + $M_{23}C_6$ + higher forms of carbides --> M_3C + increased amount of $M_{23}C_6$.

5.1.2.2.1 The $M_{23}C_6$

This carbide was positively indexed upto 900°C, 10 hours heat-treatment in all the alloys and upto 950°C, 10 hours heat-treatment in traces in B1 and B4(Table 5.42). Its possible formation and location has been a subject matter of some discussion(67-76). Through successive etching with special etching reagents and techniques, its formation along prior austenite grain boundaries has been unequivocally

demonstrated(77). This observation is consistent with an earlier finding wherein it was suggested that $M_{23}C_6$ may be present at the grain boundaries(67-73,78) or within grains in the form of fine precipitates(74,79). In the present alloys, both Cr and Mn can form this carbide ($Cr_{23}C_6$, $Mn_{23}C_6$), but the formation of $Mn_{23}C_6$ is preferred as Mn is placed ahead of Cr in the periodic table(80). Hence the tendency to form cubic carbide $Mn_{23}C_6$(81-83). In the present study, $M_{23}C_6$ has been found to be isomorphous with $Mn_{23}C_6$. The possible presence of this carbide at the grain boundaries and adjoining areas can be explained by stating that alloying element atoms in general and Mn atoms in particular have a tendency to segregate at grain boundaries giving rise to the formation of this carbide(82).

5.1.2.2.2 The M_3C

This carbide (in massive/platy form) was present upto 950°C definitely and even upto 1000°C in traces. It was found to be isomorphous with Fe_3C, although small amounts of Mn and Cr were also present in it as confirmed through EPMA (Table 5.43-5.44). This in fact made the Fe_3C little more stable(84) otherwise it might have dissolved/transformed at relatively lower temperature(s) and soaking period(s). On the other hand the presence of Cu in the alloys (although not partitioning to Fe_3C) has an opposite effect and therefore, the dissolution of this carbide was enhanced. Further, it appears that the phasing out of M_3C is in some way linked with the formation of M_7C_3 (Table 5.42). Whether this occurs singly or associated with the formation/ disappearance of $M_{23}C_6$ carbide needs to be looked at carefully. The suggestion is worthy of consideration since

formation and subsequent phasing out of $M_{23}C_6$ will generate a large amount of metal atoms. This aspect has received little attention and can form the basis of a useful future study in the experimental alloys.

5.1.2.2.3 The M_7C_3

This carbide was present in the as-cast condition and on heat-treating from higher temperatures. It may be Cr based [(Cr_7C_3), Fe (Fe_7C_3)], or Mn based (Mn_7C_3), but Cr_7C_3 is the only carbide to form singly. Others namely Fe_7C_3 or Mn_7C_3 are always present in combination as $(Cr,Fe)_7C_3$, $(Fe,Cr)_7C_3$, or $(Cr_7C_3+Mn_7C_3)$ etc(85). In the present study the carbide formed was a mixed carbide of Fe, Cr & Mn (Table 5.44) with a preponderance of Fe & Cr atoms (Table 5.44).

The formation of M_7C_3 has been the subject of a number of studies and its mechanism of formation from M_3C has been described as (i) in-situ(86-92), (ii) combination of in-situ and separate nucleation(93,94) and (iii) also as separate nucleation(95). In the present alloys, it appeared to form in-situ (Figs. 4.14, 4.20, 4.26 & 4.32) preferentially at grain boundaries and regions adjoining it (described as eutectic carbide in Section 4.1.2.) corresponding to 1050°C heat treatments. Since the formation of M_7C_3 carbide has been unequivocally established corresponding to 1000°C, 10 hours heat treatments coinciding with phasing out of M_3C, it is likely that the nucleation of M_7C_3 may be favoured at M_3C-matrix interface. However, since the location of M_7C_3 is in the close vicinity of the grain boundaries, it appears more logical to conclude that it

with the data observed from the Fe-Cr-C and Fe-Mn-C ternary systems(66). This being so it appears that a part of the dispersed carbide formed especially beyond 6 hours of holding period should correspond to the presence of M_5C_2(96). A further perusal of this table revealed that either the decrease in the volume fraction of dispersed carbide with time at 950°C is too small/ negligible or the volume fraction of the dispersed carbide initially decreases with soaking period upto 6 hours and thereafter increases on further raising the soaking period to 10 hours (Table 4.53). Both these observations in a nut shell reveal that some new carbide is definitely forming and it would not be incorrect to deduce that this is in fact M_5C_2. Further, a carbide such as the one presently under consideration i.e. forming through a precipitation process by ageing of austenite at 950°C is more likely to be of a dispersed type (excluding the possible formation of a specific type of grain boundary carbide such as the $M_{23}C_6$ whose formation has already been discussed and explained). Hence at least a part of the dispersed carbide is of the type M_5C_2. This can be established unequivocally only through selective etching technique.

5.1.2.2.5 Fe_8Si_2C

After exhausting most of the possibilities of indexing diffractograms, some peaks remained unindexed. One of the possible options considered was the presence of the aforesaid phase. From the Tables 5.2-5.41, it can be observed that this phase is indexed in all the alloys corresponding to 1000°C, 4 hrs. to 1050°C, 4 hrs. heat-treatments. Other than this no

further comment is being made as to its mechanism of formation and the morphology it assumes.

5.1.2.2.6 Presence of elemental Cu and other phases

The possible presence of Cu in the as-cast alloys is understandable because although the solubility of Cu in austenite is large, its solubility in ferrite is a maximum (≈1.5%) close to the eutectoid temperature and diminishes steeply with temperature(97). Of the two sets of alloys, presence of free Cu is more likely to be detected in the higher Cu containing alloys namely, B3 and B4 as compared with B1 and B2. The x-ray observations (Table 5.2-5.41) confirmed this to be so.

Another possibility of Cu being present is when the heat treating temperature is 1050°C - a temperature close enough to the melting point of Cu(98). Information summarized in the Table 5.42 confirms this finding.

After considering all possibilities, some reflections still remained unindexed. It was observed that this problem could be partly resolved by considering the formation of $CrMn_3$ and Cu_2S phases. The possibility of the formation of inter-metallics such as $CrMn_3$ is more on heat-treating from higher temperatures. The formation of Cu_2S is feasible in all the alloys perhaps more in the higher Cu containing alloys wherein the possibility of having free Cu to enable the formation of Cu_2S is larger. It is suggested that a more detailed investigation is required to confirm the presence of phases such as $CrMn_3$ and Cu_2S etc. in future studies.

5.2 Electron probe micro analysis results

This was carried out on the experimental alloys to ascertain (i) distribution of the major alloying elements into the matrix and the carbide phase and (ii) the manner in which the distribution was affected by heat treating/alloying. The EPMA data are reported in the Tables 5.43-5.44. Additionally, concentration profiles for Fe, Cr, Mn, Si, Cu and C (Fig. 5.3-5.5) and X-ray images for the above elements (Fig. 5.6-5.11) have also been provided.

A perusal of the above tables and figures revealed that the distribution of Cr, Mn and Cu into the matrix and the carbide phase was influenced by an increase in the alloy content and heat treating parameters. This is more effectively demonstrated with the help of the data summarized in the Tables A & B.

The abovesaid data (Tables A & B) were further rationalized by taking into account the volume fraction of different constituents and the results thus obtained are summarized in the Tables C & D. This provided additional information on the overall distribution of the alloying elements into the matrix and the carbide phases.

Table- A Element distribution in matrix and carbide (950°C, 10 Hrs., AC)

Alloy	Concentration,%					
	Matrix			Carbide		
	Cr	Mn	Cu	Cr	Mn	Cu
B1	1.20	4.61	2.11	10.11	8.51	0.04
B2	1.55	5.94	2.02	12.06	10.17	0.09
B3	---	---	----	11.56	8.06	0.15
B4	---	---	---	11.02	9.53	0.10

Table- B Element distribution in matrix and carbide (1050°C, 10 Hrs., AC)

Alloy	Concentration,%					
	Matrix			Carbide		
	Cr	Mn	Cu	Cr	Mn	Cu
B1	3.20	5.91	1.37	22.95	9.65	0.04
B2	2.98	7.00	1.69	23.30	10.47	0.00
B3	2.60	5.79	3.19	27.02	9.70	0.00
B4	2.09	8.54	5.19*	23.83	10.66	0.03

* Apparently anomalous

The data contained in the Tables A & B and the rationalized Tables C & D, is discussed as follows.

Table- C Element distribution in matrix and carbide based on their volume fractions (950°C, 10 Hrs., AC)

Alloy	Concentration,%					
	Matrix		Platy carbide		Dispersed carbide*	
	Cr	Mn	Cr	Mn	Cr	Mn
B1	0.78	2.91	2.93	2.47	0.57	0.48
B2	1.03	3.83	2.94	2.48	1.11	0.94
B3	---	---	3.92	2.73	0.87	0.60
B4	---	---	2.72	2.35	1.02	0.89

Table- D Element distribution in matrix and carbide based on their volume fractions (1050°C, 10 Hrs., AC)

Alloy	Concentration,%			
	Matrix		Carbide	
	Cr	Mn	Cr	Mn
B1	2.99	5.53	1.47	0.62
B2	2.70	6.52	1.58	0.71
B3	2.39	5.37	1.95	0.70
B4	1.92	6.93	1.92	0.86

* Assuming the overall partition ratio to be the same in the two carbides i.e. platy (massive) and the dispersed carbides.

5.2.1.1 Partitioning of the alloying elements into the matrix and the carbide phases

The abovesaid partitioning will depend upon their nature i.e. whether an element is an austenite stabilizer or a carbide former. An effective way to represent this would, therefore, be by estimating the partition ratio of elements into the carbide and the matrix phases. The data thus estimated, as influenced by heat treating is shown in the Tables E & F.

Table- E Element concentration ratio at 950°C, 10 hrs.

Alloy	C_{Cr} in carbide* / C_{Cr} in matrix	C_{Mn} in carbide* / C_{Mn} in matrix
B1	8.43	1.85
B2	7.78	1.71

* Denotes platy/massive carbide

Table- F Element concentration ratio at 1050°C, 10 hrs.

Alloy	C_{Cr} in carbide / C_{Cr} in matrix	C_{Mn} in carbide / C_{Mn} in matrix
B1	7.17	1.63
B2	7.82	1.50
B3	10.39	1.68
B4	11.40	1.25

A perusal of all the above tables revealed that :

Mn

(i) At 950°C, 10 hours heat treatment the percentage of Mn distributing into the matrix phase is approximately half of that present in the carbide phase (Table A).

(ii) However, after taking into consideration the relative volume fraction of the different constituents, it is seen

that the percentage of Mn distributing into the matrix and the carbide phases is approximately the same (Table C).

(iii) On raising the temperature to 1050°C, the percentage of Mn distributing into the matrix and the carbide phases is approximately in the ratio of 1:1.5 (Table B).

(iv) However, after correcting for the volume fraction, this ratio worked out to be approximately 8-9:1 (Table D).

(v) Since the volume fraction of the carbide phase at 1050°C is very small, the overall Mn in the carbide is small(Table D).

(vi) There is only a slight increase in the Mn content in the carbide on raising the temperature(Table A & B).

(vii) The amount of Mn distributing into the carbide phase in both the lower and the higher Cu alloys appeared to be a little higher than can be expected from an austenite stabilizing element (Table E & F).

Cr

(i) At 950°C, 10 hours heat treatment the percentage of Cr in the carbide to that in the matrix is approximately in the ratio of 8.5:1 (Alloys B3 and B4 are not considered) (Table F).

(ii) However, after correcting for the volume fraction, the ratio of Cr in the carbide to that in the matrix is 3.5-4:1 (Table C).

(iii) On heat treating from 1050°C, the percentage of Cr distributing into the carbide and the matrix phase is in the ratio of 7-7.5:1 in B1 & B2 and 11-12:1 in B3 & B4 (Table G).

(iv) However, taking into consideration the volume fraction of different constituents, these ratios work out to be 1:2 in B1 & B2 and 1:1-1.25 in B3 & B4 (Table D).

(v) Although, the overall amount of Cr distributing into the carbide is apparently small due to a reduced carbide volume fraction, it is none the less approximately 2.5 times higher than corresponding Mn distribution(Table B & D).

Cu

(i) Bulk of the Cu is partitioning to the matrix phase (Table A & B).

(ii) At lower heat treating temperature, the amount of Cu in the matrix is about 2.0% in the lower Cu alloys (Table A).

(iii) On raising the heat treating temperature, the amount of Cu in the matrix has reduced to ~1.4-1.7% in the lower Cu alloys whereas, in the higher Cu alloys its level is approximately approaching the amount in which it is present.

(iv) Barring one instance and after rationalizing for volume fraction, the overall Cu distribution appears reasonable (Table A & B).

5.2.1.2 Effect of Mn on Cr distribution

This is effectively demonstrated with the help of the Tables G & H which represent the partitioning of elements into the matrix and the carbide phases as influenced by Mn content. Its perusal revealed that

(i) Increasing the Mn content is promoting a larger partitioning of Cr both into the carbide and the matrix at lower temperature (B1 and B2).

Table- G Concentration ratio at 950°C, 10 Hrs., AC heat-treatment

Alloy	Concentration ratio of element	Matrix	Carbide
B1 & B2 (1.5% Cu)	$C_{Cr}{}_{B2}/C_{Cr}{}_{B1}$	1.29	1.19
	$C_{Mn}{}_{B2}/C_{Mn}{}_{B1}$	1.29	1.20
B3 & B4 (3.0% Cu)	$C_{Cr}{}_{B4}/C_{Cr}{}_{B3}$	----	0.96
	$C_{Mn}{}_{B4}/C_{Mn}{}_{B3}$	----	1.18

Table-H Concentration ratio at 1050°C, 10 Hrs., AC heat-treatment

Alloy	Concentration ratio of element	Matrix	Carbide
B1 & B2 (1.5% Cu)	$C_{Cr}{}_{B2}/C_{Cr}{}_{B1}$	0.93	1.02
	$C_{Mn}{}_{B2}/C_{Mn}{}_{B1}$	1.18	1.08
B3 & B4 (3.0% Cu)	$C_{Cr}{}_{B4}/C_{Cr}{}_{B3}$	0.80	0.88
	$C_{Mn}{}_{B4}/C_{Mn}{}_{B3}$	1.47	1.10

(ii) However, on raising the heat treating temperature to 1050°C, Cr partitioning (due to a higher Mn content) into both the carbide and the matrix phases was no more preferential, however, its amount in the matrix was somewhat reduced (Table G & H) [Alloys B1 & B2].

(iii) However, for the higher Cu alloys Mn is reducing the Cr distribution into the carbide (remaining unchanged if corrected for volume fraction) (Table G & H) [≈1050°C heat treatment]. At the lower heat treating temperature Mn is not influencing Cr partitioning into the carbide.

(iv) There is a definite reduction in the Cr content within the matrix (Mn is playing its customary role as austenite

Table- I Percentage variation in the element concentration between the two heat-treatments

Alloy	Variation, %					
	Matrix			Carbide		
	Cr	Mn	Cu	Cr	Mn	Cu
B1	167	28	-35	127	13	---
B2	92	18	-16	93	3	---
B3	89*	12*	----	134	20	---
B4	52*	62*	---	116	12	---

(ii) The percentage increase is very high with regard to Cr (particularly for lower Mn alloys, B1 & B3) as compared to percentage increase in Mn which is marginal (in the carbide) to moderate (in matrix).

5.2.2 DISCUSSION

The EPMA data which has been critically represented in the above sections needs to be carefully analysed to derive useful inferences regarding partitioning and its consequent impact on alloy design. Although a more extensive EPMA work would have been beneficial, none the less the limited experiments performed can serve as a basis for arriving at useful conclusions.

The primary interest in such studies centres around basic partitioning and as Mn is being given primacy, the initial interest would centre around it. The partition ratio, $Mn_{carbide}/Mn_{matrix}$ in the present study has varied from ≈1.5 to ≈1.8. This appears to be in fair agreement with an earlier study conducted by Singh(99) in which this partition ratio was found to be ≈1.5:1. The difference, however, is that whereas in the latter the heat treating temperatures did not exceed 850°C, they

(temperatures) have been relatively higher in the present study. This in itself can account for the slightly larger partition ratios obtained.

The important implications of these observations is that although Mn is considered to be an austenite stabilizer (implying a large partitioning into austenite), in the true sense its known carbide forming tendency pushes a fair proportion of it into the carbide phase. This is further made apparent when partitioning of a conventional austenite stabilizer like Ni is considered (based on data reported by Sandoz(100). Therefore, the amount of Mn is to be suitably increased to ensure that the requisite amount of Mn is available in austenite.

If the partition ratio of Mn is considered after correcting for volume fraction of different phases then at the lower of heat treating temperature the effective partition ratio is 1:1 which reduces to ≈0.11 to 0.12:1 on raising the temperature to 1050°C. The former suggests a general evening out of the partitioning at lower temperatures. However, since this data still implies that a much larger proportion of Mn is partitioning to carbide than expected, the earlier inference with regard to incorporating a larger Mn content still holds. The marked decrease in Mn concentration in the carbide can be explained by stating that the volume fraction of carbide at the higher temperature is negligible.

Talking about Cu partitioning it is seen that bulk of the Cu partitions into the matrix. This is to be expected because of its inherent tendency as austenite stabilizer and negligible carbide stabilizing tendency. On raising the heat treating temperature,

the amount of Cu in the carbide is negligible. This is again as per expectations and consistent with the behaviour of other graphitizing elements Ni and Si, which are essentially found in the matrix. It may, however, be remembered that the graphitizing tendency of Cu is not as marked as that of Ni or Si. Therefore, if Cu is being utilized to affect graphitization then it would be effective only a higher temperatures.

In so far as Cr partitioning is concerned, the partition ratio $Cr_{carbide}/Cr_{matrix}$ is ≈8:1 at lower temperature which is consistent with its known carbide forming tendency. However, on raising the heat treating temperature to 1050°C, the ratio is varying from ≈7 to 10 in the lower Mn alloys and from 8-11 in the higher Mn alloys. This is to say that higher Mn and higher Cu concentrations are ensuring a larger Cr partitioning into carbide. This is consistent with the fundamental considerations since both Mn and Cu will partition to matrix thus releasing Cr to partition to the carbide phase.

Having thus discussed the general partitioning pattern, it would now be appropriate to comment upon the nature of the carbide. The observation that approximately equal amounts of Mn and Cr partition to the carbide phase reveal that the carbides formed are mixed Fe, Mn, Cr type. This would mean that $M_{23}C_6$, M_3C and whatever M_7C_3 carbide is present are triple carbides. However, this can not be so for a M_5C_2 type carbide since only Fe and Mn form such carbides. Since it has been suggested that M_5C_2 is in fact a dispersed carbide, quite clearly the triple carbide deduction is not valid for this type of carbide. This is further

evident from the fact that our observations are mostly confined to the massive carbide and that more detailed EPM analysis is required on the dispersed carbides as well as on other carbides to clearly earmark regions representing the M_5C_2 carbides.

On raising the temperature to 1050°C, it is observed that the total Mn and Cr concentration in the carbide has increased from about 18-20% (observed at 950°C heat treatment) to about 31-36%. Since in a majority of the instances the higher temperature carbide is M_7C_3 type and since all the three elements Fe, Mn, Cr are known to form this carbide, the concentration of the elements is bound to be larger than what was observed on heat treating at 950°C.

Finally it becomes incumbent to comment upon the influence of one element on the partitioning of the others into different phases. The effect of Mn on Cu partitioning suggests no special preference on heat treating at 950°C while heat treating at 1050°C, the partitioning of Cu is more in the higher Mn alloys. This is consistent with the austenite stabilizing nature and normal affinity of Mn and Cu for one another especially when the microstructure is predominantly austenitic. Mn appears to promote larger partitioning of Cr both into the matrix and the carbide at lower temperature but not so at higher temperature. This is equivalent to saying that at higher temperature Mn and Cu together are playing a dominant role than Cr due to the microstructure being mainly austenitic.

Considering now the effect of Cu on the partitioning of Mn, it is seen that the effect on Mn partitioning is marked only at higher temperatures. Increased Mn levels both in the matrix and

in the carbide is an indication that Cu is promoting Mn to perform its customary function. A somewhat similar effect is observed on Cr partitioning; in fact, expectedly the amount of Cr in the matrix appears reduced thereby further confirming that Cu is promoting Cr to perform its usual function of forming/stabilizing the carbide.

5.3 Thermal analysis

Differential thermal analysis work comprised (i) assessment of the critical/transformation temperatures, and (ii) thermogravimetric studies, inclusive of modelling, carried out to a limited extent. The data thus obtained have been summarized in the Tables 5.45-5.46 and in the Figures 5.12-5.15. Results have been discussed in the following sections.

5.3.1 Results

5.3.1.1 Critical/transformation temperatures

(i) First set of transformations occurred in all the alloys between 722-750°C (Table 5.45).

(ii) The second set of transformation(s) similarly occurred in the temperature range of 890-955°C (Table 5.45).

(iii) A third set of transformations, observed only in B2 and B4, occurred between 1050-1075°C (Table 5.45).

5.3.1.2 DTA

(i) For the first transformation, DTA values were positive for alloys B1 and B3 (ranging from 0.2 to 0.35mV) and negative for the alloys B2 and B4 (ranging from -0.85 to -0.90mV)[Table 5.46].

(ii) For the second set of transformation(s), DTA values were negative; however, similarity between B1 and B3 (-0.52 to -0.70mV) and that between B2 and B4 (-2.15 to -2.65mV) still persisted(Table 5.46).

(iii) The third set of transformation(s), observed only in B2 and B4, were once again characterized by negative DTA values ranging from -0.90 to -0.98mV(Table 5.46).

5.3.1.3 Thermogravimetric studies

This data, summarized in the form of plots between %TG as a function of temperature, are shown in the Figure 5.16.

From the figures, the following inferences were drawn

(i) %TG increased very slowly with an increase in temperature. This was followed by an exponential increase on raising the temperature further.

(ii) The nature of these plots was a function of the microstructure.

(iii) In the as-cast state, the weight gain was nearly a constant upto approximately 600°C. %TG corresponding to this condition was a minimum for B2 followed by B1, B4 & B3. A steep increase in the %TG was observed at temperatures upwards of 600°C it being most marked in B2 followed by B4, B3 and B1.

(iv) In the 950°C, 10 hours heat-treated condition, the weight gain was nearly a constant upto approximately 700°C. %TG corresponding to this condition was a minimum for B2 followed by B3, B4 & B1 (Fig. 5.17).

(v) In the 1050°C, 10 hours heat-treated condition, the weight gain was nearly a constant upto approximately 800°C. %TG corresponding to this condition was a minimum for B2 followed by B3, B1 & B4 (Fig. 5.18).

5.3.2 Discussion

The DTA studies proved useful in substantiating the structural observations reported earlier (Chapter 4, Section 4.1.2). Such a study was expected to prove helpful in resolving some of the existing inconsistencies and to provide additional information

on the possibility of employing the experimental alloys for high temperature applications. The least that was expected from the study was by way of information on the transformation/ critical temperatures.

5.3.2.1 Critical/transformation temperature(s)

The first set of transformation temperature(s) evidently represent the $\alpha \rightarrow \tau$ transformation in the experimental alloys. The negative DTA values associated with B2 and B4 reveal a more stronger tendency to form τ and this is consistent with the composition of these alloys which contain relatively higher proportion of Mn compared with B1 and B3. A marginally more negative value of DTA associated with B4 reveals a marginally enhanced τ-stabilizing tendency which can be attributed to a higher Cu content of B4 as compared with B2.

The next set of transformation temperatures evidently represent a carbide transformation which has also been indicated through optical metallographic studies (Figs.4.7-4.32). X-ray studies (Tables 5.2-5.41) revealed that the possible carbide transformation in the temperature range 900-935°C comprises the possible formation of $M_{23}C_6$, M_5C_2 and M_7C_3 type carbides. While saying so the presence of M_3C carbide has not been commented upon since its presence is represented through approximately equivalent intensities in the diffractograms (Tables 5.2-5.41). Based on more negative DTA value it is surmised that the carbide transformation(s) are more marked in the alloys B2 and B4 in comparison with the alloys B1 and B3. In an effort to rationalize this observation further, the x-ray observation

summary Table 5.42 was scrutinized afresh. It emerged that whereas $M_{23}C_6$ formed in approximately similar amounts in all the alloys, B2 and B4 revealed a distinct preference for the formation of M_5C_2 and M_7C_3 type of carbides. Thus from all accounts the second set of transformation(s) represent the formation of $M_{23}C_6$, M_5C_2 and M_7C_3 carbides, and more distinctly the latter two types because $M_{23}C_6$ dissolves on prolonged holding at 900°C.

The third transformation is occurring only in the alloys B2 and B4 in the temperature range of 1050-1075°C. DTA values indicate this change to be not as distinctly favoured as the transformations discussed above. It is inferred that this transformation comprises yet another carbide transformation of the type M_7C_3 --> M_2C requiring a larger activation in the form of a higher temperature for initiating and sustaining it. This inference is consistent with the carbide transformation sequence as revealed from a study of the phase diagrams(66).

Although efforts have been made to arrive at definitive deductions on the basis of DTA results, perhaps a more rigorous experimentation would have enabled doing so with greater certainty. Such an experimentation would comprise (i) employing different heating rates starting from the lowest value e.g. of the order of 0.1°C/min., (ii) plotting out of the initial and peak transformation temperatures, (iii) extrapolating the initial and peak transformation temperatures to a heating rate equivalent to zero to obtain the equilibrium transformation temperatures, and (iv) calculation of heat of reaction based on the peak area finally culminating in the calculation of heat capacities of the

reactants and that of the products(101-102). It is suggested that the DTA studies be more rigorously carried out in order to arrive at precise information on the transformation behaviour of the experimental alloys.

5.3.2.2 Thermogravimetric studies

Thermogravimetric studies proved helpful in drawing inferences regarding the usefulness of the experimental alloys for high temperature applications. Since, the basic aim of the study was to optimize the microstructure (through heat treating) for getting the best in terms of corrosion resistance and the deformation behaviour, the as-cast microstructure was not expected to respond very favourably when exposed to high temperatures. All the same, its high temperature behaviour was investigated to arrive at some initial data in this regard and to use this as a reference base for assessing the high temperature response of other selected microstructures.

From a perusal of the thermogravimetric data (Fig. 5.16) it emerges that the TG data for as-cast microstructure has two distinct regions, (i) upto 600°C and (ii) beyond 600°C and extending upto 1050°C. The first of these is characterized by a very small and more or less uniform increase in %TG suggesting the usefulness of as-cast structure upto 600°C. An equally important aspect is that whereas in the first temperature region the behaviour of the alloy B2 was superior to others, there is a reversal of this trend in the second region (marked at temperature ≥700°C) such that the increase in %TG is maximum in B2 followed by B3, B4 and B1. Thus attention will have to be

given in explaining this reversal of the trend and the difference in the high temperature response of the alloys.

To understand this the TG data was re-examined in the context of critical / transformation temperatures(Table 5.45). From this it emerges that the sharp increase in %TG between 800 and 1050°C may be directly related with the susceptibility to carbide transformation (M_5C_2 formation) in general which is marked in B2 and B4 as compared to B1 and B3 (Section 5.3.2.1). This is clearly demonstrated when percentage increase in TG is considered between the temperature ranges 900-1000°C (actual temperatures representing carbide transformation are in the range of 890-935°C [Table 5.45]). The data shows percentage increase in TG to be a maximum in B2 followed by B4, B3 and B1. Amongst B1 and B3, the latter is more prone to the formation of M_5C_2. Thus, the overall superiority of B1 over all the other alloys can be attributed to its least proneness to form M_5C_2 type of carbide. A similar reasoning may explain the further sharp increase in %TG in B2, in comparison to the other alloys, on heating to 1000-1050°C.

The TG data further reflects upon the usefulness of the austenite based microstructures in influencing high temperature behaviour. This is clearly brought out by the lower %TG values observed in the temperature range 700-800°C (structure austenite based) compared to those observed in the temperature range 600-700°C (structure α based).

In the light of the abovesaid discussion when the TG data for microstructures corresponding to 950°C, 10 hrs. and 1050°C, 10 hrs. heat-treatments are compared, it is easy to assess why

the latter is proving to be more effective than the former upon heating upto 800°C. Since, both these heat-treatments stabilize austenite and exclude the carbide transformations occurring around 900°C, the present data once again favourably reflects upon the usefulness of τ based structures and supports the contention that the primary reason for the pronounced increase in the %TG is the carbide transformations. Needless to state that, the enrichment of parent austenite brought about by high temperature treatments must have further favourably contributed to the improved high temperature behaviour of these microstructures as compared with the behaviour of the as-cast microstructure.

Looking to the overall deductions based on the TG data, it is evident that where the microstructure is austenite based the high temperature behaviour would be controlled by the stability of austenite and proneness of the alloys to carbide transformations. Since these two factors are a function of the alloy content, the behaviour of the experimental alloys is expected to differ from one another. In the situation where the matrix is not austenitic, other factors need consideration e.g. an alloy with a martensitic matrix or a partly martensitic matrix may respond favourably to high temperatures till martensite decomposition has not occurred. Thereafter, its behaviour will depend upon the decomposition kinetics of martensite. On the other hand an alloy which is not fully or partly martensitic to begin with may not respond as favourably to high temperatures as the alloy in the earlier instance but its behaviour is likely to

be more consistent as compared to a martensite bearing alloy which would undergo softening after the martensite has decomposed. A somewhat similar reasoning may account for the overall superiority of B2 and B4 (more so of B2) over B1 and B3 upto about 500°C and a marginally improved performance of B1 thereafter upto 700°C. Reasons for differences in high temperature response beyond 700°C have already been discussed. It would none the less be appropriate to state that the interpretation of the overall high temperature behaviour may not be as simplistic. Furthermore, a clearer picture would have emerged if the P content of the four alloys were identical.

5.3.3 Modelling of the TG data

The discussion contained in the Section 5.3.2.1 essentially dealt with the high temperature response of some selected microstructures and of the possible impact of various transformations, occurring during heating, in affecting the overall high temperature behaviour. Having done so, it would now be appropriate to look into modelling aspect of the TG data. In order to do so, it would be necessary to examine the processes involving high temperature oxidation per se and arrive at the possible rate laws relevant to the present study, which would eventually form the basis of modelling.

Oxidation of metals can be expressed by a simple chemical reaction as

$$aMe + b/_2O_2 \dashrightarrow Me_aO_b \qquad \ldots(5.1)$$

However, the reaction path and the oxidation behaviour of a metal may depend on a variety of factors, and reaction mechanism(s) may as a result prove complex.

The initial step in the metal-oxygen reaction involves the adsorption of gas on the metal surface. As the reaction proceeds, oxygen may dissolve in the metal forming an oxide on the surface either as a film or as a separate oxide nuclei. Adsorption and the initial oxide formation are both functions of surface orientation and condition, concentration of crystal defects at the surface, and impurities in both the metal and the gas(103).

The surface oxide separates the metal from the gas. This oxide may either be in the form of thin tenacious film or as a porous oxide scale.

For a particular metal, the reaction mechanism is a function of the pre-treatment and surface condition, temperature, gas composition and pressure, and elapsed time of reaction. Looking to the possibility of a large variation in the properties of different metals and alloys and their oxides, a number of theories are needed to describe the oxidation behaviour of metals(104-106).

A detailed understanding of this phenomenon requires knowledge of reaction rates and kinetics, the temperature and oxygen pressure dependence of the reaction, the composition, structure, and growth mechanism of the reaction products.

Rate equations describing oxidation may be classified as logarithmic, parabolic, and linear. These are discussed in detail elsewhere(104-110) and are not relevant to the present study because temperature dependence of oxidation behaviour alone has been studied.

Numerous oxidation reactions have shown empirically that the

temperature dependence of oxidation rate constants at a constant ambient oxygen pressure obeys an Arrhenius-type equation

$$k = k_o \exp(-Q/RT) \qquad ...(5.2)$$

where Q is the activation energy commonly given in cal/mole, R is the gas constant(1.986 cal/°K mole), and the T the absolute temperature. The pre-exponential factor, k_o, is within experimental accuracy, usually found to be independent of temperature. Using Eq.5.2, the activation energy Q is determined by plotting $\log_{10}k$ as a function of 1/T, in which case the slope of the curve is given by Q/2.303R. The rate constant at different temperatures is commonly determined from isothermal measurements, but may also be determined from a single run under conditions of linearly increasing temperature(111).

Nucleation and growth phenomena may give rise to unusual oxygen pressure-dependence of the process of oxidation(112-114). Considering oxidation of Fe as an example, Fe_3O_4 is initially formed on the surface (FeO is unstable below 570°C), and Fe_2O_3 is subsequently nucleated in the Fe_3O_4 surface. When Fe_2O_3 has grown to form a continuous layer, the oxidation rate is substantially reduced.

A scrutiny of the Figure 5.16 reveals that although the %TG varies exponentially with temperature, the plot has two distinct parts, the nature of variation in one being opposite to that of the other. The first part (from ambient temperature to 200°C) can be represented by an asymptotic curve as

$$\%TG = A1'(\exp^{-T/A2'}-1) \qquad ...(5.3)$$

and the second part can be represented as

$$\%TG = A1 + A2(\exp^{-A3/T}) \qquad ...(5.4)$$

where, A1', A2', A1, A2, and A3 are constants, and T is temperature in °K.

The %TG increase in the first part is very small(≈2%) compared to the overall increase of upto (≈27-30%) attained at highest heating temperature. It was therefore, felt appropriate to neglect the former in arriving at the proposed model. As before multi-variable nonlinear constraint optimization technique(54,55) was employed to do so. The correlations thus obtained are summarized as follows:

Alloy B1 $\quad \%TG = 1.561878 + 2665.150 \exp(-7529.676/T) \quad ...(5.5)$

Alloy B2 $\quad \%TG = 1.310813 + 9623.292 \exp(-8771.445/T) \quad ...(5.6)$

Alloy B3 $\quad \%TG = 1.515658 + 3465.314 \exp(-7609.409/T) \quad ...(5.7)$

Alloy B4 $\quad \%TG = 1.566102 + 4004.606 \exp(-7792.101/T) \quad ...(5.8)$

The %TG calculated from the aforesaid correlations for temperatures ≥300°C revealed that predicted data are within ±6% of the experimentally determined data for the alloys B1 & B3 and within ±10% for the alloys B2 & B4 (Figs. 5.19). The scatter is within the permissible range and favourably reflects on the validity of the model.

CHAPTER VI

ELECTRO-CHEMICAL CHARACTERIZATION AND DEFORMATION BEHAVIOUR OF THE ALLOYS

The results reported thus far dealt with the transformation behaviour of the experimental alloys arrived at on the basis of hardness measurements, optical metallography, X-ray diffraction, EPMA and DTA. Having achieved this target, it was appropriate to characterize the alloys for their corrosion and deformation behaviour. Potentiostatic studies and compression testing were utilized for this purpose. The data thus obtained have been summarized and discussed in the following sections.

6.1.1 Electro-chemical characterization

The experimental alloys were characterized for their corrosion behaviour in the as-cast and in the heat-treated conditions in order to substantiate the findings of Jain(115). He investigated the alloys in 5% NaCl solution in the oil quenched condition using the weight loss method. Selection of this technique is justified because the experimental alloys undergo uniform corrosion. The study(115) had shown that :

(i) Corrosion resistance in the as-cast condition improved upon heat-treating.

(ii) Similarly, corrosion rate decreased on raising the soaking period at a given heat-treating temperature (range 900 to 1050°C) except on heat-treating at 950°C.

(iii) In general, corrosion rate decreased with an increase in the heat-treating temperature at 4 hrs soaking period.

(iv) At 10 hours soaking period, corrosion rate increased sharply on raising the temperature from 900 to 950°C

followed by a sharp decrease in it on increasing the temperature upto 1050°C.

(v) Microstructures corresponding to the following heat-treatments improved corrosion resistance :
(a) 1050,10,OQ, (b) 1050,4,OQ and (c) 1000,10,OQ

(vi) Similarly, microstructures corresponding to 900,4,OQ and 950,10,OQ heat-treatments impaired corrosion resistance.

Limited studies on the higher Cu alloys i.e. B3 and B4 in 10% $(NH_4)_2SO_4$ had revealed that(115):

(i) The experimental and the standard alloys exhibited active-passive behaviour.

(ii) In the as-cast state, B4 responded more favourably than B3 based on I_{pp} and I_{corr} values.

(iii) The 900°C, 4hours, OQ heat-treatment led to an improvement in the corrosion resistance of B3 and B4 over that observed in the as-cast state. The value of I_{pp} reduced considerably while I_{corr} was more or less unaltered. Alloy B4 again responded more favourably.

(iv) Of the two standard alloys, KC (nodular graphite) was found to be better than KC1 (flake graphite), based on I_{pp} and I_{cr} values.

The aforesaid study while establishing the usefulness of experimental alloys, none the less, did not reveal their behaviour when subjected to accelerated corrosion testing. It was therefore, decided to carry out such a study and analyze the data thus obtained. Representative microstructures were characterized for their electro-chemical response in a 5% NaCl

solution using the potentiostatic method. To facilitate a comparison, two standard alloys namely flake graphite Ni-resist and spheroidal graphite NI-resist were also investigated.

Studies were carried out in the potential range -1200mV to -300 mV by constructing polarization curves within the Tafel region (Figs.6.1 to 6.23). Corrosion potentials and the currents obtained from the plots were noted down for further analysis and are summarized in the Tables 6.1-6.3. Summary tables were also prepared for I_{corr}(Table 6.2) and for E_{corr}(Table 6.3).

A scrutiny of the Figs.6.1 to 6.23 and the Tables 6.1-6.3 revealed that:

(i) The corrosion potentials, E_{corr} (with respect to a reference electrode) essentially lie in the range of -0.426 to -0.645 V.

(ii) For the 10 hrs. soaking period, E_{corr} increased on increasing the heat-treating temperature from 900 to 950°C; a further increase in the temperature upto 1050°C made E_{corr} more noble (less -ve).

(iii) E_{corr} was a minimum for B2(1050, 10, AC heat-treatment) and a maximum for B1(950, 10, AC heat-treatment).

(iv) I_{corr} increased with an increase in the heat-treating temperature from 900 to 950°C and decreased thereafter on increasing temperature upto 1050°C (10 hrs. soaking period) in all the alloys i.e. the heat-treating parameters had an identical effect on the E_{corr} and I_{corr}.

(v) In general, 1050, 4, AC heat-treatments showed higher E_{corr} as compared to both 1000, 10, AC and 1050, 10, AC heat-treatments.

(vi) The corrosion potentials (E_{corr}) when noted from the polarization curves, were different from those measured against a reference electrode. This difference was less marked for heat-treatments such as 900,10,AC, 1000,10,AC and 1050,10,AC and more marked for the 950,10,AC heat-treatment.

(vii) The corrosion currents I_{corr} for the experimental alloys were in the range of 107-198 $\mu A/cm^2$.

(viii) The corrosion potentials and the currents for the standard alloys were lower than that for the experimental alloys. Further, the performance of KC was better than KC1(115) based on E_{corr} and I_{corr} values.

(ix) In some instances, two stepped polarization plots were obtained. In such instances it was difficult to measure I_{corr} with certainty. However, potentials corresponding to both the steps were noted.

(x) The second step was marked for the 950°C, 10 hrs., AC heat-treatment for all the alloys.

6.1.2 Discussion

A careful study of the basics of electro-chemical characterization reveals that one method of conducting accelerated aqueous corrosion testing is by determining the potentiostatic behaviour of a material. Rather than plotting the entire polarization curve, it may suffice to confine the studies to the Tafel region. The critical parameters of interest are E_{corr} and I_{corr}; the latter is determined by drawing a tangent at the linear segment of the region I (Fig.6.1) and noting down

current corresponding to the point of intersection of the tangent with the horizontal (representing E_{corr}).

A microstructure would resist corrosion if it has an E_{corr} which is less negative i.e. more closer to the H_2 electrode potential. Any heat-treatment that alters the microstructure so that the E_{corr} becomes more noble would be adjudged to be a beneficial heat-treatment. It is equally important that a given microstructure should additionally exhibit a low I_{corr} value. Thus, if two microstructures attain a nearly similar E_{corr}, the one exhibiting a lower I_{corr} value will be more preferred. Similarly, a low value of I_o is desirable irrespective of whether or not a material shows `active-passive' behaviour. This is because I_o is synonymous with H_2 liberation/ formation and a large value would signify a large H_2 adsorption/absorption and hence embrittlement(116). The abovesaid analysis is useful in explaining the data obtained.

Corrosion resistance in the heat-treated condition, in general, is improved over that in the as-cast state since most heat-treatments considered in the present study are conducive to attaining an austenite based microstructure. As against this, the microstructure in the as-cast condition is not suitable in attaining good resistance to corrosion due to the multiplicity of the microconstituents present within the matrix. On heat-treating, a general improvement in corrosion resistance is due to (i) a reduction in the Vf of MC and DC and (ii) the formation of a successively increasing amount of austenite whose stability increases with temperature as more and more amount of MC and DC dissolve in it. Needless to add that in the absence of a second

phase (both MC and DC) the corrosion resistance would have been better than what has been obtained. In order to compare the relative effects of MC and DC in influencing corrosion, it would be useful to assess the happenings corresponding to the 10 hrs. heat-treatments.

On doing so it emerges that the DC are playing a dominant role in determining the corrosion behaviour on heat-treating at 950°C. The reason is that the DC undergo maximum coarsening at this temperature as would be borne out by the coarsening index data (Section 4.2.8, p.68). The larger the coarsening, more enhanced would be the galvanic action and the lower would be the corrosion resistance. At temperatures higher than 950°C dispersed carbides have no bearing on the corrosion behaviour because they are no more present in the microstructure. Although DC are present corresponding to the 4 hrs. heat-treatment, their (i) volume fraction, (ii) size and distribution together do not enhance the galvanic action sufficient enough to adversely effect corrosion resistance. This reasoning is appropriately justified since the volume fraction of MC at the 900°C, 10 hrs., AC and 950°C, 10 hrs., AC heat-treatments is nearly the same. Quite clearly the enhanced galvanic action in the latter condition is as a consequence of (i) coarsening as would be borne out by the coarsening index and (ii) a critical volume fraction of DC.

It would be appropriate to reiterate that the massive carbides also enhance galvanic action, its magnitude being a function of the volume fraction and morphology. Thus the least that can happen in the presence of a second phase (in any form)

is that the galvanic action is enhanced; the specific effect being governed by its (second phase) nature.

On the basis of the above reasoning it would be possible to appreciate the results summarized in the Tables 6.1 to 6.3 and in the Figures 6.1 to 6.5. The overall corrosion behaviour based on potentiostatic studies also agrees well with the observations made by Jain(115) based on weight loss.

Coming to specifics, attention needs to be given to explaining (i) the presence of two steps in the polarization curves whose presence is marked corresponding to the 950°C, 10 hrs. heat-treatment, (ii) an unexpected decrease in corrosion resistance in B2 and B4 corresponding to the 1050°C, 4 hrs. heat-treatment (no mention has been made of B1 and B3 because of the non-availability of the corrosion data for 1050°C, 4 hrs. heat-treatment), (iii) 950°C, 10 hrs., AC heat-treatment impairing corrosion resistance and (iv) the standard alloys resisting corrosion better than the experimental alloys, although, the difference is marginalized when the best corrosion resistance exhibited by the experimental alloys is considered.

Presence of a two step polarization plot is a clear indication that the galvanic action is occurring in two stages. In instances such as the one experienced at 950°C, 10 hrs. heat-treatment, (effective surface area due to a combined presence of MC and DC being large enough), the corrosion resistance is being controlled predominantly by the second phase to start with (MC+DC). Evidently, the high hardness associated with the second phase has lead to a slowing down in corrosion. That this is not a true representation is revealed by a relatively large value of

E_{corr}. Generally E_{corr} is close enough to $E_{immersion}$. As potential is further superimposed, the matrix-second phase galvanic action is accelerated giving rise to an increase in current / current density which is followed by a decrease in it as is normally expected. This minimum, which is a representative of the E_{corr} normally observed (Tables 6.1 & 6.3), is occurring at currents/ current densities appreciably higher than generally attained (Figs. 6.1-6.4), primarily due to the presence of a larger number of galvanic cells. For this reason the second step is not marked. Hereafter, the plot proceeds in the usual manner. That this hypothesis, based on an enhanced galvanic action, is correct is further borne out by the coarsening index value which is the lowest corresponding to the 950°C, 10 hrs. heat-treatment (signifying maximum coarsening that has been observed in the present study).

Corrosion resistance is impaired corresponding to 1050°C, 4 hrs. heat-treatment because of the formation of a large volume fraction of an eutectic (anomalous eutectic) comprising austenite + carbide (Chapter IV, Section 4.1.2) which has platy/needle like morphology detrimental to corrosion resistance. Thus, a large volume fraction of the second phase and its unfavorable morphology have contributed to this result.

The unusual deterioration in corrosion resistance corresponding to 950°C, 10 hrs. heat-treatment is primarily due to enhanced galvanic action due to coarsening of DC and this aspect has already been discussed.

The standard alloys have a better overall corrosion

resistance (Table 6.1) primarily because the matrix is predominantly austenitic containing negligible second phase (graphite; the amount of carbide being more or less insignificant). Presence of a large Ni content has beneficially contributed to an enhanced stability of the matrix. In the experimental alloys, the total alloy content is much smaller. That the corrosion resistance of the experimental alloys approaches that of the standard alloys at the 1050°C, 10 hrs., AC heat-treatment is a clear indication that stability of austenite is a primary factor in controlling the corrosion behaviour; the other factors are the effect of the second phase and difference in electro-chemical potentials between the matrix and the second phase (which is larger for the standard alloys and smaller for the experimental alloys). It is thus clear that much improved corrosion resistance can be attained in the experimental alloys provided the deductions arrived at are duly implemented through improved alloy design.

6.2 Modelling of the corrosion behaviour

An analysis of the literature reviewed in section 1.2 reveals the manner in which different microconstituents influence corrosion behaviour. Excluding the matrix to start with, their effect depends upon their nature and size, shape and distribution. When the matrix is also considered, its characteristics (crystal structure and stability) and difference in the electro-chemical potentials between the matrix and the constituents also assume significance. Interestingly, most of the correlations have been qualitative in character. Any effort aimed at modelling the corrosion behaviour will have to incorporate the abovesaid aspects.

The first effort in this regard was made by Jain(117) who attempted to correlate corrosion rate with the microstructural features comprising austenitic matrix, massive carbides and dispersed carbides. He selected heat-treatments carried out at 900 & 950°C primarily because the different alloys constituting the study attained nearly constant hardness values at these temperatures. Whereas the hardness was more or less independent of the soaking period, the volume fraction of MC & DC varied. It was felt appropriate to examine the methodology adopted by him before enlarging upon the ideas conceived in his work reported recently by Patwardhan & Jain(118).

He conceived that the CR could be expressed as a function of different parameters namely,

CR ≈ f(austenite Vf/ stability)

CR ≈ f(Vf of MC)

CR ≈ f(Vf of DC)

CR ≈ f(distribution of the DC)

To begin with, the last term was excluded and the volume fraction of MC & DC was combined into a single term to develop the initial stage model. This was justified on the assumption that since the second phase in general would enhance CR, their overall effect can be cummulated into a single factor.

From the experimental data it was concluded that the functional relationship interrelating corrosion rate with the total volume fraction of carbides can be represented by a second order polynomial :

$$CR = A1 + A2(VCb) + A3(VCb)^2 \qquad ...(6.1)$$

The contribution of the second phase, i.e. the role of dispersed carbides, was included in the above expression by incorporating a factor based on the number of particles, NOP. This led to the following expression :

$$CR = [A1' + A2'(VCb) + A3'(VCb)^2](NOP)^{A4'} \qquad ...(6.2)$$

The constants A1', A2', A3', and A4' were calculated by using multi-variable constraint optimization technique and the final equations are (54-55):

Test duration : 168 hours

$$B1 : CR = [1516.9 - 79.6(VCb) + 1.13(VCb)^2](NOP)^{-0.48} \qquad ...(6.3)$$

$$B2 : CR = [7999.8 - 541.2(VCb) + 9.45(VCb)^2](NOP)^{-0.73} \qquad ...(6.4)$$

$$B3 : CR = [9.94 - 0.624(VCb) + 0.0099(VCb)^2](NOP)^{1.4} \qquad ...(6.5)$$

$$B4 : CR = [44.3 - 3.07(VCb) + 0.0545(VCb)^2](NOP)^{0.83} \qquad ...(6.6)$$

The above constants were determined within a limiting condition of ±8000. When this restriction over the limits was removed and a larger number of iterations were taken to obtain better optimum values, then the above equations assumed the

following form :

Test duration : 168 hours

$$B1 : CR = [3593.0 - 188.5(VCb) + 2.751(VCb)^2](NOP)^{-0.52} \quad ...(6.7)$$

$$B2 : CR = [25957.48 - 1772.55(VCb) + 30.96(VCb)^2](NOP)^{-0.99} \quad ...(6.8)$$

$$B3 : CR = [38.95 - 2.445(VCb) + 0.0389(VCb)^2](NOP)^{1.02} \quad ...(6.9)$$

$$B4 : CR = [44.69 - 3.10(VCb) + 0.0551(VCb)^2](NOP)^{0.82} \quad ...(6.10)$$

The equations 6.7-6.10 in essence are similar to those originally developed by Jain(117). In order to understand the physical implications of the aforesaid model as a whole, the values of the constants were carefully scrutinized. It emerged that whereas the first three constants are consistent from alloy to alloy i.e. they are either all positive or all negative, the last constant is negative for B1 & B2 and positive for B2 & B4. To understand its possible implications, the factor $(NOP)^{A4}$ was calculated for all the alloys and the values thus obtained are given below.

Heat-treatment	$(NOP)^{A4}$			
	B1	B2	B3	B4
900, 4,AC	----	0.056	203.68	23.59
900,10,AC	0.163	0.068	211.05	19.57
950, 4,AC	0.183	0.082	168.02	19.71
950,10,AC	0.216	0.073	154.36	17.93

Evidently, the factor $(NOP)^{A4}$ is varying widely. This gave an indication that either NOP can not be regarded as a satisfactory parameter for representing DC or the constants have been calculated without adequately understanding the physical implications of the their effect on the corrosion rate.

The latter aspect was given precedence by visualizing that

EFFECT OF SOAKING PERIOD ON HARDNESS IN A.C. CONDITION

ALLOY : B1 AS CAST HARDNESS(HV30)= 594
TABLE-4.1 TEMP.(DEG.C) = 800

TIME (HRS)	HARDNESS (HV30)										SD	AVERAGE (HV30)
2	710	710	705	702	700	700	700	698	697	697		
	695	695	692	690	690	690	690	690	685	685	7.27	696
4	752	752	752	746	746	741	741	736	736	730		
	730	730	720	720	710	710	700	695	685	685	21.90	725
6	769	763	752	741	736	736	730	730	725	725		
	725	720	720	720	720	705	705	695	690	690	21.65	724
8	763	763	752	752	752	746	741	741	741	736		
	730	730	725	725	725	725	720	720	710	695	17.45	734
10	741	741	741	736	736	736	730	730	730	725		
	720	715	715	715	715	715	710	710	710	690	13.68	723

FOR DEGREE OF 1 COEFFICIENTS ARE
701.5000 3.1500
BEST FIT VALUES 707.8 714.1 720.4 726.7 733.0
STANDARD DEVIATION IS 11.8925760
FOR DEGREE OF 2 COEFFICIENTS ARE
667.0000 17.9357 -1.2321
BEST FIT VALUES 697.9 719.0 730.3 731.6 723.1
STANDARD DEVIATION IS 6.4895508
FOR DEGREE OF 3 COEFFICIENTS ARE
654.3990 26.7864 -2.9198 0.0938
BEST FIT VALUES 697.0 720.8 730.3 729.8 724.0
STANDARD DEVIATION IS 8.7251734

TABLE-4.2 TEMP.(DEG.C) = 850

2	622	622	618	618	618	614	610	610	610	606		
	606	606	602	594	590	590	586	586	583	579	13.88	603
4	690	690	690	690	685	685	685	680	680	675		
	675	671	671	671	666	661	657	657	657	657	12.29	674
6	680	680	675	675	671	671	671	666	661	657		
	657	657	657	657	657	652	652	652	652	644	10.56	662
8	710	695	695	695	695	690	690	685	685	680		
	680	680	675	675	675	671	671	661	657	657	13.92	681
10	725	715	710	705	705	705	700	700	700	695		
	690	690	685	685	680	680	675	675	671	666	15.77	692

FOR DEGREE OF 1 COEFFICIENTS ARE
606.9000 9.2500
BEST FIT VALUES 625.4 643.9 662.4 680.9 699.4
STANDARD DEVIATION IS 22.0809110
FOR DEGREE OF 2 COEFFICIENTS ARE
562.4000 28.3214 -1.5893
BEST FIT VALUES 612.7 650.3 675.1 687.3 686.7
STANDARD DEVIATION IS 21.1768080
FOR DEGREE OF 3 COEFFICIENTS ARE
457.3993 102.0719 -15.6519 0.7813
BEST FIT VALUES 605.2 665.3 675.1 672.3 694.2
STANDARD DEVIATION IS 18.2869960

following form :

Test duration : 168 hours

$$B1 : CR = [3593.0 - 188.5(VCb) + 2.751(VCb)^2](NOP)^{-0.52} \quad ...(6.7)$$

$$B2 : CR = [25957.48 - 1772.55(VCb) + 30.96(VCb)^2](NOP)^{-0.99} \quad ...(6.8)$$

$$B3 : CR = [38.95 - 2.445(VCb) + 0.0389(VCb)^2](NOP)^{1.02} \quad ...(6.9)$$

$$B4 : CR = [44.69 - 3.10(VCb) + 0.0551(VCb)^2](NOP)^{0.82} \quad ...(6.10)$$

The equations 6.7-6.10 in essence are similar to those originally developed by Jain(117). In order to understand the physical implications of the aforesaid model as a whole, the values of the constants were carefully scrutinized. It emerged that whereas the first three constants are consistent from alloy to alloy i.e. they are either all positive or all negative, the last constant is negative for B1 & B2 and positive for B2 & B4. To understand its possible implications, the factor $(NOP)^{A4}$ was calculated for all the alloys and the values thus obtained are given below.

Heat-treatment	$(NOP)^{A4}$			
	B1	B2	B3	B4
900, 4,AC	----	0.056	203.68	23.59
900,10,AC	0.163	0.068	211.05	19.57
950, 4,AC	0.183	0.082	168.02	19.71
950,10,AC	0.216	0.073	154.36	17.93

Evidently, the factor $(NOP)^{A4}$ is varying widely. This gave an indication that either NOP can not be regarded as a satisfactory parameter for representing DC or the constants have been calculated without adequately understanding the physical implications of the their effect on the corrosion rate.

The latter aspect was given precedence by visualizing that

the presence of DC will enhance corrosion rate and as such the constants A4' should necessarily by positive. Based on this premise, the constants were redetermined in the present study and the equations now assume the form :

Test duration : 168 hours

$$B1 : CR = [2003.968-101.423(VCb)+1.290(VCb)^2](NOP)^{0.187} \quad ...(6.11)$$

$$B2 : CR = [177.200-10.94(VCb)+0.192(VCb)^2](NOP)^{0.011} \quad ...(6.12)$$

$$B3 : CR = [550.60-34.71(VCb)+0.558(VCb)^2](NOP)^{0.199} \quad ...(6.13)$$

$$B4 : CR = [105.01-6.830(VCb)+0.125(VCb)^2](NOP)^{0.199} \quad ...(6.14)$$

Test duration : 720 hours

$$B1 : CR = [2074.523-105.768(VCb)+1.356(VCb)^2](NOP)^{0.117} \quad ...(6.15)$$

$$B2 : CR = [195.200-12.28(VCb)+0.211(VCb)^2](NOP)^{0.011} \quad ...(6.16)$$

$$B3 : CR = [528.935-33.462(VCb)+0.538(VCb)^2](NOP)^{0.199} \quad ...(6.17)$$

$$B4 : CR = [16.384-0.387(VCb)+0.006(VCb)^2](NOP)^{0.199} \quad ...(6.18)$$

To understand the physical significance of the refined models emerging from this study, the relative contributions of the two factors constituting the model were assessed and the data thus computed is summarized in the following table.

The analysis of the data reveals that for the alloys B1, B3 & B4 the ratio of factor I/factor II is ranging between 5.2 to 9.6 whereas that for B2 the ratio is varying between approximately 21 to 25 i.e. at least nearly 4 times that generally attained for the alloys B1, B3 & B4. This leads to the deduction that there is an apparent anomaly in visualizing the elements of the model. A possible reason is that the term VCb already includes the effect of DC which is being represented by the NOP. Therefore, of the two options namely, VCb and DC, the latter was more representative of the

Summary of the values of the first parameter based on VCb and NOP

Test duration : 168 hours

Heat-treatment	B1	B2	B3	B4
900, 4,AC	-----	25.992	12.247	11.809
900,10,AC	10.883	22.552	10.911	11.760
950, 4,AC	18.571	21.991	11.629	12.253
950,10,AC	14.214	22.965	13.528	13.140

Test duration : 720 hours

Heat-treatment	B1	B2	B3	B4
900, 4,AC	-----	20.431	10.006	10.242
900,10,AC	13.145	18.556	8.712	10.328
950, 4,AC	18.610	16.833	9.398	10.192
950,10,AC	14.705	19.113	11.226	10.158

Summary of the values of the second parameters based on VCb and NOP

Test duration : 168 hours

Heat-treatment	B1	B2	B3	B4
900, 4,AC	-----	1.044	2.084	2.142
900,10,AC	2.020	1.041	2.094	2.052
950, 4,AC	1.934	1.038	2.029	2.052
950,10,AC	1.812	1.040	2.005	2.005

Test duration : 720 hours

Heat-treatment	B1	B2	B3	B4
900, 4,AC	-----	1.044	2.084	2.142
900,10,AC	1.553	1.041	2.094	2.040
950, 4,AC	1.511	1.038	2.029	2.052
950,10,AC	1.450	1.040	2.005	2.005

Table representing ratio of factor I/factor II (VCb & NOP)

Test duration : 168 hours

Heat-treatment	Factor I/factor II			
	B1	B2	B3	B4
900, 4,OQ	----	24.9	5.9	5.5
900,10,OQ	5.4	21.7	5.2	5.7
950, 4,OQ	9.6	21.2	5.7	6.0
950,10,OQ	7.8	22.1	6.7	6.6

Test duration : 720 hours

Heat-treatment	Factor I/factor II			
	B1	B2	B3	B4
900, 4,OQ	----	19.6	4.8	4.8
900,10,OQ	8.5	17.8	4.2	5.1
950, 4,OQ	12.3	16.2	4.6	5.0
950,10,OQ	10.1	18.4	5.6	5.1

DC as the larger the number of particles the more enhanced would be the galvanic action. VCb was replaced by VMC and therefore, the model proposed earlier is more aptly modified as

$$CR = [A1 + A2(VMC) + A3(VMC)^2] (NOP)^{A4} \quad ...(6.19)$$

The constants A1, A2, A3 and A4 were recalculated and the models thus evolved are :

Test duration : 168 hours

$$B1 : CR = [165.554-11.771(VMC)+0.232(VMC)^2] (NOP)^{0.074} \quad ...(6.20)$$

$$B2 : CR = [126.646-11.524(VMC)+0.312(VMC)^2] (NOP)^{0.013} \quad ...(6.21)$$

$$B3 : CR = [650.510-65.711(VMC)+1.715(VMC)^2] (NOP)^{0.010} \quad ...(6.22)$$

$$B4 : CR = [21.679-0.316(VMC)+0.01(VMC)^2] (NOP)^{0.067} \quad ...(6.23)$$

Test duration : 720 hours

$$B1 : CR = [67.605-4.248(VMC)+0.080(VMC)^2] (NOP)^{0.128} \quad ...(6.24)$$

$$B2 : CR = [177.124-17.133(VMC)+0.453(VMC)^2] (NOP)^{0.011} \quad ...(6.25)$$

$$B3 : CR = [732.30-74.52(VMC)+1.934(VMC)^2] (NOP)^{0.0245} \quad ...(6.26)$$

$$B4 : CR = [13.061-0.186(VMC)+0.001(VMC)^2] (NOP)^{0.199} \quad ...(6.27)$$

As before the values of the two factors constituting the modified models were computed and the data is summarized in the following table.

A scrutiny of this table reveals that based on the modified approach the discrepancies observed in the model incorporating VCb and NOP are greatly reduced in the model incorporating VMC and NOP. The superiority of the latter approach over that of the former is thus clearly established. This prompted us to refine the above model further to examine whether the actual happenings during corrosion could be more closely approximated. A possible method to do so was to represent the DC by the distribution factor, DF as was suggested by Patwardhan in the earlier study. On doing so the modified model assumes the form :

$$CR = [A1 + A2(VMC) + A3(VMC)^2] (DF)^{A4} \quad ...(6.28)$$

The constant A1, A2, A3 and A4 were recalculated as before and the models thus developed assumed the form :

Test duration : 168 hours

$$B1 : CR = [390.380-27.505(VMC)+0.528(VMC)^2] (DF)^{0.448} \quad ...(6.29)$$

$$B2 : CR = [48.300-0.091(VMC)+0.01(VMC)^2] (DF)^{0.907} \quad ...(6.30)$$

$$B3 : CR = [683.507-69.060(VMC)+1.803(VMC)^2] (DF)^{0.010} \quad ...(6.31)$$

$$B4 : CR = [26.55-0.282(VMC)-0.01(VMC)^2] (DF)^{0.010} \quad ...(6.32)$$

Summary of the values of the first parameter based on VMC and NOP

Test duration : 168 hours

Heat-treatment	B1	B2	B3	B4
900, 4,AC	-----	24.579	24.163	19.285
900,10,AC	17.549	22.134	22.992	19.186
950, 4,AC	16.865	22.234	21.433	19.413
950,10,AC	21.090	21.838	25.786	19.256

Test duration : 720 hours

Heat-treatment	B1	B2	B3	B4
900, 4,AC	-----	20.028	17.404	9.888
900,10,AC	12.221	18.964	17.086	10.280
950, 4,AC	11.229	17.104	15.077	9.654
950,10,AC	13.858	18.455	20.488	9.962

Summary of the values of the second parameters based on VMC and NOP

Test duration : 168 hours

Heat-treatment	B1	B2	B3	B4
900, 4,AC	-----	1.053	1.037	1.292
900,10,AC	1.321	1.049	1.038	1.271
950, 4,AC	1.298	1.046	1.036	1.274
950,10,AC	1.265	1.048	1.036	1.264

Test duration : 720 hours

Heat-treatment	B1	B2	B3	B4
900, 4,AC	-----	1.044	1.095	2.142
900,10,AC	1.618	1.041	1.095	2.040
950, 4,AC	1.570	1.038	1.091	2.052
950,10,AC	1.502	1.040	1.089	2.005

Table representing ratio of factor I/factor II (VMC and NOP)
Test duration : 168 hours

Heat-treatment	Factor I/factor II			
	B1	B2	B3	B4
900, 4,OQ	----	23.3	23.3	14.9
900,10,OQ	13.3	21.1	22.2	15.1
950, 4,OQ	13.0	21.3	20.7	15.2
950,10,OQ	16.7	20.8	24.9	15.2

Test duration : 720 hours

Heat-treatment	Factor I/factor II			
	B1	B2	B3	B4
900, 4,OQ	----	19.2	15.9	4.6
900,10,OQ	7.6	18.2	15.6	5.0
950, 4,OQ	7.2	16.5	13.8	4.7
950,10,OQ	9.2	17.7	18.8	5.0

Test duration : 720 hours

$$B1 : CR = [491.519-32.537(VMC)+0.589(VMC)^2] (DF)^{0.959} \quad ...(6.33)$$

$$B2 : CR = [58.24-1.292(VMC)+0.027(VMC)^2] (DF)^{0.99} \quad ...(6.34)$$

$$B3 : CR = [825.84-84.07(VMC)+2.187(VMC)^2] (DF)^{0.0270} \quad ...(6.35)$$

$$B4 : CR = [50.023-1.237(VMC)+0.01(VMC)^2] (DF)^{0.463} \quad ...(6.36)$$

Since the values of DF differ greatly from CR & VMC, an analysis of the constants in the above equations revealed a large variation in the values. Therefore, normalisation technique was used to recalculate the constants and the resulting equations are:

Test duration : 168 hours

$$B1 : CR = [10.386-19.866(VMC)+10.301(VMC)^2] (DF)^{0.518} \quad ...(6.37)$$

$$B2 : CR = [0.938 - 0.002(VMC) + 0.076(VMC)^2] (DF)^{0.878} \quad ...(6.38)$$

B3 : $CR = [25.03 - 51.85(VMC) + 27.747(VMC)^2] (DF)^{0.010}$ ...(6.39)

B4 : $CR = [0.941 - 0.001(VMC) + 0.012(VMC)^2] (DF)^{0.044}$ ...(6.40)

Test duration : 720 hours

B1 : $CR = [5.728 - 9.151(VMC) + 4.275(VMC)^2] (DF)^{0.567}$ ...(6.41)

B2 : $CR = [1.129 - 0.130(VMC) + 0.001(VMC)^2] (DF)^{0.985}$ ...(6.42)

B3 : $CR = [33.84 - 70.62(VMC) + 37.670(VMC)^2] (DF)^{0.027}$ ...(6.43)

B4 : $CR = [1.451 - 0.558(VMC) + 0.001(VMC)^2] (DF)^{0.461}$ ...(6.44)

It may however be mentioned that the predicted values of CR based on the normalized equations differ little from those predicted on the basis of un-normalized equations. Therefore the un-normalized equations were considered for further analysis.

The values of the two factors were calculated as before and the data are summarised in the following tables.

A scrutiny as before revealed that although the ratio factor I/factor II was in the range of 23 to 27 for the alloy B3 & B4, it varied from 50-82 for the alloy B1 to 99-117 for B2. Thus, on the face of it the model comprising VMC & DF did not appear to be as satisfactory as the one incorporating VMC & NOP. This was some what worrisome because DF is a more accurate representation of how heat-treating parameters influenced the distribution of the DC. One possible reason to explain this apparent anomaly is that the DF more accurately represents DC based on surface area considerations whereas NOP is more representative of the galvanic effect i.e. when DF is considered, then the surface area representation of DC is getting reflected through increased values of the factor I thereby leading to a large value of the ratio: factor I/factor II. Even if this were

Summary of the values of the first parameter based on VMC and DF
Test duration : 168 hours

Heat-treatment	B1	B2	B3	B4
900, 4,AC	-----	51.208	25.488	24.802
900,10,AC	37.077	49.404	24.202	24.615
950, 4,AC	32.657	50.799	22.576	24.984
950,10,AC	46.710	49.450	27.126	24.756

Test duration : 720 hours

Heat-treatment	B1	B2	B3	B4
900, 4,AC	-----	42.864	21.492	30.130
900,10,AC	54.749	44.480	20.656	32.426
950, 4,AC	42.401	43.615	18.503	28.784
950,10,AC	69.574	44.395	24.384	30.561

Summary of the values of the second parameters based on VMC and DF
Test duration : 168 hours

Heat-treatment	B1	B2	B3	B4
900, 4,AC	-----	0.517	0.991	0.993
900,10,AC	0.622	0.454	0.992	0.991
950, 4,AC	0.665	0.435	0.990	0.992
950,10,AC	0.570	0.482	0.990	0.990

Test duration : 720 hours

Heat-treatment	B1	B2	B3	B4
900, 4,AC	-----	0.487	0.975	0.738
900,10,AC	0.362	0.423	0.978	0.662
950, 4,AC	0.417	0.403	0.974	0.699
950,10,AC	0.300	0.451	0.973	0.622

Table representing ratio of factor I/factor II
Test duration : 168 hours

Heat-treatment	Factor I/factor II			
	B1	B2	B3	B4
900, 4,OQ	----	99.0	25.7	25.0
900,10,OQ	59.6	108.8	24.4	24.8
950, 4,OQ	49.1	116.8	22.8	25.2
950,10,OQ	81.9	102.6	27.4	25.0

Test duration : 720 hours

Heat-treatment	Factor I/factor II			
	B1	B2	B3	B4
900, 4,OQ	----	80.0	22.0	40.8
900,10,OQ	151.2	105.2	21.1	48.9
950, 4,OQ	101.7	108.2	19.0	41.2
950,10,OQ	231.9	98.4	25.1	49.1

so, the reason why the effect is more pronounced in the alloys B1 & B2 only is not clearly understood. One possible option is to represent the DC by a factor which is a combination of DF & NOP which could become a subject matter for further study.

The other possibility is to re-examine the basis on which the models were developed by considering the variation in the average values of CR, VMC, NOP and DF for all the alloys. The data thus collated is given in the following table.

This table revealed the variation to be small and this did not justify the large variation in factor I/factor II as observed in the earlier model predictions.

Parameter	Alloy(s)			
	B1	B2	B3	B4
VMC	23.6	18.8	18.7	18.6
NOP	34	40	37	38
DF	0.345	0.437	0.392	0.437
CR (168 hrs.)	23.97	23.70	24.37	24.58
CR (720 hrs.)	19.53	19.31	20.90	20.71

Evidently, therefore, there was a strong case for examining afresh the variation in CR as influenced by microstructure. This was done by constructing 3D-plots between CR vs (i) VCb & NOP (Figs. 6.6 & 6.7), (ii) VMC & NOP (Figs. 6.8 & 6.9) and (iii) VMC & DF (Figs. 6.9 & 6.10) for all the values for 168 hrs. and 720 hrs. test duration. These plots showed the variations to be irregular. This may perhaps explain the inconsistencies which have been observed during modelling as highlighted through the data summarized in the earlier tables.

Since, it has been concluded from the earlier analysis that a model incorporating VCb and NOP was not physically consistent, it was decided to determine the optimal minima for all the alloys incorporating the two physically consistent models namely, (i) CR vs VMC & NOP and (ii) CR vs VMC & DF (for both 168 and 720 hrs. test durations). The 3D-plots thus obtained are shown in Figures 6.12-6.15.

Based on the optimal minima, unified models (one model for all the alloys) for 168 and 720 hrs. test durations are given below:

CR vs VMC & NOP

168 hours

$$CR = [-7.140 + 2.790(VMC) - 0.0625(VMC)^2] (NOP)^{-0.008} \quad ...(6.45)$$

720 hours

$$CR = [\ 8.484 - 0.177(VMC) + 0.0036(VMC)^2] (NOP)^{0.2944} \quad ...(6.46)$$

CR vs VMC & DF

168 hours

$$CR = [-2.343 + 2.186(VMC) - 0.0493(VMC)^2] (DF)^{-0.069} \quad ...(6.47)$$

720 hours

$$CR = [69.680 - 3.950(VMC) + 0.0839(VMC0^2] (DF)^{0.3364} \quad ...(6.48)$$

The importance of these equations is that in order to get the best in terms of properties (corrosion resistance) for each alloy, the microstructure is to be so controlled that the constants should attain a value close enough to those indicated in the equations 6.45-5.48.

On the basis of the final unified models (Equation no. 6.45-6.48), contour plots (Figs. 6.16-6.19) were made incorporating VMC from 0 to 100%, NOP from 0 to 100 and DF from 0 to 1.0 to determine the variation of CR as influenced by these parameters. For the 168 hrs. test duration, the CR was negative beyond ≈42-47% and below ≈3% VMC. This was due to the negative constant associated with the term VMC^2 as is clear from a perusal of the plots (Figs. 6.12-6.15) which show a maxima for 168 hrs. (Figs. 6.12 & 6.14) and a minima for 720 hrs. (Figs. 6.13 & 6.15). This is the reason for the opposite nature of constants (A1, A2 and A3) for the two test durations. The constant A4 also showed an opposite nature for the two test durations. This was differently reflected in how the CR varied with NOP (Figs. 6.12-6.15) - a

decrease with an increase in NOP for 168 hrs. (Figs. 6.12 & 6.14) and an increase with an increase in NOP for 720 hrs. (Figs. 6.13 & 6.15) test duration.

This apparently anomalous behaviour can be explained easily on re-examining the final models (Eqs. 6.45-6.48) in the light of the Figures 6.12-6.15. To begin with it would be useful to realize that opposite trends can not exist for an identical variation in VMC & NOP or VMC & DF. Further, if the 3D-plots representing the overall corrosion behaviour at 168 hrs. are re-examined, it would be observed that a trend similar to that observed at 720 hrs. test duration could have been attained if one or two CR values would have been lower than what has been observed; in a more general sense if lower overall CR values were obtained. Further, the constant A4 which is making all the difference has a very small negative value. This can be considered to imply that because of certain surface/ structural features, the initial general corrosion was appreciably larger i.e. the bulk did not significantly contribute to its occurrence. However, at 720 hrs. test duration there is equilibration because of a larger period involved and as such the variation in CR with either VMC/ NOP or VMC/ DF is on the expected lines. In fact, it would not be incorrect to say that the same trend is almost indicated even at 168 hrs. on the premise that the value of the constants A4 although negative has a very small magnitude.

An additional observation which needs to be made is that slight inconsistencies in the interrelations summarized in the Figures 6.6-6.11 may have also arisen because it is difficult to

keep one of the dependent parameters as a constant and vary the other e.g. by retaining VMC constant and varying NOP/ DF or vice-versa. The problem, primarily responsible for the inconsistencies observed, also points out the complexities that exist in the system under investigation. The problem will further accentuate as the number of structural variables increase which would lead to larger degree of concentration/ structural inhomogeneities. The discussion further highlights the necessity of designing alloys based on simpler chemistries/ microstructures and of incorporating features such that the formation of extraneous constituents is minimized/ eliminated. Dispersed carbide is the unintended/ extraneous constituent in the experimental alloys. Having attained the same, the present study also records the various attempts that have been made to reduce their adverse effect on properties. Optimization studies based on modelling constitute a significant step in this regard.

Before concluding, it would be appropriate to compare the predictions based on the `unified model' with the CR experimentally determined(Fig.6.18). On doing so it emerges that:

VMC - NOP model

(i) For the 168 hrs. test duration the deviation is from as low as 0.17% to as high as 19% (observed only in one instance); in fact in most situations the deviation is within ±10%.

(ii) The maximum deviation is occurring corresponding to the 950°C, 10 hrs. heat-treatment.

(iii) For a test duration of 720 hrs., a nearly similar situation as above exists except that the deviation is a little higher.

Summary table of experimentally determined and predicted CR values based on the unified model (eqs. 64.5-6.48)

(a) VMC, NOP & CR

H/T schedule	CR exp.	CR pred.	%dev.	CR exp.	CR pred.	%dev.
		168 hours			720 hours	
B1, 900,10,AC	22.234	23.275	- 0.17	19.911	19.124	3.95
B1, 950, 4,AC	21.948	22.014	- 0.30	17.821	17.882	- 0.34
B1, 950,10,AC	26.730	23.268	12.95	20.913	16.215	22.46
B2, 900, 4,AC	26.040	23.267	10.67	20.923	20.261	3.16
B2, 900,10,AC	20.900	20.890	0.05	18.681	19.478	- 4.27
B2, 950, 4,AC	22.634	23.256	- 2.75	17.429	17.470	- 0.23
B2, 950,10,AC	25.221	21.059	16.50	20.202	18.849	6.70
B3, 900, 4,AC	25.002	23.115	7.55	21.157	18.872	10.80
B3, 900,10,AC	22.912	22.230	2.98	20.372	19.281	5.35
B3, 950, 4,AC	22.482	22.543	- 0.27	18.204	18.328	- 0.68
B3, 950,10,AC	27.092	21.938	19.02	23.870	18.170	23.88
B4, 900, 4,AC	25.782	22.622	12.26	23.728	19.825	16.45
B4, 900,10,AC	23.175	21.205	8.50	20.085	18.814	6.35
B4, 950, 4,AC	23.305	23.150	0.66	18.438	18.435	0.01
B4, 950,10,AC	26.075	22.463	13.85	20.586	18.037	12.38

(a) VMC, DF & CR

H/T schedule	CR exp.	CR pred.	%dev.	CR exp.	CR pred.	%dev.
		168 hours			720 hours	
B1, 900,10,AC	22.234	23.506	- 1.17	19.911	16.259	18.34
B1, 950, 4,AC	21.948	22.081	- 0.61	17.821	17.805	0.09
B1, 950,10,AC	26.730	23.763	11.10	20.913	15.614	25.34
B2, 900, 4,AC	26.040	23.013	11.62	20.923	18.271	12.67
B2, 900,10,AC	20.900	21.246	- 1.66	18.681	20.865	-11.69
B2, 950, 4,AC	22.634	23.246	- 2.70	17.429	17.421	0.05
B2, 950,10,AC	25.221	21.279	15.63	20.202	21.134	- 4.61
B3, 900, 4,AC	25.002	23.216	7.14	21.157	17.428	17.63
B3, 900,10,AC	22.912	22.290	2.71	20.372	19.506	4.25
B3, 950, 4,AC	22.482	22.753	- 1.21	18.204	18.198	0.04
B3, 950,10,AC	27.092	22.342	17.53	23.870	18.563	22.24
B4, 900, 4,AC	25.782	22.381	13.19	23.728	19.985	15.78
B4, 900,10,AC	23.175	21.529	7.10	20.085	20.348	- 1.31
B4, 950, 4,AC	23.305	22.959	1.49	18.438	18.430	0.05
B4, 950,10,AC	26.075	22.775	17.53	20.586	17.939	12.86

VMC - DF model

Nearly similar observations as above obtained.

Based on these deductions it can be stated that the methodology employed for developing a unified model is sound. It has also proved helpful in explaining the inconsistencies observed in the earlier models.

The model is particularly useful in predicting the best in terms of corrosion resistance that can be obtained with the present set of compositions. It also reveals the usefulness of B2. It is therefore, suggested that the alloy design in the future should incorporate the useful features of the alloy B2 as well as of other compositions.

6.3.1 Modelling of the deformation behaviour

Hardness is a very useful measure of the mechanical properties (deformation behaviour) of materials. Therefore, it is regarded as a quick yet a reliable parameter to measure. The higher the hardness the larger is the UTS and smaller the %elongation value. In ferrous materials (steels) hardness and tensile strength are related empirically by a conversion factor

$$5\ VHN_{30} \equiv 1\ tsi\ UTS \equiv 15.5\ MPa$$

A similar empirical law is not expected to be obeyed in cast irons in general and white irons in particular because, as engineering materials, they are a class apart from steels due to their brittleness and a generally complex microstructure. An attempt was, therefore, made to examine the possibility of establishing quantitative relations between the hardness and the deformation behaviour in the experimental alloys. The information thus generated was expected to provide a back up to the mathematical modelling work being actively organized(117).

6.3.1.1 Interrelation between compressive strength and hardness

To begin with CS(117) was plotted as a function of hardness (Fig. 6.19). As no definite relationship emerged, it was decided to plot CS/H as a function of hardness. The plot thus obtained (Fig.6.20) showed the behaviour to be consistent with a second order polynomial. The functional relationship between CS/H(R) and hardness can be represented as

$$R = A1 + A2\ (H) + A3\ (H)^2 \qquad ...(6.49)$$

where R = CS/H,

H = hardness, HV_{30},

A1, A2 and A3 are constants.

The constants A1, A2, and A3 were computed as before and the correlations thus obtained are :

Alloy B1 : $R = 19.87 - 0.051H + (0.3897E-04)H^2$ ...(6.50)

Alloy B2 : $R = 30.14 - 0.089H + (0.7548E-04)H^2$ ...(6.51)

Alloy B3 : $R = 23.08 - 0.061H + (0.4825E-04)H^2$ ...(6.52)

Alloy B4 : $R = 26.35 - 0.075H + (0.6306E-04)H^2$ ...(6.53)

Based on the above equations, CS was predicted for different hardness values and a plot of $CS_{exp.}$ vs $CS_{pred.}$ showed the scatter to be within ±5% except in some instances corresponding to the 1050°C, 10 hours heat-treatment (Fig. 6.21).

CS for different hardness values (air cooled condition) obtained in the present study, were determined on the basis of the above models. A comparison between the predicted and the experimentally determined values reveals that the difference in most cases does not exceed ±5% (Fig. 6.21). In some instances the experimental and the predicted values differed by a large margin due to casting defects present in the specimens.

6.3.1.2 Interrelation between %strain and hardness

Similar steps (Figs 6.22 & 6.23) as above were initiated to arrive at models interrelating %strain(117) and hardness. The quantitative relationships arrived at are :

Alloy B1 : $R = 0.1917 - 0.3909E-03H + 0.1677E-06H^2$ ...(6.54)

Alloy B2 : $R = 0.3880 - 1.1049E-03H + 0.8280E-06H^2$ ...(6.55)

Alloy B3 : $R = 0.3015 - 0.8005E-03H + 0.5465E-06H^2$ ...(6.56)

Alloy B4 : $R = 0.2709 - 0.6229E-03H + 0.3544E-06H^2$ ...(6.57)

where R = %strain/H,

H = hardness, HV_{30}

A1, A2, and A3 are constants.

%strain calculated on the basis of the above models were plotted against experimentally determined values of %strain. It was found that data points fall well within ±10% error band except one or two instances reflecting favourably on the validity of the models developed (Fig. 6.24).

6.3.2 Discussion

Models interrelating deformation behaviour with the hardness are successfully developed. Unlike in steels, the microstructure of cast irons is complex. The problem is furthermore accentuated in white irons especially with martensitic matrices because of their extreme brittleness. On heat-treating, as has been observed in the present investigation, the matrix transforms to austenite whose volume fraction and stability increase with heat-treating time and temperature. The second phase mainly comprises massive carbide and dispersed carbide which are extremely hard and therefore, further increase the embrittling behaviour when present in a martensitic matrix and will counteract the usefulness of an austenitic matrix when present in austenite-based microstructures. Therefore, the deformation behaviour will follow the following trend :

(i) A relatively low strength and % strain in the as-cast condition, wherein the matrix microstructure comprises P/B + M and the carbides are massive and mostly interconnected.

(ii) A marked improvement in strength more so the %strain as the matrix transforms to austenite.

(iii) A further improvement in these parameters as the

stability and the volume fraction of austenite increase which is simultaneously offset due to the complex nature of the massive carbides and a coarsening of dispersed carbides; their combined adverse effect reaching a peak corresponding to the 950°C, 10 hrs. heat-treatment.

(iv) A further marked improvement in CS and %strain due to a decrease in volume fraction of massive carbides and dissolution of dispersed carbide; the former will reach a maximum corresponding to 1050°C, 10 hrs. heat-treatment whereas the latter dissolve on prolonged soaking at 1000°C.

(v) Any slowing down of the above trends (involving improvement in CS and %strain) if transformation producing adverse microstructural features is initiated along with the changes mentioned in point (iv).

The models representing an interrelation involving a second order polynomial are therefore not only appropriately justified but are consistent with the transformations occurring in the experimental alloys. This deduction is evidently valid both for the compressive strength as well as for the %strain values. In purely mathematical terms, the validity of the models is duly substitiated on the basis that the predicted values in most instances are within ± 10% of the experimental values (Tables 6.4-6.11).

Models at equations 6.50-6.57 have been employed for assessing the mechanical properties corresponding to the hardness values obtained in the present investigation (Figs. 6.25-6.28;

Table 6.12). This is justified since the experimental alloys resemble those investigated in the earlier study. The models thus developed are both physically and mathematically consistent.

CHAPTER VII

GENERAL DISCUSSION, CONCLUSIONS AND SUGGESTIONS FOR FUTURE WORK

7.1 General discussion

The present investigation has succeeded in assessing the transformation behaviour of the experimental alloys in a fair detail. The alloys intended to resist corrosion, were designed to include low cost indigenously available alloying elements Mn, Cr and Cu. Possible clues to their likely transformation behaviour are provided by their composition. The least alloyed amongst them (B1) is designed to produce 'M' on air cooling from 800°C to 850°C and retain austenite in large amounts on air cooling from higher temperatures (Section 4.1.2).

Austenite stabilizing tendency of the other alloys is at least equivalent or higher than B1. Based on these considerations it is easy to comprehend the logical pattern followed by the microstructural changes on heat-treating, namely the as-cast microstructure changing into M + MC + DC (+ some austenite?), austenite + M + MC + DC , austenite + MC + DC and finally austenite + MC as the temperature is raised from 800 to 1050°C and the time varied at each of these temperatures from 2 to 10 hours. The mechanism of the formation of dispersed carbides is highlighted and temperature regime of their stability indicated.

The coarsening behaviour of the DC has been assessed on the basis of a newly evolved parameter called the 'coarsening index'. The effect of heat-treating parameters in decreasing the volume fraction and in altering the morphology of MC has been discussed in detail. This aspect of the investigation has been concluded by identifying the nature of the carbides formed by X-ray

diffraction enabling the sequence of carbide transformation to be established.

Hardness measurements were shown to be consistent with microstructural changes i.e. hardness successively decreased with temperature and time. This enabled the transformation behaviour to be mathematically modelled. The model has been shown to be 'mathematically' and 'physically' consistent. 3-D plots amongst hardness, temperature and time helped in arriving at a better understanding of the transformation behaviour of the alloys at a glance. The significance of the 'iso-hardness' plots has been explained.

X-ray diffractometry proved extremely useful in deciding upon the nature of the matrix microstructure in 'marginal' cases and in identifying carbides. This study was helpful in revealing the presence of elemental copper and Fe_3Si_2C. A part of the ambiguities, still persisting, were successfully resolved with EPM analysis which additionally proved useful in determining the partitioning of the different elements (Mn, Cr, Cu etc.) into the matrix and carbide phases.

The DTA studies, besides establishing the transformation temperatures, also predicted the high temperature response of different microstructures attained in the experimental alloys. This proved useful in deciding upon the most useful microstructure from the point of view of high temperature applications. Such a data is of considerable design interest.

Electro-chemical characterization of the different microstructures on the basis of potentiostatic studies confined

to the Tafel region, established the usefulness of a large volume fraction of austenite with enhanced stability in improving the corrosion resistance in 5% NaCl solution. The studies also revealed how an 'unfavourable' morphology of the MC and 'optimally' coarsened dispersed carbides adversely affected corrosion resistance.

High speed compression testing was useful in characterizing the different microstructures based on their deformation behaviour. The data clearly brings into 'focus' that 'brittleness' is manifested by low CS & %strain values. The study further establishes how these parameters improve as the heat-treating temperature and time are increased. It has been possible to establish qualitatively authentic interrelations between the microstructure and deformation behaviour. Models have been developed interrelating R (CS/H or %strain/H) with the hardness and this would enable prediction of mechanical properties based on 'hardness' values.

A key aspect of the present investigation has been the extensive quantification of the microstructure and the development of models interrelating (i) hardness with the heat-treating parameters, (ii) 'distribution factor' representing DC with temperature and time, (iii) weight gain with temperature and time, (iv) hardness with compressive strength and %strain, (v) corrosion rate with the microstructure and (vi) corrosion rate with the deformation behaviour. These models would prove extensively useful in optimizing the microstructures and in alloy design in general.

In fact, this idea has been put into practice while modelling the corrosion behaviour. This has been a high point of perhaps the first effort aimed at optimizing the microstructure in terms of VMC and NOP/DF. The analysis put forth has helped not only in understanding why inconsistencies arose while developing the earlier models but also in evolving what best can be achieved in terms of corrosion resistance from the compositions investigated in the present study. This has led to the development of a unified model for predicting the corrosion behaviour of all the experimental alloys.

7.2 Conclusions

Under the existing experimental conditions, the following conclusions may be arrived at:

1. Low cost elements Mn, Cu along with Cr can be usefully employed in designing alloy white irons with useful mechanical properties and corrosion behaviour. The microstructures that were characterized for their deformation and electro-chemical behaviour (mostly in 5% NaCl solution) are P/B + M + MC, M + τ + MC, M + τ + MC + DC τ + MC + DC and τ + MC. Most of the aforesaid microstructures were generated through heat-treatments. The temperature ranges over which different microstructures exist are given below:

   As-cast : P/B + M + MC with and without RA.

   Upto 900°C : M + MC + DC with and without RA depending upon ST and SP.

   Upto 1000°C : A + MC + DC or A + MC with and without M (in traces) depending upon ST and SP.

   1050°C : A + MC.

2. The volume fraction of MC decreased with temperature or with soaking period at a given heat-treating temperature. The decrease was marked at temperatures only at ≥1000°C. MC were rendered discontinuous from the early stages of heat-treatment. The 'rounding-off' tendency set in at 1000°C.

3. Dispersed carbides formed during soaking, corresponding to the 800°C, 10 hrs. heat-treatment, by a mechanism involving precipitation from austenite and also during air cooling.

Particles constituting them belonged to classes I and I. (size upto 1.16 micron). On heat-treating the overall spread of the particles extended upto class VI (size upto 3.48 micron).

4. Dispersed carbides underwent coarsening which was characterized by the 'spilling over' of the particles into the classes III to VI. Coarsening was marked at 900 and 950°C and was assessed on the basis of the coarsening index.
5. DC get dissolved on heat-treating at 1000°C.
6. The carbides to form in the experimental alloys are M_3C, $M_{23}C_6$, M_5C_2 and M_7C_3. M_3C and $M_{23}C_6$ carbides dissolved/ transformed or were replaced by the higher temperature carbides M_5C_2 and M_7C_3 (≈950-1000°C). The latter is predominant in B1 and B2 whereas both are present in B3 and B4 on prolonged soaking at 1050°C.
7. The morphology of M_7C_3 in the eutectic formed at 1050°C is harmful from the point of view of overall properties because it is in the form of plates bridging massive carbide regions. There are definite indications to suggest that the carbide begins to form even on prolonged soaking at 1000°C (soaking period ≈10 hrs. or more).
8. Hardness in general decreased with an increase in the heat-treating temperature in the order

   $H_{1050} < H_{1000} < H_{950} < H_{900} < H_{850} < H_{800}$
9. For a given heat-treating temperature, hardness varied linearly with the soaking period. It increased with an increase in soaking period on heat-treating from 800 and

850°C, remained practically unaltered on heat-treating from 900 and 950°C and decreased on heat-treating from 1000 and 1050°C. Exceptions are B2 and B4 when heat-treated from 850°C (hardness was independent of the soaking period).

10. For a given heat-treating period, the variation in hardness with temperature was in the form of a horizontal 'S' shape.

11. X-ray diffractometry revealed the presence of 'M' in marginal cases. It also revealed the presence of Fe_3Si_2C and elemental Cu.

12. Transformation behaviour of the experimental alloys, over the entire range of temperature and soaking period, can be represented by the equations:

B_1 : $H = 168.213\ e^{1471.47/T} + (0.043-0.374\times10^{-4}T)t$

B_2 : $H = 100.779\ e^{1889.66/T} + (0.026-0.223\times10^{-4}T)t$

B_3 : $H = 98.285\ e^{2021.33/T} + (0.037-0.316\times10^{-4}T)t$

B_4 : $H = 78.357\ e^{2205.77/T} + (0.027-0.244\times10^{-4}T)t$

where H = Vicker's hardness at 30 kg. load

T = temperature in °K

t = time in seconds.

The first parameter models the matrix transformation and the second parameter the carbide transformation.

13. 3-D plots interrelating temperature and time with hardness represented that the stage at which the second factor in the above model became negative can be represented by a surface.

14. The carbide transformation sequence observed is

M_3C	present upto 1000°C, 4 hours
$M_{23}C_6$	present upto 950°C, 4 hours & at best in traces upto 950°C, 10 hours
M_5C_2	present upto 1000°C,10 hours/ 1050°C, 4 hours
M_7C_3	present from 1000°C, 10 hours to 1050°C, 10 hours

15. DTA data showed that whereas the alloys B1 & B3 undergo the (i) α/α' -> austenite (722-735°C) and (ii) a carbide transformation (890-955°C), the alloys B2 & B4 undergo an additional carbide transformation at 1050-1075°C.

17. TG data showed that the as-cast microstructure was only suitable upto ≈600°C. However, on heat-treating from 950 and 1050°C, the temperature upto which the alloys could be usefully employed was increased to 800°C in the latter instance and slightly <800°C in the former.

17. Mathematical modelling of the TG data showed that %TG is related to the temperature by an equation

Alloy B1 %TG = 1.561878 + 2665.150 exp(-7529.676/T)

Alloy B2 %TG = 1.310813 + 9623.292 exp(-8771.445/T)

Alloy B3 %TG = 1.515658 + 3465.314 exp(-7609.409/T)

Alloy B4 %TG = 1.566102 + 4004.606 exp(-7792.101/T)

18. The higher the stability of austenite and larger the volume fraction, the higher the corrosion resistance.

19. Presence of second phase in general lowered corrosion resistance, its effect being a function of the morphology

& size, shape and distribution. The combined adverse effect of MC + DC approached a maximum corresponding to the 950°C, 10 hrs., AC heat-treatment. Similarly the adverse effect of MC was a maximum at the 105°C, 4 hrs., AC heat-treatment.

20. On heat-treating from 900 and 950°C, the corrosion rate is related with the volume fraction of MC+DC (VCb) and NOP through the following equations:

Test duration : 168 hours

Alloy B1: $CR = [2003.968-101.423(VCb)+1.290(VCb)^2](NOP)^{0.187}$

Alloy B2: $CR = [177.200-10.94(VCb)+0.192(VCb)^2](NOP)^{0.011}$

Alloy B3: $CR = [550.60-34.71(VCb)+0.558(VCb)^2](NOP)^{0.199}$

Alloy B4: $CR = [105.01-6.830(VCb)+0.125(VCb)^2](NOP)^{0.199}$

Test duration : 720 hours

Alloy B1: $CR = [2074.523-105.768(VCb)+1.356(VCb)^2](NOP)^{0.117}$

Alloy B2: $CR = [195.200-12.28(VCb)+0.211(VCb)^2](NOP)^{0.011}$

Alloy B3: $CR = [528.935-33.462(VCb)+0.538(VCb)^2](NOP)^{0.199}$

Alloy B4: $CR = [16.384-0.387(VCb)+0.006(VCb)^2](NOP)^{0.199}$

where VCb = total volume fraction of MC+DC

NOP = number of particles(DC)

CR = corrosion rate in mdd.

This model when modified as

$CR = [A1 + A2\ (VMC) + A3\ (VMC)^2](NOP)^{A4}$

gave a more representative idea of the physical happenings.

Test duration : 168 hours

Alloy B1: $CR = [165.554-11.771(VMC)+0.232(VMC)^2](NOP)^{0.074}$

Alloy B2: $CR = [126.646-11.524(VMC)+0.312(VMC)^2](NOP)^{0.013}$

Alloy B3: $CR = [650.510-65.711(VMC)-1.715(VMC)^2](NOP)^{0.010}$

Alloy B4: $CR = [21.679-0.316(VMC)+0.01(VMC)^2](NOP)^{0.067}$

Test duration : 720 hours

Alloy B1: $CR = [67.605-4.248(VMC)+0.080(VMC)^2](NOP)^{0.128}$

Alloy B2: $CR = [177.124-17.133(VMC)+0.453(VMC)^2](NOP)^{0.011}$

Alloy B3: $CR = [732.30-74.52(VMC)+1.934(VMC)^2](NOP)^{0.0245}$

Alloy B4: $CR = [13.061-0.186(VMC)+0.001(VMC)^2](NOP)^{0.199}$

21. On incorporating the effect of DC on the basis of the distribution factor (DF), the above equations are modified as:

Test duration : 168 hours

Alloy B1: $CR = [390.380-27.505(VMC)+0.528(VMC)^2](DF)^{0.448}$

Alloy B2: $CR = [48.300-0.091(VMC)+0.01(VMC)^2](DF)^{0.907}$

Alloy B3: $CR = [683.507-69.060(VMC)+1.803(VMC)^2](DF)^{0.010}$

Alloy B4: $CR = [26.55-0.282(VMC)-0.01(VMC)^2](DF)^{0.010}$

Test duration : 720 hours

Alloy B1: $CR = [491.519-32.537(VMC)+0.589(VMC)^2](DF)^{0.959}$

Alloy B2: $CR = [58.24-1.292(VMC)+0.027(VMC)^2](DF)^{0.99}$

Alloy B3: $CR = [825.84-84.07(VMC)+2.187(VMC)^2](DF)^{0.0270}$

Alloy B4: $CR = [50.023-1.237(VMC)+0.01(VMC)^2](DF)^{0.463}$

where VMC = volume fraction of MC

DF = distribution factor.

The above equations after normalization assumed the form

Test duration : 168 hours

Alloy B1: $CR = [10.386-19.866(VMC)+10.301(VMC)^2](DF)^{0.518}$

Alloy B2: $CR = [0.938-0.002(VMC)+0.076(VMC)^2](DF)^{0.878}$

Alloy B3: $CR = [25.035-51.8556VMC)+27.747(VMC)^2](DF)^{0.010}$

Alloy B4: $CR = [0.941-0.001(VMC)+0.012(VMC)^2](DF)^{0.044}$

Test duration : 720 hours

Alloy B1: $CR = [5.728-9.151(VMC)+4.275(VMC)^2](DF)^{0.567}$

Alloy B2: $CR = [1.129-0.130(VMC)+0.001(VMC)^2](DF)^{0.985}$

Alloy B3: $CR = [33.841-70.622(VMC)+37.670(VMC)^2](DF)^{0.027}$

Alloy B4: $CR = [1.451-0.558(VMC)+0.001(VMC)^2](DF)^{0.461}$

22. 3D plotting of the minima optimals in terms of (i) CR, VMC & NOP and (ii) CR, VMC & DF indicate the optimal conditions vis-a-vis the microstructure to attain the best in terms of corrosion resistance.

23. Using these minima optimals as the base a unified model describing the corrosion behaviour of all the experimental alloys is of the form :

CR vs VMC & NOP

168 hours

$$CR = [-7.140 + 2.790(VMC) - 0.0625(VMC)^2] (NOP)^{-0.008}$$

720 hours

$$CR = [8.484 - 0.177(VMC) + 0.0036(VMC)^2] (NOP)^{0.2944}$$

CR vs VMC & DF

168 hours

$$CR = [-2.343 + 2.186(VMC) - 0.0493(VMC)^2] (NOP)^{-0.069}$$

720 hours

$$CR = [69.680 - 3.950(VMC) + 0.0839(VMC0^2] (NOP)^{0.3364}$$

Barring few instance the deviation between the predicted and the experimentally determined values does not exceed ±10-12%.

24. From the corrosion resistance point of view the alloy B2 has again been found to be better than the rest followed by B4, B3 and B1.

25. CS and %strain are not linearly related with hardness as is found in the case of steels. It is because of the heterogeneous nature of the microstructures generally found in cast irons. It was established that the CS and %strain can be related with hardness as a second order polynomial as

Alloy B1 : $R = 19.87 - 0.051H + (0.3897E-04)H^2$

Alloy B2 : $R = 30.14 - 0.089H + (0.7548E-04)H^2$

Alloy B3 : $R = 23.08 - 0.061H + (0.4825E-04)H^2$

Alloy B4 : $R = 26.35 - 0.075H + (0.6306E-04)H^2$

where R = CS/H and CS in MPa

Alloy B1 : $R = 0.1917645 - 0.3909492E-03H + 0.1677448E-06H^2$

Alloy B2 : $R = 0.3880980 - 1.1049360E-03H + 0.8280589E-06H^2$

Alloy B3 : $R = 0.3015848 - 0.8005172E-03H + 0.5465336E-06H^2$

Alloy B4 : $R = 0.2709832 - 0.6229439E-03H + 0.3544085E-06H^2$

where R = %strain/H,

H = hardness, HV_{30}

26. From the point of view of mechanical properties, martensite bearing microstructures are brittle whereas the austenite based microstructures give high values of CS and %strain. The effect of DC on the deformation behaviour depends upon their size, shape and distribution. Similarly, the effect of MC is governed by their volume fraction, morphology and compatibility with the matrix.

27. From the point of view of overall mechanical properties, the alloy B2 has been found to be most useful followed by B4, B3 and B1. It is possible that the presence of a higher P content in B3 and B4 may have lead to some what inferior properties in them.

28. In view of 21 and 24 it is recommended that the future modifications in the alloy chemistry should incorporate the beneficial features of the composition B2. Further, the alloying elements should be so adjusted that the microstructure(s) of form on heat-treating from lower temperatures.

7.3 Suggestions for future work

The future work should be carried out on the following lines:

1. Crystal structure determination of carbides by X-ray diffractometry.
2. Detailed structural identification by EPMA.
3. Extensive use of DTA for transformation study.
4. High temperature performance study by DTA.
5. Extensive electro-chemical characterization of different microstructural couples by potentiostatic method.
6. Development of useful interrelations using numerical methods and computing devices.

REFERENCES

1. Butlef and Ison, 'Corrosion and its prevention in water', Leonard Hill, London.
2. Hurst, J.E., and Piley, R.V., JISI, 155, 172, 1974.
3. 'Corrosion', edited by Shreir, L.L., Newness-Butterworths, London, vol.1,pp.3:86, 8:123.
4. Metals Hand-book, vol.1, 'Properties and Selection; Irons and Steels', 9th edition, ASM, Metals Park, Ohio, p.76,1978.
5. Jackson, R.S., JISI, No.208, pp.163-167, 1970.
6. Kutner, C., Tech. Mitt. Krup., No.1, March 17, 1933.
7. 'Ni-resist austenitic cast irons : Propreties and applications', International Nickel Co. Inc., pp.1-21, 1965.
8. Hoar, T.P., Journal Applied Chemistry, no.11, p.121, 1961.
9. Vernon, W.H.J., 'The conservation of natural resources', Instn. of Civil Engineers, London, p.105, 1957.
10. Potter, E.C., 'Electrochemistry', Cleaver Hume, London, p.231, 1956.
11. Uhlig, H.H.(Ed.), 'The corrosion hand-book', Wiley, New York and Chapman and Hall , London, 1948.
12. Uhlig, H.H., 'Corrosion and corrosion control',Wiley, New York, 1971.
13. Fontana, M.G., and Greene, N.D., 'Corrosion Engineering', McGraw Hill, 1967.
14. Fontana, M.G., and Stachle, R.W., 'Advances in corrosion science and technology', Plenum Press, New York, 1970.
15. Evans, U.R., 'The corrosion and oxidation of metals : Scientific principles and practical applications', Edward Arnold Publishers Limited, London, p.12, 1960.

16. Webster's third new international dictionary, G and C Merriam Co., Springfield, Mass., p.512, 1966.

17. Jain, N.C., Ph.D. Thesis, University of Roorkee, Roorkee, 1986, p.14.

18. Cleary, H.J. and Greene, N.D., 'Corrosion properties of iron and steel', Corrosion Science, vol.7, pp.821-831, 1967.

20. Campbell, H.S., 'Metallurgical Factors', Hand-book of corrosion testing and evaluation, Corrosion monograph series, Ed. Ailor, W.H. etal., Reynold Metals Co., Virginia (USA), 1971,p.5.

23. Roherg, K., Gisserie, 58, 1971, pp. 697-705.

24. Boniszewski, T. Wathinson, F., 7(2), 7(3), 90, 145, (1973).

25. Benson, R.B., Jr., Dann, R.K. and Roberts, L.W., Trans. Met. Soc. AIME, Vol. 242, p. 2199-2205 (1966).

26. Steigerwald, R.F., Vol. 33, No. 9, 1977, pp. 338-342

27. Krauss, G. and Marder, A.R., Met. Trans., 2, 2345 (1971).

28. Snape, E., Schaller, F.W. and Forbesjones, R.M., Corr., Vol. 25, No. 9, Sept. 1969, p-380.

29. Lena, A., Metal progress, 66, pp. 97-99 (1954).

30. Michael, L. Streicherg, Corrosion, Vol. 30, No. 4, April, 1974.

31. Hochman, R.F., NACE Basic corrosion course, Official publication, Chapter 11, pp. 3-18, Univ. of Miami, FLA.

32. Gainer, L.J. and Wallwork, G.R.,Corr., Oct. 1979, Vol.35, No. 10, P-435.

33. Biom, K.J. and Degerbeck, J., Vol. 16, Oct. 1983, Metals abstracts, Pulp and paper industry corrosion problems, Vol.4.

34. Firivkusm, Z.P., and Uhlig, H.H., J. Electrochem. Soc., 111, 522 (1964).

35. Bain E.C., and Paxton, H.W., 'Alloying elements in steels' ASM, Metals Park, Ohio, 1962.

36. Metals Hand-book, Vol. 10, 8th edition, 'Failure analysis and prevention', ASM, Metas park, Ohio, 1975.

37. Patwardhan, A.K., Personnal communication.

38. Jain, N.C., Ph.D. Thesis, University of Roorkee, Roorkee, 1986.

39. Yang, W. and Pourbaix, A., Metal Abstracts, 8212-72-0550, Metalic corrosion, 8th International congress on metallic corrosion, Vol. 1.

40. Pearce, J.G., and Bromage, K., 'Copper in cast iron', C.D.A. publication, No. 65, Hutchinson of London for the Development Association, 1964, pp. 61-64.

41. Jain,N.C., Ph.D. Thesis, University of Roorkee, Roorkee, 1986, pp. 39-41.

42. Singh, S.S., Ph.D. Thesis, University of Roorkee, 1982.

43. Jain,N.C., Ph.D. Thesis, University of Roorkee, Roorkee, 1986, pp.43-44.

44. Angus, H.T., 'Cast iron', Butterworths, London, 1976, p-53.

45. Kumar,V. and Mohanty,B.,'X-ray diffractogram index', Software Section, Scripta Metallurgica, Vol.20, Dec.1986.

46. Index (Inorganic) to the Powder diffraction File 1971, compiled and published by JCPDS, Pennsylvania.

47. Fink's (six-entry) Inorganic Index to the Powder Diffraction File 1971, ibid.

48. Selected Powder Diffraction Data for Metals and Alloys,

JCPDS, Pennsylvania, First ed., 1978, vol.1 & 2.

49. Pearson, W.B., 'A Handbook of Lattice Spacings and Structures of Metals and Alloys', Pergammon Press, Oxford, vol.2, 1967.

50. Singh, S.S., Ph.D. Thesis, University of Roorkee, 1982.

51. Greene, N.D., Experimental electrode Kinetics, Ressenlaer polytechnic Institute, Troy, New York (1965).

52. G-1-72, Standard practice for preparation, cleaning and evaluating corrosion test specimens, Annual book of ASTM standards, part 10, Philadeiphia, 1978.

53. G.31, Standars recommendation practice for preparation, cleaning and evaluating corrosion test specimens, Annual book of ASTM standards, part 10, Philadeiphia, 1978.

54. Himmelblau, D.M., 'Applied Non- Linear Programming', McGraw-Hill book company, 1975.

55. Non-Linear Programming-2, Editted by Mangasarian, O.L., Meyer, R.R., and Robinson, S.M., Academic Press, Inc., New York, San Francisco, London, 1975.

56. Singh, S.S., Ph.D. Thesis, University of Roorkee, 1982.

57. Bolten, J.D., Petty, E.R., and Allen, G.B., JISI, 209, 1314 (1969).

58. Orowan, E., 'Symposium on internal Stresses in metals and alloys', 451 (1948).

59. Smallman, R.E., 'Modern physical netallurgy', Third edition, Butterworths, London, 1970, pp. 405-459.

60. Reiss, M., Rosenthal, P.C., Loper, C.R., and Heine, R.W., AFS Transactions, 79, 1971, p-565.

61. Burgess, P.B., AFS Trans., 71, 1963, p.477.

62. Pearce, J.G. and Bromage, K., 'Copper in Cast Iron', Copper Development Association, London, 1964, pp.41-43.

63. Pearce, J.G. and Bromage, K., ibid., pp.91.

64. Heine, R.W. and Rosenthal, P.C.,'Principles of Metal Casting', McGraw-Hill, New York, 1967.

65. Wagner,C., Z. Elecktrochem., 65(61), 581.

66. Metals Handbook, ASM, Vol.8, 8th ed., Metals Park, Chio.

67. Lewis, M.H. and Hattersley, B., Acta Met., 1965, 13, p.1159.

68. Mahla, E.M. and Nielsen, N.A., Trans.ASM, 1951, 43, p.290.

69. Kinzel, A.B., J.Met., 1952, 4, p.469.

70. Stickler, R. and Vinckier, A., Trans. ASM, 1961, 54, p.362.

71. Stickler, R. and Vinckier, A., Corros. Sci., 1963, 3, p.1.

72. Stickler, R. and Vinckier, A., Rev. Met., 1963, 60, p.489.

73. Stickler, R. and Vinckier, A., Trans. Met. Soc. AIME, 1962, 224, p.1021.

74. Lewis, M.H. and Hattersley : as above

75. Ronald, T.M.F. and Bodsworth, C., JISI, 1965, 203, p.352.

76. Beech, J. and Warrington, D.H., JISI, May 1966, pp.460-467.

77. Martray, F. and Usseglio, R.,'Atlas of Transformation Charatectristics of Cr and Cr-Mo White Irons', Climax-Molybdenum, S.A., pp.7-8.

78. Metals Handbook, ASM, Metals Park, Ohio, Vol.7, pp.166-169.

79. Metals Handbook, ASM, Metals Park, Ohio, Vol.7, p.141.

80. Goldschmidt, H.J., 'Interstitial Alloys', 1967, p.88.

81. Westgren, A., Nature, Lond., 132, 1933, p.480.

82. Goldschmidt, H.J., 'Interstitial Alloys', 1967, pp.108-113.

83. Beckitt, F.R. and Clark, B.R., Acta Met., 1967, 15, p.113.

84. Goldschmidt, H.J., 'Interstitial Alloys', 1967.

85. Goldschmidt, H.J., 'Interstitial Alloys', 1967.

86. Wever, F. and Koch, W., Stehl Eisen, 1954, 74, p.989.

87. Smith, E. and Nutting. J, JISI, 1957, 187, pp.314-329.

88. Pickering, F.B., 4th Int. Conf. on Electronmicroscopy, 1958, Berlin, 668.

89. Nutting, J., JISI, Vol.207, June 1969, pp.872-893.

90. Woodhead, J.H. and Quarrell, A.G., JISI, 605, 1965, p.203.

91. Mills, K.C., Argent, B.B. and Quarrell, A.G., JISI, Jan 1961, pp.9-21.

92. Kuo,K., JISI, 1953,173, pp.363-374.

93. Honeycombe, R.W.K. and Seal, A.K., JISI, 188, 1958, p.9

94. Bilby, B.A. and Pickering, F.B., ISI Sp. Report 64, 313.

95. Balluffi, R.W. et al., Trans. ASM. 1951, 43, p.493.

96. Patwardhan, A. K., Ph.D. Thesis, University of Roorkee, Roorkee, 1979.

97. May, I.L. and Schetky, L.M.'Copper in Iron and Steel', John Wiley & Sons, New York, 1982.

98. Swarup, D. and Rastogi, A.,'Elements of metallurgy', Rastogi Publications, Meerut, p.16.

99. Singh, S.S., Ph.D. Thesis, University of Roorkee, Roorkee, 1983.

100. Sandoz, G.,'Recent research in cast iron', Ed. H. Merchant, Gordon and Beach, New York, 1968, p.50.

101. Schutze, D., 'Differential Thermal Analysis', Weinhim Verlag, Cherie, 1969.

102. Mackenzie, R.C., 'Differential Thermal Analysis', Vol.1,

Academic Press, London, 1970, p.32.

103. Kofstad, P., 'High Temperature Oxidation of Metals', John Wiley & Sons Inc., New York, 1966.

104. Kubaschewski, O. and Hopkins, B.E., 'Pxidation of Metals and Alloys', Butterworths, London, 1962.

105. Hauffi, K., 'Oxydation Von Metallen Und Metallefierungen, Springer', Berlin, 1957.

106. Benard, J.,'Oxydation des Metaux', Gauthier Villars et C, Paris, 1962.

107. Evans, U.R., 'The Corrosion and Oxidation of Metals', Edward Arnold Ltd., London, 1960.

108. Loviers, J., Compt. rend., 229(1949), p.547.

109. Webb, W.W., Norton, J.J. and Wgner, C., J. Electrochem. Soc., 103, 1956, p.107.

110. Haycock, E.W., J. Electrochem. Soc., 106, 1059, p.771.

111. Kofstad, P., Acta Chem. Scand. 12, 1959, p.501.

112. Sewell, P.B. and Cohen, M., J. Electrochem. Soc., 111, 1964, p.501.

113. Sewell, P.B. and Cohen, M., J. Electrochem. Soc., 111, 1964, p.508.

114. Rahmel, A., Z. Elektrochem., 66, 1962, 363, p.284.

115. Jain, N.C., Ph.D. Thesis, University of Roorkee, Roorkee, 1986, pp.67-70.

116. Patwardhan, A.K., Ph.D. Thesis, University of Roorkee, Roorkee.

117. Jain, N.C., Ph.D. Thesis, University of Roorkee, Roorkee, 1986, pp. T-65 to T-75.

118. Patwardhan, A.K. and Jain, N.C., Met. Trans. (to appear).

Table-1.3(a) Chemical composition of Ni-resist irons, Percent

	Type 1 Aus101a	Type 1B Aus101b	Type 2 Aus102a	Type 2B Aus102b	Type 3 Aus105	Type 4	Type 5
C	3.00 max	3.00 max	3.00 max	3.00 max	2.60 max	2.60 max	2.40 max
Si	1.00-2.80	1.00-2.80	1.00-2.80	1.00-2.80	1.00-2.00	5.00-6.00	1.00-2.00
Mn	1.00-1.50	1.00-1.50	0.80-1.50	0.80-1.50	0.40-0.80	0.40-0.80	0.40-0.80
Ni	13.50-17.50	13.50-17.50	18.00-22.00	18.00-22.00	28.00-32.00	29.00-32.00	34.00-36.00
Cu	5.50-7.50	5.50-7.50	0.50 max	0.50 max	0.50 max	0.50 max	0.50 max
Cr	1.75-2.50	2.75-3.50	1.75-2.50	3.00-6.00	2.50-3.50	4.50-5.00	0.01 max

1 Where the presence of copper offers corrosion resistance advantages, type 1 is recommeneded.
2 For handling caustics, food, etc., where copper contamination can not be tolerated, type 2 is recommended.
3 Where some machining is required, the 3.0 to 4.0 Cr level is recommended.
4 Where higher hardness, greater strength and added heat resistance are desired, the chromium may be 2.5-3.0% at the expense of increased expansivity.

Table-1.3(b) Chemical composition of SG Ni-resist irons, percent

	Type D-2	Type D-2B	Type D-2C	Type D-2M	Type D-3	Type D-3A	Type D-4	Type D-5	Type D-5B
C	3.00 max	3.00 max	2.90 max	2.70 max	2.60 max	2.60 max	2.60 max	2.40 max	2.40 max
Si	1.75-3.00	1.75-3.00	2.0-3.0	1.5-2.6	1.50-2.80	1.50-2.80	5.0-6.0	1.50-2.75	1.50-2.75
Mn	0.70-1.0	0.70-1.0	1.80-2.40	3.75-4.50	0.50 max	0.50 max	0.50 max	0.50 max	0.50 max
P	0.08 max	0.08 max	0.08 max	0.08 max	0.08 max	0.08 max	0.08 max	0.08 max	0.08 max
Ni	18.0-22.0	18.0-22.0	21.0-24.0	21.5-24.0	28.0-32.0	28.0-32.0	29.0-32.0	34.0-36.0	34.0-36.0
Cr	1.75-2.50	2.75-4.0	0.50 max	0.2 max	2.50-3.50	1.00-5.50	4.50-5.50	0.10 max	2.0-3.0

Table-1.4a Mechanical properties of Ni-resist irons

	Type 1 Aus 101a	Type 1B Aus 101b	Type 2 Aus 102a	Type 2B Aus 102b	Type 3 Aus 103	Type 4	Type 5
Tensile Strength	11-13.5	11-15.5	11-13.5	11-15.5	11-15.5	11-13.5	9-11
ton/in² (Kg/m²)	(17-21)	(17-24)	(17-21)	(17-24)	(17-24)	(17-24)	(14-17)
Compressive Strength	(44-53)		44-53	58-71	44-50	36	36-44
ton/in² (Kg/m²)	(69-84)		(69-84)	(91-112)	(69-79)	(57)	(57-69)
Torsional Strength	35-40		35-40	45-60	35-45	29	30-35
lb/in²x10³(Kg/mm²)	(25-28)		(25-28)	(32-42)	(25-32)	(20)	(21-25)
Modulus of Elasticity							
lb/in²x10⁶(Kg/mm²x10³)	12-14	14-16	15-16.2	15-16.2	15-16.5	15	10.5
(at 25% of Tensile Strength)	(8.4-9.8)	(9.8-11.2)	(10.5-11.4)	(10.5-11.6)	(10.5-10.0)	(10.5)	(7.4)
Permanent Set Point	3000		3000				
lb/in²(Kg/mm²)	(2.1)		(2.1)				
Transverse Properties(18 in)	2.0-2.2		2.0-2.2	2.4-2.8	2.0-2.4	1.8	1.8-2.0
load-lbx10³(Kgx10³)	(0.9-1.0)		(0.9-1.0)	(1.1-1.3)	(0.9-1.1)	(0.8)	1.8-0.9
deflection-inch(cm)	0.3-0.6		0.3-0.6	0.2-0.4	0.5-0.6	0.3-0.6	0.5-1.0
	(0.8-1.5)		(0.8-1.5)	(0.5-1.0)	(1.3-1.5)	(0.8-1.5)	(1.3-2.5)
Vibration Damping							
Capacity	High	medium	High	Medium	High	Medium	High
Endurance Limit	12,000		12,000	18,000	13,500	9,000	9,900
lb/in²(Kg/mm²)	(8.4)		(8.4)	(12.6)	(9.5)	(6.3)	(7.0)
Hardness Brinell	130-170	150-210	125-170	170-250	120-160	150-210	100-125
Toughness by Impact(Izod)	100	90	100	60	150	80	150
ft./lbf(Kgm)‡	(14)	(11)	(14)	(8)	(21)	(11)	(21)

Table-1.4b Mechanical properties of SG Ni-resist irons

	Type D-2 Aus 202a	Type D-2b Aus 202b	Type D-2c Aus 203	Type D-3 Aus 205	Type D-3a	Type D-4	Type D-5	Type D-5b
Tensile Strength ton/in²(kg/mm²)	24-30 (38-47)	26-31 (41-49)	24-29 (38-46)	24-30 (38-47)	24-29 (38-46)	27-32 (43-50)	24-27 (38-43)	24-29 (38-46)
Yield Strength (2% offset) ton/in²(kg/mm²)	14-16 (22-25)	14.5-16.5 (23-26)	13.5-15.5 (21-24)	14.5-16.5 (23-26)	14-17 (22-27)	17-20 (27-32)	13.5-16.5 (21-26)	16.5-19 (26-30)
Elongation, % on 2 in (5.1 cm)	8-20	7-15	20-40	7-18	13-18	1.5-4.0	20-40	5-10
Proportional Limit ton/in²(kg/mm²)	7.3-8.3 (11.6-13.0)	7.1-8.5 (11.2-13.4)	5.4-7.1 (8.4-11.2)	7.1-8.5 (11.2-13.4)	6.7-8.5 (10.5-13.4)	5.4-7.1 (8.4-11.2)	4.2-4.9 (6.7-7.7)	4.7-5.8 (7.4-9.1)
Modulus of Elasticity lb/in² x 10^6(kg/mm² x 10^3)	16.5-18.5 (11.6-13.0)	16.5-19 (11.6-13.4)	15 (10.5)	13.5-14.5 (9.5-10.2)	16-18.5 (11.2-13.0)	13 (9.1)	16-20 (11.2-14.1)	16-17.5 (11.2-12.3)
Hardness Brinell	140-200	150-200	130-170	140-200	130-190	170-240	130-180	140-190
Impact ft-lbf(kgm/cm²) Charpy V-notch Room Temperature	12 (2.075)	10 (1.73)	28 (4.84)	7 (1.21)	14 (2.42)		17 (2.94)	6 (1.04)

TABLE 1.6 EFFECT OF ALLOYING ELEMENTS (41)

Element	Ferrite stabilization	Austenite stabilization	Graphitization	Carbide forming tendency	Eutectoid carbon
Al		-		-	-
B		-			-
C	-		-	-	-
Co	-		-	(Fe)	
Cr		-		W<Cr<Mn	<Si
Cu	-	>1.2%		-	<Ni
Mn	-		-	Cr<Mn<Fe	<Cr
Mo		-		>Cr	<Nb
Nb		-			<V
Ni	-			-	<Mn
P	-	-	mild	-	-
S		-	-	-	-
Si		-		-	<Mo
Ti		-	-		
V		-			<Ti
W		-	-		

Eutectoid temperature	Chill depth	Hardenability	Partitioning	Corrosion resistance
-		if dissolved	,Al_2O_3 ,AlxNy	
-			-	-
-				-
-				-
<Si	<1%Si	Mn	>Cb, CrxOy	>12%Cr
<Ni	<4%Si >4%Si	When in solution pronounced (0.5-2%Mo)	(>0.8%Cu) elemental	(3-10%Cu) (atmospheric CR)
<Cr	in presence of sulphur	>Cr	>Cb, Mns MnO,SiO_2	helpful in reducing Ni
<Nb	1/3Cr		,Cb	0.25-0.75 Mo for pitting (1-4% Cl ions)
<V	-		,Cb	
<Mn	1/4 Si		NiSi(?)Ni_3Al	(14-36%)
				-
	in presence of Mn		(Mn Fe)S, ZrS	
<Mo		>Ni	SiO_2 MxOy Cb,TixOy	
<Ti			TixNyC2 ,TixNy Cb,VxOy ,VxNy	
		Strong	Cb	-

Heat resistance	Remarks
	Modifies corrosion behaviour, much better scaling resistance than Fe & Si alloys,limited use due to brittleness and castability.
.B.strengh-ening	provides resistance to inter-granular corrosion in Austenitic S.S., pitting resistance improves slightly.
Retains strength	Helpful in retaining high hardness at high temperatures by maintaining coherency.
	CrS inclusions ---> resistance to pitting and crevice corrosion improves.
-	Atmospheric corrosion resistance is improved.
-	Mn<0.03% - pitting corrosion resistance improves, better C.R. to Austenitic stainless steel but poorer to high Si irons.
	Helpful in reducing temper-embrittlement, at high temperature applications(oxidizing atmosphere).
	Extremely helpful in preventing stress corrosion cracking in stainless steels.
	Improves corrosion resistance and high temperature oxidation resistance by forming austenitic matrix.
-	Ni increases the ability of phosphorous to enhance corrosion.
t shortness	Improves machinability but produces hot shortness.
	Helpful in designing corrosion resistant and oxidation resistant irons, only useful in the presence of other alloying elements like Ni, Mn, Si, ect.
	Phosphorous-induced embrittlement is reduced, useful in attaining secondary hardening.
	Useful in attaining secondary hardening
	Same as V but less effective.

TABLE- 3.1 CHEMICAL ANALYSIS OF RAW MATERIALS

RAW MATERIAL	C	Si	P	S	Mn	Cr	Cu
PIG IRON	3.55	2.15	0.40	0.05	1.12	....	....
FERRO-CHROMIUM (LOW CARBON)	0.10 MAX	0.70 MAX	0.03 MAX	0.01 MAX	....	67.0-75.0	....
FERRO-MANGANESE LOW CARBON)	0.03 MAX	....	0.03 MAX	0.008	97.0	....	....
FERRO-SILICON (LOW CARBON)	0.03 MAX	75.0	....	....	....	....	....
COPPER (ELECTROLYTIC)	....	....	....	....	....	....	99.99

TABLE- 3.2 CHEMICAL ANALYSIS OF ALLOYS

ALLOY	C	S	P	Si	Mn	Cr	Cu
B1	3.05	0.07	0.183	2.24	6.1	4.8	1.46
B2	2.90	0.065	0.173	2.14	7.5	4.8	1.48
B3	2.90	0.068	0.280	1.80	6.2	4.7	2.84
B4	2.85	0.072	0.305	1.80	7.3	4.5	2.86

EFFECT OF SOAKING PERIOD ON HARDNESS IN A.C. CONDITION

ALLOY : B1 AS CAST HARDNESS(HV30)= 594
TABLE-4.3 TEMP.(DEG.C) = 900

TIME (HRS)	HARDNESS (HV30)										SD	AVERAGE (HV30)
2	602	602	598	594	594	594	594	588	586	586		
	586	586	586	583	583	579	579	579	575	575	8.21	587
4	583	575	571	568	568	568	561	561	561	561		
	557	557	557	554	550	550	550	540	540	537	11.95	558
6	594	594	590	586	586	586	583	583	579	579		
	579	575	571	571	568	568	564	557	557	550	12.54	576
8	598	594	594	590	590	586	586	586	586	583		
	583	583	579	579	579	575	571	571	568	554	10.35	581
10	606	602	598	594	594	590	590	590	590	586		
	586	586	586	583	583	583	583	579	571	557	10.58	586

FOR DEGREE OF 1 COEFFICIENTS ARE
571.3000 1.0500
BEST FIT VALUES 573.4 575.5 577.6 579.7 581.8
STANDARD DEVIATION IS 13.0779700
FOR DEGREE OF 2 COEFFICIENTS ARE
598.8000 -10.7357 0.9821
BEST FIT VALUES 581.3 571.6 569.7 575.8 589.7
STANDARD DEVIATION IS 12.1866440
FOR DEGREE OF 3 COEFFICIENTS ARE
664.6009 -56.9530 9.7948 -0.4896
BEST FIT VALUES 586.0 562.2 569.7 585.2 585.0
STANDARD DEVIATION IS 8.7251705

TABLE-4.4 TEMP.(DEG.C) = 950

2	575	568	568	564	564	561	557	557	557	557		
	554	554	554	554	550	550	547	543	540	540	9.33	555
4	564	561	557	554	550	547	547	547	547	547		
	543	543	540	540	540	540	540	537	530	530	8.98	545
6	543	537	537	537	533	533	533	533	530	530		
	530	527	527	527	523	523	523	523	523	514	6.77	529
8	530	523	520	520	520	520	520	520	517	517		
	517	517	517	514	514	511	511	508	508	508	5.57	516
10	550	550	547	543	543	543	540	533	530	530		
	527	523	520	520	520	520	517	517	511	505	13.54	529

FOR DEGREE OF 1 COEFFICIENTS ARE
559.1000 -4.0500
BEST FIT VALUES 551.0 542.9 534.8 526.7 518.6
STANDARD DEVIATION IS 9.6038187
FOR DEGREE OF 2 COEFFICIENTS ARE
583.6000 -14.5500 0.8750
BEST FIT VALUES 558.0 539.4 527.8 523.2 525.6
STANDARD DEVIATION IS 7.2525858
FOR DEGREE OF 3 COEFFICIENTS ARE
538.7993 16.9172 -5.1251 0.3333
BEST FIT VALUES 554.8 545.8 527.8 516.8 528.8
STANDARD DEVIATION IS 1.6733191

EFFECT OF SOAKING PERIOD ON HARDNESS IN A.C. CONDITION

ALLOY : B1 AS CAST HARDNESS(HV30)= 594
TABLE-4.5 TEMP.(DEG.C) =1000

TIME (HRS)	HARDNESS (HV30)										SD	AVERAGE (HV30)
2	554	543	543	540	540	540	537	533	533	533		
	530	530	530	530	530	527	527	527	527	520	7.79	533
4	493	487	487	487	481	481	481	478	476	476		
	476	473	473	470	470	470	465	457	457	451	10.95	474
6	493	490	490	487	487	481	478	478	476	476		
	473	473	473	473	470	470	470	467	465	451	10.07	476
8	425	425	422	422	418	413	412	411	411	409		
	409	406	406	406	406	404	404	404	400	398	8.04	410
10	393	391	385	383	383	379	377	377	375	373		
	370	370	370	370	358	358	358	358	358	349	12.24	371

FOR DEGREE OF 1 COEFFICIENTS ARE
569.2000 -19.4000
BEST FIT VALUES 530.4 491.6 452.8 414.0 375.2
STANDARD DEVIATION IS 17.2085260
FOR DEGREE OF 2 COEFFICIENTS ARE
555.2000 -13.4000 -0.5000
BEST FIT VALUES 526.4 493.6 456.8 416.0 371.2
STANDARD DEVIATION IS 20.4009830
FOR DEGREE OF 3 COEFFICIENTS ARE
602.8001 -46.8334 5.8750 -0.3542
BEST FIT VALUES 529.8 486.8 456.8 422.8 367.8
STANDARD DEVIATION IS 26.7731200

TABLE-4.6 TEMP.(DEG.C) =1050

2	473	473	467	465	465	459	457	457	451	451		
	451	449	446	446	446	446	446	441	441	436	10.76	453
4	379	377	377	375	371	370	370	368	368	366		
	366	364	358	358	355	355	349	349	346	346	10.68	363
6	373	370	370	366	366	364	362	360	360	357		
	357	351	351	351	349	348	348	348	344	336	9.92	356
8	329	329	328	328	328	325	323	323	321	321		
	321	318	317	315	315	315	314	314	314	308	6.23	320
10	280	278	277	276	276	276	276	276	275	275		
	275	275	274	274	274	271	268	266	266	266	4.11	273

FOR DEGREE OF 1 COEFFICIENTS ARE
473.9000 -20.1500
BEST FIT VALUES 433.6 393.3 353.0 312.7 272.4
STANDARD DEVIATION IS 21.2689140
FOR DEGREE OF 2 COEFFICIENTS ARE
502.4000 -32.3643 1.0179
BEST FIT VALUES 441.7 389.2 344.9 308.6 280.5
STANDARD DEVIATION IS 23.7173840
FOR DEGREE OF 3 COEFFICIENTS ARE
634.0007 -124.7981 18.6429 -0.9792
BEST FIT VALUES 451.1 370.4 344.9 327.4 271.1
STANDARD DEVIATION IS 15.5379730

EFFECT OF SOAKING PERIOD ON HARDNESS IN A.C. CONDITION

ALLOY : B2 AS CAST HARDNESS(HV30)= 590
TABLE-4.7 TEMP.(DEG.C) = 800

TIME (HRS)	HARDNESS (HV30)										SD	AVERAGE (HV30)
2	659	635	631	626	626	622	618	618	610	610		
	610	606	606	606	606	606	602	602	602	602	14.61	615
4	652	652	648	648	648	644	644	635	635	635		
	631	631	626	626	626	622	622	618	618	618	11.93	633
6	652	652	648	648	648	648	644	644	639	639		
	639	639	635	635	635	631	631	631	618	618	9.82	638
8	675	675	666	666	666	661	661	657	657	648		
	648	644	644	644	644	644	644	639	639	634	12.40	652
10	695	690	680	680	680	680	671	671	671	666		
	666	666	661	661	661	661	661	657	657	644	12.30	668

FOR DEGREE OF 1 COEFFICIENTS ARE
603.7000 6.2500
BEST FIT VALUES 616.2 628.7 641.2 653.7 666.2
STANDARD DEVIATION IS 3.4785053
FOR DEGREE OF 2 COEFFICIENTS ARE
606.2000 5.1786 0.0893
BEST FIT VALUES 616.9 628.3 640.5 653.3 666.9
STANDARD DEVIATION IS 4.1541702
FOR DEGREE OF 3 COEFFICIENTS ARE
585.1999 19.9287 -2.7232 0.1563
BEST FIT VALUES 615.4 631.3 640.5 650.3 668.4
STANDARD DEVIATION IS 3.4661620

TABLE-4.8 TEMP.(DEG.C) = 850

2	533	533	533	533	530	527	527	527	523	523		
	523	520	520	520	511	511	508	508	508	499	10.18	520
4	547	540	540	540	540	537	537	537	533	530		
	530	527	527	523	523	520	520	520	514	511	9.94	529
6	550	540	537	533	533	533	530	530	530	530		
	527	527	520	520	517	517	517	514	514	511	10.08	526
8	543	543	543	540	540	537	533	533	533	530		
	530	530	530	527	523	520	511	511	508	502	12.30	528
10	543	540	540	537	537	533	533	533	530	530		
	527	527	527	523	520	514	514	505	505	505	12.05	526

FOR DEGREE OF 1 COEFFICIENTS ARE
522.5000 0.5500
BEST FIT VALUES 523.6 524.7 525.8 526.9 528.0
STANDARD DEVIATION IS 3.4976163
FOR DEGREE OF 2 COEFFICIENTS ARE
514.0000 4.1929 -0.3036
BEST FIT VALUES 521.2 525.9 528.2 528.1 525.6
STANDARD DEVIATION IS 2.8334728
FOR DEGREE OF 3 COEFFICIENTS ARE
502.7993 12.0601 -1.8037 0.0833
BEST FIT VALUES 520.4 527.5 528.2 526.5 526.4
STANDARD DEVIATION IS 3.1075953

EFFECT OF SOAKING PERIOD ON HARDNESS IN A.C. CONDITION

ALLOY : B2 AS CAST HARDNESS(HV30)= 590
TABLE- 4.9 TEMP.(DEG.C) = 900

TIME (HRS)	HARDNESS (HV30)										SD	AVERAGE (HV30)
2	517	514	511	511	511	511	508	508	505	505		
	505	505	499	499	499	493	490	484	484	484	10.32	502
4	508	508	508	502	499	499	496	496	493	493		
	490	487	487	487	487	484	481	481	481	478	9.53	492
6	511	505	502	499	496	493	493	487	487	484		
	484	484	478	478	478	478	476	476	473	473	11.25	486
8	505	505	505	499	499	499	493	490	487	487		
	476	478	476	473	473	473	470	468	465	465	14.20	484
0	508	508	505	505	499	496	496	493	493	493		
	490	487	481	481	481	481	478	476	473	467	12.06	489

FOR DEGREE OF 1 COEFFICIENTS ARE
500.8000 -1.7000
BEST FIT VALUES 497.4 494.0 490.6 487.2 483.8
STANDARD DEVIATION IS 5.2788894
FOR DEGREE OF 2 COEFFICIENTS ARE
517.8000 -8.9857 0.6071
BEST FIT VALUES 502.3 491.6 485.7 484.8 488.7
STANDARD DEVIATION IS 0.7171372
FOR DEGREE OF 3 COEFFICIENTS ARE
513.6004 -6.0360 0.0447 0.0312
BEST FIT VALUES 502.0 492.2 485.7 484.2 489.0
STANDARD DEVIATION IS 0.3585704

TABLE-4.10 TEMP.(DEG.C) = 950

2	470	465	465	465	462	459	459	457	454	454		
	454	451	451	451	451	451	449	449	444	444	7.28	455
4	459	459	459	457	454	454	454	451	449	446		
	446	444	444	444	444	439	434	432	427	425	10.41	446
6	457	454	451	451	451	451	449	449	446	446		
	446	444	444	439	439	439	432	432	422	422	9.85	443
8	465	459	457	457	454	454	454	451	449	446		
	444	444	441	441	441	439	436	432	432	427	10.21	446
10	462	457	454	451	451	446	446	446	444	444		
	444	444	444	441	441	441	436	434	429	427	8.61	444

FOR DEGREE OF 1 COEFFICIENTS ARE
453.4000 -1.1000
BEST FIT VALUES 451.2 449.0 446.8 444.6 442.4
STANDARD DEVIATION IS 3.7594329
FOR DEGREE OF 2 COEFFICIENTS ARE
463.4000 -5.3857 0.3571
BEST FIT VALUES 454.1 447.6 443.9 443.2 445.3
STANDARD DEVIATION IS 2.6295041
FOR DEGREE OF 3 COEFFICIENTS ARE
478.8003 -16.2026 2.4197 -0.1146
BEST FIT VALUES 455.2 445.4 443.9 445.4 444.2
STANDARD DEVIATION IS 1.3147510

EFFECT OF SOAKING PERIOD ON HARDNESS IN A.C. CONDITION

ALLOY : B2 AS CAST HARDNESS(HV30)= 590
TABLE-4.11 TEMP.(DEG.C) =1000

TIME (HRS)	HARDNESS (HV30)										SD	AVERAGE (HV30)
2	439	439	439	436	434	432	432	432	429	428		
	427	427	425	420	418	418	418	418	415	406	9.18	426
4	425	422	420	420	418	418	418	418	415	415		
	415	415	415	413	411	411	406	406	404	402	6.13	414
6	413	409	409	406	406	406	404	404	404	404		
	400	400	400	400	400	398	398	398	398	391	5.05	402
8	387	387	387	387	377	377	377	377	375	375		
	373	373	373	373	373	370	370	370	357	353	8.86	374
10	370	366	364	364	362	362	358	357	353	353		
	341	341	341	341	341	341	337	337	337	336	11.82	350

FOR DEGREE OF 1 COEFFICIENTS ARE
450.8000 -9.6000
BEST FIT VALUES 431.6 412.4 393.2 374.0 354.8
STANDARD DEVIATION IS 6.6932794
FOR DEGREE OF 2 COEFFICIENTS ARE
430.8000 -1.0286 -0.7143
BEST FIT VALUES 425.9 415.3 398.9 376.9 349.1
STANDARD DEVIATION IS 3.1713009
FOR DEGREE OF 3 COEFFICIENTS ARE
425.2002 2.9046 -1.4643 0.0417
BEST FIT VALUES 425.5 416.1 398.9 376.1 349.5
STANDARD DEVIATION IS 4.3028225

TABLE-4.12 TEMP.(DEG.C) =1050

2	429	427	427	413	413	411	411	409	409	409		
	406	406	406	406	404	402	402	400	396	396	9.36	409
4	375	375	371	371	371	371	371	371	370	368		
	368	364	364	362	362	362	358	353	353	351	7.31	365
6	353	349	348	346	344	343	343	343	341	337		
	329	326	320	317	317	314	314	309	302	301	16.82	329
8	309	309	308	307	305	305	305	305	295	295		
	295	294	294	294	289	289	289	289	287	282	8.53	297
10	278	278	274	269	269	269	268	268	264	263		
	261	261	260	260	260	258	256	254	252	249	8.05	263

FOR DEGREE OF 1 COEFFICIENTS ARE
440.6000 -18.0000
BEST FIT VALUES 404.6 368.6 332.6 296.6 260.6
STANDARD DEVIATION IS 4.1311823
FOR DEGREE OF 2 COEFFICIENTS ARE
452.6000 -23.1429 0.4286
BEST FIT VALUES 408.0 366.9 329.2 294.9 264.0
STANDARD DEVIATION IS 2.2424451
FOR DEGREE OF 3 COEFFICIENTS ARE
466.6001 -32.9763 2.3036 -0.1042
BEST FIT VALUES 409.0 364.9 329.2 296.9 263.0
STANDARD DEVIATION IS 0.2390430

EFFECT OF SOAKING PERIOD ON HARDNESS IN A.C. CONDITION

ALLOY : B3 AS CAST HARDNESS(HV30)= 652
TABLE-4.13 TEMP.(DEG.C) = 800

TIME (HRS)	HARDNESS (HV30)										SD	AVERAGE (HV30)
2	710	705	705	705	700	700	700	700	700	695		
	695	695	695	690	690	690	690	690	685	685	7.05	696
4	720	720	715	715	710	710	705	705	700	700		
	700	700	700	700	695	695	695	690	690	685	9.93	702
6	730	730	725	725	725	720	720	715	715	715		
	715	715	715	710	710	710	710	710	710	710	6.93	716
8	757	752	752	752	752	746	746	746	746	746		
	741	741	741	741	736	736	736	736	730	730	7.66	743
10	763	763	763	757	752	752	752	746	746	741		
	741	741	741	736	736	736	736	736	736	736	9.98	745

FOR DEGREE OF 1 COEFFICIENTS ARE
678.7000 6.9500
BEST FIT VALUES 692.6 706.5 720.4 734.3 748.2
STANDARD DEVIATION IS 6.7601779
FOR DEGREE OF 2 COEFFICIENTS ARE
681.2000 5.8786 0.0893
BEST FIT VALUES 693.3 706.1 719.7 733.9 748.9
STANDARD DEVIATION IS 8.2253956
FOR DEGREE OF 3 COEFFICIENTS ARE
727.3999 -26.5713 6.2768 -0.3437
BEST FIT VALUES 696.6 699.5 719.7 740.5 745.6
STANDARD DEVIATION IS 5.1394821

TABLE-4.14 TEMP.(DEG.C) = 850

2	583	583	583	579	579	575	571	571	571	568		
	568	568	568	564	564	561	561	557	557	554	8.97	569
4	594	594	594	594	590	590	586	582	579	575		
	575	575	571	571	571	571	568	564	564	564	10.99	578
6	631	631	626	622	618	618	618	618	618	618		
	618	618	618	614	610	610	606	602	602	602	8.54	615
8	644	635	631	631	626	622	622	622	622	622		
	618	618	618	618	618	614	614	610	610	610	8.77	621
10	652	652	652	648	648	648	648	648	648	644		
	644	644	644	644	644	631	631	631	631	622	8.63	642

FOR DEGREE OF 1 COEFFICIENTS ARE
548.3000 9.4500
BEST FIT VALUES 567.2 586.1 605.0 623.9 642.8
STANDARD DEVIATION IS 7.7006512
FOR DEGREE OF 2 COEFFICIENTS ARE
544.8000 10.9500 -0.1250
BEST FIT VALUES 566.2 586.6 606.0 624.4 641.8
STANDARD DEVIATION IS 9.3380964
FOR DEGREE OF 3 COEFFICIENTS ARE
562.9997 -1.8331 2.3125 -0.1354
BEST FIT VALUES 567.5 584.0 606.0 627.0 640.5
STANDARD DEVIATION IS 12.5498980

EFFECT OF SOAKING PERIOD ON HARDNESS IN A.C. CONDITION

ALLOY : B3 AS CAST HARDNESS(HV30)= 652
TABLE-4.15 TEMP.(DEG.C) = 900

TIME (HRS)	HARDNESS (HV30)										SD	AVERAGE (HV30)
2	533	533	533	530	527	520	517	514	514	511		
	511	511	511	508	505	502	502	499	496	496	12.28	513
4	523	523	520	517	517	517	511	505	505	505		
	505	505	505	505	502	499	499	499	499	493	8.86	507
6	527	523	523	520	520	517	517	514	514	514		
	514	514	514	508	508	508	505	505	505	505	6.70	513
8	530	530	523	520	517	514	514	511	511	511		
	508	505	505	502	502	499	499	496	496	496	10.66	509
10	533	533	530	530	527	523	523	523	523	523		
	520	520	517	517	517	511	511	508	508	505	8.38	520

FOR DEGREE OF 1 COEFFICIENTS ARE
507.6000 0.8000
BEST FIT VALUES 509.2 510.8 512.4 514.0 515.6
STANDARD DEVIATION IS 4.9531122
FOR DEGREE OF 2 COEFFICIENTS ARE
519.6000 -4.3429 0.4286
BEST FIT VALUES 512.6 509.1 509.0 512.3 519.0
STANDARD DEVIATION IS 4.0284694
FOR DEGREE OF 3 COEFFICIENTS ARE
515.4004 -1.3932 -0.1339 0.0312
BEST FIT VALUES 512.3 509.7 509.0 511.7 519.3
STANDARD DEVIATION IS 5.6175745

TABLE-4.16 TEMP.(DEG.C) = 950

2	499	499	499	496	496	496	496	496	496	496		
	493	493	493	493	493	487	487	481	481	473	6.95	492
4	517	511	508	508	508	505	505	505	505	499		
	496	496	496	496	496	493	493	493	493	493	7.31	500
6	514	514	502	502	502	502	499	499	496	496		
	496	493	493	490	490	490	490	490	490	484	7.88	496
8	505	505	496	490	490	490	490	487	487	487		
	484	481	481	481	481	478	473	473	473	470	9.74	485
10	499	499	499	496	496	496	496	496	493	487		
	487	487	484	484	484	481	481	481	481	481	7.13	489

FOR DEGREE OF 1 COEFFICIENTS ARE
498.7000 -1.0500
BEST FIT VALUES 496.6 494.5 492.4 490.3 488.2
STANDARD DEVIATION IS 5.5707570
FOR DEGREE OF 2 COEFFICIENTS ARE
491.2000 2.1643 -0.2679
BEST FIT VALUES 494.5 495.6 494.5 491.4 486.1
STANDARD DEVIATION IS 6.2059871
FOR DEGREE OF 3 COEFFICIENTS ARE
453.3993 28.7148 -5.3305 0.2813
BEST FIT VALUES 491.8 501.0 494.5 486.0 488.8
STANDARD DEVIATION IS 2.0318891

EFFECT OF SOAKING PERIOD ON HARDNESS IN A.C. CONDITION

ALLOY : B3 AS CAST HARDNESS(HV30)= 652
TABLE-4.17 TEMP.(DEG.C) =1000

TIME (HRS)	HARDNESS (HV30)										SD	AVERAGE (HV30)
2	490	490	490	487	484	484	481	478	478	476		
	476	476	476	470	470	470	470	470	467	467	7.84	477
4	436	429	429	429	428	427	427	425	425	422		
	422	422	420	418	418	418	418	415	415	415	5.83	422
6	393	393	391	389	389	387	387	385	383	383		
	383	377	377	375	375	373	370	370	368	364	8.83	380
8	398	397	396	393	391	383	381	381	381	377		
	377	375	375	371	371	366	366	366	366	362	11.41	378
10	375	375	373	371	370	370	368	368	368	362		
	358	357	353	351	351	348	346	346	343	341	11.57	359

FOR DEGREE OF 1 COEFFICIENTS ARE
  487.2000 -14.0000
BEST FIT VALUES 459.2 431.2 403.2 375.2 347.2
STANDARD DEVIATION IS 19.0333040
FOR DEGREE OF 2 COEFFICIENTS ARE
  543.2000 -38.0000 2.0000
BEST FIT VALUES 475.2 423.2 387.2 367.2 363.2
STANDARD DEVIATION IS 9.7672923
FOR DEGREE OF 3 COEFFICIENTS ARE
  585.2003 -67.5002 7.6250 -0.3125
BEST FIT VALUES 478.2 417.2 387.2 373.2 360.2
STANDARD DEVIATION IS 10.0399190

TABLE-4.18 TEMP.(DEG.C) =1050

2	411	409	409	409	406	406	404	404	404	402		
	398	398	398	396	396	393	391	391	385	381	8.35	399
4	377	373	373	373	371	370	368	368	368	368		
	366	366	366	360	360	360	357	355	351	344	8.30	364
6	370	368	364	362	360	358	358	358	358	358		
	358	358	357	357	355	353	351	349	344	344	6.64	357
8	312	307	304	302	302	301	299	295	295	295		
	289	289	287	287	287	287	285	285	282	270	10.02	293
10	270	270	270	269	269	269	265	264	263	263		
	262	262	260	260	258	257	254	251	251	246	7.12	261

FOR DEGREE OF 1 COEFFICIENTS ARE
  438.9000 -17.3500
BEST FIT VALUES 404.2 369.5 334.8 300.1 265.4
STANDARD DEVIATION IS 14.3747460
FOR DEGREE OF 2 COEFFICIENTS ARE
  413.4000 -6.4214 -0.9107
BEST FIT VALUES 396.9 373.1 342.1 303.7 258.1
STANDARD DEVIATION IS 14.7328590
FOR DEGREE OF 3 COEFFICIENTS ARE
  407.8002 -2.4882 -1.6607 0.0417
BEST FIT VALUES 396.5 373.9 342.1 302.9 258.5
STANDARD DEVIATION IS 20.7969760

EFFECT OF SOAKING PERIOD ON HARDNESS IN A.C. CONDITION

ALLOY : B4 AS CAST HARDNESS(HV30)= 621
TABLE-4.19 TEMP.(DEG.C) = 800

TIME (HRS)	HARDNESS (HV30)										SD	AVERAGE (HV30)
2	671	671	671	666	666	666	666	657	657	657		
	652	652	652	648	644	644	644	644	644	644	10.40	655
4	657	657	657	652	652	652	648	648	648	644		
	639	639	639	639	639	639	639	639	635	635	7.59	644
6	671	666	661	661	661	661	657	657	657	657		
	657	652	652	648	648	648	644	644	644	631	9.23	653
8	680	675	671	671	671	671	666	661	661	661		
	657	657	657	657	657	657	652	652	648	648	9.10	661
10	690	690	690	685	680	680	680	680	680	675		
	675	675	675	675	675	671	671	671	671	666	6.86	677

FOR DEGREE OF 1 COEFFICIENTS ARE
639.7000 3.0500
BEST FIT VALUES 645.8 651.9 658.0 664.1 670.2
STANDARD DEVIATION IS 8.7158861
FOR DEGREE OF 2 COEFFICIENTS ARE
666.2000 -8.3071 0.9464
BEST FIT VALUES 653.4 648.1 650.4 660.3 677.8
STANDARD DEVIATION IS 3.6916896
FOR DEGREE OF 3 COEFFICIENTS ARE
683.0006 -20.1075 3.1965 -0.1250
BEST FIT VALUES 654.6 645.7 650.4 662.7 676.6
STANDARD DEVIATION IS 3.5856849

TABLE-4.20 TEMP.(DEG.C) = 850

2	557	557	554	554	550	550	550	543	543	540		
	540	537	537	537	533	533	527	527	527	523	10.74	540
4	537	537	533	533	533	533	533	530	527	523		
	523	523	523	523	523	523	520	520	514	511	7.28	526
6	557	557	554	554	554	554	550	550	550	550		
	550	547	547	547	543	543	543	533	530	530	8.15	547
8	543	543	543	543	540	537	537	537	533	533		
	533	530	530	530	527	527	527	517	514	514	9.14	531
10	523	520	517	517	517	517	517	517	517	514		
	514	514	511	511	511	511	508	508	508	508	4.35	514

FOR DEGREE OF 1 COEFFICIENTS ARE
545.7000 -2.3500
BEST FIT VALUES 541.0 536.3 531.6 526.9 522.2
STANDARD DEVIATION IS 11.9485000
FOR DEGREE OF 2 COEFFICIENTS ARE
524.2000 6.8643 -0.7679
BEST FIT VALUES 534.9 539.4 537.7 530.0 516.1
STANDARD DEVIATION IS 12.1702250
FOR DEGREE OF 3 COEFFICIENTS ARE
574.6006 -28.5361 5.9822 -0.3750
BEST FIT VALUES 538.5 532.2 537.7 537.2 512.5
STANDARD DEVIATION IS 12.9084710

EFFECT OF SOAKING PERIOD ON HARDNESS IN A.C. CONDITION

ALLOY : B4 AS CAST HARDNESS(HV30)= 621
TABLE-4.21 TEMP.(DEG.C) = 900

TIME (HRS)	HARDNESS (HV30)										SD	AVERAGE (HV30)
2	487	484	481	481	476	473	473	473	473	473		
	473	473	470	470	470	470	470	467	467	462	6.03	473
4	493	493	493	493	493	484	484	481	481	481		
	481	478	478	476	476	473	473	465	465	462	9.71	480
6	484	484	484	481	478	478	476	476	476	476		
	476	476	476	473	470	470	470	470	467	465	5.48	475
8	493	493	490	487	487	487	487	487	484	484		
	484	484	484	484	484	481	476	476	476	476	5.17	484
10	499	493	493	493	493	493	493	493	493	490		
	487	487	487	487	484	484	484	481	481	476	5.68	488

FOR DEGREE OF 1 COEFFICIENTS ARE
469.8000 1.7000
BEST FIT VALUES 473.2 476.6 480.0 483.4 486.8
STANDARD DEVIATION IS 3.5777094
FOR DEGREE OF 2 COEFFICIENTS ARE
473.8000 -0.0143 0.1429
BEST FIT VALUES 474.3 476.0 478.9 482.8 487.9
STANDARD DEVIATION IS 4.1126981
FOR DEGREE OF 3 COEFFICIENTS ARE
463.9995 6.8694 -1.1697 0.0729
BEST FIT VALUES 473.6 477.4 478.9 481.4 488.6
STANDARD DEVIATION IS 5.3785287

TABLE-4.22 TEMP.(DEG.C) = 950

2	499	487	481	478	478	473	470	470	467	467		
	465	465	465	465	465	462	462	462	462	457	10.15	470
4	481	478	478	478	476	476	473	473	467	467		
	467	467	467	465	465	465	462	459	454	454	7.88	468
6	465	465	462	459	459	457	457	457	457	457		
	457	454	451	449	449	449	446	444	444	441	6.98	453
8	467	454	454	454	454	451	451	446	446	441		
	441	441	441	439	439	439	434	434	434	434	8.99	444
10	454	452	451	451	451	451	449	449	449	446		
	446	446	444	444	444	436	436	436	436	434	6.37	445

FOR DEGREE OF 1 COEFFICIENTS ARE
478.2000 -3.7000
BEST FIT VALUES 470.8 463.4 456.0 448.6 441.2
STANDARD DEVIATION IS 4.7046076
FOR DEGREE OF 2 COEFFICIENTS ARE
484.2000 -6.2714 0.2143
BEST FIT VALUES 472.5 462.5 454.3 447.7 442.9
STANDARD DEVIATION IS 5.2968990
FOR DEGREE OF 3 COEFFICIENTS ARE
452.0002 16.3451 -4.0982 0.2396
BEST FIT VALUES 470.2 467.1 454.3 443.1 445.2
STANDARD DEVIATION IS 1.7928424

EFFECT OF SOAKING PERIOD ON HARDNESS IN A.C. CONDITION

ALLOY : B4 AS CAST HARDNESS(HV30)= 621
TABLE-4.23 TEMP.(DEG.C) =1000

TIME (HRS)	HARDNESS (HV30)										SD	AVERAGE (HV30)
2	444	444	436	436	436	436	432	432	432	429		
	429	427	427	427	427	427	422	418	415	415	8.11	429
4	406	396	393	393	389	387	385	385	385	385		
	385	385	383	383	381	379	379	379	379	366	8.07	385
6	396	393	391	389	389	387	387	383	381	381		
	377	377	377	375	371	370	370	368	368	368	9.12	379
8	360	360	353	351	348	346	346	346	345	343		
	341	341	341	341	339	339	337	336	334	323	8.62	343
10	301	301	294	291	290	290	287	287	283	282		
	282	280	280	278	275	274	274	274	270	270	9.33	283

FOR DEGREE OF 1 COEFFICIENTS ARE
464.0000 -16.7000
BEST FIT VALUES 430.6 397.2 363.8 330.4 297.0
STANDARD DEVIATION IS 15.6758840
FOR DEGREE OF 2 COEFFICIENTS ARE
433.0000 -3.4143 -1.1071
BEST FIT VALUES 421.7 401.6 372.7 334.8 288.1
STANDARD DEVIATION IS 15.2090190
FOR DEGREE OF 3 COEFFICIENTS ARE
519.8010 -64.3817 10.5180 -0.6458
BEST FIT VALUES 427.9 389.2 372.7 347.2 281.9
STANDARD DEVIATION IS 8.8446902

TABLE-4.24 TEMP.(DEG.C) =1050

2	418	413	413	413	411	406	406	406	404	404		
	402	402	400	396	389	389	387	383	381	379	11.74	400
4	348	348	343	343	339	339	334	333	333	331		
	328	328	326	325	325	320	311	309	308	307	12.87	328
6	317	314	314	309	309	309	308	307	305	302		
	302	302	301	295	295	295	295	294	294	289	7.98	302
8	283	282	281	280	277	261	260	260	258	257		
	256	256	256	254	254	252	250	250	250	250	11.93	261
10	253	253	252	251	250	249	248	248	240	239		
	239	239	239	238	238	237	236	236	236	236	6.63	242

FOR DEGREE OF 1 COEFFICIENTS ARE
421.5000 -19.1500
BEST FIT VALUES 383.2 344.9 306.6 268.3 230.0
STANDARD DEVIATION IS 16.1895030
FOR DEGREE OF 2 COEFFICIENTS ARE
467.0000 -38.6500 1.6250
BEST FIT VALUES 396.2 338.4 293.6 261.8 243.0
STANDARD DEVIATION IS 9.8691452
FOR DEGREE OF 3 COEFFICIENTS ARE
500.6000 -62.2500 6.1250 -0.2500
BEST FIT VALUES 398.6 333.6 293.6 266.6 240.6
STANDARD DEVIATION IS 11.7132400

EFFECT OF SOAKING TEMPERATURE ON HARDNESS IN A. C. CONDITION

ALLOY : B1 AS CAST HARDNESS(HV30)= 594
TABLE-4.25 TIME(HRS) = 2

TEMP (DEG.C)	HARDNESS (HV30)										SD	AVERAGE (HV30)
800	710	710	705	702	700	700	700	698	697	697		
	695	695	692	690	690	690	690	690	685	685	7.27	696
850	622	622	618	618	618	614	610	610	610	606		
	606	606	602	594	590	590	586	586	583	579	13.88	603
900	602	602	598	594	594	594	594	588	586	586		
	586	586	586	583	583	579	579	579	575	575	8.21	587
950	575	568	568	564	564	561	557	557	557	557		
	554	554	554	554	550	550	547	543	540	540	9.33	555
1000	554	543	543	540	540	540	537	533	533	533		
	530	530	530	530	530	527	527	527	527	520	7.79	533
1050	473	473	467	465	465	459	457	457	451	451		
	451	449	446	446	446	446	446	441	441	436	10.76	453

FOR DEGREE OF 1 COEFFICIENTS ARE
134.12947000 -0.83257087
BEST FIT VALUES 675.2 633.6 592.0 550.4 508.7 467.1
STANDARD DEVIATION IS 23.4649700
FOR DEGREE OF 2 COEFFICIENTS ARE
158.96311000 -1.37412950 0.00292734
BEST FIT VALUES 677.7 633.1 590.0 548.4 508.2 469.5
STANDARD DEVIATION IS 26.9716360
FOR DEGREE OF 3 COEFFICIENTS ARE
2691.59370000 -84.34636400 0.90449701 -0.00324940
BEST FIT VALUES 689.7 616.1 580.4 558.2 525.3 457.2
STANDARD DEVIATION IS 13.0705310

TABLE-4.26 TIME(HRS) = 4

800	752	752	752	746	746	741	741	736	736	730		
	730	730	720	720	710	710	700	695	685	685	21.90	725
850	690	690	690	690	685	685	685	680	680	675		
	675	671	671	671	666	661	657	657	657	657	12.29	674
900	583	575	571	568	568	568	561	561	561	561		
	557	557	557	554	550	550	550	540	540	537	11.95	558
950	564	561	557	554	550	547	547	547	547	547		
	543	543	540	540	540	540	540	537	530	530	8.98	545
1000	493	487	487	487	481	481	481	478	476	476		
	476	473	473	470	470	470	465	457	457	451	10.95	474
1050	379	377	377	375	371	370	370	368	368	366		
	366	364	358	358	355	355	349	349	346	346	10.68	363

FOR DEGREE OF 1 COEFFICIENTS ARE
183.72286000 -1.38457140
BEST FIT VALUES 729.6 660.3 591.1 521.9 452.7 383.4
STANDARD DEVIATION IS 26.0340420
FOR DEGREE OF 2 COEFFICIENTS ARE
111.01688000 0.20096165 -0.00857045
BEST FIT VALUES 722.4 661.8 596.8 527.6 454.1 376.3
STANDARD DEVIATION IS 29.0955730
FOR DEGREE OF 3 COEFFICIENTS ARE
1636.71170000 -49.78276100 0.53454867 -0.00195748
BEST FIT VALUES 729.7 651.5 591.0 533.5 464.4 368.9
STANDARD DEVIATION IS 30.6306150

EFFECT OF SOAKING TEMPERATURE ON HARDNESS IN A.C. CONDITION

ALLOY : B1 AS CAST HARDNESS(HV30)= 594
TABLE-4.27 TIME(HRS) = 6

TEMP (DEG.C)	HARDNESS (HV30)										SD	AVERAGE (HV30)
800	769	763	752	741	736	736	730	730	725	725		
	725	720	720	720	720	705	705	695	690	690	21.65	724
850	680	680	675	675	671	671	671	666	661	657		
	657	657	657	657	657	652	652	652	652	644	10.56	662
900	594	594	590	586	586	586	583	583	579	579		
	579	575	571	571	568	568	564	557	557	550	12.54	576
950	543	537	537	537	533	533	533	533	530	530		
	530	527	527	527	523	523	523	523	523	514	6.77	529
1000	493	490	490	487	487	481	478	478	476	476		
	473	473	473	473	470	470	470	467	465	451	10.07	476
1050	373	370	370	366	366	364	362	360	360	357		
	357	351	351	351	349	348	348	348	344	336	9.92	356

FOR DEGREE OF 1 COEFFICIENTS ARE
184.61905000 -1.39714290
BEST FIT VALUES 728.5 658.6 588.8 518.9 449.0 379.2
STANDARD DEVIATION IS 19.7514260
FOR DEGREE OF 2 COEFFICIENTS ARE
88.89708500 0.69031054 -0.01128353
BEST FIT VALUES 719.1 660.5 596.3 526.4 450.9 369.8
STANDARD DEVIATION IS 20.5206060
FOR DEGREE OF 3 COEFFICIENTS ARE
1586.27530000 -48.36572500 0.52175542 -0.00192115
BEST FIT VALUES 726.2 650.4 590.6 532.2 461.0 362.5
STANDARD DEVIATION IS 17.7254870

TABLE-4.28 TIME(HRS) = 8

800	763	763	752	752	752	746	741	741	741	736		
	730	730	725	725	725	725	720	720	710	695	17.45	734
850	710	695	695	695	695	690	690	685	685	680		
	680	680	675	675	675	671	671	661	657	657	13.92	681
900	598	594	594	590	590	586	586	586	586	583		
	583	583	579	579	579	575	571	571	568	554	10.35	581
950	530	523	520	520	520	520	520	520	517	517		
	517	517	517	514	514	511	511	508	508	508	5.57	516
1000	425	425	422	422	418	413	412	411	411	409		
	409	406	406	406	406	404	404	404	400	398	8.04	410
1050	329	329	328	328	328	325	323	323	323	321		
	321	318	317	315	315	315	314	314	314	309	6.16	320

FOR DEGREE OF 1 COEFFICIENTS ARE
209.85614000 -1.68457090
BEST FIT VALUES 750.9 666.7 582.4 498.2 414.0 329.8
STANDARD DEVIATION IS 15.1692070
FOR DEGREE OF 2 COEFFICIENTS ARE
83.21141500 1.07722960 -0.01492865
BEST FIT VALUES 738.5 669.2 592.4 508.2 416.5 317.3
STANDARD DEVIATION IS 11.5528800
FOR DEGREE OF 3 COEFFICIENTS ARE
-281.50552000 13.02582600 -0.14476114 0.00046794
BEST FIT VALUES 736.7 671.6 593.8 506.8 414.0 319.1
STANDARD DEVIATION IS 13.4445410

EFFECT OF SOAKING TEMPERATURE ON HARDNESS IN A.C. CONDITION

ALLOY : B1 AS CAST HARDNESS(HV30)= 594

TABLE-4.29 TIME(HRS) = 10

TEMP (DEG.C)	HARDNESS (HV30)										SD (HV30)	AVERAGE
800	741	741	741	736	736	736	730	730	730	725		
	720	715	715	715	715	715	710	710	710	690	13.68	723
850	725	715	710	705	705	705	700	700	700	695		
	690	690	685	685	680	680	675	675	671	666	15.77	692
900	606	602	598	594	594	590	590	590	590	586		
	586	586	586	583	583	583	583	579	571	557	10.58	586
950	550	550	547	543	543	543	540	533	530	530		
	527	523	520	520	520	520	517	517	511	505	13.54	529
1000	393	391	385	383	383	379	377	377	375	373		
	370	370	370	370	358	358	358	358	358	349	12.24	371
1050	280	278	277	276	276	276	276	276	275	275		
	275	275	274	274	274	271	268	266	266	266	4.11	273

FOR DEGREE OF 1 COEFFICIENTS ARE

225.74281000 -1.86857090

BEST FIT VALUES 762.6 669.1 575.7 482.3 388.9 295.4

STANDARD DEVIATION IS 36.0495660

FOR DEGREE OF 2 COEFFICIENTS ARE

-103.25174000 5.30596630 -0.03878128

BEST FIT VALUES 730.3 675.6 601.6 508.1 395.3 263.1

STANDARD DEVIATION IS 23.7218540

FOR DEGREE OF 3 COEFFICIENTS ARE

-1035.43200000 35.84539000 -0.37062021 0.00119600

BEST FIT VALUES 725.8 681.9 605.1 504.5 389.0 267.6

STANDARD DEVIATION IS 26.7335330

EFFECT OF SOAKING TEMPERATURE ON HARDNESS IN A.C. CONDITION

ALLOY : B2 AS CAST HARDNESS(HV30)= 590
TABLE-4.30 TIME(HRS) = 2

TEMP (DEG.C)	HARDNESS (HV30)										SD	AVERAGE (HV30)
800	659	635	631	626	626	622	618	618	610	610		
	610	606	606	606	606	606	602	602	602	602	14.61	615
850	533	533	533	533	530	527	527	527	523	523		
	523	520	520	520	511	511	508	508	508	499	10.18	520
900	517	514	511	511	511	511	508	508	505	505		
	505	505	499	499	499	493	490	484	484	484	10.32	502
950	470	465	465	465	462	459	459	457	454	454		
	454	451	451	451	451	451	449	449	444	444	7.28	455
1000	439	439	439	436	434	432	432	432	429	428		
	427	427	425	420	418	418	418	418	415	406	9.18	426
1050	429	427	427	413	413	411	411	409	409	409		
	406	406	406	406	404	402	402	400	396	396	9.36	409

FOR DEGREE OF 1 COEFFICIENTS ARE
120.61619000 -0.77657143
BEST FIT VALUES 584.9 546.1 507.2 468.4 429.6 390.8
STANDARD DEVIATION IS 23.1236830
FOR DEGREE OF 2 COEFFICIENTS ARE
330.24797000 -5.34810920 0.02471102
BEST FIT VALUES 605.5 542.0 490.8 451.9 425.5 411.4
STANDARD DEVIATION IS 15.4232360
FOR DEGREE OF 3 COEFFICIENTS ARE
1098.19240000 -30.50695400 0.29808500 -0.00098528
BEST FIT VALUES 609.2 536.8 487.8 454.9 430.7 407.6
STANDARD DEVIATION IS 16.4314860

TABLE-4.31 TIME(HRS) = 4

800	652	652	648	648	648	644	644	635	635	635		
	631	631	626	626	626	622	622	618	618	618	11.93	633
850	547	540	540	540	540	537	537	537	533	530		
	530	527	527	523	523	520	520	520	514	511	9.94	529
900	508	508	508	502	499	499	496	496	493	493		
	490	487	487	487	487	484	481	481	481	478	9.53	492
950	459	459	459	457	454	454	454	451	449	446		
	446	444	444	444	444	439	434	432	427	425	10.41	446
1000	425	422	420	420	418	418	418	418	415	415		
	415	415	415	413	411	411	406	406	404	402	6.13	414
1050	375	375	371	371	371	371	371	371	370	368		
	368	364	364	362	362	362	358	353	353	351	7.31	365

FOR DEGREE OF 1 COEFFICIENTS ARE
139.47910000 -0.98914342
BEST FIT VALUES 603.5 554.0 504.6 455.1 405.6 356.2
STANDARD DEVIATION IS 21.7121890
FOR DEGREE OF 2 COEFFICIENTS ARE
318.22220000 -4.88707740 0.02106991
BEST FIT VALUES 621.0 550.5 490.5 441.1 402.1 373.7
STANDARD DEVIATION IS 16.8291880
FOR DEGREE OF 3 COEFFICIENTS ARE
1797.47790000 -53.34939400 0.54765756 -0.00189790
BEST FIT VALUES 628.1 540.6 484.9 446.8 412.1 366.6
STANDARD DEVIATION IS 10.3715980

EFFECT OF SOAKING TEMPERATURE ON HARDNESS IN A.C. CONDITION

ALLOY : B2 AS CAST HARDNESS(HV30)= 590
TABLE-4.32 TIME(HRS) = 6

TEMP (DEG.C)	HARDNESS (HV30)										SD	AVERAGE (HV30)
800	652	652	648	648	648	648	644	644	639	639		
	639	639	635	635	635	631	631	631	618	618	9.82	638
850	550	540	537	533	533	533	530	530	530	530		
	527	527	520	520	517	517	517	514	514	511	10.08	526
900	511	505	502	499	496	493	493	487	487	484		
	484	484	478	478	478	478	476	476	473	473	11.25	486
950	457	454	451	451	451	451	449	449	446	446		
	446	444	444	439	439	439	432	432	422	422	9.85	443
1000	413	409	409	406	406	406	404	404	404	404		
	400	400	400	400	400	398	398	398	398	391	5.05	402
1050	353	349	348	346	344	343	343	343	341	337		
	329	326	320	317	317	314	314	309	302	301	16.82	329

FOR DEGREE OF 1 COEFFICIENTS ARE
150.66672000 -1.12000060
BEST FIT VALUES 610.7 554.7 498.7 442.7 386.7 330.7
STANDARD DEVIATION IS 22.1773150
FOR DEGREE OF 2 COEFFICIENTS ARE
266.39419000 -3.64372330 0.01364174
BEST FIT VALUES 622.0 552.4 489.6 433.6 384.4 342.0
STANDARD DEVIATION IS 22.6055760
FOR DEGREE OF 3 COEFFICIENTS ARE
2402.59340000 -73.62835500 0.77408914 -0.00274077
BEST FIT VALUES 632.2 538.0 481.4 441.9 398.8 331.7
STANDARD DEVIATION IS 10.4284190

TABLE-4.33 TIME(HRS) = 8

800	675	675	666	666	666	661	661	657	657	648		
	648	644	644	644	644	644	644	639	639	634	12.40	652
850	543	543	543	540	540	537	533	533	533	530		
	530	530	530	527	523	520	511	511	508	502	12.30	528
900	505	505	505	499	499	499	493	490	487	487		
	476	478	476	473	473	473	470	468	465	465	14.20	484
950	465	459	457	457	454	454	454	451	449	446		
	444	444	441	441	441	439	436	432	432	427	10.21	446
1000	387	387	387	387	377	377	377	377	375	375		
	373	373	373	373	373	370	370	370	357	353	8.86	374
1050	309	309	308	307	305	305	305	305	295	295		
	295	294	294	294	289	289	289	289	287	282	8.53	297

FOR DEGREE OF 1 COEFFICIENTS ARE
166.60000000 -1.30000000
BEST FIT VALUES 626.0 561.0 496.0 431.0 366.0 301.0
STANDARD DEVIATION IS 23.5265790
FOR DEGREE OF 2 COEFFICIENTS ARE
241.12362000 -2.92517140 0.00878471
BEST FIT VALUES 633.3 559.5 490.1 425.1 364.5 308.3
STANDARD DEVIATION IS 26.0377420
FOR DEGREE OF 3 COEFFICIENTS ARE
2550.62010000 -78.58724200 0.83092270 -0.00296311
BEST FIT VALUES 644.3 544.0 481.3 434.1 380.1 297.1
STANDARD DEVIATION IS 15.8201170

EFFECT OF SOAKING TEMPERATURE ON HARDNESS IN A.C. CONDITION

ALLOY : B2 AS CAST HARDNESS(HV30)= 590

TABLE-4.34 TIME(HRS) = 10

TEMP (DEG.C)	HARDNESS (HV30)										SD	AVERAGE (HV30)
800	695	690	680	680	680	680	671	671	671	666		
	666	666	661	661	661	661	661	657	657	644	12.30	668
850	543	540	540	537	537	533	533	533	530	530		
	527	527	527	523	520	514	514	505	505	505	12.05	526
900	508	508	505	505	499	496	496	493	493	493		
	490	487	481	481	481	481	478	476	473	467	12.06	489
950	462	457	454	451	451	446	446	446	444	444		
	444	444	444	441	441	441	436	434	429	427	8.61	444
1000	370	366	364	364	362	362	358	357	353	353		
	341	341	341	341	341	341	337	337	337	336	11.82	350
1050	278	278	274	269	269	269	268	268	264	263		
	261	261	260	260	260	258	256	254	252	249	8.05	263

FOR DEGREE OF 1 COEFFICIENTS ARE

182.98952000 -1.48457140

BEST FIT VALUES 642.2 568.0 493.8 419.6 345.3 271.1

STANDARD DEVIATION IS 28.0018760

FOR DEGREE OF 2 COEFFICIENTS ARE

211.46982000 -2.10565450 0.00335721

BEST FIT VALUES 645.0 567.4 491.5 417.3 344.8 273.9

STANDARD DEVIATION IS 32.1979400

FOR DEGREE OF 3 COEFFICIENTS ARE

2814.32540000 -87.37855100 0.92992567 -0.00333949

BEST FIT VALUES 657.4 549.9 481.6 427.4 362.3 261.3

STANDARD DEVIATION IS 24.1729740

EFFECT OF SOAKING TEMPERATURE ON HARDNESS IN A.C. CONDITION

ALLOY : B3 AS CAST HARDNESS(HV30)= 652
TABLE-4.35 TIME(HRS) = 2

TEMP (DEG.C)	HARDNESS (HV30)										SD	AVERAGE (HV30)
800	710	705	705	705	700	700	700	700	700	695		
	695	695	695	690	690	690	690	690	685	685	7.05	696
850	583	583	583	579	579	575	571	571	571	568		
	568	568	568	564	564	561	561	557	557	554	8.97	569
900	533	533	533	530	527	520	517	514	514	511		
	511	511	511	508	505	502	502	499	496	496	12.28	513
950	499	499	499	496	496	496	496	496	496	496		
	493	493	493	493	493	487	487	481	481	473	6.95	492
1000	490	490	490	487	484	484	481	478	478	476		
	476	476	476	470	470	470	470	470	467	467	7.84	477
1050	411	409	409	409	406	406	404	404	404	402		
	398	398	398	396	396	393	391	391	385	381	8.35	399

FOR DEGREE OF 1 COEFFICIENTS ARE
146.62476000 -1.01828570
BEST FIT VALUES 651.6 600.7 549.8 498.9 448.0 397.0
STANDARD DEVIATION IS 36.1341440
FOR DEGREE OF 2 COEFFICIENTS ARE
394.42719000 -6.42222840 0.02921050
BEST FIT VALUES 676.0 595.8 530.3 479.4 443.1 421.4
STANDARD DEVIATION IS 32.8190190
FOR DEGREE OF 3 COEFFICIENTS ARE
3591.93000000 -111.17653000 1.16746240 -0.00410243
BEST FIT VALUES 691.2 574.3 518.1 491.8 464.7 405.9
STANDARD DEVIATION IS 11.7699700

TABLE-4.36 TIME(HRS) = 4

800	720	720	715	715	710	710	705	705	700	700		
	700	700	700	700	695	695	695	690	690	685	9.93	702
850	594	594	594	594	590	590	586	582	579	575		
	575	575	571	571	571	571	568	564	564	564	10.99	578
900	523	523	520	517	517	517	511	505	505	505		
	505	505	505	505	502	499	499	499	499	493	8.86	507
950	517	511	508	508	508	505	505	505	505	499		
	496	496	496	496	496	493	493	493	493	493	7.31	500
1000	436	429	429	429	428	427	427	425	425	422		
	422	422	420	418	418	418	418	415	415	415	5.83	422
1050	377	373	373	373	371	370	368	368	368	368		
	366	366	366	360	360	360	357	355	351	344	8.30	364

FOR DEGREE OF 1 COEFFICIENTS ARE
165.65243000 -1.23714340
BEST FIT VALUES 666.8 605.0 543.1 481.2 419.4 357.5
STANDARD DEVIATION IS 30.2839720
FOR DEGREE OF 2 COEFFICIENTS ARE
348.63293000 -5.22748420 0.02156941
BEST FIT VALUES 684.8 601.4 528.7 466.9 415.8 375.5
STANDARD DEVIATION IS 29.3411710
FOR DEGREE OF 3 COEFFICIENTS ARE
2756.67090000 -84.11790300 0.87878636 -0.00308954
BEST FIT VALUES 696.3 585.2 519.5 476.2 432.0 363.8
STANDARD DEVIATION IS 21.3031590

EFFECT OF SOAKING TEMPERATURE ON HARDNESS IN A.C. CONDITION

ALLOY : B3 AS CAST HARDNESS(HV30)= 652
TABLE-4.37 TIME(HRS) = 6

TEMP (DEG.C)	HARDNESS (HV30)										SD	AVERAGE (HV30)
800	730	730	725	725	725	720	720	715	715	715		
	715	715	715	710	710	710	710	710	710	710	6.93	716
850	631	631	626	622	618	618	618	618	618	618		
	618	618	618	614	610	610	606	602	602	602	8.54	615
900	527	523	523	520	520	517	517	514	514	514		
	514	514	514	508	508	508	505	505	505	505	6.70	513
950	514	514	502	502	502	502	499	499	496	496		
	496	493	493	490	490	490	490	490	490	484	7.88	496
1000	393	393	391	389	389	387	387	385	383	383		
	383	377	377	375	375	373	370	370	368	364	8.83	380
1050	370	368	364	362	360	358	358	358	358	358		
	358	358	357	357	355	353	351	349	344	344	6.64	357

FOR DEGREE OF 1 COEFFICIENTS ARE
184.32482000 -1.43828630
BEST FIT VALUES 692.6 620.7 548.8 476.9 405.0 333.0
STANDARD DEVIATION IS 29.2519460
FOR DEGREE OF 2 COEFFICIENTS ARE
386.69736000 -5.85151860 0.02385531
BEST FIT VALUES 712.5 616.7 532.9 461.0 401.0 352.9
STANDARD DEVIATION IS 26.4238410
FOR DEGREE OF 3 COEFFICIENTS ARE
724.23041000 -16.90953500 0.14401084 -0.00043306
BEST FIT VALUES 714.1 614.5 531.6 462.3 403.3 351.3
STANDARD DEVIATION IS 32.0965920

TABLE-4.38 TIME(HRS) = 8

800	757	752	752	752	752	746	746	746	746	746		
	741	741	741	741	736	736	736	736	730	730	7.66	743
850	644	635	631	631	626	622	622	622	622	622		
	618	618	618	618	618	614	614	610	610	610	8.77	621
900	530	530	523	520	517	514	514	511	511	511		
	508	505	505	502	502	499	499	496	496	496	10.66	509
950	505	505	496	490	490	490	490	487	487	487		
	484	481	481	481	481	478	473	473	473	470	9.74	485
1000	398	397	396	393	391	383	381	381	381	377		
	377	375	375	371	371	366	366	366	366	362	11.41	378
1050	312	307	304	302	302	301	299	295	295	295		
	289	289	287	287	287	287	285	285	282	270	10.02	293

FOR DEGREE OF 1 COEFFICIENTS ARE
209.21328000 -1.71599940
BEST FIT VALUES 719.3 633.5 547.7 461.9 376.1 290.3
STANDARD DEVIATION IS 26.2684870
FOR DEGREE OF 2 COEFFICIENTS ARE
333.41554000 -4.42453590 0.01464074
BEST FIT VALUES 731.5 631.1 538.0 452.2 373.7 302.5
STANDARD DEVIATION IS 27.4459230
FOR DEGREE OF 3 COEFFICIENTS ARE
2252.14380000 -67.28454000 0.69767250 -0.00246175
BEST FIT VALUES 740.7 618.2 530.7 459.6 386.6 293.2
STANDARD DEVIATION IS 24.5021170

EFFECT OF SOAKING TEMPERATURE ON HARDNESS IN A.C. CONDITION

ALLOY : B3 AS CAST HARDNESS(HV30)= 652

TABLE-4.39 TIME(HRS) = 10

TEMP (DEG.C)	HARDNESS (HV30)										SD	AVERAGE (HV30)
800	763	763	763	757	752	752	752	746	746	741		
	741	741	741	736	736	736	736	736	736	736	9.98	745
850	652	652	652	648	648	648	648	648	648	644		
	644	644	644	644	644	631	631	631	631	622	8.63	642
900	533	533	530	530	527	523	523	523	523	523		
	520	520	517	517	517	511	511	508	508	505	8.38	520
950	499	499	499	496	496	496	496	496	493	487		
	487	487	484	484	484	481	481	481	481	481	7.13	489
1000	375	375	373	371	370	370	368	368	368	362		
	358	357	353	351	351	348	346	346	343	341	11.57	359
1050	270	270	270	269	269	269	265	264	263	263		
	262	262	260	260	258	257	254	251	251	246	7.12	261

FOR DEGREE OF 1 COEFFICIENTS ARE

224.69519000 -1.88571370

BEST FIT VALUES 738.4 644.1 549.8 455.5 361.2 267.0

STANDARD DEVIATION IS 22.9014420

FOR DEGREE OF 2 COEFFICIENTS ARE

220.44643000 -1.79305910 -0.00050084

BEST FIT VALUES 738.0 644.2 550.1 455.9 361.3 266.5

STANDARD DEVIATION IS 26.4406330

FOR DEGREE OF 3 COEFFICIENTS ARE

1559.25210000 -45.65405300 0.47608921 -0.00171770

BEST FIT VALUES 744.3 635.2 545.0 461.1 370.4 260.0

STANDARD DEVIATION IS 28.1466160

EFFECT OF SOAKING TEMPERATURE ON HARDNESS IN A.C. CONDITION

ALLOY : B4 AS CAST HARDNESS(HV30)= 621
TABLE-4.40 TIME(HRS) = 2

TEMP (DEG.C)	HARDNESS (HV30)										SD	AVERAGE (HV30)
800	671	671	671	666	666	666	666	657	657	657		
	652	652	652	648	644	644	644	644	644	644	10.40	655
850	557	557	554	554	550	550	550	543	543	540		
	540	537	537	537	533	533	527	527	527	523	10.74	540
900	487	484	481	481	476	473	473	473	473	473		
	473	473	470	470	470	470	470	467	467	462	6.03	473
950	499	487	481	478	478	473	470	470	467	467		
	465	465	465	465	465	462	462	462	462	457	10.15	470
1000	444	444	436	436	436	436	432	432	432	429		
	429	427	427	427	427	427	422	418	415	415	8.11	429
1050	418	413	413	413	411	406	406	406	404	404		
	402	402	400	396	389	389	387	383	381	379	11.74	400

FOR DEGREE OF 1 COEFFICIENTS ARE
134.60291000 -0.92057199
BEST FIT VALUES 609.6 563.5 517.5 471.5 425.5 379.4
STANDARD DEVIATION IS 35.4876230
FOR DEGREE OF 2 COEFFICIENTS ARE
458.15587000 -7.97644200 0.03813984
BEST FIT VALUES 641.4 557.2 492.1 446.1 419.1 411.2
STANDARD DEVIATION IS 23.4006410
FOR DEGREE OF 3 COEFFICIENTS ARE
2502.60940000 -74.95537000 0.76592751 -0.00262306
BEST FIT VALUES 651.1 543.4 484.3 454.0 432.9 401.3
STANDARD DEVIATION IS 14.6154630

TABLE-4.41 TIME(HRS) = 4

800	657	657	657	652	652	652	648	648	648	644		
	639	639	639	639	639	639	639	639	635	635	7.59	644
850	537	537	533	533	533	533	533	530	527	523		
	523	523	523	523	523	523	520	520	514	511	7.28	526
900	493	493	493	493	493	484	484	481	481	481		
	481	478	478	476	476	473	473	465	465	462	9.71	480
950	481	478	478	478	476	476	473	473	467	467		
	467	467	467	465	465	465	462	459	454	454	7.88	468
1000	406	396	393	393	389	387	385	385	385	385		
	385	385	383	383	381	379	379	379	379	366	8.07	385
1050	348	348	343	343	339	339	334	333	333	331		
	328	328	326	325	325	320	311	309	308	307	12.87	328

FOR DEGREE OF 1 COEFFICIENTS ARE
153.69053000 -1.15142910
BEST FIT VALUES 615.8 558.2 500.6 443.0 385.5 327.9
STANDARD DEVIATION IS 26.8403570
FOR DEGREE OF 2 COEFFICIENTS ARE
248.81040000 -3.22575240 0.01121256
BEST FIT VALUES 625.1 556.3 493.1 435.6 383.6 337.2
STANDARD DEVIATION IS 29.3722070
FOR DEGREE OF 3 COEFFICIENTS ARE
2553.77610000 -78.73939300 0.83173773 -0.00295730
BEST FIT VALUES 636.1 540.8 484.4 444.5 399.2 326.1
STANDARD DEVIATION IS 22.9796110

EFFECT OF SOAKING TEMPERATURE ON HARDNESS IN A.C. CONDITION

ALLOY : B4 AS CAST HARDNESS(HV30)= 621
TABLE-4.42 TIME(HRS) = 6

TEMP (DEG.C)	HARDNESS (HV30)										SD	AVERAGE (HV30)
800	671	666	661	661	661	661	657	657	657	657		
	657	652	652	648	648	648	644	644	644	631	9.23	653
850	557	557	554	554	554	554	550	550	550	550		
	550	547	547	547	543	543	543	533	530	530	8.15	547
900	484	484	484	481	478	478	476	476	476	476		
	476	476	476	473	470	470	470	470	467	465	5.48	475
950	465	465	462	459	459	457	457	457	457	457		
	457	454	451	449	449	449	446	444	444	441	6.98	453
1000	396	393	391	389	389	387	387	383	381	381		
	377	377	377	375	371	370	370	368	368	368	9.12	379
1050	317	314	314	309	309	309	308	307	305	302		
	302	302	301	295	295	295	295	294	294	289	7.98	302

FOR DEGREE OF 1 COEFFICIENTS ARE
167.38386000 -1.30342910
BEST FIT VALUES 631.1 565.9 500.8 435.6 370.4 305.2
STANDARD DEVIATION IS 21.7302740
FOR DEGREE OF 2 COEFFICIENTS ARE
250.39364000 -3.11366200 0.00978504
BEST FIT VALUES 639.2 564.3 494.2 429.1 368.8 313.4
STANDARD DEVIATION IS 23.5611160
FOR DEGREE OF 3 COEFFICIENTS ARE
2328.82720000 -71.20581500 0.74966891 -0.00266666
BEST FIT VALUES 649.2 550.3 486.3 437.1 382.8 303.3
STANDARD DEVIATION IS 14.5159450

TABLE-4.43 TIME(HRS) = 8

800	680	675	671	671	671	671	666	661	661	661		
	657	657	657	657	657	657	652	652	648	648	9.10	661
850	543	543	543	543	540	537	537	537	533	533		
	533	530	530	530	527	527	527	517	514	514	9.14	531
900	493	493	490	487	487	487	487	487	484	484		
	484	484	484	484	484	481	476	476	476	476	5.17	484
950	467	454	454	454	454	451	451	446	446	441		
	441	441	441	439	439	439	434	434	434	434	8.99	444
1000	360	360	353	351	348	346	346	346	346	343		
	341	341	341	341	339	339	337	336	334	323	8.62	343
1050	283	282	281	280	277	261	260	260	258	257		
	256	256	256	254	254	252	250	250	250	250	11.93	261

FOR DEGREE OF 1 COEFFICIENTS ARE
183.03995000 -1.48799940
BEST FIT VALUES 640.0 565.6 491.2 416.8 342.4 268.0
STANDARD DEVIATION IS 24.8957840
FOR DEGREE OF 2 COEFFICIENTS ARE
197.58114000 -1.80510610 0.00171409
BEST FIT VALUES 641.4 565.3 490.1 415.7 342.1 269.4
STANDARD DEVIATION IS 28.7073940
FOR DEGREE OF 3 COEFFICIENTS ARE
2426.65870000 -74.83254900 0.79522442 -0.00285993
BEST FIT VALUES 652.1 550.3 481.6 424.3 357.1 258.6
STANDARD DEVIATION IS 22.9414350

EFFECT OF SOAKING TEMPERATURE ON HARDNESS IN A.C. CONDITION

ALLOY : B4 AS CAST HARDNESS(HV30)= 621

TABLE-4.44 TIME(HRS) = 10

TEMP (DEG.C)	HARDNESS (HV30)										SD (HV30)	AVERAGE
800	690	690	690	685	680	680	680	680	680	675		
	675	675	675	675	675	671	671	671	671	666	6.86	677
850	523	520	517	517	517	517	517	517	517	514		
	514	514	511	511	511	511	508	508	508	508	4.35	514
900	499	493	493	493	493	493	493	493	493	490		
	487	487	487	487	484	484	484	481	481	476	5.68	488
950	454	452	451	451	451	451	449	449	449	446		
	446	446	444	444	444	436	436	436	436	434	6.37	445
1000	301	301	294	291	290	290	287	287	283	282		
	280	280	278	275	275	274	274	274	270	269	9.57	282
1050	253	253	252	251	250	249	248	248	240	239		
	239	239	239	238	238	237	236	236	236	236	6.63	242

FOR DEGREE OF 1 COEFFICIENTS ARE

198.15910000 -1.66514340

BEST FIT VALUES 649.5 566.2 483.0 399.7 316.4 233.2

STANDARD DEVIATION IS 41.3088310

FOR DEGREE OF 2 COEFFICIENTS ARE

238.76084000 -2.55056460 0.00478606

BEST FIT VALUES 653.5 565.4 479.8 396.5 315.6 237.2

STANDARD DEVIATION IS 47.5122370

FOR DEGREE OF 3 COEFFICIENTS ARE

1847.13990000 -55.24312900 0.57733924 -0.00206357

BEST FIT VALUES 661.1 554.6 473.6 402.8 326.5 229.4

STANDARD DEVIATION IS 54.9100730

Table 4.45 Summary table of effect of heat-treatment on hardness

h/t temp. (deg.C)	B1					B2					B3					B4				
	2	4	6	8	10	2	4	6	8	10	2	4	6	8	10	2	4	6	8	10
800	696	725	724	734	723	615	633	638	652	668	696	702	716	743	745	655	644	653	661	677
850	603	674	662	681	692	520	529	526	528	526	569	578	615	621	642	540	526	547	531	514
900	587	558	576	581	586	502	492	486	484	489	513	507	513	509	520	473	480	475	484	488
950	555	545	529	516	529	455	446	443	446	444	492	500	496	485	489	470	468	453	444	445
1000	533	474	476	410	371	426	414	402	374	350	477	422	380	378	359	429	385	379	343	283
1050	453	363	356	320	273	409	365	329	297	263	399	364	357	293	261	400	328	302	261	242

TABLE 4.46 EFFECT OF HEAT-TREATMENT ON THE AMOUNT OF MASSIVE CARBIDE

Alloy	Temp. (Deg.)	Soaking Duration(hrs.) 2	4	6	8	10
B1	800	26.7	26.5	26.3	26.2	25.8
	850	27.2	26.8	26.5	25.8	24.9
	900	26.5	24.7	24.2	23.8	24.0
	950	25.9	23.6	20.2	20.1	19.7
	1000	18.1	17.9	15.9	14.8	13.9
B2	800	22.5	21.6	20.7	20.0	19.5
	850	22.9	22.2	21.8	20.5	19.7
	900	20.4	19.3	18.4	17.8	17.4
	950	20.1	17.9	17.4	16.5	16.3
	1000	15.3	14.2	14.0	13.5	13.2
B3	800	23.3	22.2	21.3	20.6	20.5
	850	22.5	21.8	21.1	20.8	20.8
	900	21.4	20.3	20.4	20.0	19.5
	950	20.7	19.6	19.1	18.1	17.3
	1000	16.9	13.8	15.0	13.5	12.6
B4	800	21.3	20.8	19.8	20.0	20.1
	850	21.8	21.2	21.5	20.6	19.7
	900	20.3	19.4	18.7	18.5	18.3
	950	20.0	18.9	18.4	18.1	17.8
	1000	17.8	17.4	16.8	16.5	16.3

Effect of heat-treatment on size and dispersion of 2nd phase particles

Table-4.47 (Alloy B1) As-cast hardness = 594

Temp. Deg.C	Time Hrs.	HV30	MD μ	1st class %area	1st class %NOP	2nd class %area	2nd class %NOP	3rd class %area	3rd class %NOP	4th class %area	4th class %NOP	5th class %area	5th class %NOP	6th class %area	6th class %NOP
800	2	696	0.52	1.14	72	3.98	28	0.00	0	0.00	0	0.00	0	0.00	0
800	10	723	0.55	1.01	68	4.09	30	0.16	0	0.00	0	0.00	0	0.00	0
850	2	603	0.61	1.12	61	6.14	37	0.79	1	0.00	0	0.00	0	0.00	0
850	4	674	0.62	1.10	62	5.57	35	1.10	2	0.00	0	0.00	0	0.00	0
850	6	662	0.65	0.90	56	5.74	40	0.95	2	0.31	0	0.00	0	0.00	0
850	10	692	0.66	0.93	55	6.02	40	1.58	3	0.00	0	0.00	0	0.00	0
900	2	587	0.54	1.30	71	4.49	27	0.47	1	0.00	0	0.00	0	0.00	0
900	4	558	0.67	0.91	56	5.62	38	1.74	4	0.00	0	0.00	0	0.00	0
900	6	576	0.73	0.82	52	5.62	39	2.84	7	0.31	0	0.00	0	0.00	0
900	10	586	0.67	0.79	62	3.58	31	1.89	5	0.31	0	0.00	0	0.00	0
950	2	555	0.70	0.93	61	3.98	29	3.16	8	0.62	0	0.00	0	0.00	0
950	4	545	0.67	0.91	65	3.69	29	1.42	4	0.62	0	0.51	0	0.00	0
950	6	529	0.77	0.66	51	4.55	39	2.05	6	0.93	1	0.51	0	0.00	0
950	10	529	0.81	0.61	55	3.35	33	1.89	6	1.86	3	0.51	0	0.00	0

Table-4.48 (Alloy B2) As-cast hardness = 590

Temp. Deg.C	Time Hrs.	Hv30	MD μ	1st class %area	1st class %NOP	2nd class %area	2nd class %NOP	3rd class %area	3rd class %NOP	4th class %area	4th class %NOP	5th class %area	5th class %NOP	6th class %area	6th class %NOP
800	2	615	0.62	1.13	59	6.70	39	0.63	1	0.00	0	0.00	0	0.00	0
800	10	668	0.63	1.00	59	5.85	38	0.47	1	0.31	0	0.00	0	0.00	0
850	2	520	0.60	1.07	63	5.28	35	0.47	1	0.00	0	0.00	0	0.00	0
850	4	529	0.62	0.93	64	4.15	31	1.26	3	0.00	0	0.00	0	0.00	0
850	6	526	0.65	0.95	55	6.42	41	1.10	2	0.00	0	0.00	0	0.00	0
850	10	526	0.67	0.88	52	6.82	44	1.26	2	0.00	0	0.00	0	0.00	0
900	2	502	0.65	0.98	56	6.48	41	0.95	2	0.31	0	0.00	0	0.00	0
900	4	492	0.63	1.00	59	5.74	37	1.10	2	0.00	0	0.00	0	0.00	0
900	6	486	0.68	0.80	52	6.08	44	1.10	2	0.31	0	0.00	0	0.00	0
900	10	489	0.64	1.02	61	5.00	33	1.89	4	0.00	0	0.00	0	0.00	0
950	2	455	0.69	0.74	53	5.11	40	1.89	5	0.00	0	0.00	0	0.00	0
950	4	446	0.69	1.05	66	3.69	26	2.21	5	0.62	0	1.02	0	0.00	0
950	6	443	0.66	0.85	69	2.56	23	1.58	5	0.62	1	0.51	0	0.00	0
950	10	444	0.77	0.90	70	2.16	18	2.05	6	2.17	3	0.51	0	0.76	0

Effect of heat-treatment on size and dispersion of 2nd phase particles

Table-4.49 (Alloy B3) As-cast hardness = 652

Temp. Deg.C	Time Hrs.	Hv30	MD μ	1st class %area	1st class %NOP	2nd class %area	2nd class %NOP	3rd class %area	3rd class %NOP	4th class %area	4th class %NOP	5th class %area	5th class %NOP	6th class %area	6th class %NOP
800	2	696	0.63	1.05	57	6.76	41	0.47	1	0.00	0	0.00	0	0.00	0
800	10	745	0.63	0.99	62	5.00	34	1.10	2	0.31	0	0.00	0	0.00	0
850	2	569	0.65	1.07	56	6.82	40	1.58	3	0.00	0	0.00	0	0.00	0
850	4	578	0.69	0.82	54	5.57	40	1.74	4	0.31	0	0.00	0	0.00	0
850	6	615	0.67	0.96	55	6.42	40	1.74	3	0.00	0	0.00	0	0.00	0
850	10	642	0.61	1.00	60	5.62	38	0.47	1	0.00	0	0.00	0	0.00	0
900	2	513	0.54	1.30	71	4.49	27	0.47	1	0.00	0	0.00	0	0.00	0
900	4	507	0.67	0.78	56	4.83	38	1.58	4	0.00	0	0.00	0	0.00	0
900	6	513	0.54	1.30	71	4.49	27	0.47	1	0.00	0	0.00	0	0.00	0
900	10	520	0.65	0.98	58	5.62	37	1.42	3	0.00	0	0.00	0	0.00	0
950	2	492	0.68	0.95	54	6.48	41	1.42	3	0.31	0	0.00	0	0.00	0
950	4	500	0.75	0.74	54	4.49	36	2.84	8	0.62	0	0.00	0	0.00	0
950	6	496	0.74	0.83	55	4.83	36	2.53	6	1.24	1	0.00	0	0.00	0
950	10	489	0.79	0.81	64	2.67	23	1.74	5	3.71	6	0.00	0	0.00	0

Table-4.50 (Alloy B4) As-cast hardness = 621

Temp. Deg.C	Time Hrs.	Hv30	MD μ	1st class %area	1st class %NOP	2nd class %area	2nd class %NOP	3rd class %area	3rd class %NOP	4th class %area	4th class %NOP	5th class %area	5th class %NOP	6th class %area	6th class %NOP
800	2	655	0.60	1.02	61	5.62	37	0.32	0	0.00	0	0.00	0	0.00	0
800	10	677	0.61	1.03	61	5.68	37	0.63	1	0.00	0	0.00	0	0.00	0
850	2	540	0.65	0.98	60	5.11	34	1.74	4	0.31	0	0.00	0	0.00	0
850	4	526	0.68	0.90	50	7.39	45	1.58	3	0.00	0	0.00	0	0.00	0
850	6	547	0.62	1.09	62	5.45	34	1.42	3	0.00	0	0.00	0	0.00	0
850	10	514	0.67	0.88	57	5.11	37	1.74	4	0.31	0	0.00	0	0.00	0
900	2	473	0.62	1.13	62	5.68	34	1.42	3	0.00	0	0.00	0	0.00	0
900	4	480	0.62	1.10	62	5.57	35	1.10	2	0.00	0	0.00	0	0.00	0
900	6	475	0.66	0.95	55	6.42	41	1.42	3	0.00	0	0.00	0	0.00	0
900	10	488	0.64	0.80	60	4.37	36	1.10	3	0.00	0	0.00	0	0.00	0
950	2	470	0.69	0.82	54	5.57	40	1.74	4	0.31	0	0.00	0	0.00	0
950	4	468	0.67	0.91	65	3.69	29	1.42	4	0.62	0	0.51	0	0.00	0
950	6	453	0.71	0.76	56	4.37	36	2.05	6	0.62	0	0.00	0	0.00	0
950	10	445	0.82	0.66	59	2.61	26	3.31	11	1.24	2	0.51	0	0.00	0

Table-4.51 Effect of h/t on mean diameter of dispersed carbides

Temp. Deg.C	Alloy	Soaking period(Hrs.) 2	4	6	10	Alloy	Soaking period(Hrs.) 2	4	6	10
800	B1	0.52	----	----	0.55	B3	0.63	----	----	0.63
850		0.61	0.62	0.65	0.66		0.65	0.69	0.67	0.61
900		0.54	0.67	0.73	0.67		0.54	0.67	0.54	0.65
950		0.70	0.67	0.77	0.81		0.68	0.75	0.74	0.79
800	B2	0.62	----	----	0.63	B4	0.60	----	----	0.61
850		0.60	0.62	0.65	0.67		0.65	0.68	0.62	0.67
900		0.65	0.63	0.68	0.64		0.62	0.62	0.66	0.64
950		0.69	0.69	0.66	0.77		0.69	0.67	0.71	0.82

Table-4.52 Effect of h/t on the average no. of dispersed carbides

Temp. Deg.C	Alloy	Soaking period(Hrs.) 2	4	6	10	Alloy	Soaking period(Hrs.) 2	4	6	10
800	B1	50	--	--	46	B3	56	--	--	49
850		57	54	49	52		59	47	54	50
900		56	49	48	39		56	43	56	51
950		47	42	39	33		53	41	46	38
800	B2	58	--	--	51	B4	51	--	--	52
850		51	44	53	53		51	56	54	47
900		54	52	47	51		56	54	53	41
950		43	48	37	38		47	42	41	33

Table-4.53 Effect of h/t on volume percent of dispersed carbides

Temp. Deg.C	Alloy	Soaking period(Hrs.) 2	4	6	10
800	B1	10.63	-----	-----	10.93
850		16.71	16.15	16.41	17.52
900		13.01	17.19	19.94	13.66
950		18.04	14.86	18.08	17.08
800	B2	17.59	-----	-----	15.87
850		14.18	13.18	17.62	18.63
900		18.10	16.31	17.24	16.45
950		16.11	17.87	12.70	17.76
800	B3	17.22	-----	-----	15.39
850		19.66	17.53	18.94	14.75
900		13.01	14.94	13.01	16.67
950		19.03	18.05	19.57	18.55
800	B4	14.47	-----	-----	15.26
850		16.92	20.50	16.56	16.70
900		17.11	16.15	18.27	13.04
950		17.53	14.86	16.23	17.32

Table-4.55 Effect of h/t on percent area of dispersed carbides in different classes

Alloy	Temp. Deg.C	Class 1				Class 2				Class 3				Class 4				Class 5				Class 6			
		Soaking period (Hrs.)																							
		2	4	6	10	2	4	6	10	2	4	6	10	2	4	6	10	2	4	6	10	2	4	6	10
B1	800	1.14	....	....	1.01	3.98	....	....	4.09	0.00	....	....	0.16	0.00	....	....	0.00	0.00	....	....	0.00	0.00	....	....	0.00
	850	1.12	1.10	0.90	0.93	6.14	5.57	5.74	6.02	0.79	1.10	0.95	1.58	0.00	0.00	0.31	0.00	0.00	0.00	0.00	0.00	0.00	0.00	0.00	0.00
	900	1.30	0.91	0.82	0.79	4.49	5.62	5.62	3.58	0.47	1.74	2.84	1.89	0.00	0.00	0.31	0.31	0.00	0.00	0.00	0.00	0.00	0.00	0.00	0.00
	950	0.93	0.91	0.66	0.61	3.98	3.69	4.55	3.35	3.16	1.42	2.05	1.89	0.62	0.62	0.93	1.86	0.00	0.51	0.51	0.51	0.00	0.00	0.00	0.00
B2	800	1.13	....	....	1.00	6.70	....	....	5.85	0.63	....	....	0.47	0.00	....	....	0.31	0.00	....	....	0.00	0.00	....	....	0.00
	850	1.07	0.93	0.95	0.88	5.28	4.15	6.42	6.82	0.47	1.26	1.10	1.26	0.00	0.00	0.00	0.00	0.00	0.00	0.00	0.00	0.00	0.00	0.00	0.00
	900	0.98	1.00	0.80	1.02	6.48	5.74	6.08	5.00	0.95	1.10	1.10	1.89	0.31	0.00	0.31	0.00	0.00	0.00	0.00	0.00	0.00	0.00	0.00	0.00
	950	0.74	1.05	0.85	0.90	5.11	3.69	2.56	2.16	1.89	2.21	1.58	2.05	0.00	0.62	0.62	2.17	0.00	1.02	0.51	0.51	0.00	0.00	0.00	0.76
B3	800	1.05	....	....	0.99	6.76	....	....	5.00	0.47	....	....	1.10	0.00	....	....	0.31	0.00	....	....	0.00	0.00	....	....	0.00
	850	1.07	0.82	0.96	1.00	6.82	5.57	6.42	5.62	1.58	1.74	1.74	0.47	0.00	0.31	0.00	0.00	0.00	0.00	0.00	0.00	0.00	0.00	0.00	0.00
	900	1.30	0.78	1.30	0.98	4.49	4.83	4.49	5.62	0.47	1.58	0.47	1.42	0.00	0.00	0.00	0.00	0.00	0.00	0.00	0.00	0.00	0.00	0.00	0.00
	950	0.95	0.74	0.83	0.81	6.48	4.49	4.83	2.67	1.42	2.84	2.53	1.74	0.31	0.62	1.24	3.71	0.00	0.00	0.00	0.00	0.00	0.00	0.00	0.00
B4	800	1.02	....	....	1.03	5.62	....	....	5.68	0.32	....	....	0.63	0.00	....	....	0.00	0.00	....	....	0.00	0.00	....	....	0.00
	850	0.98	0.90	1.09	0.88	5.11	7.39	5.45	5.11	1.74	1.58	1.42	1.74	0.31	0.00	0.00	0.31	0.00	0.00	0.00	0.00	0.00	0.00	0.00	0.00
	900	1.13	1.10	0.95	0.80	5.68	5.57	6.42	4.37	1.42	1.10	1.42	1.10	0.00	0.00	0.00	0.00	0.00	0.00	0.00	0.00	0.00	0.00	0.00	0.00
	950	0.82	0.91	0.76	0.66	5.57	3.69	4.37	2.61	1.74	1.42	2.05	3.31	0.31	0.62	0.62	1.24	0.00	0.51	0.00	0.51	0.00	0.00	0.00	0.00

Frame area = 207.81 μm^2

TABLE-5.1 PHASES UNDER CONSIDERATION

X-RAY WAVE LENGTH(A°)= 1.9373

PHASE(S) UNDER CONSIDERATION:

NO. (S)	ASTM CODE	PHASE(S)	LATTICE TYPE	LATTICE PARAMETER A	B	C
1	06-0696	ALPHA IRON	CUBIC(BCC)	2.8664	0.0000	0.0000
2	23-298	AUSTENITE	CUBIC(FCC)	3.6000	0.0000	0.0000
3	-------	MARTENSITE	CUBIC(BCT)	0.0000	0.0000	0.0000
4	14-0407	CR23C6	CUBIC	10.6380	0.0000	0.0000
5	--------	MN23C6	-------	0.0000	0.0000	0.0000
6	06-0670	FE3C(CEMENTITE)	ORTHORHOMBIC	2.7540	0.0000	4.3490
7	20-509	FE5C2	MONOCLINIC	11.5630	4.5730	5.0580
8	20-508	FE5C2(HAGG)	MONOCLINIC	11.5600	4.5600	5.0300
9	14-176	MN5C2	MONOCLINIC	5.0660	4.5730	11.6600
10	6-0038	MN5C2(PD5C2)	MONOCLINIC	11.6600	4.5730	5.0860
11	-----	FE7C3(2)	HEXAGONAL	6.8820	0.0000	4.5400
12	-------	CR7C3(2)	HEXAGONAL	13.9000	0.0000	4.5400
13	11-0550	CR7C3	HEXAGONAL(TRIGO)	13.9800	0.0000	4.5230
14	05-0720	(CR,FE)7C3	HEXAGONAL	13.9800	0.0000	4.5230
15	03-0975	(CR7C3+MN7C3)	-------	2.2220	0.0000	0.0000
16	14-519	CR2C	HEXAGONAL	2.7900	0.0000	4.4600
17	4-406	CR3C2	ORTHORHOMBIC	11.4600	5.5200	2.8210
18	26-782	FE2C(NETA)	ORTHORHOMBIC	4.7040	4.2180	2.8300
19	20-522	FE0.6MN5.4C2	HEXAGONAL	5.7700	0.0000	6.9800
20	23-0064	C(GRAPHITE)	HEXAGONAL	2.4630	0.0000	6.7140
21	13-534	FE2O3	RHOMBOHEDRAL	5.0340	0.0000	13.7520
22	6-504	CR2O3	HEXAGONAL	4.9540	0.0000	13.5840
23	26-1116	CU2S(1)	HEAXGONAL	3.9610	0.0000	36.7220
24	6-518	MNS	CUBIC	5.2236	0.0000	0.0000
25	4-836	COPPER	CUBIC	3.6150	0.0000	0.0000
26	26-798	FE8SI2C	TRICLINIC	6.3470	6.4140	9.7200
27	05-0708	FE-CR	TETRAGONAL	8.7990	0.0000	4.5440
28	06-645	CRMN3	TETRAGONAL	8.8000	0.0000	4.5880
29	20-706	MN15C4	HEXAGONAL	7.4920	0.0000	12.0700
30	17-897	FE2C	MONOCLINIC	2.7940	2.7940	4.3600

TABLE 5.2-A SUMMARY TABLE OF DIFFRACTOGRAM INDEXING

ALLOY : B1
HEAT-TREATMENT : AS CAST

DIFF. ANGLE	PHASE(S) 1	3	5	7	9	11	13	15	17	19	21	23	25	27	29	INT
48.0	0 0 0	1 1	1 0	1 0	0 0	0 0	0 0	1 0	0 1	0 0	0 0	0 0	0 0	0 0	0 0	8.3
56.0	0 0 1	0 0	1 0	1 1	1 0	0 0	0 0	0 0	0 1	0 0	1 0	0 0	0 0	1 1	1 0	11.3
57.3	1 0 1	0 0	1 0	1 1	0 1	1 1	0 0	0 0	0 1	0 0	0 0	0 0	0 0	0 0	0 0	100.0
58.8	0 0 0	0 0	1 0	1 0	1 0	0 0	0 0	0 0	0 0	0 0	0 0	1 0	0 0	1 0	1 0	7.5
* 62.4	0 0 0	0 0	1 0	0 0	0 0	0 0	0 0	0 0	0 0	0 0	0 0	1 1	0 0	0 1	0 1	7.5
85.1	1 0 0	0 0	0 0	0 0	0 0	0 0	0 0	0 0	0 0	0 0	0 1	0 0	0 0	0 0	0 0	5.8
93.7	0 0 0	0 1	0 0	0 0	0 0	0 1	0 0	0 1	0 0	0 0	0 0	0 0	0 0	0 1	0 0	5.0
97.2	0 0 1	1 0	0 0	0 0	0 0	1 0	0 0	0 0	0 1	0 0	0 0	0 0	0 0	0 0	0 0	15.8
111.9	1 0 1	1 0	0 1	0 0	0 1	0 0	1 0	1 0	0 1	0 0	0 0	0 0	1 0	0 1	0 0	5.8
118.2	0 0 0	0 0	0 1	0 0	0 0	0 0	0 0	0 0	0 0	0 0	0 0	0 0	0 0	0 0	0 0	5.0
	3 0 0	3 4	5 0	6 0	0 0	0 0	4 0	0 0	0 0	3 0	0 0	0 0	0 0	0 0	4 0	0

0 = ABSENT 1 = PRESENT * = PROBABLE DIFF. ANGLE FOR K-BETA RADIATION

TABLE 5.2-B DETAILED ANALYSIS OF PHASE(S) ACTUALLY PRESENT

S.N.	PHASE PRESENT	DIFF ANGLE	PEAK INT	I/IO	D MEAS	D STD	DIFF PLANESTD	INT	CONF LIMIT
(1)	ALPHA IRON	57.3	100	100	2.021	2.027	110	100	99.8
		85.1	5	5	1.433	1.433	200	20	100.0
		111.9	5	5	1.169	1.170	211	30	99.9
(2)	CR23C6	48.0	8	52	2.382	2.370	420	50	99.7
		97.2	15	100	1.292	1.293	644	60	99.9
		111.9	5	36	1.169	1.170	753	90	99.9
(3)	MN23C6	48.0	8	52	2.382	2.380	420	50	100.0
		93.7	5	31	1.328	1.330	622	35	99.8
		97.2	15	100	1.292	1.290	800	30	99.8
		111.9	5	36	1.169	1.169	753	40	100.0
(4)	FE3C(CEMENTITE)	48.0	8	8	2.382	2.380	112	65	100.0
		56.0	11	11	2.064	2.060	210	70	99.9
		57.3	100	100	2.021	2.020	022	60	100.0
		58.8	7	7	1.974	1.970	211	55	99.9
		62.4	7	7	1.870	1.870	113	30	100.0
(5)	FE5C2(HAGG)	48.0	8	8	2.382	2.390	202	20	99.8
		56.0	11	11	2.064	2.060	510	100	99.9
		57.3	100	100	2.021	2.030	312	100	99.7
		58.8	7	7	1.974	1.980	511	20	99.8
		111.9	5	5	1.169	1.170	623	20	99.9
		118.2	5	5	1.129	1.130	133	50	99.8
(6)	CR7C3	57.3	100	100	2.021	2.020	---	50	100.0
		93.7	5	5	1.328	1.330	---	50	99.8
		97.2	15	15	1.292	1.290	---	60	99.8
		111.9	5	5	1.169	1.170	---	100	99.9

TABLE 5.3-A SUMMARY TABLE OF DIFFRACTOGRAM INDEXING

ALLOY : B1
SOAKING TEMPERATURE : 900°C SOAKING DURATION : 4 HOURS
COOLING MEDIA : AIR COOLED

	DIFF. ANGLE	PHASE(S) 1	3	5	7	9	11	13	15	17	19	21	23	25	27	29	INT
	48.3	0 0 0 1	1 1 0	0 0 0	1 0 0	0 0 0	1 0 0	0 0 0	1 0 0	1 0 0	0 0 0	0 0 0	1 0 0	0 0 0	0 0 0	0 0 0	2.0
	55.8	0 1 0 0	0 0 1	0 0 1	0 0 1	0 0 1	0 0 0	0 0 0	0 0 0	0 0 0	0 0 0	1 0 0	0 0 0	0 0 1	0 1 0	1 0 0	15.0
	56.1	0 0 1	0 0 1	0 1 0	1 1 1	0 0 0	0 0 0	0 0 0	0 0 0	1 0 0	0 0 0	0 0 0	0 0 0	0 0 0	1 0 0	0 0 0	9.0
	56.3	0 0 1	1 1 0	0 0 0	0 0 0	0 0 0	0 0 0	0 0 0	0 0 0	0 0 0	0 0 0	0 0 1	0 0 0	0 0 1	1 0 0	0 0 0	6.0
	57.8	0 0 0 0	0 1 1	0 0 0	0 0 0	0 0 0	0 0 0	0 0 0	0 0 0	0 0 0	0 0 0	0 0 0	0 0 0	0 0 1	0 0 1	0 0 1	13.0
	59.0	0 0 0 0	0 1 0	0 0 1	0 0 0	0 0 0	0 0 0	0 0 0	0 0 0	0 0 0	0 0 0	0 0 0	0 0 0	0 0 1	0 1 0	0 1 0	4.0
*	62.7	0 0 0 0	0 1 0	0 0 0	0 0 0	0 0 0	0 0 0	0 0 0	1 0 1	0 0 0	0 0 0	0 0 0	0 0 1	0 0 0	0 0 0	0 0 0	4.0
	65.1	0 1 0 1	1 0 0	1 0 0	1 0 0	0 0 1	0 0 0	0 0 0	0 0 0	0 0 0	0 1 0	0 0 0	0 0 1	0 0 0	0 0 1	0 0 1	6.0
	99.5	0 1 0 0	0 0 0	0 1 0	0 0 0	1 0 0	0 0 0	1 0 0	0 0 0	0 0 0	1 0 0	0 0 0	0 0 0	0 0 0	0 0 0	0 0 0	4.0
	126.1	0 0 0 0	1 0 0	0 0 0	0 0 0	0 0 0	0 0 0	0 0 0	0 0 0	0 0 0	0 0 0	0 0 1	0 0 0	0 0 0	0 0 0	0 0 0	6.0
		0 3 0 3	4 5 0	3 0 3	0 0 0	0 0 0	0 0 0	0 0 0	0 0 0	0 0 0	0 0 0	0 0 0	0 0 0	0 0 0	4 0 0	0	

0 = ABSENT 1 = PRESENT * = PROBABLE DIFF. ANGLE FOR K-BETA RADIATION

TABLE 5.3-B DETAILED ANALYSIS OF PHASE(S) ACTUALLY PRESENT

S.N.	PHASE PRESENT	DIFF ANGLE	PEAK INT	I/IO	D MEAS	D STD	DIFF PLANES	INT STD	CONF LIMIT
(1)	AUSTENITE	55.8	100	100	2.071	2.080	111	100	99.7
		65.1	40	40	1.801	1.800	200	80	100.0
		99.5	26	26	1.269	1.270	220	50	99.9
(2)	CR23C6	48.3	13	33	2.368	2.370	420	50	100.0
		56.3	40	100	2.054	2.050	511	100	99.9
		65.1	40	100	1.801	1.800	531	50	100.0
(3)	MN23C6	48.3	13	33	2.368	2.380	420	50	99.7
		56.3	40	100	2.054	2.053	511	100	100.0
		65.1	40	100	1.801	1.799	531	50	99.9
		126.1	40	100	1.087	1.087	555	75	100.0
(4)	FE3C(CEMENTITE)	48.3	13	15	2.368	2.380	112	65	99.7
		56.1	60	69	2.061	2.060	210	70	100.0
		57.8	86	100	2.005	2.010	103	100	99.8
		59.0	26	30	1.968	1.970	211	55	99.9
		62.7	26	30	1.864	1.870	113	30	99.8
(5)	FE5C2(HAGG)	56.1	60	100	2.061	2.060	510	100	100.0
		65.1	40	66	1.801	1.800	312	70	100.0
		99.5	26	44	1.269	1.270	531	20	99.9
(6)	MN5C2(PD5B2)	55.8	100	100	2.071	2.078	510	100	99.8
		56.1	60	60	2.061	2.058	402	80	99.9
		59.0	26	26	1.968	1.972	312	80	99.9
(7)	FE8SI2C	55.8	100	100	2.071	2.070	210	80	100.0
		56.3	40	40	2.054	2.050	121	80	99.9
		57.8	86	86	2.005	2.010	322	100	99.8
		59.0	26	26	1.968	1.960	224	60	99.7

TABLE 5.4-A SUMMARY TABLE OF DIFFRACTOGRAM INDEXING

ALLOY : B1
SOAKING TEMPERATURE : 900°C SOAKING DURATION : 10 HOURS
COOLING MEDIA : AIR COOLED

DIFF. ANGLE	PHASE(S) 1	3	5	7	9	11	13	15	17	19	21	23	25	27	29	INT
48.1	0 0 0	1 1 1	0 0	0 0	0 0	0 0	0 0	1 0	0 1	0 0	0 0	0 0	0 0	0 0	0 0	4.0
50.9	0 0 0	0 0 1	0 1	0 0	1 0	0 1	0 0	0 0	0 0	0 0	0 1	0 0	0 0	0 1	0 1	3.0
55.1	0 0 0	0 0 1	0 0	0 0	0 0	0 1	0 0	0 0	0 0	0 1	0 0	0 1	0 1	1 0	0 1	5.0
55.6	0 1 0	0 0 0	1 0	1 0	0 1	0 1	1 0	0 0	0 0	0 0	1 0	0 0	0 0	1 0	1 0	54.0
56.1	0 0 1	0 1 1	0 1	1 0	1 1	1 0	0 0	0 0	0 0	1 0	0 0	0 0	0 0	0 0	0 0	16.0
57.2	1 0 0	0 0 1	0 1	0 1	1 1	0 1	1 1	0 0	0 0	0 0	1 0	0 0	0 0	0 0	0 0	24.0
57.6	0 0 1	0 0 0	1 0	0 1	0 1	0 0	0 0	0 0	0 0	0 0	0 0	0 0	0 1	1 0	0 1	24.0
58.8	0 0 0	0 0 1	0 1	0 1	0 1	0 0	0 0	0 0	0 0	0 0	0 0	0 1	0 0	1 1	1 0	12.0
61.8	0 0 0	0 1 1	0 0	0 0	0 0	0 1	0 0	0 0	0 1	0 0	0 0	0 0	0 0	1 0	1 0	4.0
* 62.4	0 0 0	0 0 1	0 0	0 0	0 0	0 0	0 0	0 0	0 0	0 0	0 0	0 1	0 0	0 1	0 1	8.0
63.3	0 0 0	0 0 1	0 0	0 0	0 0	0 0	0 0	0 1	0 0	0 0	0 0	0 0	1 0	0 0	0 0	5.0
65.1	0 1 0	1 1 0	0 1	0 0	1 0	0 1	0 0	0 0	0 0	0 0	1 0	0 0	0 1	1 0	0 1	22.0
66.8	0 0 0	0 0 1	0 1	0 0	1 0	0 0	0 0	0 0	0 0	0 0	0 0	0 1	0 0	0 1	1 1	5.0
99.2	0 1 0	0 0 0	0 1	0 0	1 0	0 0	0 0	1 0	0 0	0 0	0 0	0 1	0 0	0 0	0 0	11.0
125.9	0 0 0	0 1 0	0 0	0 0	0 0	0 0	0 0	0 0	0 0	0 0	0 0	1 0	0 0	0 0	0 0	7.0
	0 3 0	3 5 9	0 7	3 4	4 0	0 0	0 0	0 0	0 0	0 0	0 0	3 3	0 0	6 5	4 6	

0 = ABSENT 1 = PRESENT * = PROBABLE DIFF. ANGLE FOR K-BETA RADIATION

TABLE 5.4-B DETAILED ANALYSIS OF PHASE(S) ACTUALLY PRESENT

S.N.	PHASE PRESENT	DIFF ANGLE	PEAK INT	I/IO	D MEAS	D STD	DIFF PLANESTD	INT	CONF LIMIT
(1)	AUSTENITE	55.6	100	100	2.077	2.080	111	100	99.9
		65.1	40	40	1.801	1.800	200	80	100.0
		99.2	20	20	1.272	1.270	220	50	99.7
(2)	CR23C6	48.1	7	18	2.378	2.370	420	50	99.8
		61.8	7	18	1.887	1.880	440	50	99.8
		65.1	40	100	1.801	1.800	531	50	100.0
(3)	MN23C6	48.1	7	18	2.378	2.380	420	50	99.9
		56.1	35	86	2.061	2.053	511	100	99.8
		61.8	7	18	1.887	1.881	440	70	99.8
		65.1	40	100	1.801	1.799	531	50	99.9
		125.9	12	31	1.088	1.087	555	75	99.9
(4)	FE3C(CEMENTITE)	48.1	7	16	2.378	2.380	112	65	99.9
		50.9	5	12	2.255	2.260	200	25	99.9
		55.1	9	20	2.097	2.100	121	60	99.9
		56.1	35	79	2.061	2.060	210	70	100.0
		57.2	44	100	2.024	2.020	022	60	99.9
		58.8	22	50	1.972	1.970	211	55	99.9
		62.4	14	33	1.871	1.870	113	30	100.0
		63.3	9	20	1.848	1.850	122	40	99.9
		66.8	9	20	1.760	1.760	212	16	100.0
(5)	FE5C2(HAGG)	50.9	5	12	2.255	2.260	020	50	99.9
		56.1	35	79	2.061	2.060	510	100	100.0
		57.2	44	100	2.024	2.030	312	100	99.8
		58.8	22	50	1.972	1.980	511	20	99.7
		65.1	40	91	1.801	1.800	312	70	100.0
		66.8	9	20	1.760	1.760	402	10	100.0
		99.2	20	45	1.272	1.270	531	20	99.7
(6)	MN5C2(PD5B2)	55.6	100	100	2.077	2.078	510	100	100.0
		56.1	35	35	2.061	2.058	402	80	99.9
		57.6	44	44	2.013	2.016	511	80	99.9
		58.8	22	22	1.972	1.972	312	80	100.0
(7)	FE8SI2C	55.1	9	9	2.097	2.090	130	80	99.8
		55.6	100	100	2.077	2.070	210	80	99.8
		57.6	44	44	2.013	2.010	322	100	99.9
		58.8	22	22	1.972	1.970	212	60	99.9
		61.8	7	7	1.887	1.880	323	10	99.8
		65.1	40	40	1.801	1.794	015	20	99.7
(8)	CRMN3	55.6	100	100	2.077	2.069	330	100	99.8
		58.8	22	22	1.972	1.970	420	100	99.9
		61.8	7	7	1.887	1.888	777	90	100.0
		66.8	9	9	1.760	1.764	500	60	99.8

TABLE 5.5-A SUMMARY TABLE OF DIFFRACTOGRAM INDEXING

ALLOY : B1
SOAKING TEMPERATURE : 950°C SOAKING DURATION : 4 HOURS
COOLING MEDIA : AIR COOLED

	DIFF. ANGLE	PHASE(S) 1	3	5	7	9	11	13	15	17	19	21	23	25	27	29	INT
	48.2	0 0 0 1	1 1 0	0 0 0	0 0 1	0 0 0	0 0 0	1 0 0	1 0 0	0 0 0	0 0 0	0 0 0	0 0 0	0 0 0	0 0 0	0 0 0	7.0
	50.2	0 0 0 0	0 0 1	0 1 1	0 0 0	0 0 0	0 0 0	0 0 0	0 0 0	0 0 0	0 0 1	0 0 0	0 0 0	0 0 0	0 1 1	0 0 0	4.0
	50.9	0 0 0 0	0 1 0	1 0 0	1 0 0	0 0 0	0 0 0	0 0 0	0 0 0	0 0 0	0 0 0	0 1 0	0 0 0	0 0 0	0 1 0	1 0 1	8.0
*	55.8	0 1 0 0	0 0 1	0 0 1	0 0 0	0 0 0	0 0 0	0 0 0	0 0 0	0 0 0	0 0 0	0 0 1	0 0 0	0 0 0	1 0 1	0 0 0	94.0
	56.1	0 0 1 0	1 1 0	1 1 1	0 0 0	0 0 0	0 0 0	0 0 0	0 0 0	0 0 1	0 0 0	0 0 0	0 0 0	0 0 0	0 1 0	0 0 0	36.0
	57.2	1 0 1 0	0 1 0	1 1 0	1 1 0	1 1 1	0 0 0	0 0 0	0 0 0	0 0 1	0 0 0	0 0 0	0 0 0	0 0 0	0 0 0	0 0 0	18.0
	57.7	0 0 0 0	0 1 1	0 0 1	0 0 0	0 0 0	0 0 0	0 0 0	0 0 0	0 0 0	0 0 0	0 0 0	0 0 0	0 0 1	1 1 0	1 0 1	38.0
	58.9	0 0 0 0	0 1 0	0 0 1	0 0 0	0 0 0	0 0 0	0 0 0	0 0 0	0 0 0	0 0 0	0 0 0	0 0 0	0 0 0	1 1 1	0 0 0	17.0
*	62.4	0 0 0 0	0 1 0	0 0 0	0 0 0	0 0 0	0 0 0	0 0 0	0 0 0	0 0 0	0 0 0	0 0 0	0 1 1	0 0 0	0 1 0	1 0 1	12.0
	63.3	0 0 0 0	0 1 0	0 0 0	0 0 0	0 0 0	0 0 0	0 0 1	0 0 0	0 0 0	0 0 0	0 0 0	0 0 0	0 1 0	0 0 0	0 0 0	8.0
	65.1	0 1 0 1	1 0 0	1 0 0	0 0 0	0 0 0	0 0 0	0 0 0	0 0 1	0 0 0	0 0 0	1 0 0	0 0 0	0 0 0	1 0 0	1 0 1	22.0
	66.5	0 0 0 0	0 0 0	0 0 0	0 0 0	0 0 0	0 0 0	0 0 0	0 0 1	0 0 0	0 0 0	0 0 0	0 0 0	0 0 0	0 0 1	1 0 1	4.0
	66.9	0 0 0 0	0 1 0	1 0 0	0 0 0	0 0 0	0 0 0	0 0 0	0 0 0	0 0 0	0 0 0	0 0 0	0 1 0	0 0 0	0 1 0	1 0 1	7.0
	99.2	0 1 0 0	0 0 1	0 1 0	0 0 0	0 1 0	0 0 0	0 1 0	0 0 0	0 0 0	0 0 0	0 0 0	0 1 0	0 0 0	0 0 0	0 0 0	9.0
	118.1	0 0 0 0	0 0 0	1 0 0	1 0 0	1 0 0	1 0 0	0 0 0	0 0 0	0 0 0	0 0 0	0 0 0	0 0 0	0 0 0	0 0 0	0 0 0	6.0
	126.0	0 0 0 0	1 0 0	0 0 0	0 0 0	0 0 0	0 0 0	0 0 0	0 0 0	0 0 0	0 0 0	0 0 0	1 0 0	0 0 0	0 0 0	0 0 0	40.0
		0 3 0 0	4 9 3	7 3 5	3 0 3	0 0 0	0 0 0	0 0 0	0 0 0	0 0 0	0 0 0	0 0 0	0 0 0	0 0 0	4 6 4	7	

0 = ABSENT 1 = PRESENT * = PROBABLE DIFF. ANGLE FOR K-BETA RADIATION

TABLE 5.5-B DETAILED ANALYSIS OF PHASE(S) ACTUALLY PRESENT

S.N.	PHASE PRESENT	DIFF ANGLE	PEAK INT	I/IO	D MEAS	D STD	DIFF PLANES	INT STD	CONF LIMIT
(1)	AUSTENITE	55.8	100	100	2.071	2.080	111	100	99.7
		65.1	23	23	1.801	1.800	200	80	100.0
		99.2	9	9	1.272	1.270	220	50	99.8
(2)	MN23C6	48.2	7	17	2.375	2.380	420	50	99.9
		56.1	38	90	2.061	2.053	511	100	99.8
		65.1	23	54	1.801	1.799	531	50	99.9
		126.0	42	100	1.087	1.087	555	75	100.0
(3)	FE3C(CEMENTITE)	48.2	7	18	2.375	2.380	112	65	99.9
		50.9	8	21	2.255	2.260	200	25	99.9
		56.1	38	94	2.061	2.060	210	70	100.0
		57.2	19	47	2.024	2.020	022	60	99.9
		57.7	40	100	2.008	2.010	103	100	99.9
		58.9	18	44	1.969	1.970	211	55	100.0
		62.4	12	31	1.869	1.870	113	30	100.0
		63.3	8	21	1.848	1.850	122	40	99.9
		66.9	7	18	1.759	1.760	212	16	100.0
(4)	FE5C2(HAGG)	50.9	8	22	2.255	2.260	020	50	99.9
		56.1	38	100	2.061	2.060	510	100	100.0
		57.2	19	50	2.024	2.030	312	100	99.8
		65.1	23	61	1.801	1.800	312	70	100.0
		66.9	7	19	1.759	1.760	402	10	100.0
		99.2	9	25	1.272	1.270	531	20	99.8
		118.1	6	16	1.130	1.130	133	50	99.9
(5)	MN5C2(PD5B2)	50.2	4	4	2.284	2.282	020	70	99.9
		55.8	100	100	2.071	2.078	510	100	99.8
		56.1	38	38	2.061	2.058	402	80	99.9
		57.7	40	40	2.008	2.016	511	80	99.8
		58.9	18	18	1.969	1.972	312	80	99.9
(6)	FE7C3(2)	50.9	8	40	2.255	2.255	120	31	100.0
		57.2	19	90	2.024	2.019	121	100	99.8
		118.1	6	30	1.130	1.131	501	13	99.8
(7)	FE8SI2C	55.8	100	100	2.071	2.070	210	80	100.0
		57.7	40	40	2.008	2.010	322	100	99.9
		58.9	18	18	1.969	1.970	212	60	100.0
		65.1	23	23	1.801	1.794	015	20	99.7
(8)	CRMN3	50.2	4	4	2.284	2.272	002	60	99.7
		55.8	100	100	2.071	2.069	330	100	99.9
		58.9	18	18	1.969	1.970	420	100	100.0
		66.5	4	4	1.767	1.764	500	60	99.9

TABLE 5.6-A SUMMARY TABLE OF DIFFRACTOGRAM INDEXING

ALLOY : B1
SOAKING TEMPERATURE : 950°C SOAKING DURATION : 10 HOURS
COOLING MEDIA : AIR COOLED

	DIFF. ANGLE	PHASE(S) 1	3	5	7	9	11	13	15	17	19	21	23	25	27	29	INT
	47.8	0	0	1	1	0	1	0	0	0	1	1	0	0	0	0	4.0
	50.8	0	0	0	1	0	1	0	0	0	0	0	1	0	1	1	3.0
*	55.5	1	0	0	0	1	0	1	1	0	0	0	0	1	1	0	42.0
	57.4	0	1	0	1	1	0	1	1	1	0	0	0	0	1	1	19.0
	58.8	0	0	0	0	1	0	1	0	0	0	0	1	0	1	0	5.0
	61.4	0	0	0	0	0	0	0	1	1	0	0	0	0	0	1	2.0
*	61.8	0	0	1	1	0	0	0	0	0	0	0	0	1	0	0	2.0
	62.4	0	0	0	0	1	0	0	0	0	0	0	1	0	1	1	6.0
	63.3	0	0	0	0	1	0	0	0	0	0	0	0	1	0	0	3.0
	64.9	0	1	1	0	1	0	1	0	1	0	0	0	0	1	1	8.0
	66.6	0	0	0	1	0	1	0	0	0	0	0	0	1	0	0	3.0
	98.6	0	0	0	0	0	0	0	1	0	0	0	0	0	1	0	6.0
	125.5	0	0	0	0	0	1	0	0	0	0	0	0	0	1	0	6.0
		0	0	0	3	7	0	6	0	3	4	3	4	0	3	0	5	0	0	0	0	3	3	0	4	5	3	4	6	

0 = ABSENT 1 = PRESENT * = PROBABLE DIFF. ANGLE FOR K-BETA RADIATION

TABLE 5.6-B DETAILED ANALYSIS OF PHASE(S) ACTUALLY PRESENT

S.N.	PHASE PRESENT	DIFF ANGLE	PEAK INT	I/I0	D MEAS	D STD	DIFF PLANE	INT STD	CONF LIMIT
(1)	MN23C6	47.8	9	50	2.389	2.380	420	50	99.8
		61.8	4	25	1.887	1.881	440	70	99.8
		64.9	19	100	1.806	1.799	531	50	99.7
(2)	FE3C(CEMENTITE)	47.8	9	21	2.389	2.380	112	65	99.8
		50.8	7	15	2.260	2.260	200	25	100.0
		57.4	45	100	2.017	2.010	103	100	99.8
		58.8	11	26	1.975	1.970	211	55	99.8
		62.4	14	31	1.870	1.870	113	30	100.0
		63.3	7	15	1.848	1.850	122	40	99.9
		66.6	7	15	1.764	1.760	212	16	99.8
(3)	FE5C2(HAGG)	47.8	9	50	2.389	2.390	202	20	100.0
		50.8	7	37	2.260	2.260	020	50	100.0
		58.8	11	62	1.975	1.980	511	20	99.8
		64.9	19	100	1.806	1.800	312	70	99.7
		66.6	7	37	1.764	1.760	402	10	99.8
		125.5	14	75	1.090	1.090	404	20	99.9
(4)	MN5C2(PD5B2)	55.5	100	100	2.081	2.078	510	100	99.9
		57.4	45	45	2.017	2.016	511	80	100.0
		58.8	11	11	1.975	1.972	312	80	99.9
(5)	FE7C3(2)	50.8	7	15	2.260	2.255	120	31	99.9
		57.4	45	100	2.017	2.019	121	100	99.9
		61.4	4	10	1.898	1.895	112	5	99.9
		64.9	19	42	1.806	1.807	022	22	100.0
(6)	CR7C3(2)	50.8	7	15	2.260	2.270	120	50	99.8
		57.4	45	100	2.017	2.020	121	100	99.9
		61.4	4	10	1.898	1.900	112	10	99.9
(7)	COPPER	55.5	100	100	2.081	2.088	111	100	99.8
		64.9	19	19	1.806	1.808	200	46	99.9
		98.6	14	14	1.278	1.278	220	20	100.0
		125.5	14	14	1.090	1.090	311	17	99.9
(8)	FE8SI2C	55.5	100	100	2.081	2.080	131	80	100.0
		57.4	45	45	2.017	2.010	322	100	99.8
		58.8	11	11	1.975	1.970	212	60	99.8
		61.8	4	4	1.887	1.880	323	10	99.7
		64.9	19	19	1.806	1.810	031	20	99.9
(9)	CRMN3	50.8	7	60	2.260	2.272	002	60	99.7
		58.8	11	100	1.975	1.970	420	100	99.8
		61.8	4	40	1.887	1.888	777	90	100.0
		66.6	7	60	1.764	1.764	500	60	100.0
(10)	AUSTENITE	55.5	100	100	2.081	2.080	111	100	99.9
		64.9	19	19	1.806	1.800	200	80	99.8

TABLE 5.8-A SUMMARY TABLE OF DIFFRACTOGRAM INDEXING

ALLOY : B1
SOAKING TEMPERATURE : 1000°C SOAKING DURATION : 10 HOURS
COOLING MEDIA : AIR COOLED

	DIFF. ANGLE	PHASE(S) 1		3		5		7		9		11		13		15		17		19		21		23		25		27		29		INT
	48.2	0	0	0	1	1	1	0	0	0	0	0	0	0	0	1	0	0	1	0	0	0	0	0	1	0	0	0	0	0	0	2.5
	50.1	0	0	0	0	0	0	1	0	1	1	0	0	1	1	0	0	1	0	0	0	1	0	0	0	0	0	0	0	0	0	3.0
*	55.6	0	1	0	0	0	0	1	0	1	1	0	0	0	0	0	0	0	0	0	0	1	0	0	0	0	0	0	1	0	1	0	115.0
	56.3	0	0	1	1	1	1	0	1	1	1	0	0	0	0	0	0	0	1	0	0	0	1	0	0	0	0	0	1	1	0	0	5.0
	57.7	0	0	0	0	0	1	1	0	0	1	0	0	0	0	0	0	0	0	0	0	0	0	0	0	0	0	0	1	1	0	1	7.0
*	62.7	0	0	0	0	0	1	0	0	0	0	0	0	0	0	1	0	1	0	0	0	0	0	0	1	0	0	0	0	0	0	25.0
	65.1	0	1	0	1	1	0	0	1	0	0	1	0	0	0	0	0	0	0	0	1	0	0	0	0	0	1	1	0	0	1	24.0
	100.7	0	0	0	0	0	0	0	0	0	0	0	0	1	0	1	0	1	0	0	0	1	0	0	0	0	0	0	1	0	0	16.0
	101.2	0	0	0	1	0	0	0	0	0	0	0	0	0	0	0	0	0	0	0	0	0	0	0	0	0	0	0	0	0	0	11.0
	101.6	0	0	0	0	0	0	0	1	0	0	0	0	0	0	0	0	0	0	0	0	0	0	0	0	0	0	0	0	1	0	5.0
	126.0	0	0	0	0	1	0	0	0	0	0	0	0	0	0	0	0	0	0	0	0	0	0	1	0	0	0	0	0	0	0	10.0
	126.4	0	0	0	0	0	0	0	0	0	0	0	0	0	0	0	0	0	0	0	0	0	0	0	0	0	0	0	0	0	0	14.0
	126.9	0	1	0	0	0	0	0	0	0	0	0	0	0	0	0	0	0	0	0	0	0	0	1	0	0	0	0	0	0	0	16.0
	127.3	0	0	0	0	0	0	0	0	0	0	0	0	0	0	0	0	0	0	0	0	0	0	0	0	0	0	0	0	0	0	7.0
	127.8	0	0	0	0	0	0	0	0	0	0	0	0	0	0	0	0	0	0	0	0	0	0	0	0	0	0	0	0	0	0	3.0
		0	3	0	4	4	4	3	3	3	4	0	0	0	0	3	0	3	0	0	0	3	0	0	0	0	0	4	3	0	0	

0 = ABSENT 1 = PRESENT * = PROBABLE DIFF. ANGLE FOR K-BETA RADIATION

TABLE 5.8-B DETAILED ANALYSIS OF PHASE(S) ACTUALLY PRESENT

S.N.	PHASE PRESENT	DIFF ANGLE	PEAK INT	I/I0	D MEAS	D STD	DIFF PLANESTD	INT	CONF LIMIT
(1)	AUSTENITE	55.6	100	100	2.078	2.080	111	100	99.9
		65.1	20	20	1.801	1.800	200	80	100.0
		126.9	13	13	1.083	1.083	311	80	100.0
(2)	FE3C(CEMENTITE)	48.2	2	35	2.373	2.380	112	65	99.8
		56.3	4	71	2.054	2.060	210	70	99.8
		57.7	6	100	2.008	2.010	103	100	99.9
		62.7	2	35	1.862	1.870	113	30	99.7
(3)	FE5C2(HAGG)	56.3	4	20	2.054	2.060	510	100	99.8
		65.1	20	100	1.801	1.800	312	70	100.0
		101.6	4	20	1.250	1.250	712	20	100.0
(4)	MN5C2(PD5B2)	50.1	2	2	2.288	2.282	020	70	99.8
		55.6	100	100	2.078	2.078	510	100	100.0
		56.3	4	4	2.054	2.058	402	80	99.9
		57.7	6	6	2.008	2.016	511	80	99.8
(5)	(CR7C3+MN7C3)	48.2	2	15	2.373	2.380	333	80	99.8
		62.7	2	15	1.862	1.860	888	100	99.9
		100.7	13	100	1.258	1.260	555	60	99.8
(6)	FE8SI2C	55.6	100	100	2.078	2.070	210	80	99.8
		56.3	4	4	2.054	2.050	121	80	99.9
		57.7	6	6	2.008	2.010	322	100	99.9
		65.1	20	20	1.801	1.794	015	20	99.7

TABLE 5.10-A SUMMARY TABLE OF DIFFRACTOGRAM INDEXING

ALLOY : B1
SOAKING TEMPERATURE : 1050°C SOAKING DURATION : 6 HOURS
COOLING MEDIA : AIR COOLED

	DIFF. ANGLE	PHASE(S) 1	3	5	7	9	11	13	15	17	19	21	23	25	27	29	INT
	31.0	0	0	0	0	0	0	0	0	0	0	1	1	0	0	0	3.0
	36.8	0	0	0	0	0	0	0	0	0	0	0	1	0	0	0	2.0
	42.3	0	0	0	0	0	0	1	1	0	0	1	1	0	0	0	3.0
	49.8	0	0	0	0	0	0	0	1	0	0	0	0	0	0	0	4.0
	50.0	0	0	0	0	1	0	1	0	0	0	1	0	0	0	0	4.0
*	55.3	0	0	0	0	0	0	0	0	0	0	0	0	1	1	1	137.5
*	55.6	1	0	0	0	0	0	0	0	0	0	1	0	0	0	0	205.0
	57.2	1	1	0	0	1	1	1	1	0	0	1	0	0	1	0	6.5
	64.7	0	0	0	0	1	0	1	1	1	0	0	1	1	0	0	40.0
	65.4	0	0	0	1	0	0	0	0	0	0	0	0	1	0	1	2.5
	96.4	0	0	0	0	0	0	0	0	1	0	0	0	0	0	0	20.5
	96.6	0	0	0	0	0	0	0	0	1	0	0	0	0	0	0	16.5
	96.9	0	0	1	0	0	0	0	0	0	1	0	1	0	0	0	6.0
	120.6	0	0	0	0	0	0	0	0	0	0	0	0	0	0	0	2.0
	122.6	0	0	0	0	0	0	0	0	0	0	0	0	0	0	0	9.0
	126.8	0	1	0	0	0	0	0	0	0	0	0	1	0	0	0	10.0
		0	0	0	0	0	3	0	3	3	0	0	4	4	3	0	0	0	4	0	0	0	

0 = ABSENT 1 = PRESENT * = PROBABLE DIFF. ANGLE FOR K-BETA RADIATION

TABLE 5.10-B DETAILED ANALYSIS OF PHASE(S) ACTUALLY PRESENT

S.N.	PHASE PRESENT	DIFF ANGLE	PEAK INT	I/IO	D MEAS	D STD	DIFF PLANES	INT STD	CONF LIMIT
(1)	FE5C2	50.0	1	1	2.293	2.287	020	20	99.9
		55.6	100	100	2.078	2.080	021	70	99.9
		64.7	19	19	1.811	1.814	312	25	99.9
(2)	MN5C2	55.3	67	100	2.088	2.084	120	80	99.9
		57.2	3	4	2.024	2.019	213	100	99.8
		64.7	19	29	1.811	1.818	213	60	99.7
(3)	MN5C2(PD5B2)	50.0	1	1	2.293	2.282	020	70	99.7
		55.6	100	100	2.078	2.078	510	100	100.0
		57.2	3	3	2.024	2.016	511	80	99.7
(4)	CR7C3	42.3	1	7	2.683	2.680	311	20	100.0
		50.0	1	10	2.293	2.280	411	70	99.7
		57.2	3	16	2.024	2.020	---	50	99.9
		64.7	19	100	1.811	1.810	431	70	100.0
(5)	FE8SI2C	55.3	67	67	2.088	2.080	131	80	99.8
		55.6	100	100	2.078	2.080	131	80	99.9
		64.7	19	19	1.811	1.810	031	20	100.0
		65.4	1	1	1.792	1.794	015	20	99.9
(6)	AUSTENITE	55.6	100	100	2.078	2.080	111	100	99.9
		126.8	10	10	1.084	1.083	311	50	99.9

TABLE 5.12-A SUMMARY TABLE OF DIFFRACTOGRAM INDEXING

ALLOY : B2
HEAT-TREATMENT : AS CAST

	DIFF. ANGLE	PHASE(S) 1	3	5	7	9	11	13	15	17	19	21	23	25	27	29	INT
	47.9	0 0 0 0	1 1 0 1	0 0 0	0 1 1	0 0 0	0 0 0	1 1 0	0 0 0	0 0 0	0 0 0	0 0 0	1 0 0	0 0 0	0 0 0	0 0 0	22.5
	50.8	0 0 0 0	0 1 0 1	0 0 1	1 0 0	0 0 0	1 1 0	0 0 0	0 0 0	0 0 0	0 0 0	0 1 0	0 0 0	0 0 1	0 1 0	1 0 0	30.0
	54.8	0 0 0 0	0 1 1 0	0 0 0	1 0 0	0 0 0	1 0 0	0 0 0	1 1 0	1 0 0	1 0 0	0 0 0	0 0 0	0 0 0	0 0 0	0 0 0	10.0
	55.9	0 0 1 0	0 1 0 1	1 1 0	0 0 0	0 0 0	0 0 0	0 0 0	0 1 0	1 0 0	1 0 0	1 0 0	0 0 0	0 0 0	1 1 1	0 0 0	3.9
	57.2	1 0 0 0	0 1 0 1	0 0 0	1 0 0	1 0 0	0 0 0	1 1 0	0 0 0	0 0 0	0 1 0	1 0 0	0 0 0	0 0 0	0 0 0	0 0 0	70.5
	57.5	0 0 1 0	0 0 0 0	0 1 1	0 0 0	1 1 0	0 0 0	0 0 0	0 0 0	0 0 0	0 0 0	0 0 0	0 0 0	0 0 0	0 1 0	0 0 0	100.0
	58.8	0 0 0 0	0 1 0 1	0 0 0	1 0 0	1 0 0	1 0 0	0 0 0	0 0 0	0 0 0	0 0 0	0 0 0	1 0 0	0 1 0	1 0 1	0 1 0	25.0
*	62.3	0 0 0 1	1 1 0 0	0 0 0	0 0 0	0 0 0	0 0 0	0 0 0	0 0 0	0 0 0	0 0 0	0 0 0	1 1 0	0 1 1	0 1 0	1 0 1	17.5
	63.1	0 0 0 0	0 1 0 0	0 0 0	0 0 0	0 0 0	0 0 0	0 0 0	1 0 0	0 0 0	0 0 0	0 0 0	0 0 1	0 0 0	0 0 0	0 0 0	7.5
	66.8	0 0 0 0	0 1 0 1	0 0 0	0 0 0	0 0 0	0 0 0	0 0 0	0 0 0	0 0 0	0 0 0	0 0 0	0 1 0	0 0 1	1 1 1	1 0 0	15.5
	85.1	1 0 0 0	0 0 0 0	0 0 0	0 0 0	0 0 0	0 0 0	0 1 0	0 0 0	0 0 0	0 0 0	0 1 0	0 0 0	0 0 0	0 0 0	0 0 0	8.8
	93.6	0 0 0 0	1 0 0 0	0 0 0	0 0 0	0 0 0	0 0 0	1 0 0	0 0 0	0 0 0	0 0 0	0 0 0	0 0 0	0 0 0	0 1 0	0 0 0	10.0
	105.7	0 0 0 0	0 0 0 0	0 0 0	0 0 0	0 0 0	0 0 0	1 0 0	0 0 0	0 0 0	0 0 0	0 0 0	0 0 0	0 0 0	0 0 1	0 1 0	10.0
	111.8	1 0 0 1	1 0 0 1	0 0 0	1 0 0	0 0 0	1 1 0	1 0 0	1 0 0	1 0 0	0 0 0	0 0 0	0 0 1	0 1 0	0 1 0	0 0 0	20.0
	118.2	0 0 0 0	0 0 0 1	0 0 0	0 0 0	1 0 0	0 0 0	0 0 0	0 0 0	0 0 0	0 0 0	0 0 0	0 0 0	0 0 0	0 0 0	0 0 0	10.0
	119.0	0 0 0 0	0 0 0 0	0 0 0	0 0 0	0 0 0	0 0 0	0 0 0	0 0 0	0 0 0	0 0 0	0 0 0	1 0 0	0 0 0	0 0 0	0 0 0	10.0
		3 0 0 0	4 9 0 8	0 3 0	4 4 0	3 0 0	0 0 0	3 3 0	0 0 0	3 7 4	3						

0 = ABSENT 1 = PRESENT * = PROBABLE DIFF. ANGLE FOR K-BETA RADIATION

TABLE 5.12-B DETAILED ANALYSIS OF PHASE(S) ACTUALLY PRESENT

S.N.	PHASE PRESENT	DIFF ANGLE	PEAK INT	I/IO	D MEAS	D STD	DIFF PLANES	INT STD	CONF LIMIT
(1)	ALPHA IRON	57.2	70	100	2.024	2.027	110	100	99.9
		85.1	8	12	1.433	1.433	200	20	100.0
		111.8	20	28	1.170	1.170	211	30	100.0
(2)	FE3C(CEMENTITE)	47.9	22	31	2.387	2.380	112	65	99.9
		50.8	30	42	2.259	2.260	200	25	100.0
		54.8	10	14	2.106	2.100	121	60	99.8
		55.9	3	5	2.067	2.060	210	70	99.8
		57.2	70	100	2.024	2.020	022	60	99.9
		58.8	25	35	1.974	1.970	211	55	99.9
		62.3	17	24	1.873	1.870	113	30	99.9
		63.1	7	10	1.852	1.850	122	40	99.9
		66.8	15	21	1.760	1.760	212	16	100.0
(3)	FE5C2(HAGG)	47.9	22	31	2.387	2.390	202	20	99.9
		50.8	30	42	2.259	2.260	020	50	100.0
		55.9	3	5	2.067	2.060	510	100	99.8
		57.2	70	100	2.024	2.030	312	100	99.8
		58.8	25	35	1.974	1.980	511	20	99.8
		66.8	15	21	1.760	1.760	402	10	100.0
		111.8	20	28	1.170	1.170	623	20	100.0
		118.2	10	14	1.129	1.130	133	50	99.8
(4)	MN5C2(PD5B2)	55.9	3	3	2.067	2.058	402	80	99.7
		57.5	100	100	2.014	2.016	511	80	100.0
		58.8	25	25	1.974	1.972	312	80	99.9
(5)	CR7C3(2)	50.8	30	42	2.259	2.270	120	50	99.7
		54.8	10	14	2.106	2.100	012	60	99.8
		57.2	70	100	2.024	2.020	121	100	99.9
		111.8	20	28	1.170	1.172	501	50	99.7
(6)	CU2S(1)	47.9	22	90	2.387	2.401	102	88	99.7
		58.8	25	100	1.974	1.980	110	100	99.8
		62.3	17	70	1.873	1.876	103	98	99.9
(7)	FE8SI2C	55.9	3	15	2.067	2.070	210	80	99.9
		58.8	25	100	1.974	1.970	212	60	99.9
		62.3	17	70	1.873	1.880	323	10	99.7

TABLE 5.13-A SUMMARY TABLE OF DIFFRACTOGRAM INDEXING

ALLOY : B2
SOAKING TEMPERATURE : 900°C SOAKING DURATION : 4 HOURS
COOLING MEDIA : AIR COOLED

	DIFF. ANGLE	PHASE(S) 1	3	5	7	9	11	13	15	17	19	21	23	25	27	29	INT
	48.2	0 0 0	1 1	1 0	0 0	0 0	0 0	0	1 0	0 1	0 0	0	1 0	0 0	0 0	0 0	3.0
	55.7	0 1 0	0 0	0 1	0 1	1 0	0 0	0	0 0	0 0	1 0	0	0 0	0 1	0 1	1 0	35.0
	57.1	1 0 0	0 0	0 0	1 1	1 0	0 0	0	0 0	0 0	1 0	0	1 0	0 0	1 1	1 1	10.0
	57.5	0 0 1	0 0	1 1	0 1	0 1	1 1	0	0 0	0 0	0 0	0	0 0	1 1	0 1		7.0
	58.9	0 0 0	0 0	1 0	0 0	1 0	0 0	0	0 0	0 0	0 0	0	0 0	1 1	1 0		3.0
	60.4	0 0 0	0 0	0 0	0 0	1 0	0 0	0	0 0	0 0	0 0	0	0 0	1 1	0 0		1.5
	63.2	0 0 0	0 0	0 1	0 0	0 0	0 0	0	1 0	0 0	0 0	0	0 0	1 0	0 0		4.0
	64.5	0 0 0	0 0	0 1	0 1	1 1	1 1	1	0 0	1 0	0 0	0	1 0	0 1	0 0		4.0
	65.1	0 1 0	1 1	0 0	1 0	0 0	1 0	0	0 0	0 0	0 1	0	0 0	0 1	0 0	0 1	9.0
*	65.6	0 0 0	0 0	0 0	0 0	0 0	0 1	0	0 0	0 0	0 0	0	0 0	0 1	0 0	0 1	4.5
	65.9	0 0 0	1 0	0 0	0 0	0 1	0 0	1	0 1	0 1	0 0	0	1 0	0 1	0 0	0 1	2.5
	70.2	0 0 0	0 1	0 0	0 0	0 1	0 0	0	0 0	1 0	0 0	1	0 0	0 0	0 0	0 0	2.5
*	70.6	0 0 0	0 0	1 0	0 0	0 0	0 0	0	0 0	0 1	0 0	0	1 0	0 0	1 0	0 0	2.0
	99.0	0 0 0	0 0	0 0	0 0	0 0	0 0	0	0 0	0 0	0 0	0	1 0	0 0	0 0	0 0	2.0
	99.8	0 0 0	0 0	0 0	0 0	0 0	0 0	0	0 1	0 0	1 0	0	0 0	0 0	0 0	1 0	2.0
	118.9	0 0 0	0 0	0 0	0 0	0 0	0 0	0	0 0	0 0	0 0	1	0 0	0 0	0 0	0 0	2.5
	125.2	0 0 0	0 0	0 0	0 1	0 0	0 0	0	0 0	0 0	0 0	0	0 0	1 0	0 0	0 0	9.0
	125.9	0 0 0	0 1	0 0	0 0	0 0	0 0	0	0 0	0 0	0 0	0	1 0	0 0	0 0	0 0	18.5
		0 0 0	3 4	5 3	3 5	6 3	3 3	3	0 3	0 3	0 0	0	3 3	3 0	0 8	3 4	5

0 = ABSENT 1 = PRESENT * = PROBABLE DIFF. ANGLE FOR K-BETA RADIATION

TABLE 5.13-B DETAILED ANALYSIS OF PHASE(S) ACTUALLY PRESENT

S.N.	PHASE PRESENT	DIFF ANGLE	PEAK INT	I/IO	D MEAS	D STD	DIFF PLANES	INT STD	CONF LIMIT
(1)	CR23C6	48.2	8	33	2.373	2.370	420	50	99.9
		65.1	25	100	1.801	1.800	531	50	100.0
		65.9	7	27	1.781	1.780	422	40	100.0
(2)	MN23C6	48.2	8	16	2.373	2.380	420	50	99.8
		65.1	25	48	1.801	1.799	531	50	99.9
		70.2	7	13	1.685	1.686	422	20	99.9
		125.9	52	100	1.088	1.087	555	75	99.9
(3)	FE3C(CEMENTITE)	48.2	8	42	2.373	2.380	112	65	99.8
		57.5	20	100	2.014	2.020	022	60	99.8
		58.9	8	42	1.971	1.970	211	55	100.0
		63.2	11	57	1.849	1.850	122	40	100.0
		70.6	5	28	1.677	1.680	023	16	99.8
(4)	FE5C2(HAGG)	57.1	28	100	2.027	2.030	312	100	99.9
		65.1	25	90	1.801	1.800	312	70	100.0
		125.2	25	90	1.091	1.090	404	20	99.8
(5)	MN5C2(PD5B2)	55.7	100	100	2.074	2.078	510	100	99.9
		57.1	28	28	2.027	2.035	312	70	99.8
		58.9	8	8	1.971	1.972	312	80	100.0
		64.5	11	11	1.816	1.820	421	70	99.8
		65.9	7	7	1.781	1.779	512	70	99.9
		70.2	7	7	1.685	1.690	602	10	99.8
(6)	FE7C3(2)	57.5	20	77	2.014	2.019	121	100	99.9
		64.5	11	44	1.816	1.820	301	11	99.8
		65.1	25	100	1.801	1.807	022	22	99.8
(7)	CR7C3(2)	57.5	20	100	2.014	2.020	121	100	99.8
		64.5	11	57	1.816	1.820	301	30	99.8
		65.6	12	64	1.789	1.790	022	50	99.9
(8)	CRMN3	55.7	100	100	2.074	2.069	330	100	99.8
		57.1	28	28	2.027	2.036	202	70	99.7
		58.9	8	8	1.971	1.970	420	100	100.0
		99.8	5	5	1.267	1.265	700	40	99.8
(9)	AUSTENITE	55.7	100	100	2.074	2.080	111	100	99.8
		65.1	26	26	1.801	1.800	200	80	100.0

TABLE 5.15-A SUMMARY TABLE OF DIFFRACTOGRAM INDEXING

ALLOY : B2
SOAKING TEMPERATURE : 950°C SOAKING DURATION : 4 HOURS
COOLING MEDIA : AIR COOLED

	DIFF. ANGLE	PHASE(S) 1	3	5	7	9	11	13	15	17	19	21	23	25	27	29	INT
	47.9	0	0	0	1	1	0	1	0	0	0	0	0	1	0	0	5.0
	49.8	0	0	0	0	0	0	0	0	0	0	0	0	0	0	0	7.0
	53.4	0	0	0	0	0	0	0	0	0	0	0	0	0	1	1	2.5
	53.8	0	0	0	0	0	0	0	0	0	0	0	0	0	1	0	3.5
	55.5	0	1	0	0	0	1	0	1	1	0	0	0	0	0	0	32.5
	55.9	0	0	1	0	0	1	0	1	1	0	0	0	0	0	0	10.5
	57.5	0	0	0	0	0	1	1	0	0	0	0	0	0	0	1	15.0
	58.8	0	0	0	0	0	1	0	1	0	1	0	0	0	0	0	7.0
	62.4	0	0	0	0	0	1	0	0	0	0	0	1	0	0	1	4.5
	63.1	0	0	0	0	0	1	0	0	0	0	0	0	1	0	0	3.5
	64.9	0	0	0	0	0	0	1	0	0	0	0	0	0	0	0	5.0
*	65.4	0	1	0	1	0	0	0	1	0	0	0	0	0	0	1	2.0
	66.7	0	0	0	0	0	1	0	1	0	0	0	0	0	1	1	3.0
	67.6	0	0	0	0	0	0	0	0	0	0	0	0	0	0	0	1.5
	70.2	0	0	0	0	1	1	0	0	0	1	0	1	0	0	0	3.0
	97.9	0	0	0	0	0	0	0	0	0	0	0	0	0	0	0	2.0
	98.8	0	0	0	0	0	0	0	0	0	0	0	0	0	0	0	8.5
	125.6	0	0	0	0	0	0	1	0	0	0	0	0	0	0	0	24.0
	126.0	0	0	0	1	0	0	0	0	0	0	0	1	0	0	0	17.0
		0	0	0	3	8	3	6	0	4	0	0	0	3	3	0	4	3	0	0	0	0	4	5	0	4	8	3	5	5	

0 = ABSENT 1 = PRESENT * = PROBABLE DIFF. ANGLE FOR K-BETA RADIATION

TABLE 5.15-B DETAILED ANALYSIS OF PHASE(S) ACTUALLY PRESENT

S.N.	PHASE PRESENT	DIFF ANGLE	PEAK INT	D I/IO	D MEAS	D STD	DIFF PLANES	INT STD	CONF LIMIT
(1)	MN23C6	47.9	15	29	2.387	2.380	420	50	99.9
		70.2	9	17	1.685	1.686	422	20	100.0
		126.0	52	100	1.087	1.087	555	75	99.9
(2)	FE3C(CEMENTITE)	47.9	15	33	2.387	2.380	112	65	99.9
		55.9	32	70	2.066	2.060	210	70	99.8
		57.5	46	100	2.014	2.010	103	100	99.9
		58.8	21	46	1.975	1.970	211	55	99.8
		62.4	13	30	1.870	1.870	113	30	100.0
		63.1	10	23	1.853	1.850	122	40	99.9
		66.7	9	20	1.762	1.760	212	16	99.9
		70.2	9	20	1.685	1.680	023	16	99.8
(3)	FE5C2(HAGG)	47.9	15	20	2.387	2.390	202	20	99.9
		55.9	32	43	2.066	2.060	510	100	99.8
		58.8	21	29	1.975	1.980	511	20	99.8
		65.4	6	8	1.794	1.800	312	70	99.7
		66.7	9	12	1.762	1.760	402	10	99.9
		125.6	73	100	1.089	1.090	404	20	99.8
(4)	MN5C2(PD5B2)	55.5	100	100	2.081	2.078	510	100	99.9
		55.9	32	32	2.066	2.058	402	80	99.8
		58.8	21	21	1.975	1.972	312	80	99.9
		70.2	9	9	1.685	1.690	602	10	99.8
(5)	COPPER	55.5	100	100	2.081	2.088	111	100	99.8
		64.9	15	15	1.807	1.808	200	46	100.0
		98.8	26	26	1.277	1.278	220	20	99.8
		125.6	73	73	1.089	1.090	311	17	99.8
(6)	CRMN3	53.4	7	23	2.156	2.162	321	40	99.9
		53.8	10	33	2.142	2.132	410	100	99.7
		55.9	32	100	2.066	2.069	330	100	99.9
		58.8	21	66	1.975	1.970	420	100	99.8
		66.7	9	28	1.762	1.764	500	60	99.9
(7)	AUSTENITE	55.5	100	100	2.081	2.080	111	100	100.0
		65.4	7	7	1.794	1.800	200	80	99.7

TABLE 5.16-A SUMMARY TABLE OF DIFFRACTOGRAM INDEXING

ALLOY : B2
SOAKING TEMPERATURE : 950°C SOAKING DURATION : 10 HOURS
COOLING MEDIA : AIR COOLED

	DIFF. ANGLE	PHASE(S) 1	3	5	7	9	11	13	15	17	19	21	23	25	27	29	INT
	47.9	0 0 0 0 1 1 0 1	0 0 0	0 0 0	0 1 1	0 0 0	0 0 0	0 1 0	0 1 0	0 0 0	0 0 0	0 0 0	0 1 0	0 0 0	0 0 0	0 0 0	5.5
	49.8	0 0 0 0 0 0 0 0	0 0 0	0 0 0	0 0 0	0 0 0	0 0 0	0 0 1	0 1 0	0 0 0	0 0 0	0 0 0	0 0 0	0 0 0	0 0 0	0 0 0	7.5
	53.4	0 0 0 0 0 0 0 0	0 0 0	0 0 0	0 0 0	0 0 0	0 0 0	0 0 1	0 1 0	0 0 1	0 0 0	0 0 0	0 0 1	0 0 0	0 0 1	1 1	3.0
	55.5	0 1 0 0 0 0 1 0	1 1 0	0 0 0	0 0 0	0 0 0	0 0 0	0 0 0	0 0 0	0 0 0	0 0 0	0 0 0	0 0 1	0 1 1	1 0 0	0 0 0	32.5
	55.9	0 0 1 0 0 1 0 1	1 1 0	0 0 0	0 0 0	0 0 0	0 0 0	0 0 0	0 0 0	0 0 1	0 0 1	0 0 0	0 0 0	0 1 1	1 1 0	0 0 0	10.5
	57.4	0 0 1 0 0 1 0 0	1 1 1	1 1 1	0 0 0	0 0 0	0 0 0	0 0 0	0 0 0	0 0 0	0 0 0	0 0 0	0 0 0	0 0 0	0 0 0	0 0 0	14.0
	58.8	0 0 0 0 0 1 0 1	0 1 0	0 0 0	0 0 0	0 0 0	0 0 0	0 0 0	0 0 0	0 0 0	0 0 0	0 0 0	0 1 0	0 0 0	0 1 0	1 0	7.0
	62.4	0 0 0 0 0 1 0 0	0 0 0	0 0 0	0 0 0	0 0 0	0 0 0	0 0 0	0 0 0	0 0 0	0 0 0	0 0 0	0 1 1	0 0 0	0 1 0	1 1	4.5
	63.1	0 0 0 0 0 0 1 0	0 0 0	0 0 0	0 0 1	0 0 0	0 0 0	0 0 0	0 1 0	1 0 0	0 0 0	0 0 0	0 0 0	1 0 0	0 0 0	0 0 0	3.5
	64.6	0 0 0 0 0 0 0 1	0 0 1	1 1 1	0 0 0	0 0 0	0 0 0	0 0 0	0 0 0	0 0 0	0 0 0	0 0 0	1 0 0	0 0 1	0 0 0	0 0 0	3.0
	64.9	0 0 0 0 0 0 0 0	0 0 1	1 0 0	0 1 1	0 0 0	0 0 0	0 0 0	0 0 0	1 0 0	0 0 0	0 0 0	0 0 0	0 0 1	1 0 0	0 0 0	5.0
*	65.4	0 1 0 1 0 0 0 1	0 0 0	1 0 0	0 0 0	1 0 0	0 0 0	1 0 0	0 0 0	0 0 0	0 0 1	0 0 0	0 0 0	0 1 1	0 0 0	1 1	2.5
	66.7	0 0 0 0 0 1 0 1	0 0 0	0 0 0	0 0 0	0 0 0	0 0 0	0 0 0	0 0 0	0 0 0	0 0 0	0 0 0	0 0 0	1 0 0	0 0 1	1 1	3.0
	67.6	0 0 0 0 0 0 0 0	0 0 0	0 0 0	0 0 0	0 0 0	0 0 1	0 0 0	0 0 0	0 0 0	0 0 0	0 0 0	0 0 0	0 0 1	0 0 0	0 0	2.0
	70.2	0 0 0 0 1 1 0 0	0 1 0	0 0 0	0 0 0	0 1 0	0 0 0	0 0 0	0 0 0	1 1 0	0 1 0	1 0 1	0 0 0	0 1 0	0 0 0	0 0	2.5
	98.8	0 0 0 0 0 0 0 0	0 0 0	0 0 0	0 0 0	0 0 0	0 0 0	0 0 0	0 0 0	0 0 0	0 0 0	0 0 0	0 0 0	0 0 1	0 0 0	0 0	8.0
	117.7	0 0 0 0 0 0 0 0	0 0 1	0 0 0	0 0 0	0 0 0	0 0 0	0 0 0	0 0 0	0 0 0	0 0 0	0 0 0	0 0 0	0 0 0	0 0 0	0 0	3.0
	125.6	0 0 0 0 0 0 0 1	0 0 0	0 0 0	0 0 0	0 0 0	0 0 0	0 0 0	0 0 0	0 0 0	0 0 0	0 0 0	0 0 0	0 0 1	0 0 0	0 0	24.0
	126.0	0 0 0 0 1 0 0 0	0 0 0	0 0 0	0 0 0	0 0 0	0 0 0	0 0 0	0 0 0	0 0 0	0 0 0	0 0 1	0 0 0	0 0 0	0 0 0	0 0	17.0
	127.0	0 1 0 0 0 0 0 0	0 0 0	0 0 0	0 0 0	0 0 0	0 0 0	0 0 0	0 0 0	0 0 0	0 0 0	0 0 0	1 0 0	0 0 0	0 0 0	0 0	2.0
		0 3 0 0 3 8 0 6	4 6 4	3 3 3	3 0 4	3 0 0	0 0 5	4 0 4	8 0 4	4							

0 = ABSENT 1 = PRESENT * = PROBABLE DIFF. ANGLE FOR K-BETA RADIATION

TABLE 5.16-B DETAILED ANALYSIS OF PHASE(S) ACTUALLY PRESENT

S.N.	PHASE PRESENT	DIFF ANGLE	PEAK INT	I/IO	D MEAS	D STD	DIFF PLANES	INT STD	CONF LIMIT
(1)	AUSTENITE	55.5	100	100	2.081	2.080	111	100	100.0
		65.4	7	7	1.794	1.800	200	80	99.7
		127.0	6	6	1.083	1.083	311	80	99.9
(2)	MN23C6	47.9	16	32	2.387	2.380	420	50	99.9
		70.2	7	14	1.685	1.686	422	20	100.0
		126.0	52	100	1.087	1.087	555	75	99.9
(3)	FE3C(CEMENTITE)	47.9	16	36	2.387	2.380	112	65	99.9
		55.9	32	70	2.066	2.060	210	70	99.8
		58.8	21	46	1.975	1.970	211	55	99.8
		62.4	13	30	1.870	1.870	113	30	100.0
		63.1	10	23	1.853	1.850	122	40	99.9
		66.7	9	20	1.762	1.760	212	16	99.9
		70.2	7	16	1.685	1.680	023	16	99.8
(4)	MN5C2(PD5B2)	55.5	100	100	2.081	2.078	510	100	99.9
		55.9	32	32	2.066	2.058	402	80	99.8
		57.4	43	43	2.016	2.016	511	80	100.0
		58.8	21	21	1.975	1.972	312	80	99.9
		64.6	9	9	1.813	1.820	421	70	99.7
		70.2	7	7	1.685	1.690	602	10	99.8
(5)	FE7C3(2)	57.4	43	100	2.016	2.019	121	100	99.9
		64.6	9	21	1.813	1.807	022	22	99.7
		64.9	15	35	1.807	1.807	022	22	100.0
		117.7	9	21	1.132	1.131	501	13	99.8
(6)	CR7C3(2)	57.4	43	100	2.016	2.020	121	100	99.9
		64.6	9	21	1.813	1.820	301	30	99.7
		65.4	7	17	1.794	1.790	022	50	99.9
(7)	COPPER	55.5	100	100	2.081	2.088	111	100	99.8
		64.9	15	15	1.807	1.808	200	46	100.0
		98.8	24	24	1.277	1.278	220	20	99.8
		125.6	73	73	1.089	1.090	311	17	99.8
(8)	CRMN3	53.4	9	28	2.156	2.162	321	40	99.9
		53.8	10	33	2.142	2.132	410	100	99.7
		55.9	32	100	2.066	2.069	330	100	99.9
		58.8	21	66	1.975	1.970	420	100	99.8
		66.7	9	28	1.762	1.764	500	60	99.9

TABLE 5.17-A SUMMARY TABLE OF DIFFRACTOGRAM INDEXING

ALLOY : B2
SOAKING TEMPERATURE : 1000°C SOAKING DURATION : 4 HOURS
COOLING MEDIA : AIR COOLED

DIFF. ANGLE	PHASE(S) 1	3	5	7	9	11	13	15	17	19	21	23	25	27	29	INT
42.1	0 0 0	0 0	0 0	0 0	0 0	0 1	0 0	1 0	0 0	0 0	1 0	0 0	0 0	0 0	0 0	1.5
47.0	0 0 0	0 0	0 0	1 0	0 1	0 0	0 0	0 0	0 1	0 0	0 0	0 0	0 0	0 0	0 0	2.0
48.4	0 0 0	1 0	0 0	0 0	0 0	0 0	0 0	0 0	1 0	0 0	0 0	1 0	0 0	0 0	0 0	2.0
54.8	0 0 0	0 0	1 1	0 0	0 0	1 0	0 0	1 0	1 0	1 0	0 0	0 0	0 0	0 0	0 1	3.0
55.8	0 1 0	0 0	0 1	0 0	0 1	0 0	0 0	0 0	0 0	0 0	1 0	0 0	0 0	1 0	0 0	37.0
55.9	0 0 1	0 0	0 0	0 1	1 0	0 0	0 0	0 0	0 1	0 0	0 0	0 0	0 0	1 1	0 0	37.5
57.7	0 0 0	0 0	0 1	1 0	0 1	0 0	0 0	0 0	0 0	0 0	0 0	0 0	0 0	1 1	0 1	6.0
57.8	0 0 0	0 0	0 0	0 0	0 0	0 0	0 0	0 0	0 0	0 0	0 0	0 0	0 0	0 0	0 0	8.0
59.0	0 0 0	0 0	0 1	0 0	0 1	0 0	0 1	0 0	0 0	0 0	0 0	0 0	0 0	1 1	1 0	3.0
62.7	0 0 0	0 0	0 1	0 0	0 0	0 0	0 0	1 0	1 0	0 0	0 0	0 1	0 0	0 0	0 0	2.5
65.1	0 1 0	1 1	0 0	1 0	0 1	0 0	0 0	0 0	0 0	0 1	0 0	0 0	0 1	0 0	0 1	15.0
67.2	0 0 0	0 0	0 0	0 0	0 0	0 0	1 0	0 0	1 0	0 0	0 0	0 0	0 0	0 1	0 0	2.5
80.2	0 0 0	0 0	0 0	0 1	0 0	0 0	0 0	0 0	0 0	0 0	0 0	0 0	0 0	1 0	0 0	3.0
99.0	0 0 0	0 0	0 0	0 0	0 0	0 0	0 0	0 0	0 0	0 0	0 0	1 0	0 0	0 0	0 0	4.0
125.5	0 0 0	0 0	0 0	1 0	0 0	0 0	0 0	0 0	0 0	0 0	0 0	0 0	1 0	0 0	0 0	7.5
	0 0 0	0 0	4 4	4 0	5 0	0 3	0 0	0 3	3 0	0 0	0 0	0 0	0 0	4 4	0 3	

0 = ABSENT 1 = PRESENT * = PROBABLE DIFF. ANGLE FOR K-BETA RADIATION

TABLE 5.17-B DETAILED ANALYSIS OF PHASE(S) ACTUALLY PRESENT

S.N.	PHASE PRESENT	DIFF ANGLE	PEAK INT	I/IO	D MEAS	D STD	DIFF PLANESTD	INT	CONF LIMIT
(1)	FE3C(CEMENTITE)	54.8	8	50	2.104	2.100	121	60	99.9
		57.7	16	100	2.008	2.010	103	100	99.9
		59.0	8	50	1.968	1.970	211	55	99.9
		62.7	6	41	1.862	1.870	113	30	99.7
(2)	FE5C2	47.0	5	5	2.430	2.421	311	15	99.8
		54.8	8	8	2.104	2.112	112	25	99.8
		55.8	98	100	2.071	2.080	021	70	99.7
		57.7	16	16	2.008	2.010	312	40	99.9
(3)	FE5C2(HAGG)	55.9	100	100	2.067	2.060	510	100	99.8
		65.1	40	40	1.802	1.800	312	70	99.9
		80.2	8	8	1.504	1.500	422	10	99.7
		125.5	20	20	1.090	1.090	404	20	99.9
(4)	MN5C2(PD5B2)	47.0	5	5	2.430	2.429	202	50	100.0
		55.8	98	98	2.071	2.078	510	100	99.8
		55.9	100	100	2.067	2.058	402	80	99.7
		57.7	16	16	2.008	2.016	511	80	99.8
		59.0	8	8	1.968	1.972	312	80	99.9
(5)	CR7C3	42.1	4	50	2.698	2.680	311	20	99.7
		59.0	8	100	1.968	1.960	511	70	99.7
		67.2	6	83	1.751	1.750	412	70	100.0
(6)	FE2C(NETA)	47.0	5	5	2.430	2.420	101	80	99.8
		48.4	5	5	2.364	2.370	011	40	99.9
		55.9	100	100	2.067	2.060	210	100	99.8
(7)	FE8SI2C	55.8	98	100	2.071	2.070	210	80	100.0
		57.7	16	16	2.008	2.010	322	100	99.9
		59.0	8	8	1.968	1.960	224	60	99.7
		80.2	8	8	1.504	1.500	421	10	99.7
(8)	AUSTENITE	55.8	98	100	2.071	2.080	111	100	99.7
		65.1	40	39	1.802	1.800	200	80	100.0

TABLE 5.19-A SUMMARY TABLE OF DIFFRACTOGRAM INDEXING

ALLOY : B2
SOAKING TEMPERATURE : 1050°C SOAKING DURATION : 4 HOURS
COOLING MEDIA : AIR COOLED

	DIFF. ANGLE	PHASE(S) 1	3	5	7	9	11	13	15	17	19	21	23	25	27	29	INT
	41.6	0	0	0	0	0	0	0	0	1	0	0	0	0	0	0	3.0
	49.8	0	0	0	0	0	0	0	1	1	0	0	0	0	0	0	3.5
	54.1	0	0	0	0	0	1	1	1	0	1	0	0	0	1	1	4.5
*	55.3	0	1	0	0	0	1	1	0	0	0	0	1	1	0	1	125.0
	57.2	1	0	1	0	0	1	1	1	0	0	0	0	0	1	0	6.0
	58.7	0	0	0	0	1	0	1	0	0	0	0	1	0	0	1	3.0
	59.4	0	0	0	0	0	1	0	0	0	0	0	0	0	1	0	2.5
	62.9	0	0	0	0	1	0	0	0	1	0	0	0	0	0	0	2.5
	64.6	0	0	0	0	0	1	1	0	0	0	0	1	0	0	0	20.0
	64.9	0	1	0	1	0	0	0	0	0	0	0	0	1	0	0	19.0
	108.4	0	0	0	0	0	0	0	1	1	0	1	0	0	1	0	3.5
	123.9	0	0	0	0	0	0	0	0	0	0	0	0	0	0	0	6.5
	124.6	0	0	0	0	0	0	0	0	0	0	0	0	0	0	0	9.5
	124.8	0	0	0	0	0	0	0	0	0	0	0	0	0	0	0	9.5
		0	0	0	0	3	3	0	4	3	3	0	5	3	0	0	5	0	0	0	0	0	0	0	0	4	3	3	0	

0 = ABSENT 1 = PRESENT * = PROBABLE DIFF. ANGLE FOR K-BETA RADIATION

TABLE 5.19-B DETAILED ANALYSIS OF PHASE(S) ACTUALLY PRESENT

S.N.	PHASE PRESENT	DIFF ANGLE	PEAK INT	I/IO	D MEAS	D STD	DIFF PLANES	INT STD	CONF LIMIT
(1)	FE5C2	55.3	100	100	2.088	2.080	021	70	99.8
		59.4	2	2	1.956	1.950	221	45	99.8
		64.6	16	16	1.812	1.814	312	25	99.9
(2)	MN5C2(PD5B2)	55.3	100	100	2.088	2.078	510	100	99.7
		57.2	4	4	2.024	2.016	511	80	99.7
		58.7	2	2	1.977	1.972	312	80	99.8
(3)	FE7C3(2)	54.1	3	23	2.131	2.122	012	41	99.8
		57.2	4	31	2.024	2.019	121	100	99.8
		64.9	15	100	1.807	1.807	022	22	100.0
(4)	CR7C3	54.1	3	22	2.131	2.120	202	70	99.7
		57.2	4	30	2.024	2.020	---	50	99.9
		59.4	2	12	1.956	1.960	511	70	99.9
		64.6	16	100	1.812	1.810	431	70	99.9
		108.4	2	17	1.195	1.194	---	50	99.9
(5)	FE8SI2C	55.3	100	100	2.088	2.080	131	80	99.8
		58.7	2	2	1.977	1.970	212	60	99.8
		59.4	2	2	1.956	1.960	224	60	99.9
		64.6	16	16	1.812	1.810	031	20	99.9
(6)	AUSTENITE	55.3	100	100	2.088	2.080	111	100	99.8
		64.9	15	15	1.807	1.800	200	80	99.8

TABLE 5.20-A SUMMARY TABLE OF DIFFRACTOGRAM INDEXING

ALLOY :B2
SOAKING TEMPERATURE : 1050°C SOAKING DURATION : 6 HOURS
COOLING MEDIA : AIR COOLED

	DIFF. ANGLE	PHASE(S) 1	3	5	7	9	11	13	15	17	19	21	23	25	27	29	INT
	44.9	0 0 0 0	0 1	0 0	0 0	0 0	0 0	0 0	0 0	0 1	0 0	0 0	0 1	0 0	0 0	0 1	2.5
*	49.8	0 0 0 0	0 0	0 0	0 0	0 0	0 0	0 1	0 0	0 1	0 0	0 0	0 0	0 0	0 0	0 0	2.0
	50.7	0 0 0 0	0 1	0 1	0 0	1 1	0 0	0 0	0 0	0 0	0 0	0 1	0 0	0 0	0 1	1 1	3.0
*	55.3	0 1 0 0	0 0	0 1	0 1	1 1	0 0	0 0	0 0	0 0	0 0	0 0	0 1	0 1	1 0	0 1	79.5
	55.9	0 0 1 0	0 1	0 1	0 1	1 1	0 0	0 0	0 0	0 1	0 0	1 0	0 0	0 1	1 1	1 0	4.0
	57.6	0 0 1 0	0 1	1 0	0 1	1 1	1 1	0 0	0 0	0 0	0 0	0 0	0 0	0 1	1 0	1 1	3.0
*	62.3	0 0 0 1	1 1	0 0	0 0	0 0	0 0	0 0	0 0	0 0	0 0	0 0	1 1	0 0	1 1	0 1	2.5
*	64.2	0 0 0 0	0 0	0 1	0 1	1 1	1 1	0 0	0 0	0 0	0 1	0 0	0 0	0 0	1 1	0 0	3.5
	64.6	0 0 0 0	0 0	0 1	0 0	0 0	0 0	0 0	0 0	0 0	0 0	0 0	1 0	0 0	0 0	0 0	16.5
	64.8	0 0 0 0	0 0	0 0	0 1	0 0	0 1	0 1	1 0	0 1	0 0	0 0	0 0	0 1	1 0	0 0	15.5
	90.2	0 0 0 0	0 0	0 0	1 0	0 0	0 0	0 0	0 0	1 0	0 0	0 0	0 0	0 0	0 0	0 0	2.0
	98.3	0 0 0 0	0 0	0 0	0 0	0 0	0 0	0 1	0 0	0 1	0 0	0 0	1 1	0 1	0 0	0 0	4.0
	99.0	0 0 0 0	0 0	0 0	0 0	0 0	0 0	0 0	0 0	0 0	0 0	0 0	1 0	0 0	0 0	0 0	2.0
	124.7	0 0 0 0	0 0	0 0	0 0	0 0	0 0	0 0	0 0	0 0	0 0	0 0	0 0	0 0	0 0	0 0	4.5
	125.4	0 0 0 0	0 0	0 0	0 1	0 0	0 0	0 0	0 0	0 0	0 0	0 0	0 0	0 1	0 0	0 0	4.0
		0 0 0 0	0 5	4 4	4 4	4 3	3 0	0 0	0 5	0 0	0 0	0 3	4 0	4 6	5 0	5	

0 = ABSENT 1 = PRESENT * = PROBABLE DIFF. ANGLE FOR K-BETA RADIATION

TABLE 5.20-B DETAILED ANALYSIS OF PHASE(S) ACTUALLY PRESENT

S.N.	PHASE PRESENT	DIFF ANGLE	PEAK INT	I/I0	D MEAS	D STD	DIFF PLANES	INT STD	CONF LIMIT
(1)	FE5C2(HAGG)	50.7	3	75	2.263	2.260	020	50	99.9
		55.9	5	100	2.067	2.060	510	100	99.8
		90.2	2	50	1.368	1.370	331	10	99.8
		125.4	5	100	1.090	1.090	404	20	100.0
(2)	MN5C2(PD5B2)	55.3	100	100	2.088	2.078	510	100	99.7
		55.9	5	5	2.067	2.058	402	80	99.7
		57.6	3	3	2.011	2.016	511	80	99.9
		64.2	4	4	1.823	1.820	421	70	99.9
(3)	FE7C3(2)	50.7	3	19	2.263	2.255	120	31	99.8
		57.6	3	19	2.011	2.019	121	100	99.8
		64.2	4	22	1.823	1.820	301	11	99.9
		64.8	19	100	1.808	1.807	022	22	99.9
(4)	CR7C3(2)	50.7	3	85	2.263	2.270	120	50	99.8
		57.6	3	85	2.011	2.020	121	100	99.7
		64.2	4	100	1.823	1.820	301	30	99.9
(5)	COPPER	55.3	100	100	2.088	2.088	111	100	100.0
		64.8	19	19	1.808	1.808	200	46	100.0
		98.3	5	5	1.281	1.278	220	20	99.7
		125.4	5	5	1.090	1.090	311	17	100.0
(6)	FE8SI2C	55.3	100	100	2.088	2.080	131	80	99.8
		55.9	5	5	2.067	2.070	210	80	99.9
		57.6	3	3	2.011	2.010	322	100	100.0
		62.3	3	3	1.874	1.880	323	10	99.8
		64.2	4	4	1.823	1.820	015	60	99.9
		64.8	19	19	1.808	1.810	031	20	99.9
(7)	AUSTENITE	55.3	80	100	2.088	2.080	111	100	99.8

TABLE 5.31-A SUMMARY TABLE OF DIFFRACTOGRAM INDEXING

ALLOY : B3
SOAKING TEMPERATURE : 1050°C SOAKING DURATION : 10 HOURS
COOLING MEDIA : AIR COOLED

DIFF. ANGLE	PHASE(S) 1	3	5	7	9	11	13	15	17	19	21	23	25	27	29	INT
49.9	0	0	0	1	0	0	0	1	0	0	1	0	0	0	0	2.0
55.6	0	1	0	1	1	0	0	0	0	0	1	0	1	1	0	53.5
56.8	1	0	0	0	1	1	0	1	0	0	1	0	0	0	1	2.0
64.8	0	0	0	1	0	0	1	0	1	0	0	0	1	1	0	14.0
98.6	0	0	0	0	0	0	0	0	1	0	0	0	1	0	0	3.0
125.9	0	0	0	0	0	0	0	0	0	0	1	0	0	0	0	11.0
126.1	0	0	1	0	0	0	0	0	0	0	0	0	0	0	0	12.0
	0	0	0	3	0	0	3	3	0	0	3	0	0	3	0	

0 = ABSENT 1 = PRESENT * = PROBABLE DIFF. ANGLE FOR K-BETA RADIATION

TABLE 5.31-B DETAILED ANALYSIS OF PHASE(S) ACTUALLY PRESENT

S.N.	PHASE PRESENT	DIFF ANGLE	PEAK INT	I/I0	D MEAS	D STD	DIFF PLANE	INT STD	CONF LIMIT
(1)	FE5C2	49.9	3	3	2.297	2.287	020	20	99.8
		55.6	100	100	2.079	2.080	021	70	100.0
		64.8	26	26	1.808	1.814	312	25	99.8
(2)	CR7C3	56.8	3	14	2.036	2.040	421	100	99.9
		64.8	26	100	1.808	1.810	431	70	99.9
		98.6	5	21	1.277	1.280	---	60	99.7
(3)	(CR,FE)7C3	49.9	3	14	2.297	2.300	141	40	99.9
		56.8	3	14	2.036	2.040	122	100	99.9
		64.8	26	100	1.808	1.810	431	60	99.9
(4)	COPPER	55.6	100	100	2.079	2.088	111	100	99.7
		64.8	26	26	1.808	1.808	200	46	100.0
		98.6	5	5	1.277	1.278	220	20	99.9
(5)	AUSTENITE	55.6	54	100	2.079	2.080	111	100	99.9

TABLE 5.33-A SUMMARY TABLE OF DIFFRACTOGRAM INDEXING

ALLOY : B4
SOAKING TEMPERATURE : 900°C SOAKING DURATION : 4 HOURS
COOLING MEDIA : AIR COOLED

	DIFF. ANGLE	PHASE(S) 1	3	5	7	9	11	13	15	17	19	21	23	25	27	29	INT
	47.9	0	0	0	1	1	0	1	0	0	0	0	1	0	0	0	5.0
	50.8	0	0	0	0	1	0	1	0	0	1	0	0	0	1	1	3.0
	51.6	0	0	0	0	0	0	0	0	0	0	0	0	0	1	0	3.0
	54.9	0	0	0	0	1	0	0	0	0	1	0	0	0	0	1	3.0
*	55.6	0	1	0	0	0	1	0	1	1	0	0	0	0	0	0	160.0
	56.0	0	0	1	0	0	1	0	1	1	1	0	0	0	1	0	28.0
	57.1	1	0	0	0	0	0	1	1	1	0	0	0	0	0	1	7.0
	57.5	0	0	1	0	0	1	1	0	1	1	1	0	0	1	1	20.0
	58.9	0	0	0	0	0	1	0	0	0	0	0	0	0	1	0	5.0
*	62.4	0	0	0	0	0	1	0	0	0	0	0	0	0	0	1	3.0
	63.2	0	0	0	0	0	1	0	0	0	0	0	0	0	0	0	3.0
	65.0	0	1	0	1	1	0	0	1	0	1	1	0	0	1	1	17.0
	66.0	0	0	0	1	0	0	0	0	1	0	1	0	1	0	1	2.5
	66.6	0	0	0	0	0	1	0	1	0	0	0	0	0	1	1	5.0
	93.6	0	0	0	0	1	0	0	0	0	0	0	0	0	0	0	4.0
	98.9	0	0	0	0	0	0	0	0	0	0	0	0	0	0	0	7.0
	118.1	0	0	0	0	0	0	1	0	0	0	0	0	0	0	0	3.5
	126.0	0	0	0	0	1	0	0	0	0	0	0	1	0	0	0	19.0
	126.9	0	1	0	0	0	0	0	0	0	0	0	0	1	0	0	3.0
		0	3	0	0	4	9	0	7	4	4	4	3	5	0	3	3	5	0	0	0	0	0	4	6	0	0	7	5	4	8	

0 = ABSENT 1 = PRESENT * = PROBABLE DIFF. ANGLE FOR K-BETA RADIATION

TABLE 5.33-B DETAILED ANALYSIS OF PHASE(S) ACTUALLY PRESENT

S.N.	PHASE PRESENT	DIFF ANGLE	PEAK INT	I/IO	D MEAS	D STD	DIFF PLANESTD	INT	CONF LIMIT
(1)	AUSTENITE	55.6	100	100	2.078	2.080	111	100	99.9
		65.0	10	10	1.803	1.800	200	80	99.9
		126.9	1	1	1.083	1.083	311	80	100.0
(2)	MN23C6	47.9	3	26	2.387	2.380	420	50	99.9
		65.0	10	89	1.803	1.799	531	50	99.9
		93.6	2	21	1.329	1.330	622	35	99.9
		126.0	11	100	1.087	1.087	555	75	99.9
(3)	FE3C(CEMENTITE)	47.9	3	17	2.387	2.380	112	65	99.9
		50.8	1	10	2.259	2.260	200	25	100.0
		54.9	1	10	2.101	2.100	121	60	100.0
		56.0	17	100	2.064	2.060	210	70	99.9
		57.5	12	71	2.014	2.020	022	60	99.8
		58.9	3	17	1.970	1.970	211	55	100.0
		62.4	1	10	1.870	1.870	113	30	100.0
		63.2	1	10	1.849	1.850	122	40	99.9
		66.6	3	17	1.764	1.760	212	16	99.8
(4)	FE5C2(HAGG)	47.9	3	17	2.387	2.390	202	20	99.9
		50.8	1	10	2.259	2.260	020	50	100.0
		56.0	17	100	2.064	2.060	510	100	99.9
		57.1	4	25	2.027	2.030	312	100	99.9
		65.0	10	60	1.803	1.800	312	70	99.9
		66.6	3	17	1.764	1.760	402	10	99.8
		118.1	2	12	1.130	1.130	133	50	99.9
(5)	MN5C2(PD5B2)	55.6	100	100	2.078	2.078	510	100	100.0
		56.0	17	17	2.064	2.058	402	80	99.8
		57.1	4	4	2.027	2.035	312	70	99.8
		66.0	1	1	1.779	1.779	512	70	100.0
(6)	FE7C3(2)	50.8	1	15	2.259	2.255	120	31	99.9
		57.5	12	100	2.014	2.019	121	100	99.9
		65.0	10	85	1.803	1.807	022	22	99.8
		118.1	2	17	1.130	1.131	501	13	99.8
(7)	CRMN3	56.0	17	100	2.064	2.069	330	100	99.9
		57.1	4	25	2.027	2.036	202	70	99.7
		58.9	3	17	1.970	1.970	420	100	100.0
		66.6	3	17	1.764	1.764	500	60	100.0

TABLE 5.34-A SUMMARY TABLE OF DIFFRACTOGRAM INDEXING

ALLOY : B4
SOAKING TEMPERATURE : 900°C SOAKING DURATION : 10 HOURS
COOLING MEDIA : AIR COOLED

	DIFF. ANGLE	PHASE(S) 1	3	5	7	9	11	13	15	17	19	21	23	25	27	29	INT
	48.0	0 0 0 1	1 1 0 1	0 0 0	0 0 0	1 0 0	0 0 0	0 0 0	1 0 0	1 0 0	0 0 0	0 0 0	0 0 0	0 0 0	0 0 0	0 0 0	5.0
	50.9	0 0 0 0	0 1 0 1	0 0 1	0 0 0	0 0 0	0 0 0	0 0 0	0 0 0	0 0 0	0 0 0	0 0 1	0 0 0	0 0 1	0 1 0	1 0 1	3.0
*	55.6	0 1 0 0	0 0 1 0	1 1 0	0 0 0	0 0 0	0 0 0	0 0 0	0 0 0	0 0 0	0 0 0	0 1 0	0 0 0	0 0 0	1 0 1	0 0 0	332.0
	56.1	0 0 1 0	0 1 0 1	1 1 0	0 0 0	0 0 0	0 0 0	0 0 0	0 0 0	0 1 0	0 0 0	0 0 0	0 0 0	0 0 0	0 1 0	0 0 0	17.0
	56.4	0 0 0 1	1 0 0 0	0 0 0	0 0 0	0 0 0	0 0 0	0 0 0	0 0 0	0 0 0	0 0 0	0 0 1	0 0 0	0 0 1	0 0 0	0 0 0	6.0
	57.2	1 0 0 0	0 1 0 1	0 0 1	1 1 0	0 0 0	0 0 0	0 0 0	0 0 0	0 0 0	0 0 1	0 0 0	0 0 0	0 0 0	0 0 0	0 0 0	12.0
	57.6	0 0 1 0	0 0 0 0	1 1 0	0 0 0	0 0 0	0 0 0	0 0 0	0 0 0	0 0 0	0 0 0	0 0 0	0 0 0	0 0 0	1 1 0	1 0 1	27.0
	58.8	0 0 0 0	0 1 0 1	0 1 0	0 0 0	0 0 0	0 0 0	0 0 0	0 0 0	0 0 0	0 0 0	0 0 0	0 1 0	0 0 0	1 0 1	0 0 0	9.0
*	62.4	0 0 0 0	0 1 0 0	0 0 0	0 0 0	0 0 0	0 0 0	0 0 0	0 0 0	0 0 0	0 0 0	0 0 0	0 1 1	0 0 0	0 1 0	1 0 1	6.0
*	63.2	0 0 0 0	0 1 0 0	0 0 0	0 0 0	0 0 0	0 0 0	0 0 1	0 0 0	0 0 0	0 0 0	0 0 0	0 0 0	1 0 0	0 0 0	0 0 0	4.0
	64.6	0 0 0 0	0 0 1 0	1 1 1	1 1 1	1 0 0	1 0 0	0 0 0	1 0 0	0 0 0	0 0 0	0 0 1	0 0 0	0 0 1	0 0 0	0 0 0	10.0
	65.0	0 1 0 1	1 0 0 1	0 0 1	0 1 0	1 0 0	1 0 0	1 1 0	0 1 0	1 0 0	1 0 0	0 0 0	0 0 1	0 0 1	1 0 0	0 1 1	12.0
	66.6	0 0 0 0	0 1 0 1	0 0 0	0 0 0	0 0 0	0 0 0	0 0 0	0 0 0	1 0 0	0 0 0	0 0 0	0 0 1	0 0 0	0 0 1	1 0 0	2.0
	125.8	0 0 0 0	1 0 0 0	0 0 0	0 0 0	0 0 0	0 0 0	0 0 0	0 0 0	0 0 0	0 0 0	0 0 0	1 0 0	0 0 0	0 0 0	0 0 0	7.0
		0 0 0 3	4 7 0 7	4 5 4	0 3 0	0 0 0	3 0 0	0 0 0	4 0 0	0 0 0	6 4 3	5					

0 = ABSENT 1 = PRESENT * = PROBABLE DIFF. ANGLE FOR K-BETA RADIATION

TABLE 5.34-B DETAILED ANALYSIS OF PHASE(S) ACTUALLY PRESENT

S.N.	PHASE PRESENT	DIFF ANGLE	PEAK INT	I/IO	D MEAS	D STD	DIFF PLANES	INT STD	CONF LIMIT
(1)	CR23C6	48.0	1	83	2.383	2.370	420	50	99.7
		56.4	1	100	2.050	2.050	511	100	100.0
		65.0	0	33	1.803	1.800	531	50	99.9
(2)	MN23C6	48.0	1	71	2.383	2.380	420	50	99.9
		56.4	1	85	2.050	2.053	511	100	99.9
		65.0	0	28	1.803	1.799	531	50	99.8
		125.8	2	100	1.088	1.087	555	75	99.8
(3)	FE3C(CEMENTITE)	48.0	1	29	2.383	2.380	112	65	99.9
		50.9	0	17	2.255	2.260	200	25	99.9
		56.1	5	100	2.061	2.060	210	70	100.0
		57.2	3	70	2.025	2.020	022	60	99.9
		58.8	2	52	1.974	1.970	211	55	99.9
		62.4	1	35	1.870	1.870	113	30	100.0
		63.2	1	23	1.849	1.850	122	40	100.0
		66.6	0	11	1.764	1.760	212	16	99.8
(4)	FE5C2(HAGG)	48.0	1	29	2.383	2.390	202	20	99.9
		50.9	0	17	2.255	2.260	020	50	99.9
		56.1	5	100	2.061	2.060	510	100	100.0
		57.2	3	70	2.025	2.030	312	100	99.8
		58.8	2	52	1.974	1.980	511	20	99.8
		65.0	0	11	1.803	1.800	312	70	99.9
		66.6	0	11	1.764	1.760	402	10	99.8
(5)	MN5C2(PD5B2)	55.6	100	100	2.077	2.078	510	100	100.0
		56.1	5	5	2.061	2.058	402	80	99.9
		57.6	8	8	2.012	2.016	511	80	99.9
		58.8	2	2	1.974	1.972	312	80	99.9
		64.6	3	3	1.813	1.820	421	70	99.7
(6)	FE7C3(2)	50.9	0	25	2.255	2.255	120	31	100.0
		57.2	3	100	2.025	2.019	121	100	99.8
		64.6	3	83	1.813	1.807	022	22	99.7
		65.0	0	16	1.803	1.807	022	22	99.8
(7)	FE8SI2C	55.6	100	100	2.077	2.070	210	80	99.8
		56.4	1	1	2.050	2.050	121	80	100.0
		57.6	8	8	2.012	2.010	322	100	99.9
		58.8	2	2	1.974	1.970	212	60	99.9
		64.6	3	3	1.813	1.810	031	20	99.9
		65.0	0	0	1.803	1.810	031	20	99.7
(8)	CRMN3	55.6	100	100	2.077	2.069	330	100	99.8
		58.8	2	2	1.974	1.970	420	100	99.9
		66.6	0	0	1.764	1.764	500	60	100.0
(9)	AUSTENITE	55.6	100	100	2.077	2.080	111	100	99.9
		65.0	12	12	1.803	1.800	200	80	99.9

TABLE 5.36-A SUMMARY TABLE OF DIFFRACTOGRAM INDEXING

ALLOY : B4
SOAKING TEMPERATURE : 950°C SOAKING DURATION : 10 HOURS
COOLING MEDIA : AIR COOLED

	DIFF. ANGLE	PHASE(S) 1	3	5	7	9	11	13	15	17	19	21	23	25	27	29	INT
	48.1	0	0	1	1	0	0	0	1	0	0	0	0	0	0	0	5.0
	50.8	0	0	0	0	1	1	0	0	0	0	0	0	0	1	1	3.0
	54.9	0	0	0	1	1	0	0	0	1	1	0	0	0	0	1	11.0
	55.6	1	0	0	0	1	0	1	0	0	0	1	0	0	1	0	63.0
	57.6	0	1	0	1	1	0	1	0	0	0	0	0	0	1	1	21.0
	58.8	0	0	0	0	1	0	1	0	0	0	0	0	0	1	0	7.0
	62.4	0	0	0	0	1	0	0	0	0	0	0	0	0	0	1	8.0
	63.2	0	0	0	0	1	0	0	0	0	0	0	1	0	0	0	5.0
*	64.6	0	0	0	0	0	1	0	1	1	0	0	0	1	0	0	7.0
*	65.1	1	0	1	1	0	0	1	0	0	0	1	0	0	1	1	13.0
	66.7	0	0	0	0	1	0	1	0	0	0	0	1	0	0	1	4.0
	125.8	0	0	0	1	0	0	0	0	0	0	0	0	0	0	0	49.0
	126.8	1	0	0	0	0	0	0	0	0	0	0	0	0	0	0	8.0
		3	0	4	9	7	6	7	8	6	5	7	0	3	0	3	0	3	0	3	3	0	0	0	3	8	5	6	8

0 = ABSENT 1 = PRESENT * = PROBABLE DIFF. ANGLE FOR K-BETA RADIATION

TABLE 5.36-B DETAILED ANALYSIS OF PHASE(S) ACTUALLY PRESENT

S.N.	PHASE PRESENT	DIFF ANGLE	PEAK INT	I/I0	D MEAS	D STD	DIFF PLANESTD	INT	CONF LIMIT
(1)	AUSTENITE	55.6	100	100	2.077	2.080	111	100	99.9
		65.1	20	20	1.801	1.800	200	80	100.0
		126.8	12	12	1.084	1.083	311	80	99.9
(2)	MN23C6	48.1	7	10	2.378	2.380	420	50	99.9
		65.1	20	26	1.801	1.799	531	50	99.9
		125.8	77	100	1.088	1.087	555	75	99.7
(3)	FE3C(CEMENTITE)	48.1	7	23	2.378	2.380	112	65	99.9
		50.8	4	14	2.259	2.260	200	25	100.0
		54.9	17	52	2.102	2.100	121	60	99.9
		57.6	33	100	2.011	2.010	103	100	100.0
		58.8	11	33	1.974	1.970	211	55	99.9
		62.4	12	38	1.870	1.870	113	30	100.0
		63.2	7	23	1.849	1.850	122	40	100.0
		66.7	6	19	1.762	1.760	212	16	99.9
(4)	FE5C2(HAGG)	48.1	7	10	2.378	2.390	202	20	99.8
		50.8	4	6	2.259	2.260	020	50	100.0
		58.8	11	14	1.974	1.980	511	20	99.8
		65.1	20	26	1.801	1.800	312	70	100.0
		66.7	6	8	1.762	1.760	402	10	99.9
(5)	MN5C2(PD5B2)	55.6	100	100	2.077	2.078	510	100	100.0
		57.6	33	33	2.011	2.016	511	80	99.9
		58.8	11	11	1.974	1.972	312	80	99.9
		64.6	11	11	1.813	1.820	421	70	99.7
(6)	FE7C3(2)	50.8	4	14	2.259	2.255	120	31	99.9
		57.6	33	100	2.011	2.019	121	100	99.8
		64.6	11	33	1.813	1.807	022	22	99.7
		64.9	23	71	1.805	1.807	022	22	99.9
		65.1	20	61	1.801	1.807	022	22	99.8
(7)	CRMN3	55.6	100	100	2.077	2.069	330	100	99.8
		58.8	11	11	1.974	1.970	420	100	99.9
		66.7	6	6	1.762	1.764	500	60	99.9

TABLE 5.37-A SUMMARY TABLE OF DIFFRACTOGRAM INDEXING

ALLOY : B4
SOAKING TEMPERATURE : 1000°C SOAKING DURATION : 4 HOURS
COOLING MEDIA : AIR COOLED

	DIFF. ANGLE	PHASE(S) 1	3	5	7	9	11	13	15	17	19	21	23	25	27	29	INT
	49.9	0	0	0	1	0	0	0	1	0	0	1	0	0	0	0	2.0
	51.4	0	0	0	0	0	0	0	0	1	0	0	1	0	0	0	2.5
*	55.6	0	1	0	0	1	0	0	0	0	0	0	1	1	0	0	38.0
	55.6	0	0	0	0	0	1	0	0	0	0	1	0	1	1	0	38.0
	55.8	0	1	0	0	0	1	0	0	0	0	1	0	0	1	0	36.0
	56.3	0	0	1	0	1	1	0	0	0	1	0	1	0	0	0	9.0
	57.8	0	0	0	0	1	1	0	0	0	0	0	0	0	1	1	9.0
	57.9	0	0	0	0	0	0	0	1	0	0	0	0	0	0	0	9.0
	58.9	0	0	0	0	1	0	0	0	1	0	0	0	0	1	0	3.0
	59.2	0	0	0	0	0	0	0	0	0	1	0	0	0	0	0	3.0
*	62.1	0	0	0	1	1	0	0	0	0	0	0	1	0	0	0	2.0
*	62.8	0	0	0	0	0	0	0	0	0	0	0	0	1	0	0	3.0
	64.0	0	0	0	0	0	1	0	1	1	1	0	0	0	0	0	3.5
	65.1	0	1	0	1	1	0	0	1	0	0	0	0	0	0	1	15.5
*	66.0	0	0	0	1	0	0	0	0	1	0	0	0	1	0	0	3.0
	66.6	0	0	0	0	0	1	0	0	0	0	0	0	0	0	1	2.0
	67.4	0	0	0	0	0	0	0	0	0	1	0	0	0	0	0	2.0
	67.8	0	0	0	0	0	0	0	0	1	0	0	0	0	1	0	1.5
	68.6	0	0	0	0	0	0	1	0	0	0	0	0	0	0	1	1.5
	93.8	0	0	0	1	0	0	0	0	0	0	0	0	0	1	0	2.5
	98.5	0	0	0	0	0	0	0	0	0	0	0	1	0	0	0	3.5
	106.0	0	0	0	0	0	0	0	0	0	0	1	0	0	0	1	3.0
	125.0	0	0	0	0	0	0	0	0	0	0	0	0	0	0	0	10.0
	126.0	0	0	0	0	0	0	0	0	0	0	0	1	0	0	0	6.0
		0	3	0	3	5	4	5	4	4	7	0	0	6	0	0	0	9	0	0	0	4	0	0	5	0	0	11	5	5	5	

0 = ABSENT 1 = PRESENT * = PROBABLE DIFF. ANGLE FOR K-BETA RADIATION

TABLE 5.37-B DETAILED ANALYSIS OF PHASE(S) ACTUALLY PRESENT

S.N.	PHASE PRESENT	DIFF ANGLE	PEAK INT	I/IO	D MEAS	D STD	DIFF PLANES	INT STD	CONF LIMIT
(1)	AUSTENITE	55.6	100	100	2.079	2.080	111	100	100.0
		55.8	94	94	2.072	2.080	111	100	99.8
		65.1	40	40	1.800	1.800	200	80	100.0
(2)	FE3C(CEMENTITE)	56.3	23	100	2.052	2.060	210	70	99.8
		57.8	23	100	2.003	2.010	103	100	99.8
		58.9	7	33	1.970	1.970	211	55	100.0
		66.6	5	22	1.765	1.760	212	16	99.8
(3)	FE5C2(HAGG)	56.3	23	58	2.052	2.060	510	100	99.8
		65.1	40	100	1.800	1.800	312	70	100.0
		66.6	5	12	1.765	1.760	402	10	99.8
		68.6	3	9	1.720	1.720	421	10	100.0
(4)	MN5C2(PD5B2)	55.6	100	100	2.077	2.078	510	100	100.0
		55.8	94	94	2.072	2.078	510	100	99.8
		56.3	23	23	2.052	2.058	402	80	99.8
		58.9	7	7	1.970	1.972	312	80	99.9
		64.0	9	9	1.827	1.820	421	70	99.7
		66.0	7	7	1.779	1.779	512	70	100.0
		67.8	3	3	1.737	1.732	022	80	99.8
(5)	CR7C3	59.2	7	20	1.961	1.960	511	70	100.0
		66.0	7	20	1.779	1.780	521	50	99.9
		67.4	5	13	1.746	1.750	412	70	99.8
		93.8	6	16	1.327	1.330	---	50	99.7
		98.5	9	23	1.279	1.280	---	60	99.9
		106.0	7	20	1.213	1.215	---	60	99.8
(6)	COPPER	55.6	100	100	2.079	2.088	111	100	99.7
		98.5	9	9	1.279	1.278	220	20	99.9

TABLE 5.38-A SUMMARY TABLE OF DIFFRACTOGRAM INDEXING

ALLOY : B4
SOAKING TEMPERATURE : 1000°C SOAKING DURATION : 10 HOURS
COOLING MEDIA : AIR COOLED

DIFF. ANGLE	PHASE(S) 1	3	5	7	9	11	13	15	17	19	21	23	25	27	29	INT
36.0	0	0	0	0	0	0	0	0	0	0	0	0	0	0	0	1.0
42.1	0	0	0	0	0	0	0	0	0	0	0	0	0	0	0	1.5
43.2	0	0	0	0	0	0	0	0	0	0	0	0	0	0	0	1.5
49.0	0	0	0	0	0	0	0	0	0	0	0	0	0	1	0	1.0
53.2	0	0	0	1	0	0	0	0	0	0	0	0	0	1	1	1.5
54.0	0	0	0	0	0	0	0	0	0	0	0	0	0	1	1	1.5
55.3	0	0	0	0	0	0	0	0	0	0	0	0	1	1	0	26.5
55.4	0	1	0	0	0	1	0	0	0	0	0	0	0	1	0	25.5
56.9	1	0	0	0	0	0	1	1	0	0	0	0	0	0	1	2.0
57.4	0	0	1	0	0	1	1	1	1	1	0	0	0	1	1	1.5
63.0	0	0	0	0	0	1	0	0	0	0	0	0	1	0	0	1.5
64.6	0	0	0	0	0	1	0	1	1	1	1	0	0	1	0	6.5
65.3	0	1	0	1	1	0	0	1	0	0	0	0	0	1	0	2.0
65.6	0	0	0	0	0	0	0	0	0	0	0	0	1	0	0	1.5
66.2	0	0	0	1	0	0	0	0	0	1	0	0	0	1	0	3.0
66.4	0	0	0	0	0	0	0	0	0	0	0	0	0	0	1	3.0
67.2	0	0	0	0	0	0	0	0	0	0	0	0	0	0	1	1.5
68.1	0	0	0	0	0	0	0	0	0	0	0	0	0	0	1	1.5
70.5	0	0	0	0	1	0	0	0	0	0	0	0	1	0	0	1.0
72.7	0	0	0	0	1	0	0	0	0	0	0	0	0	1	0	2.0
73.0	0	0	0	0	0	0	0	0	0	0	0	0	0	1	0	2.5
98.5	0	0	0	0	0	0	0	0	0	0	0	0	0	1	0	2.5
125.0	0	0	0	0	0	0	0	0	0	0	0	0	0	0	0	4.5
124.7	0	0	0	0	0	0	0	0	0	0	0	0	0	0	0	4.0
126.0	0	0	0	0	0	0	0	0	0	0	0	0	0	0	0	3.0
	0	0	0	3	0	4	3	3	4	7	0	4	7	0	4	0	6	0	0	4	0	0	0	5	0	3	8	4	5	9	

0 = ABSENT 1 = PRESENT * = PROBABLE DIFF. ANGLE FOR K-BETA RADIATION

TABLE 5.38-B DETAILED ANALYSIS OF PHASE(S) ACTUALLY PRESENT

S.N.	PHASE PRESENT	DIFF ANGLE	PEAK INT	I/I0	D MEAS	D STD	DIFF PLANES	INT STD	CONF LIMIT
(1)	FE5C2	55.4	96	100	2.084	2.080	021	70	99.9
		57.4	5	5	2.018	2.010	312	40	99.8
		64.6	24	25	1.813	1.814	312	25	100.0
(2)	FE5C2(HAGG)	43.2	5	75	2.631	2.620	311	10	99.8
		56.9	7	100	2.035	2.030	312	100	99.9
		65.3	7	100	1.795	1.800	312	70	99.8
(3)	MN5C2(FD5B2)	55.4	96	100	2.084	2.078	510	100	99.8
		56.9	7	7	2.035	2.035	312	70	100.0
		57.4	5	5	2.018	2.016	511	80	99.9
		64.6	24	25	1.813	1.820	421	70	99.7
		66.2	11	11	1.774	1.779	512	70	99.8
		68.1	5	5	1.731	1.732	022	80	100.0
		72.7	7	7	1.635	1.636	999	50	99.9
(4)	CR7C3(2)	57.4	5	23	2.018	2.020	121	100	99.9
		64.6	24	100	1.813	1.820	301	30	99.7
		65.6	5	23	1.789	1.790	022	50	100.0
		68.1	5	23	1.731	1.730	122	30	100.0
(5)	COPPER	55.3	100	100	2.087	2.088	111	100	100.0
		64.6	24	24	1.813	1.808	200	46	99.8
		98.5	9	9	1.279	1.278	220	20	99.9
(6)	FE8SI2C	55.3	100	100	2.087	2.080	131	80	99.8
		55.4	96	96	2.084	2.080	131	80	99.9
		57.4	5	5	2.018	2.010	322	100	99.8
		64.6	24	24	1.813	1.810	031	20	99.9
		65.3	7	7	1.795	1.794	015	20	100.0
		66.2	11	11	1.774	1.780	312	20	99.7
		70.5	3	3	1.678	1.680	303	20	99.9
		73.0	9	9	1.629	1.625	302	10	99.8
(7)	AUSTENITE	55.4	26	100	2.084	2.080	111	100	99.9
		65.3	2	7	1.795	1.800	200	80	99.8

TABLE 5.39-A SUMMARY TABLE OF DIFFRACTOGRAM INDEXING

ALLOY : B4
SOAKING TEMPERATURE : 1050°C SOAKING DURATION : 4 HOURS
COOLING MEDIA : AIR COOLED

DIFF. ANGLE	PHASE(S) 1	3	5	7	9	11	13	15	17	19	21	23	25	27	29	INT
48.9	0 0	0 0	0 0	0 0	0 0	0 0	1 0	0 0	0 1	0 0	0 0	0 0	0 0	0 1	1 1	1.5
49.5	0 0	0 0	0 0	0 0	0 0	0 0	0 0	0 0	0 1	0 0	0 0	0 0	0 1	0 0	1 0	2.5
53.5	0 0	0 0	0 0	0 0	0 0	0 0	0 0	1 0	0 1	0 0	0 0	0 1	0 0	0 1	0 0	2.5
55.5	0 1	0 0	0 0	1 0	1 1	0 0	0 0	0 0	0 0	0 0	1 0	0 1	0 1	1 0	0 0	39.0
57.7	0 0	0 0	0 1	1 0	0 1	0 0	0 0	0 0	0 0	0 0	0 0	0 0	0 1	1 0	0 1	3.5
58.3	0 0	0 0	0 0	0 1	1 1	1 1	0 0	0 0	0 1	0 0	0 0	1 0	0 0	1 0	0 0	2.0
61.8	0 0	0 1	1 0	0 0	0 0	1 0	0 0	0 0	1 0	0 0	0 0	0 0	0 1	0 1	0 0	1.5
64.0	0 0	0 0	0 0	0 0	1 1	0 0	0 0	0 0	0 0	1 0	0 0	0 0	0 0	1 0	0 0	3.0
64.4	0 0	0 0	0 0	1 0	1 1	1 1	0 0	0 0	0 0	0 0	0 0	0 0	0 1	0 0	0 0	7.5
64.7	0 0	0 0	0 0	1 0	0 0	0 1	1 0	0 0	1 0	0 0	0 1	0 0	0 1	0 0	0 0	13.0
64.8	0 0	0 0	0 0	1 0	0 0	1 0	0 0	0 0	0 0	0 0	0 0	0 0	1 0	0 0	0 0	14.5
65.1	0 1	0 1	1 0	0 1	0 0	0 0	0 0	0 0	0 0	1 0	0 0	0 0	0 1	0 0	0 1	11.0
66.0	0 0	0 1	1 0	0 0	1 0	0 1	0 0	1 0	0 1	0 0	0 0	0 1	0 0	1 0	0 1	2.5
97.9	0 0	0 0	0 0	0 0	0 0	0 0	0 0	0 0	0 0	0 0	0 0	0 1	0 0	0 0	0 0	3.0
98.4	0 0	0 0	0 0	0 0	0 0	0 0	1 0	0 0	0 1	0 0	0 0	1 0	0 0	0 0	0 0	6.5
99.0	0 0	0 0	0 0	0 0	0 0	0 0	0 0	0 0	0 0	0 0	0 0	1 0	0 0	0 0	0 0	4.0
100.2	0 0	0 0	0 0	0 0	0 0	0 0	0 0	0 0	0 1	0 0	0 0	0 0	0 0	0 0	1 0	2.5
101.6	0 0	0 0	0 0	0 1	0 0	0 0	0 0	0 0	0 0	0 0	0 0	0 0	0 0	0 0	1 0	2.5
124.6	0 0	0 0	0 0	0 0	0 0	0 0	0 0	0 0	0 0	0 0	0 0	0 0	0 0	0 0	0 0	8.0
125.9	0 0	0 0	1 0	0 0	0 0	0 0	0 0	0 0	0 0	0 0	0 1	0 0	0 0	0 0	0 0	4.5
	0 0	0 3	3 0	5 3	4 6	4 0	4 0	0 0	6 0	0 0	0 0	0 3	4 0	3 8	0 5	4

0 = ABSENT 1 = PRESENT * = PROBABLE DIFF. ANGLE FOR K-BETA RADIATION

TABLE 5.39-B DETAILED ANALYSIS OF PHASE(S) ACTUALLY PRESENT

S.N.	PHASE PRESENT	DIFF ANGLE	PEAK INT	I/IO	D MEAS	D STD	DIFF PLANES	INT STD	CONF LIMIT
(1)	FE5C2(HAGG)	58.3	5	18	1.989	1.980	511	20	99.7
		65.1	28	100	1.802	1.800	312	70	99.9
		101.6	6	22	1.250	1.250	712	20	100.0
(2)	MN5C2(PD5B2)	55.5	100	100	2.080	2.078	510	100	99.9
		57.7	8	8	2.007	2.016	511	80	99.7
		58.3	5	5	1.989	1.990	600	80	100.0
		64.0	7	7	1.829	1.829	402	70	100.0
		64.4	19	19	1.818	1.820	421	70	99.9
		66.0	6	6	1.779	1.779	512	70	100.0
(3)	FE7C3(2)	58.3	5	13	1.989	1.989	300	13	100.0
		61.8	3	10	1.887	1.895	112	5	99.7
		64.4	19	51	1.818	1.820	301	11	99.9
		64.8	37	100	1.808	1.807	022	22	100.0
(4)	CR7C3	48.9	3	11	2.341	2.350	321	20	99.8
		64.7	33	100	1.811	1.810	431	70	100.0
		66.0	6	19	1.779	1.780	521	50	99.9
		98.4	16	50	1.280	1.280	---	60	100.0
(5)	COPPER	55.5	100	100	2.080	2.088	111	100	99.8
		64.8	37	37	1.808	1.808	200	46	100.0
		65.1	28	28	1.802	1.808	200	46	99.8
		98.5	15	15	1.279	1.278	220	20	99.9
(6)	FE8SI2C	49.5	6	6	2.314	2.320	104	40	99.9
		55.5	100	100	2.080	2.070	210	80	99.7
		57.7	8	8	2.007	2.010	322	100	99.9
		58.3	5	5	1.989	1.980	114	60	99.7
		61.8	3	3	1.887	1.880	323	10	99.7
		64.4	19	19	1.818	1.820	015	60	99.9
		64.7	33	33	1.811	1.810	031	20	100.0
		66.0	6	6	1.779	1.780	312	20	99.9
(7)	AUSTENITE	55.5	100	100	2.080	2.080	111	100	100.0
		65.1	11	11	1.802	1.800	200	80	100.0

TABLE 5.40-A: SUMMARY TABLE OF DIFFRACTOGRAM INDEXING

ALLOY : B4
SOAKING TEMPERATURE : 1050°C SOAKING DURATION : 6 HOURS
COOLING MEDIA : AIR COOLED

DIFF. ANGLE	PHASE(S) 1	2	3	4	5	6	7	8	9	10	11	12	13	14	15	16	17	18	19	20	21	22	23	24	25	26	27	28	29	30	INT
48.7	0	0	0	0	0	0	0	0	0	0	0	0	1	0	0	0	0	1	0	0	0	0	0	1	0	0	0	0	1	1	1.5
49.9	0	0	0	0	0	0	1	0	0	0	0	0	0	1	0	0	1	0	0	0	1	0	0	0	0	0	0	0	0	0	1.5
51.0	0	0	0	0	0	1	0	1	0	0	1	0	0	0	0	0	0	0	0	0	0	0	0	0	0	0	0	1	0	0	2.0
55.5	0	1	0	0	0	0	1	0	1	1	0	0	0	0	0	0	0	0	0	0	0	0	0	1	0	1	1	0	0	0	49.5
56.6	0	0	0	1	0	0	0	0	0	0	0	0	1	1	1	0	0	0	0	0	0	1	0	0	0	0	1	0	1	1	2.5
57.1	1	0	0	0	0	0	0	1	1	1	0	0	0	0	0	0	0	0	0	1	0	0	0	1	0	0	0	0	0	0	2.0
57.4	0	0	1	0	0	1	0	0	1	1	1	1	1	0	0	0	0	0	0	0	0	0	0	0	0	0	0	1	0	1	2.5
57.8	0	0	0	0	0	1	1	0	0	0	0	0	0	0	0	0	0	0	0	0	0	0	0	0	0	0	1	0	0	0	3.0
63.8	0	0	0	0	0	0	0	0	1	1	0	0	1	0	0	0	0	0	0	0	1	0	0	0	0	0	1	1	1	0	2.0
64.2	0	0	0	0	0	0	1	0	0	0	1	1	0	0	0	0	0	0	1	0	0	1	0	0	0	0	1	0	0	0	3.5
65.1	0	1	0	1	1	0	0	1	0	0	1	0	0	0	0	0	0	0	0	1	0	0	0	0	0	0	1	0	0	1	39.5
67.4	0	0	0	0	0	0	0	0	0	0	0	0	1	1	0	0	1	0	0	0	0	0	0	0	0	0	1	0	0	0	2.0
68.1	0	0	0	0	0	0	0	0	0	1	0	1	0	0	0	0	0	0	0	0	0	0	0	0	0	0	0	0	0	1	1.5
98.4	0	0	0	0	0	0	0	0	0	0	0	0	1	0	0	0	1	0	0	0	0	0	0	0	0	1	0	0	0	0	11.5
125.0	0	0	0	0	0	0	0	0	0	0	0	0	0	0	0	0	0	0	0	0	0	0	0	0	0	0	0	0	0	0	3.5
125.6	0	0	0	0	0	0	0	1	0	0	0	0	0	0	0	0	0	0	0	0	0	0	0	0	0	1	0	0	0	0	2.0
126.0	0	0	0	0	1	0	0	0	0	0	0	0	0	0	0	0	0	0	0	0	0	1	0	0	0	0	0	0	0	0	2.0
	0	0	0	0	0	3	4	4	4	5	4	3	6	3	0	0	3	0	0	0	0	3	0	3	0	3	7	3	3	5	

0 = ABSENT 1 = PRESENT * = PROBABLE DIFF. ANGLE FOR K-BETA RADIATION

TABLE 5.40-B: DETAILED ANALYSIS OF PHASE(S) ACTUALLY PRESENT

S.N.	PHASE PRESENT	DIFF ANGLE	PEAK INT	I/IO	D MEAS	D STD	DIFF PLANE	INT STD	CONF LIMIT
(1)	FE5C2(HAGG)	51.0	4	5	2.249	2.260	020	50	99.7
		57.1	4	5	2.028	2.030	312	100	99.9
		65.1	79	100	1.800	1.800	312	70	100.0
		125.6	4	5	1.089	1.090	404	20	99.8
(2)	MN5C2(PD5B2)	55.5	100	100	2.080	2.078	510	100	99.9
		57.1	4	4	2.028	2.035	312	70	99.8
		57.4	5	5	2.017	2.016	511	80	100.0
		63.8	4	4	1.833	1.829	402	70	99.8
		68.1	3	3	1.730	1.732	022	80	99.9
(3)	FE7C3(2)	51.0	4	5	2.249	2.255	120	31	99.9
		57.4	5	6	2.017	2.019	121	100	99.9
		64.2	7	8	1.823	1.820	301	11	99.9
		65.1	79	100	1.800	1.807	022	22	99.7
(4)	CR7C3	48.7	3	13	2.348	2.350	321	20	100.0
		56.6	5	21	2.043	2.040	421	100	99.9
		57.4	5	21	2.017	2.020	---	50	99.9
		63.8	4	17	1.833	1.840	601	60	99.7
		67.4	4	17	1.747	1.750	412	70	99.8
		98.4	23	100	1.280	1.280	---	60	100.0
(5)	COPPER	55.5	100	100	2.080	2.088	111	100	99.8
		98.4	23	23	1.280	1.278	220	20	99.8
		125.6	4	4	1.089	1.090	311	17	99.8
(6)	FE8SI2C	55.5	100	100	2.080	2.080	131	80	100.0
		56.6	5	5	2.043	2.050	121	80	99.8
		57.8	6	6	2.005	2.010	322	100	99.8
		63.8	4	4	1.833	1.840	331	60	99.7
		64.2	7	7	1.823	1.820	015	60	99.9
		65.1	79	79	1.800	1.794	015	20	99.7
		67.4	4	4	1.747	1.740	301	20	99.7
(7)	AUSTENITE	55.5	100	100	2.080	2.080	111	100	100.0
		65.1	40	40	1.800	1.800	200	80	100.0

TABLE 5.41-A SUMMARY TABLE OF DIFFRACTOGRAM INDEXING

ALLOY :B4
SOAKING TEMPERATURE :1050 SOAKING DURATION :10
QUENCHING MEDIA :AIR COOLED

DIFF. ANGLE	PHASE(S) 1	3	5	7	9	11	13	15	17	19	21	23	25	27	29	INT
49.9	0	0	0	0	1	0	0	0	1	0	0	1	0	0	0	2.0
55.6	0	1	0	0	1	0	1	1	0	0	1	0	1	1	0	53.5
56.8	1	0	0	0	0	1	1	1	0	0	1	0	0	0	1	2.0
64.8	0	0	0	0	1	0	0	0	1	0	0	0	1	1	0	14.0
65.1	0	1	0	1	0	0	1	0	0	0	1	0	0	0	1	41.0
98.6	0	0	0	0	0	0	0	1	0	0	0	0	1	0	0	3.0
125.9	0	0	0	0	0	0	0	0	0	0	0	1	0	0	0	11.0
126.1	0	0	0	1	0	0	0	0	0	0	0	0	0	0	0	12.0
	0	0	0	0	0	3	0	0	0	3	0	0	0	0	0	

0 = ABSENT 1 = PRESENT * = PROBABLE DIFF. ANGLE FOR K-BETA RADIATION

TABLE 5.41-B DETAILED ANALYSIS OF PHASE(S) ACTUALLY PRESENT

S.N.	PHASE PRSENT	DIFF ANGLE	PEAK INT	I/IO	D MEAS	D STD	DIFF PLANES	INT STD	CONF LIMIT
(1)	FE5C2	49.9	3	3	2.297	2.287	020	20	99.8
		55.6	100	100	2.079	2.080	021	70	100.0
		64.8	26	26	1.808	1.814	312	25	99.8
(2)	CR7C3	56.8	3	14	2.036	2.040	421	100	99.9
		64.8	26	100	1.808	1.810	431	70	99.9
		98.6	5	21	1.277	1.280	---	60	99.7
(3)	(CR,FE)7C3	49.9	3	14	2.297	2.300	141	40	99.9
		56.8	3	14	2.036	2.040	122	100	99.9
		64.8	26	100	1.808	1.810	431	60	99.9
(4)	CR3C2	49.9	3	14	2.297	2.300	211	100	99.9
		64.8	26	100	1.808	1.810	130	30	99.9
		98.6	5	21	1.277	1.280	531	5	99.7
(5)	COPPER	55.6	100	100	2.079	2.088	111	100	99.7
		64.8	26	26	1.808	1.808	200	46	100.0
		98.6	5	5	1.277	1.278	220	20	99.9
(6)	AUSTENITE	55.6	100	100	2.079	2.080	111	100	100.0
		65.1	78	78	1.800	1.800	200	80	100.0

TABLE-5.42 SUMMARY OF X-RAY DIFFRACTOGRAM ANALYSIS

H/T	MATRIX	M23	M3	M5	M7	FE8SI2C	CrMn3	Cu	Cu2S
ALLOY B1									
AS CAST	P/B	S/P	P	P	P				
900, 4, AC	A	P	P	T?	T?	S/T			
900,10, AC	A	P	P	S/T		P	T		
950, 4, AC	A	P	P	S	T?	S/T	T		
950,10, AC	A*	S/T	P	S/T	S/P		T	T/S	
1000, 4, AC	A	P	P	T	S/T	T/S		T	
1000,10, AC	A		T	T	T	T/S			
1050, 4, AC	A*			T	S/P	S			
1050, 6, AC	A*			T?	P	S/P			
1050,10, AC	A*			T?	P	S/P		T/S	
ALLOY B2									
AS CAST	P/B	P	P	P	P	S?			
900, 4, AC	A*	P	P	P	S		S		
900,10, AC	A*	P	P	T/S	S/T		S		
950, 4, AC	A*	T	P	P/S			S/P	S/P	
950,10, AC	A	T	P	P	T/S		S/P	S/P	
1000, 4, AC	A*		S	S/P	T/S	T/S			
1000,10, AC	A*			T	P	S		S/T	
1050, 4, AC	A*			T?	P	P			
1050, 6, AC	A*			S	P			S	
1050,10, AC	A*			S	P			S	
ALLOY B3									
AS CAST	P/B+ M		P	P	P	P			
900, 4, AC	A*	P	P	P	T?		S/T	T?	
900,10, AC	A	P	P	P	T		S/T		
950, 4, AC	A*	T/S	P	P/S			S	T/S	
950,10, AC	A*	S/P	P	P	P		S/P	S/T	
1000, 4, AC	A*		S/T	T	P	S		S/T	
1000,10, AC	A*		S	T	P			S/T	
1050, 4, AC	A*		T	T	P/S	S			
1050, 6, AC	A*			T	P			T/S	
1050,10 ,AC	A*			T?	P			T/S	
ALLOY B4									
AS CAST	α*/B		P	P	S	P			
900, 4, AC	A	P	P	P	P		P/S		
900,10, AC	A*	P	P	P	S	P	T		
950, 4, AC	A	P	P	P	S		S		
950,10, AC	A	S	P	P	S		S/T		
1000, 4, AC	A*	S/T	S	P	P			T	
1000,10, AC	A*			T/P	P	P		S/T	
1050, 4, AC	A*			T/P	P	P		P/S	
1050, 6, AC	A*			T/P	P	P		S	
1050,10, AC	A*			T	P	P		S	

P = PRESENT, S = SOME, T = TRACE, * = PROBABLE

TABLE 5.43 ELEMENT DISTRIBUTION IN MATRIX

Heat treatment : 950°C, 10 hours, AC

Alloy	Fe	C	Si	Cr	Mn	Cu
B1	86.10	2.48	3.50	1.20	4.61	2.11
B2	84.41	2.94	3.15	1.55	5.94	2.02

Heat treatment : 1050°C, 10 hours, AC

Alloy	Fe	C	Si	Cr	Mn	Cu
B1	85.41	2.33	1.78	3.20	5.91	1.37
B2	85.56	1.42	2.43	2.98	7.00	1.69
B3	84.37	1.78	2.07	2.60	5.79	3.19
B4	80.84	1.28	2.07	2.09	8.54	5.19

TABLE 5.44 ELEMENT DISTRIBUTION IN CARBIDE

Heat treatment : 950°C, 10 hours, AC

Alloy	Fe	C	Si	Cr	Mn	Cu
B1	74.57	6.75	0.02	10.11	8.51	0.04
B2	70.93	6.76	0.00	12.06	10.17	0.09
B3	73.48	6.75	0.00	11.56	8.06	0.15
B4	72.56	6.76	0.03	11.02	9.53	0.10

Heat treatment : 1050°C, 10 hours, AC

Alloy	Fe	C	Si	Cr	Mn	Cu
B1	58.72	8.60	0.04	22.95	9.65	0.04
B2	57.63	8.60	0.00	23.30	10.47	0.00
B3	54.60	8.62	0.00	27.02	9.70	0.00
B4	56.87	8.60	0.00	23.83	10.66	0.03

TABLE 5.45 TRANSFORMATION TEMPERATURE, °C

Alloy Desgination	Transformation temperature, °C I	II	III
B1	722	935	---
B2	750	920	1050
B3	745	890	----
B4	735	925	1075

TABLE 5.46 DTA, mV

Alloy Desgination	DTA, mV I	II	III
B1	0.35	-0.52	---
B2	-0.85	-2.15	-0.90
B3	0.20	-0.70	----
B4	-0.90	-2.65	-0.98

Table 5.47 Effect of heating temperature on the %TG

Alloy	Heating temperature, °C										
	RT	100	200	300	400	500	600	700	800	900	1000	1050
B1	0.0	2.5	3.1	3.27	3.27	3.88	4.49	6.48	8.62	12.37	18.11	23.62
B2	0.0	1.52	2.51	2.58	3.03	3.27	4.03	6.15	8.66	13.10	22.66	30.71
B3	0.0	2.31	3.07	3.38	3.53	4.00	4.78	7.07	9.22	14.47	23.07	27.69
B4	0.0	2.15	2.64	2.96	3.22	3.63	4.70	6.93	9.25	13.15	21.78	27.23

Table 5.48 Percent increase in %TG on heating in the different temperature ranges

Alloy	Temperature range										
	I	II	III	IV	V	VI	VII	VIII	IX	X	XI
B1	..	24.0	5.5	0.0	18.6	15.7	44.3	33.0	43.5	46.4	30.4
B2	..	65.1	2.8	17.4	7.9	23.2	52.6	40.8	51.3	73.0	35.5
B3	..	32.9	10.1	4.4	13.3	19.5	47.9	30.4	56.9	59.4	20.0
B4	..	22.8	12.1	8.8	12.7	29.5	47.4	33.5	41.1	66.9	25.0

Table 6.1 Polarization curve data

h/t schedule	Ecorr (ref.) mV	Ecorr mV I	Ecorr mV II	Icorr µA	Icorr µA/SQ.CM
B1, 950,10,AC	-0.645	-0.830	-0.655	225	160
1050,10,AC	-0.542	-0.540	-0.400*	220	124
B2 900,10,AC	-0.644	-0.625	-----	190	170
950,10,AC	-0.609	-0.920	-0.650	190	181
1000,10,AC	-0.570	-0.620	------	130	112
1050, 4,AC	-0.600	-0.885	-0.610	295	154
1050,10,AC	-0.386	-0.580	-0.435*	64	107
B3 950,10,AC	-0.632	-0.925	-0.645	182	198
1050, 4,AC	-0.590	-0.715	-0.650*	230	149
1050,10,AC	-0.487	-0.530	------	210	132
B4 900,10,AC	-0.573	-0.580	------	120	182
950,10,AC	-0.600	-0.870	-0.625	170	172
1000,10,AC	-0.573	-0.580	------	270	121
1050, 4,AC	-0.624	-0.710	-0.660*	280	167
1050,10,AC	-0.543	-0.550	------	185	111
KC	-0.390	-0.570	-0.360*	48	68
KC1	-0.350	-0.520	-0.350*	88	95

Note: Ecorr corresponding to II denotes second distinct peak and * represents a change in the slope (probable reduction process).

Table 6.2 Summary table of I_{corr}

h/t schedule	B1	B2	B3	B4
900,10,AC	---	170	--	162
950,10,AC	160	181	198	172
1000,10,AC	---	112	---	121
1050, 4,AC	---	154	149	167
1050,10,AC	124	107	132	111

Table 6.3 Summary table of E_{corr} (ref.)

h/t schedule	B1	B2	B3	B4
900,10,AC	-----	-0.644	-----	-0.593
950,10,AC	-0.645	-0.609	-0.632	-0.629
1000,10,AC	------	-0.570	------	-0.573
1050, 4,AC	------	-0.600	-0.590	-0.624
1050,10,AC	-0.542	-0.426	-0.487	-0.543

Table 6.4 Summary table of compressive strength and hardness

Alloy B1

H/T schedule	hardness	CSexp.	Rexp.	Rpred.	CSpred.	%error
AS-CAST	594	1972.08	3.32	3.33	1975.66	- 0.18
900, 4,OQ	486	2008.08	4.13	4.29	2084.24	- 3.84
900,10,OQ	530	2091.73	3.94	3.79	2006.94	3.89
950, 4,OQ	481	2094.34	4.35	4.36	2094.82	- 0.12
950,10,OQ	476	2022.91	4.25	4.42	2105.67	- 4.09
1000, 4,OQ	433	2305.35	5.32	5.09	2205.46	4.26
1000,10,OQ	349	2444.66	7.00	6.82	2379.34	2.61
1050, 4,OQ	363	2350.58	6.47	6.49	2356.61	- 0.34
1050, 6,OQ	307	2337.40	7.61	7.89	2420.97	- 3.63
1050,10,OQ	272	2450.40	9.00	8.88	2415.68	1.32

Table 6.5 Summary table of compressive strength and hardness

Alloy B2

H/T schedule	hardness	CSexp.	Rexp.	Rpred.	CSpred.	%error
AS-CAST	590	2116.22	3.58	3.64	2145.72	- 1.59
900, 4,OQ	499	2083.67	4.16	4.30	2144.50	- 3.31
900,10,OQ	496	2132.18	4.30	4.34	2152.97	- 0.95
950, 4,OQ	457	2400.95	5.25	5.02	2296.06	4.30
950,10,OQ	446	2464.66	5.52	5.26	2345.30	4.74
1000, 4,OQ	386	2747.53	7.12	6.86	2647.23	3.68
1000,10,OQ	339	2886.49	8.51	8.49	2878.36	0.23
1050, 4,OQ	332	2647.93	7.97	8.76	2909.13	- 9.94
1050, 6,OQ	342	2756.52	8.06	8.38	2864.79	- 3.93
1050,10,OQ	289	3218.40	11.17	10.59	3061.57	5.16

CS in MN/m^2

Table 6.6 **Summary table of compressive strength and hardness**

Alloy B3

H/T schedule	hardness	CSexp.	Rexp.	Rpred.	CSpred.	%error
AS-CAST	652	2253.03	3.45	3.51	2287.79	- 1.71
900, 4,OQ	486	2175.03	4.47	4.60	2234.76	- 2.87
900,10,OQ	487	2228.90	4.58	4.58	2232.28	- 0.08
950, 4,OQ	455	2434.43	5.33	5.10	2318.86	4.38
950,10,OQ	463	2353.39	5.08	4.96	2296.00	2.38
1000, 4,OQ	383	2533.79	6.62	6.61	2532.07	0.13
1000,10,OQ	349	2779.35	7.96	7.50	2617.63	5.77
1050, 4,OQ	307	2416.63	7.87	8.75	2687.12	-11.22
1050, 6,OQ	272	2559.21	9.41	9.93	2700.03	- 5.49
1050,10,OQ	245	2863.30	11.68	10.91	2673.65	6.57

Table 6.7 **Summary table of compressive strength and hardness**

Alloy B4

H/T schedule	hardness	CSexp.	Rexp.	Rpred.	CSpred.	%error
AS-CAST	621	2352.37	3.79	3.79	2355.24	- 0.07
900, 4,OQ	476	2219.33	4.66	4.71	2241.34	- 1.05
900,10,OQ	476	2287.96	4.81	4.71	2241.34	2.11
950, 4,OQ	441	2340.50	5.31	5.33	2349.23	- 0.32
950,10,OQ	444	2297.35	5.11	5.27	2338.99	- 3.09
1000, 4,OQ	375	2682.59	7.15	6.91	2592.52	3.31
1000,10,OQ	347	2845.30	8.20	7.75	2690.06	5.46
1050, 4,OQ	322	2552.70	7.92	8.58	2764.35	- 8.40
1050, 6,OQ	306	2772.33	9.06	9.16	2902.70	- 1.09
1050,10,OQ	266	2909.22	10.94	10.74	2855.77	1.86

CS in MN/m^2

Table 6.8 **Summary table of %strain and hardness**

Alloy B1

H/T schedule	hardness	%Sexp.	Rexp.	Rpred.	%Spred.	%error
AS-CAST	594	28.66	.105	.097	26.62	- 7.15
900, 4,OQ	486	25.98	.084	.087	26.88	- 3.45
900,10,OQ	530	24.60	.070	.075	26.44	- 7.47
950, 4,OQ	481	23.87	.065	.071	26.12	- 9.42
950,10,OQ	476	23.47	.054	.053	23.35	.49
1000, 4,OQ	433	21.18	.044	.043	20.79	1.84
1000,10,OQ	349	21.00	.043	.042	20.46	2.59
1050, 4,OQ	363	21.96	.045	.041	20.11	8.42
1050, 6,OQ	307	20.56	.038	.031	16.79	18.33
1050,10,OQ	272	7.39	.012	.018	11.12	-50.54

Table 6.9 **Summary table of %strain and hardness**

Alloy B2

H/T schedule	hardness	%Sexp.	Rexp.	Rpred.	%Spred.	%error
AS-CAST	590	42.68	.147	.137	39.86	6.60
900, 4,OQ	499	38.67	.116	.112	37.36	3.39
900,10,OQ	496	32.07	.094	.108	36.84	-14.89
950, 4,OQ	457	35.97	.105	.107	36.62	-1.79
950,10,OQ	446	29.22	.075	.084	32.80	-12.25
1000, 4,OQ	386	28.63	.064	.060	26.76	6.51
1000,10,OQ	339	28.38	.062	.056	25.63	9.69
1050, 4,OQ	332	23.58	.048	.044	21.71	7.94
1050, 6,OQ	342	22.43	.044	.043	21.42	4.51
1050,10,OQ	289	11.79	.020	.024	14.42	-22.29

Table 6.10 **Summary table of %strain and hardness**

Alloy B3

H/T schedule	hardness	%Sexp.	Rexp.	Rpred.	%Spred.	%error
AS-CAST	652	30.14	.143	.138	33.87	3.60
900, 4,OQ	486	31.54	.116	.124	33.80	- 7.17
900,10,OQ	487	33.91	.110	.107	32.95	2.82
950, 4,OQ	455	31.28	.090	.089	30.98	0.96
950,10,OQ	463	28.07	.073	.075	28.79	- 2.55
1000, 4,OQ	383	22.58	.050	.051	22.98	- 1.74
1000,10,OQ	349	22.17	.048	.048	22.27	- 0.47
1050, 4,OQ	307	20.41	.042	.042	20.22	0.90
1050, 6,OQ	272	21.25	.044	.041	20.14	5.22
1050,10,OQ	245	7.47	.011	.012	7.81	- 4.55

Table 6.11 **Summary table of %strain and hardness**

Alloy B4

H/T schedule	hardness	%Sexp.	Rexp.	Rpred.	%Spred.	%error
AS-CAST	621	34.81	.130	.130	34.67	0.38
900, 4,OQ	476	34.48	.112	.113	34.75	- 0.76
900,10,OQ	476	35.80	.111	.107	34.50	3.63
950, 4,OQ	441	31.79	.091	.097	33.83	- 6.42
950,10,OQ	444	30.90	.082	.087	32.71	- 5.85
1000, 4,OQ	375	28.10	.063	.065	28.75	- 2.31
1000,10,OQ	347	28.43	.064	.064	28.53	- 0.36
1050, 4,OQ	322	28.31	.059	.054	26.07	7.92
1050, 6,OQ	306	27.25	.057	.054	26.07	4.35
1050,10,OQ	266	12.01	.019	.020	12.92	- 7.60

Table 6.12 Summary table of the predicted and experimentally determined compressive strength and %strain values (based on Eqs. 6.45-6.48)

H/T schedule	CS pred.	CS exp.	%dev.	%strain pred.	%strain exp.	%dev.
B1, 900,10,AC	2308.84	2579.29	-11.71	22.73	31.13	-36.96
B1, 950, 4,AC	2370.75	2240.73	5.48	23.79	14.13	40.60
B2, 900, 10,AC	2102.70	2607.47	-24.01	23.25	21.73	6.54
B2,1050,10,AC*	3218.40	1260.02	60.85	42.68	12.22	71.37
B3, 900, 4,AC	2266.29	2393.89	-5.63	21.29	20.48	3.82
B3, 900,10,AC	2381.60	1706.41	28.35	22.69	22.82	-.55
B3, 950, 4,AC	2665.00	3167.60	-18.86	24.82	34.30	-38.19
B3, 950,10,AC*	2484.12	1228.24	50.56	23.41	14.14	39.59
B3,1000, 4,AC	2793.64	2581.28	7.60	30.93	36.89	-19.28
B3,1000,10,AC*	2857.64	1658.31	41.97	32.18	18.98	41.01
B3,1050, 4,AC*	2864.68	693.27	75.80	40.20	16.02	60.15
B3,1050,10,AC*	3048.48	979.54	67.87	37.44	25.85	30.95
B4, 950, 4,AC	2485.08	1844.97	25.76	29.82	20.93	29.81
B4, 950,10,AC	2273.95	1849.45	18.67	28.49	30.25	-6.17
B4,1000, 4,AC*	2752.75	1610.61	41.49	31.72	23.72	25.22
B4,1050, 4,AC*	2597.76	1349.73	48.04	36.47	19.81	45.68

CS in MN/m^2

* Experiment revealed either the presence of inclusions inside the specimen or voids.

Fig. 4.2 Effect of h/t time on hardness as influenced by h/t temperature (comparative plots)

(a) 800 deg.C

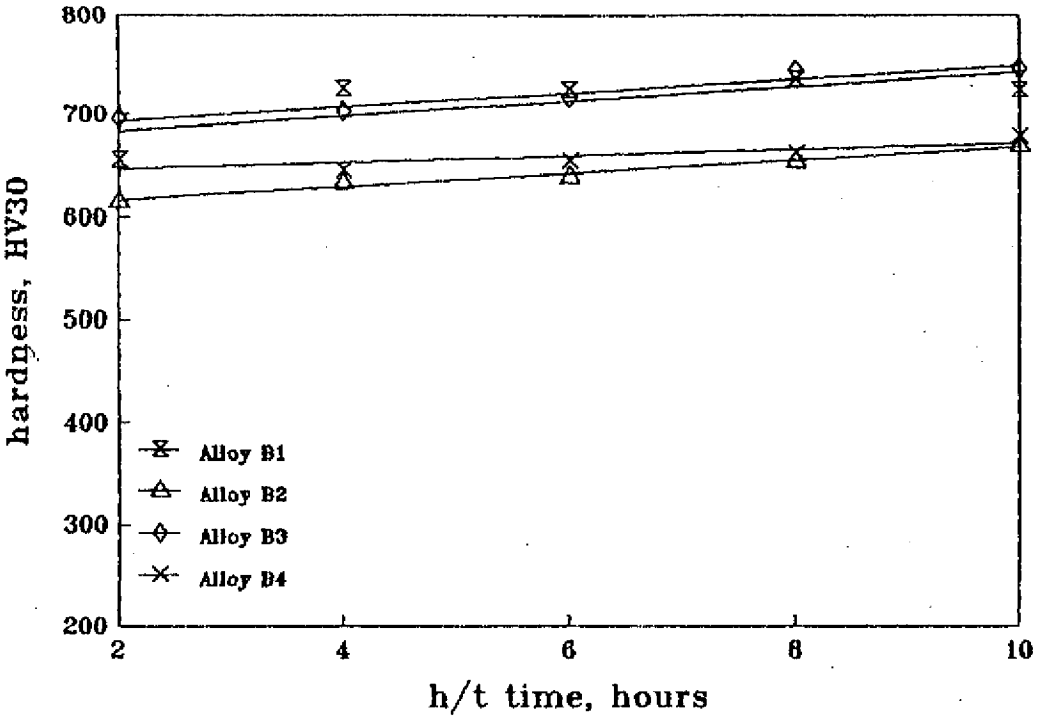

(b) 850 deg.C

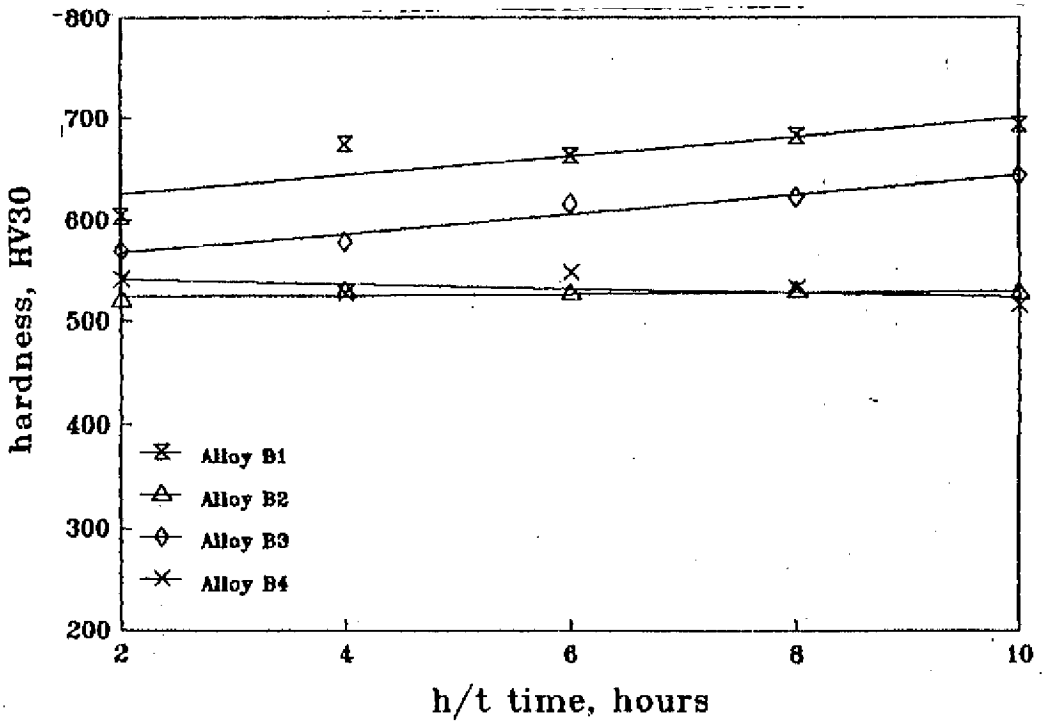

(c) 900 deg.C

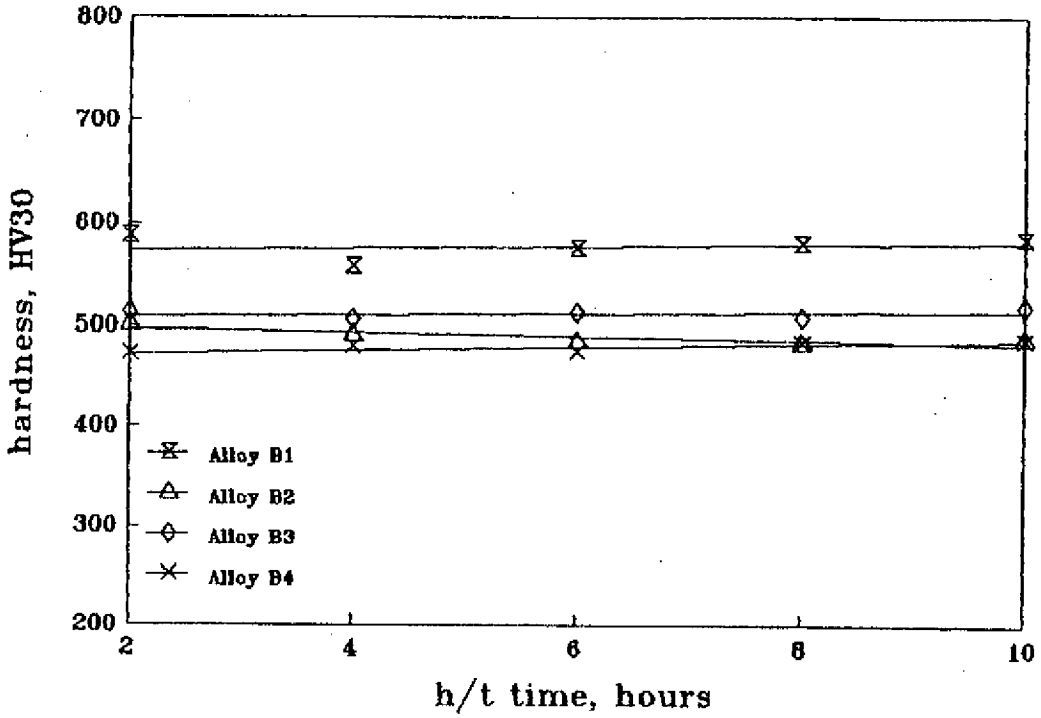

(d) 950 deg.C

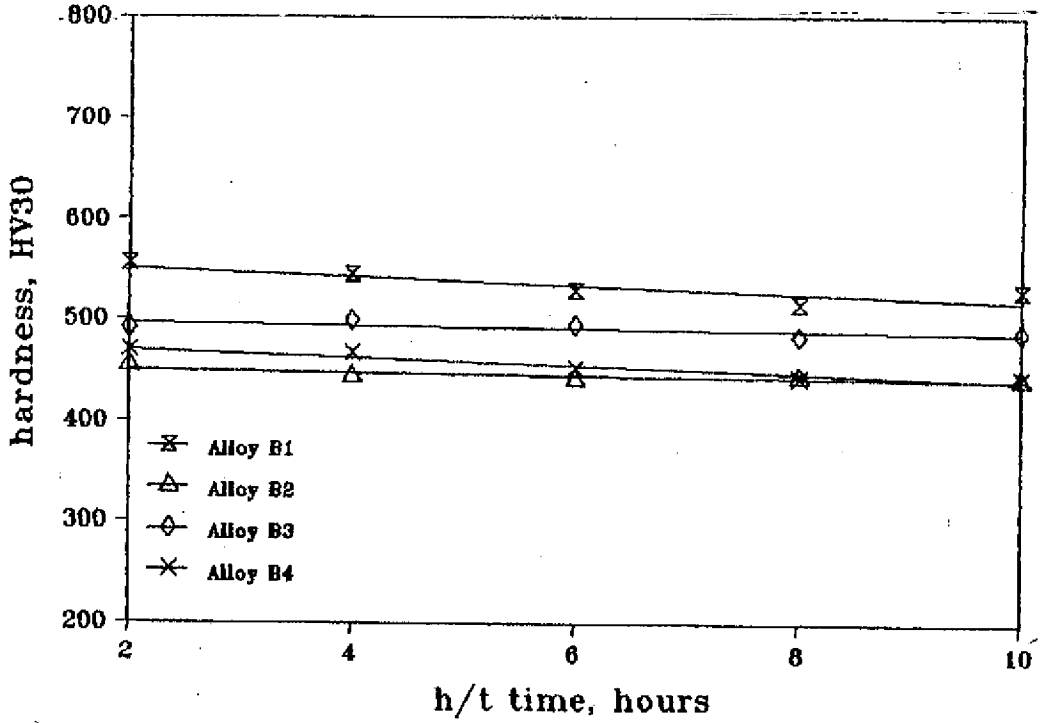

Fig. 4.3 Effect of h/t temperature on hardness as influenced by h/t time

(a) Alloy B1

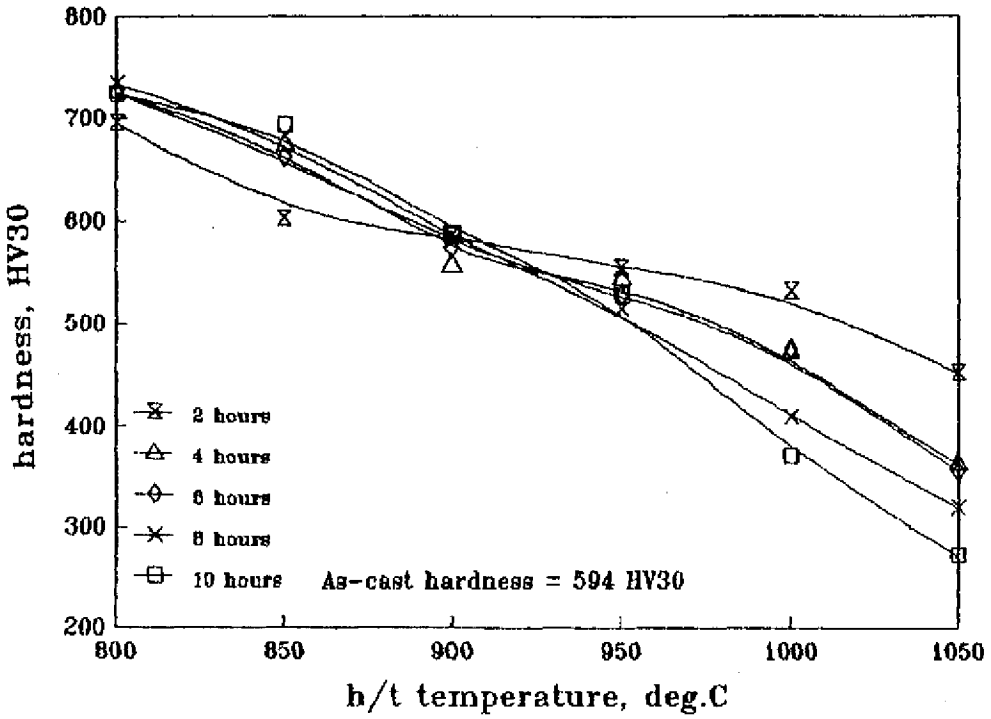

(b) Alloy B2

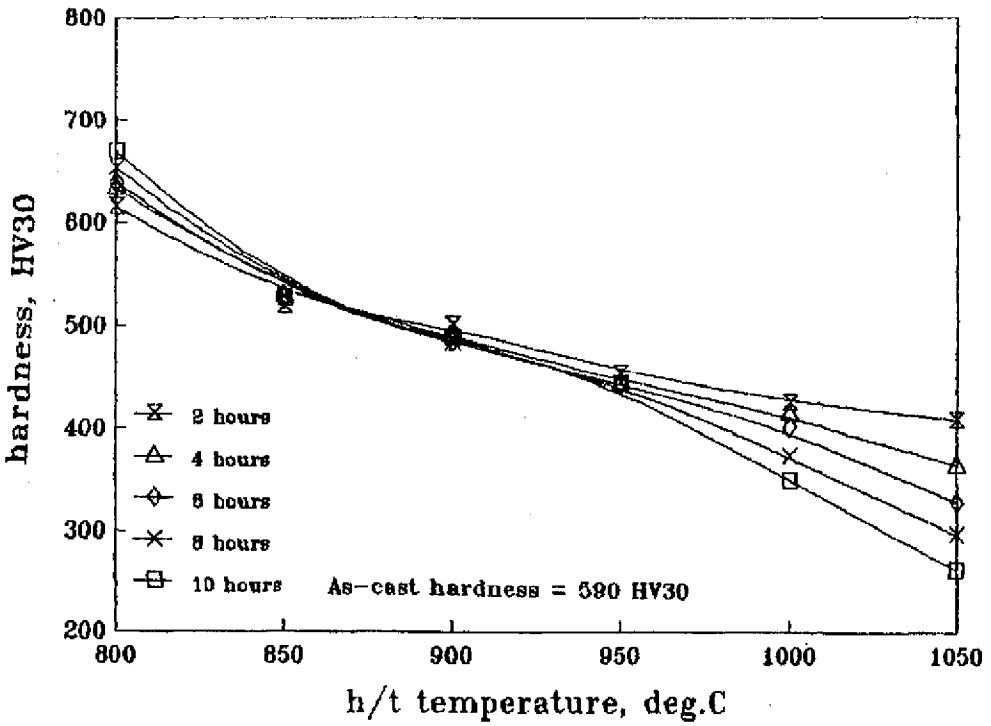

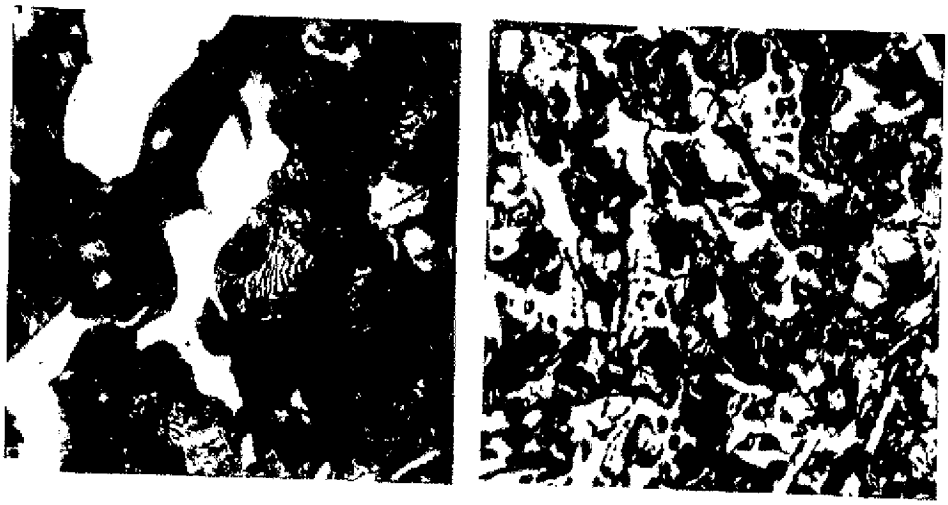

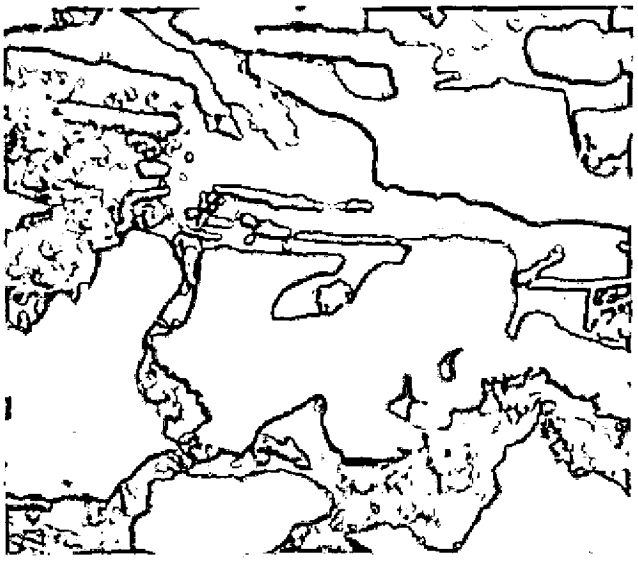

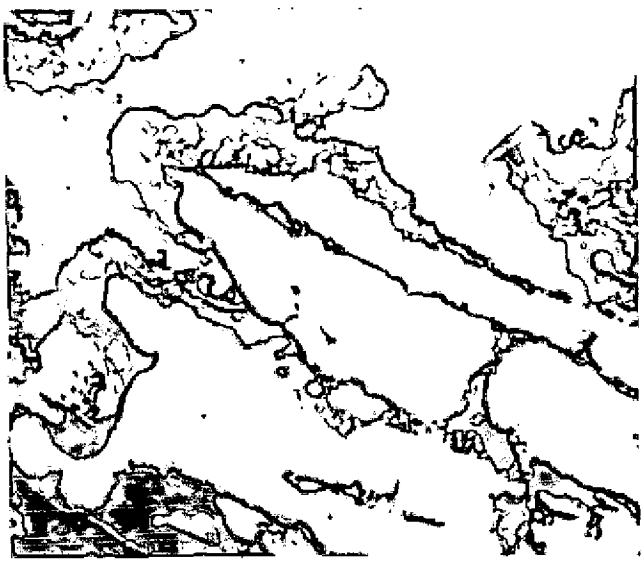

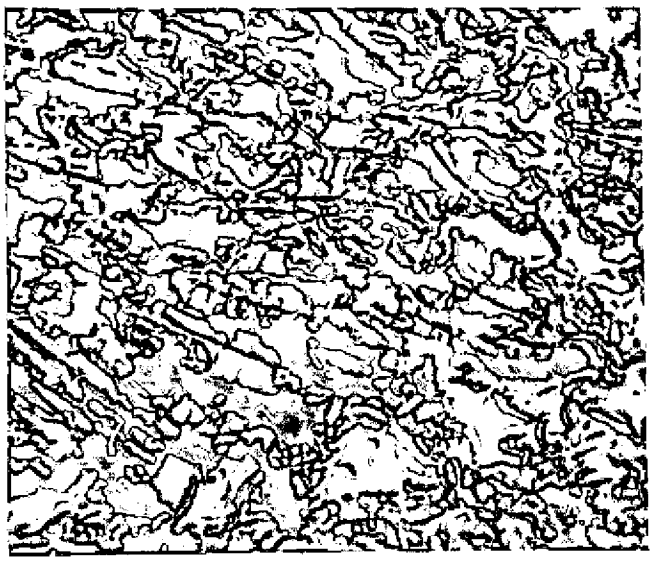

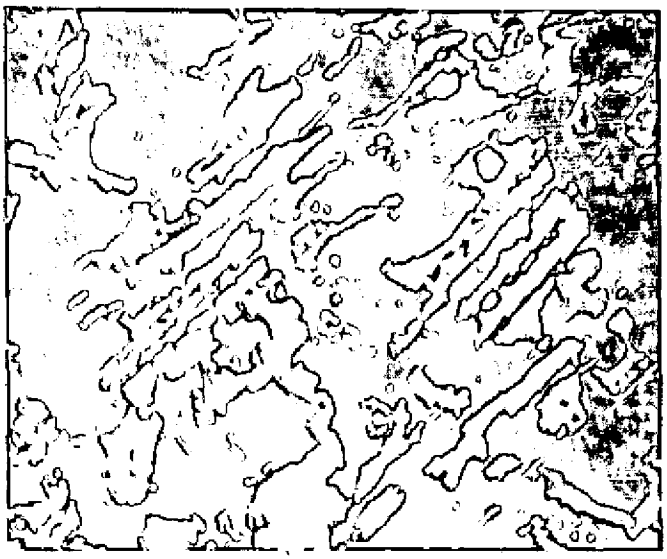

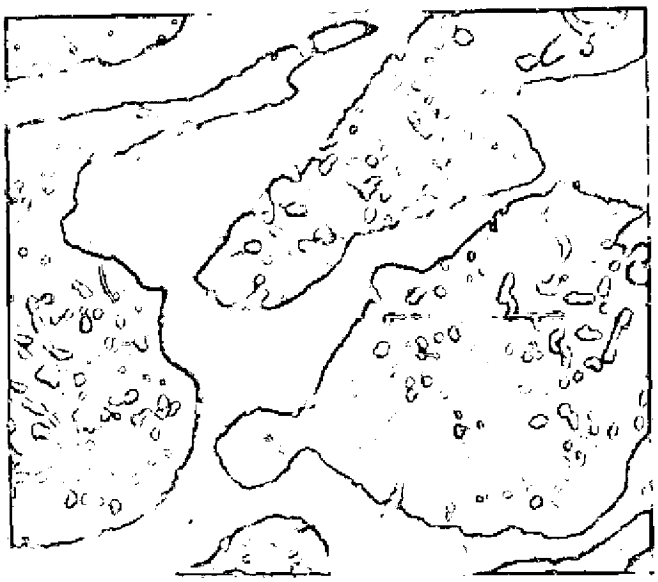

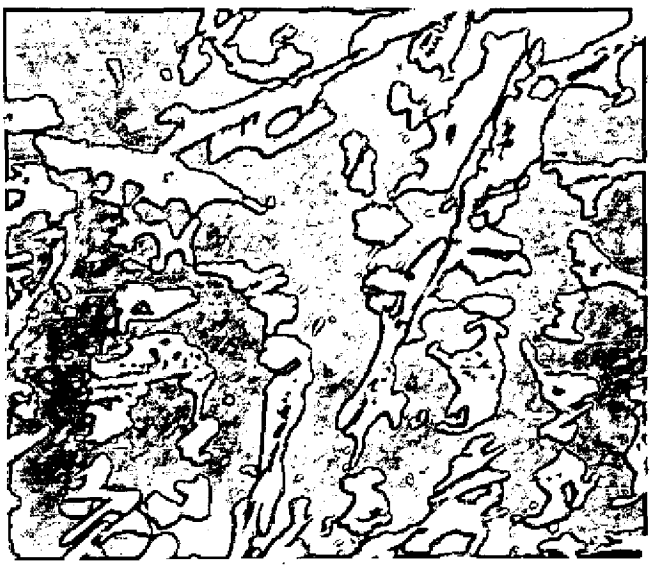

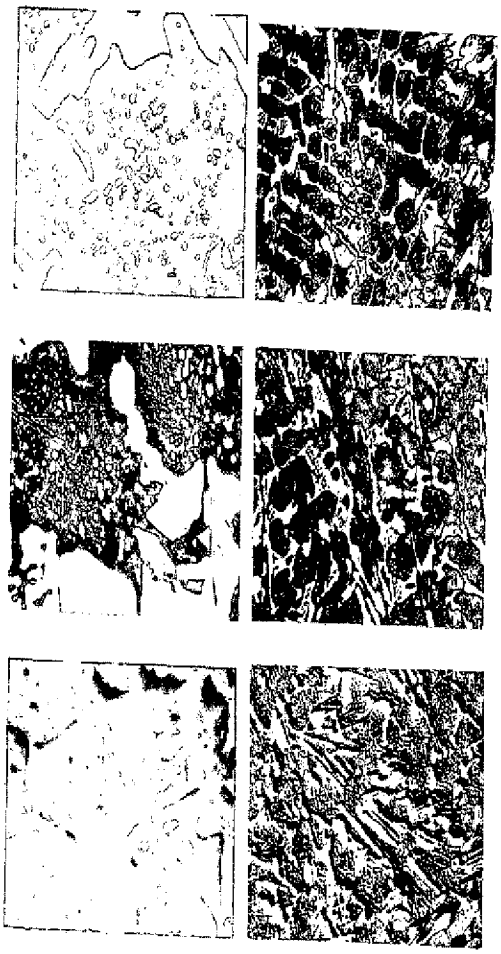

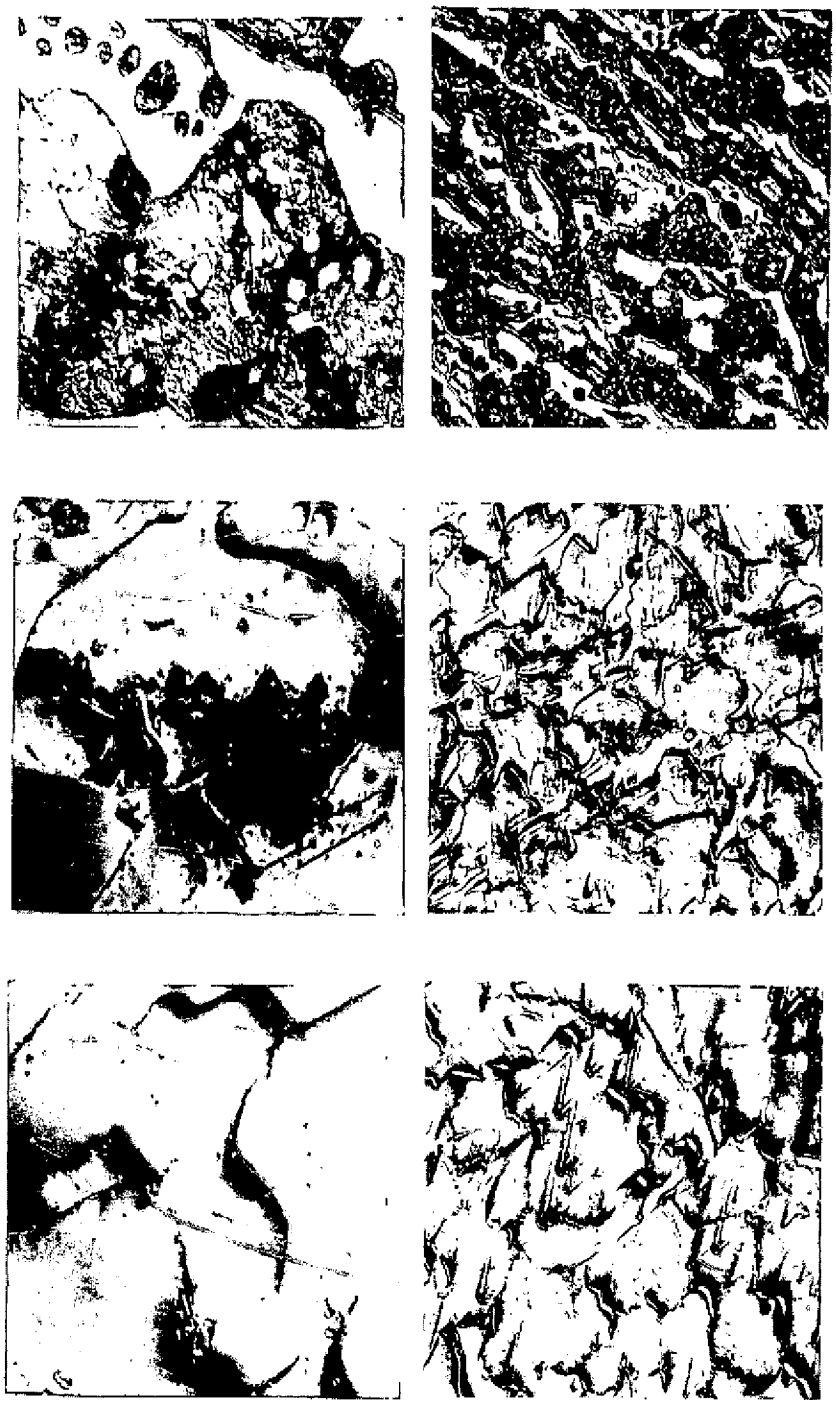

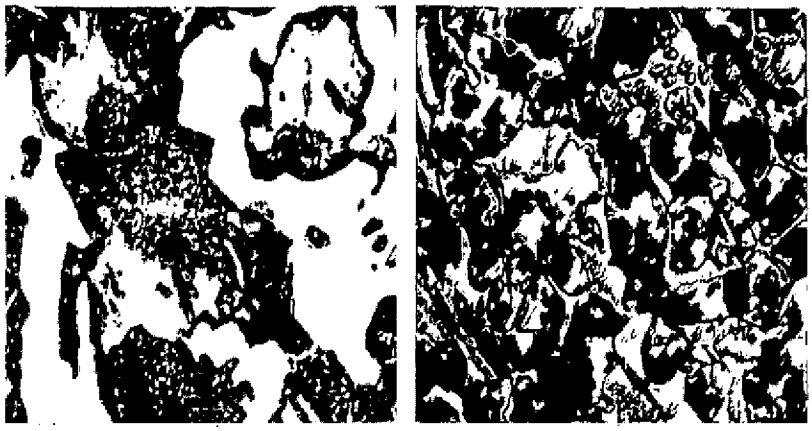

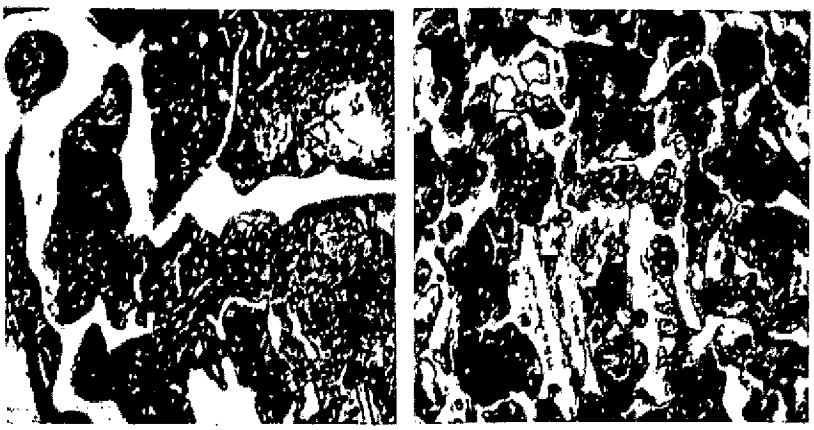

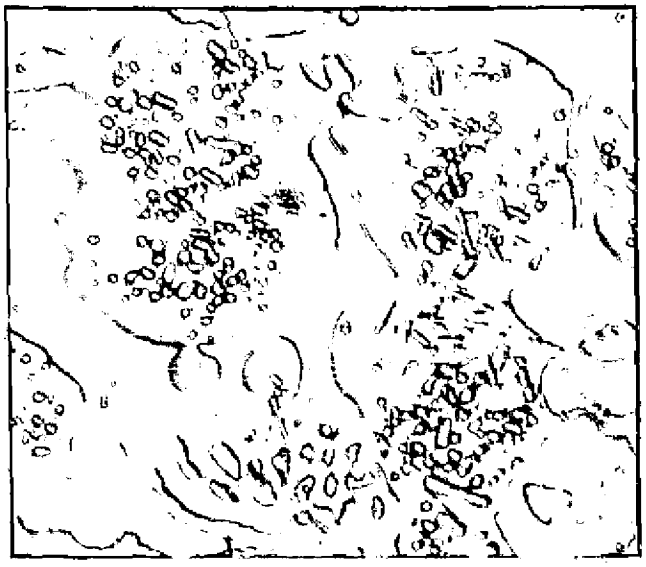

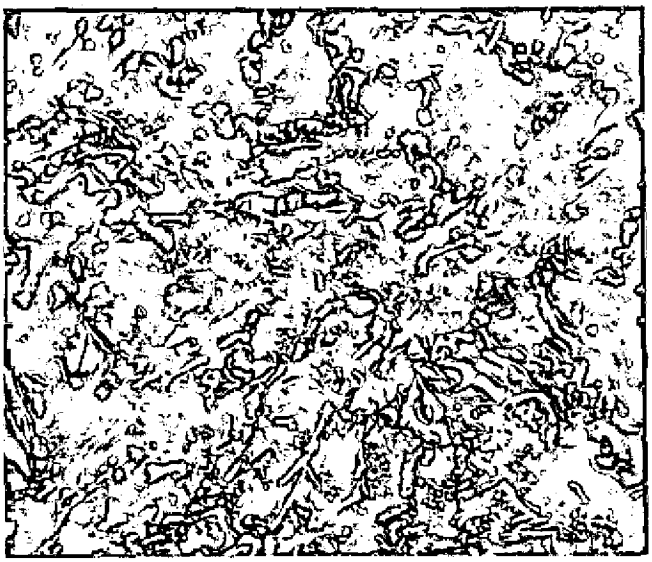

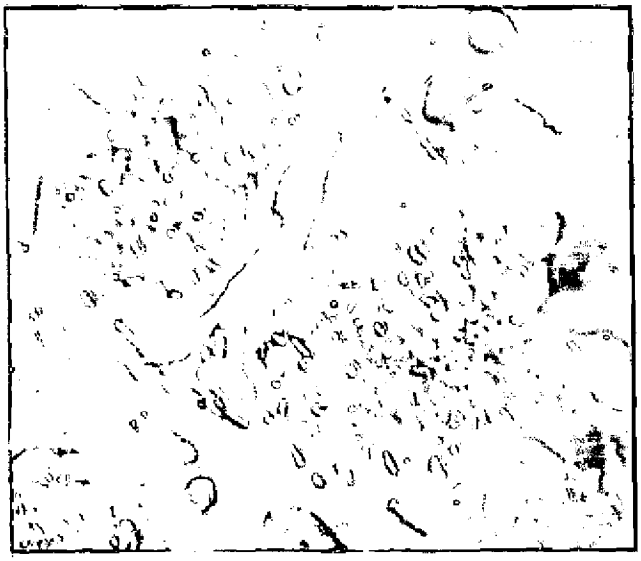

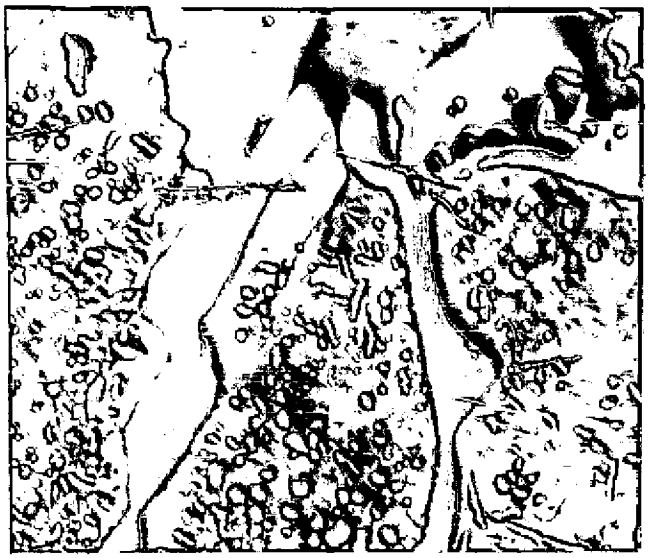

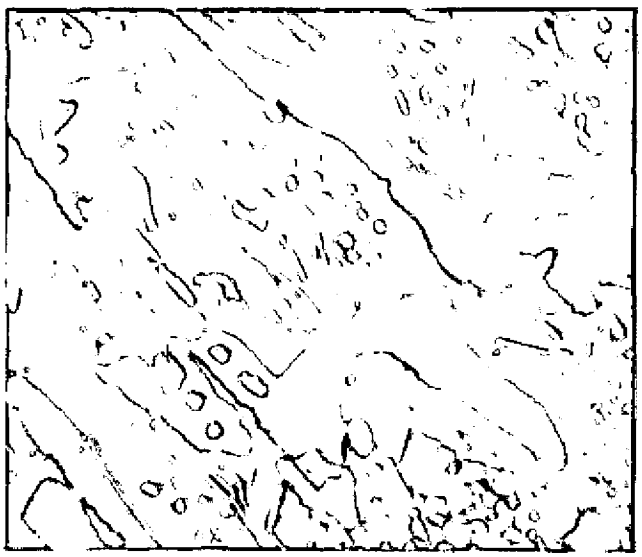

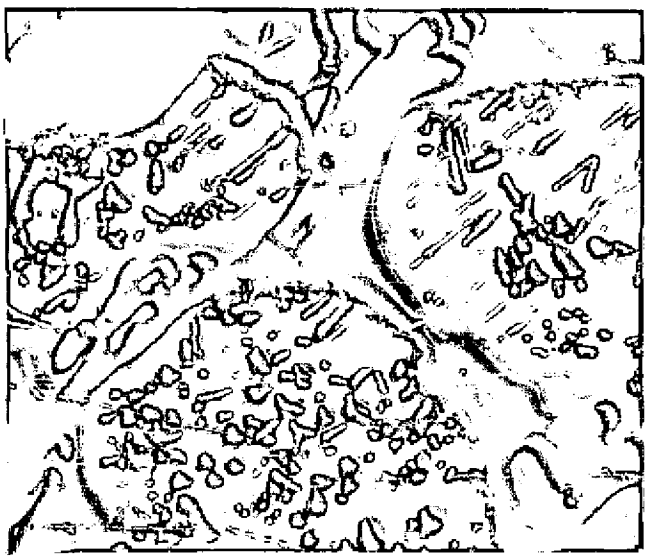

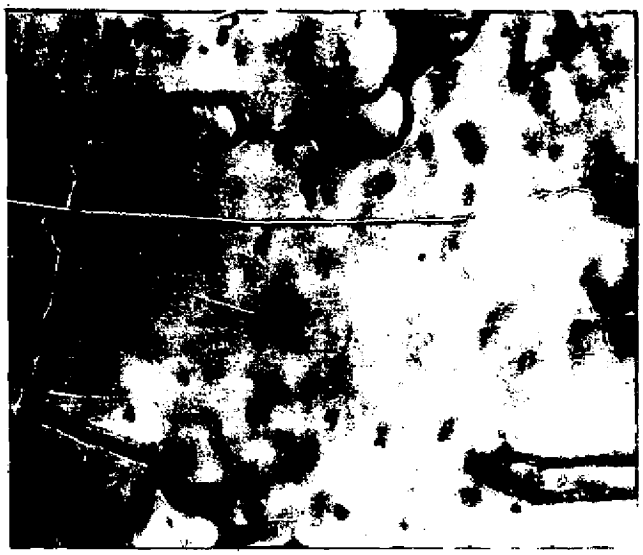

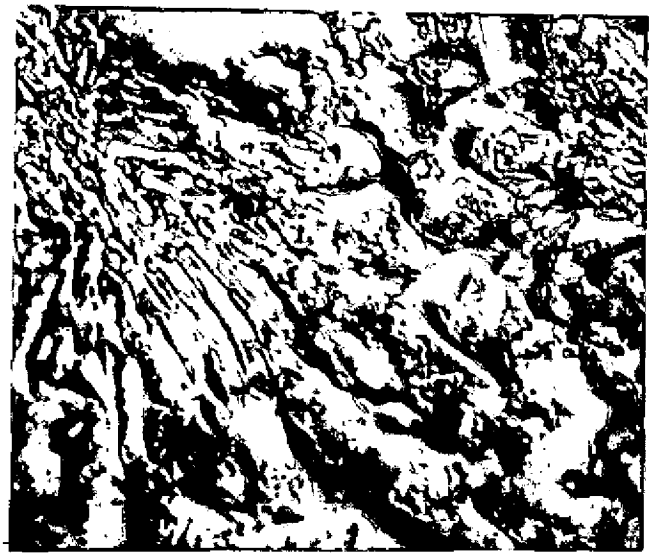

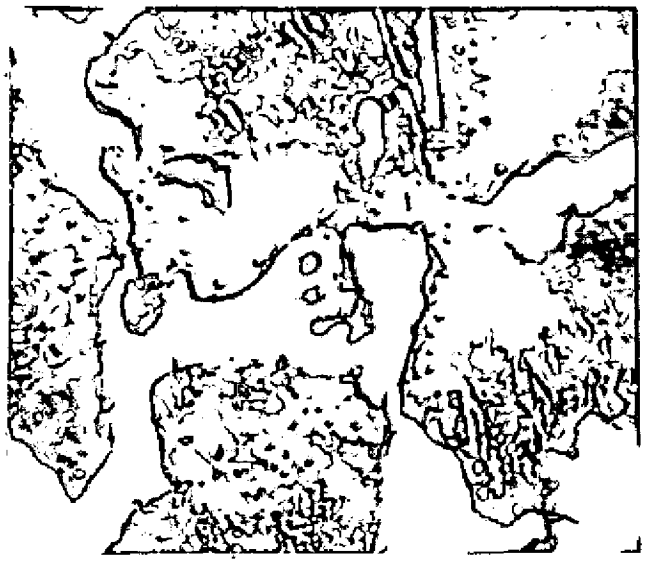

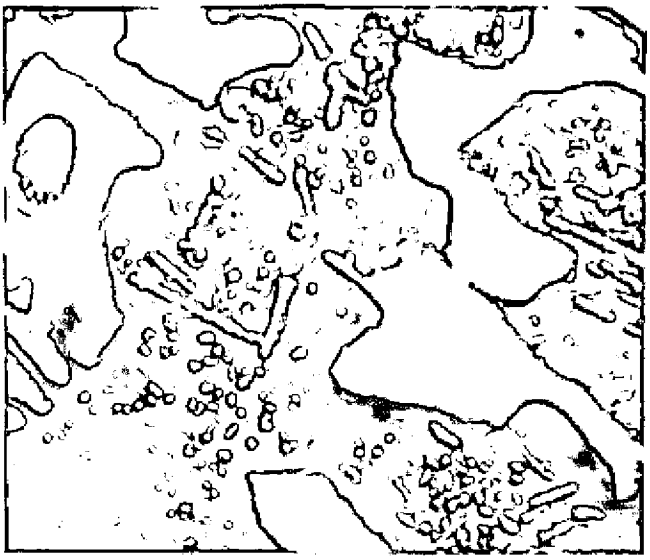

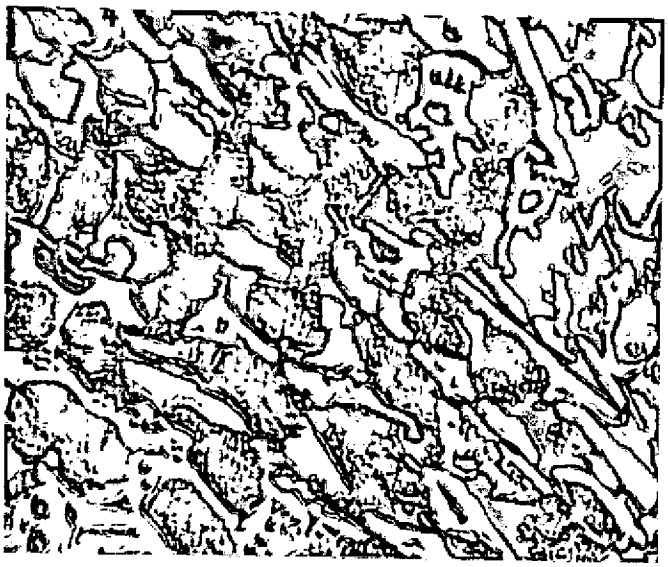

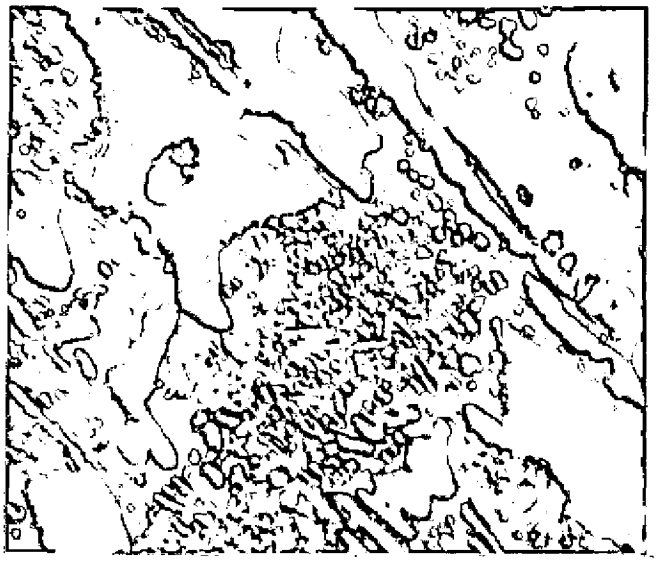

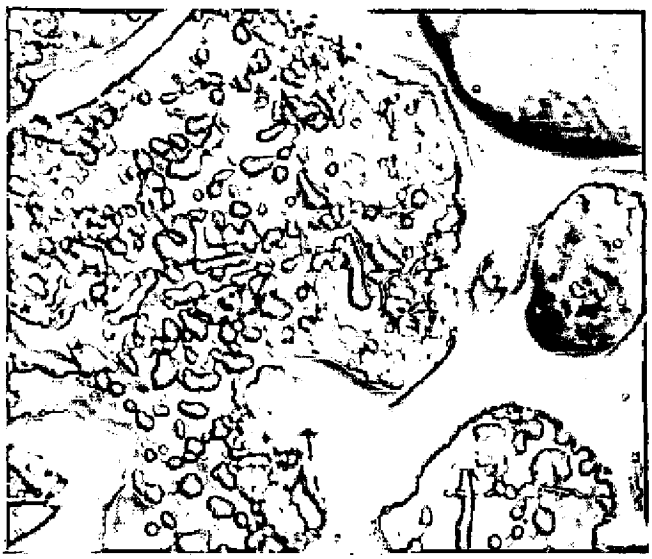

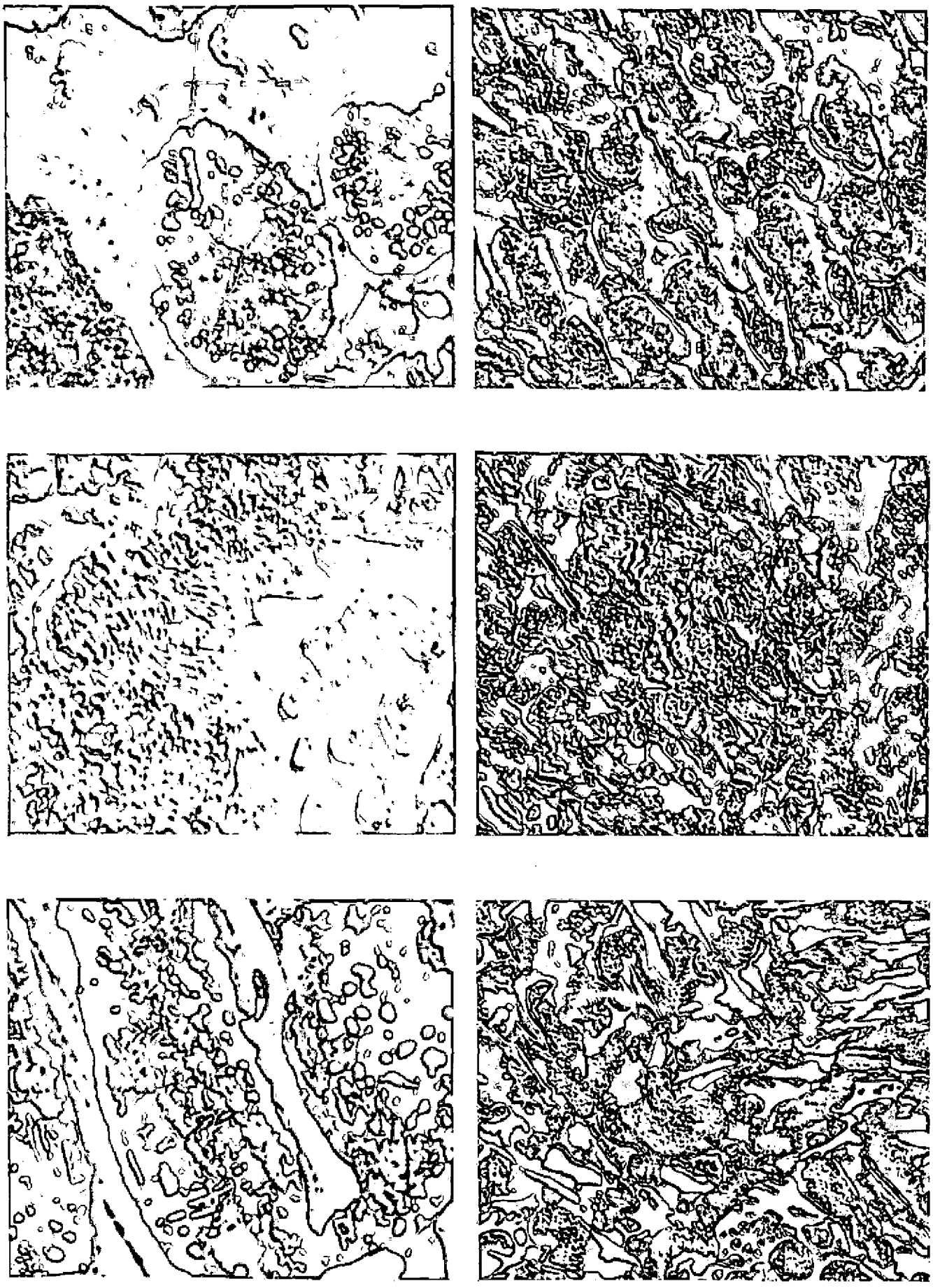

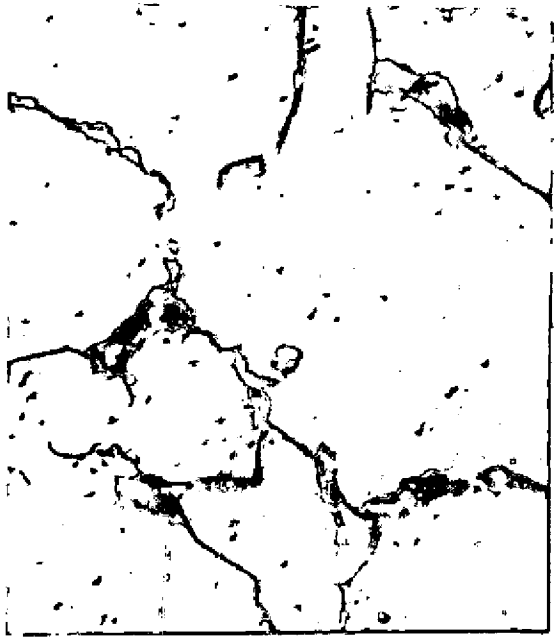




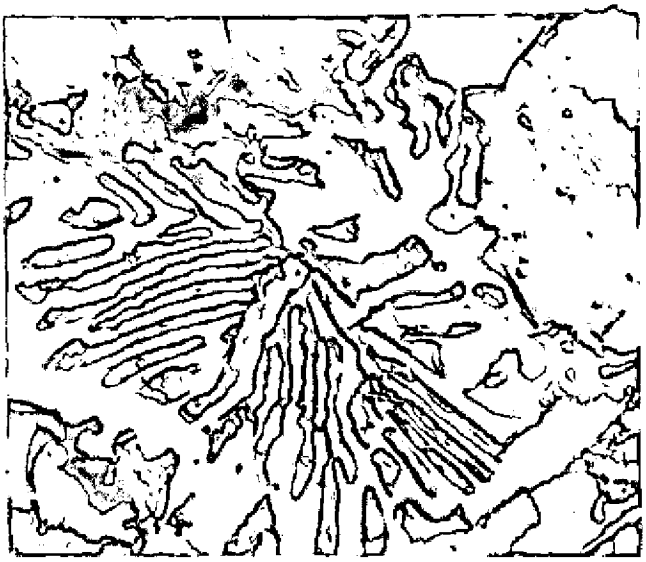

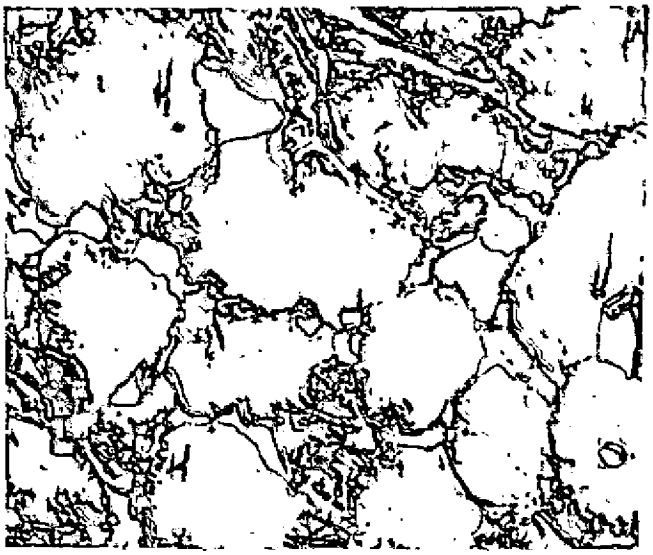

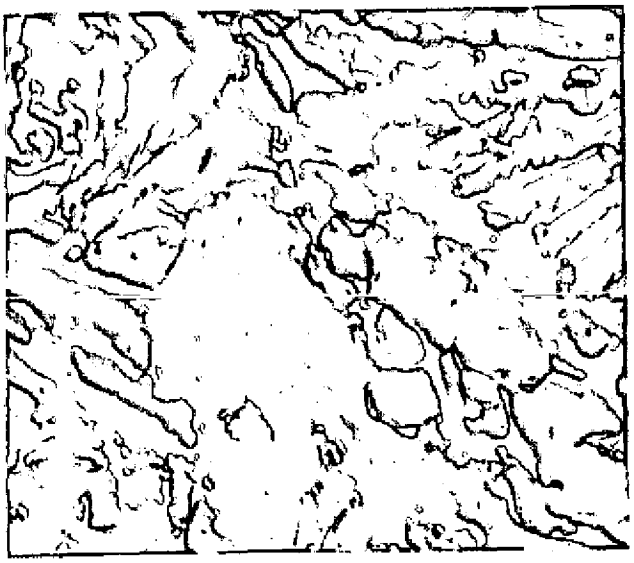

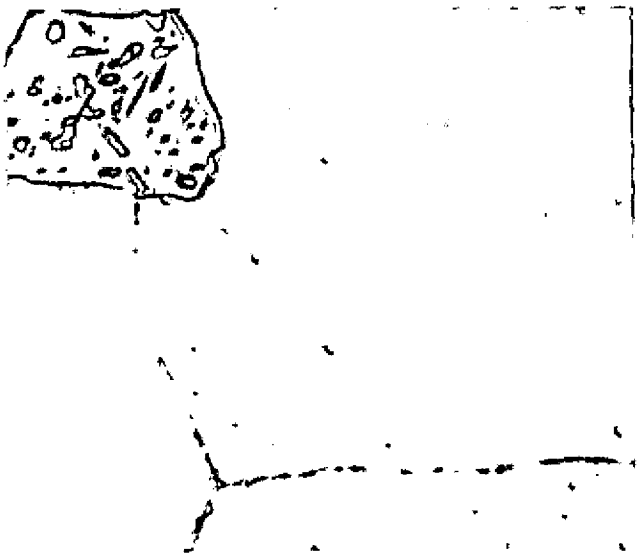

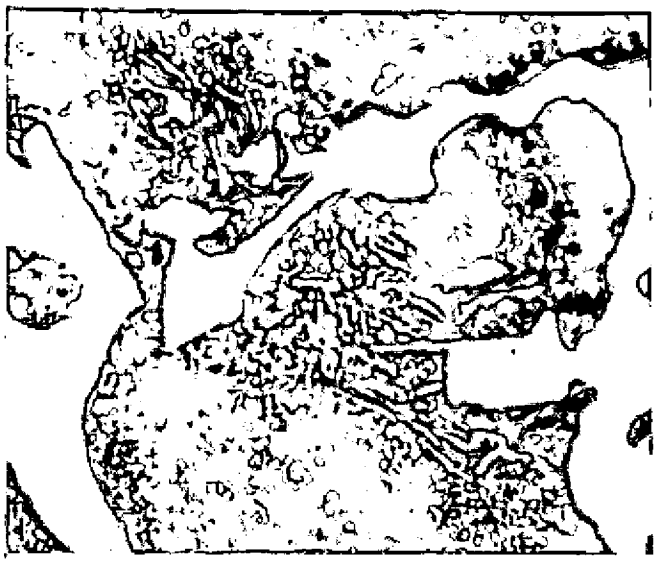

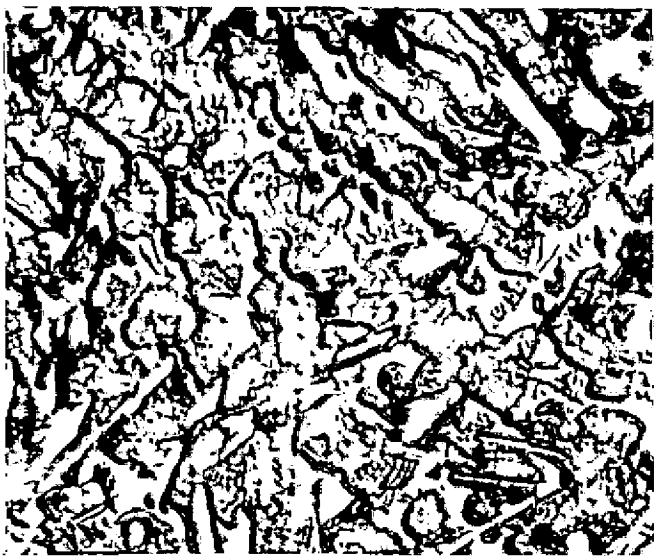

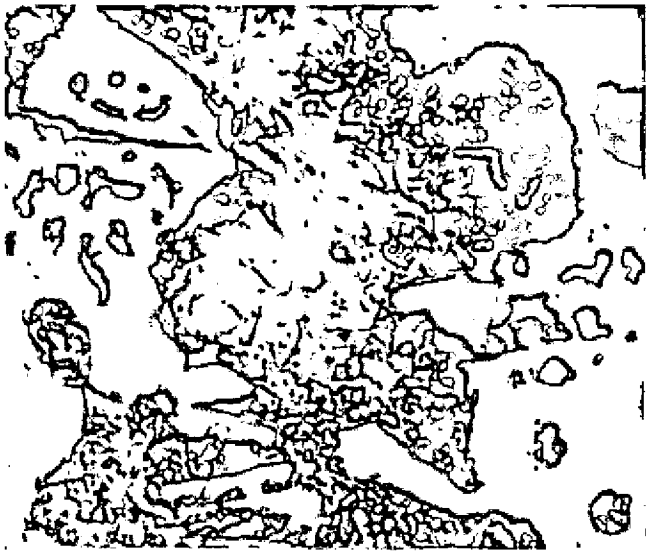

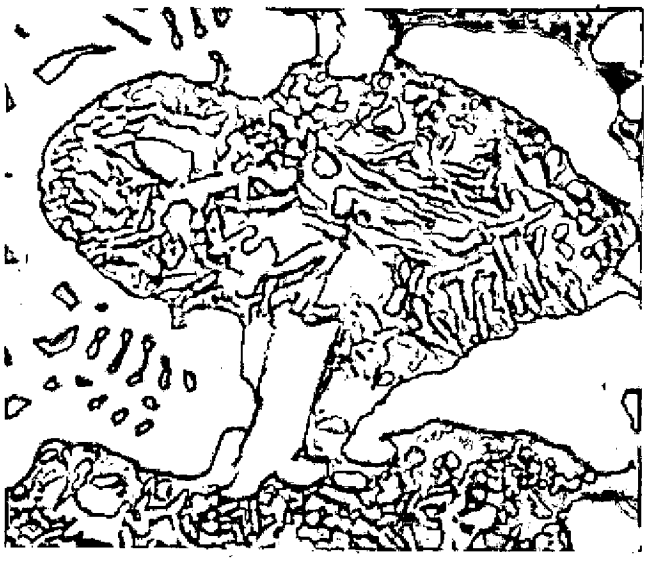

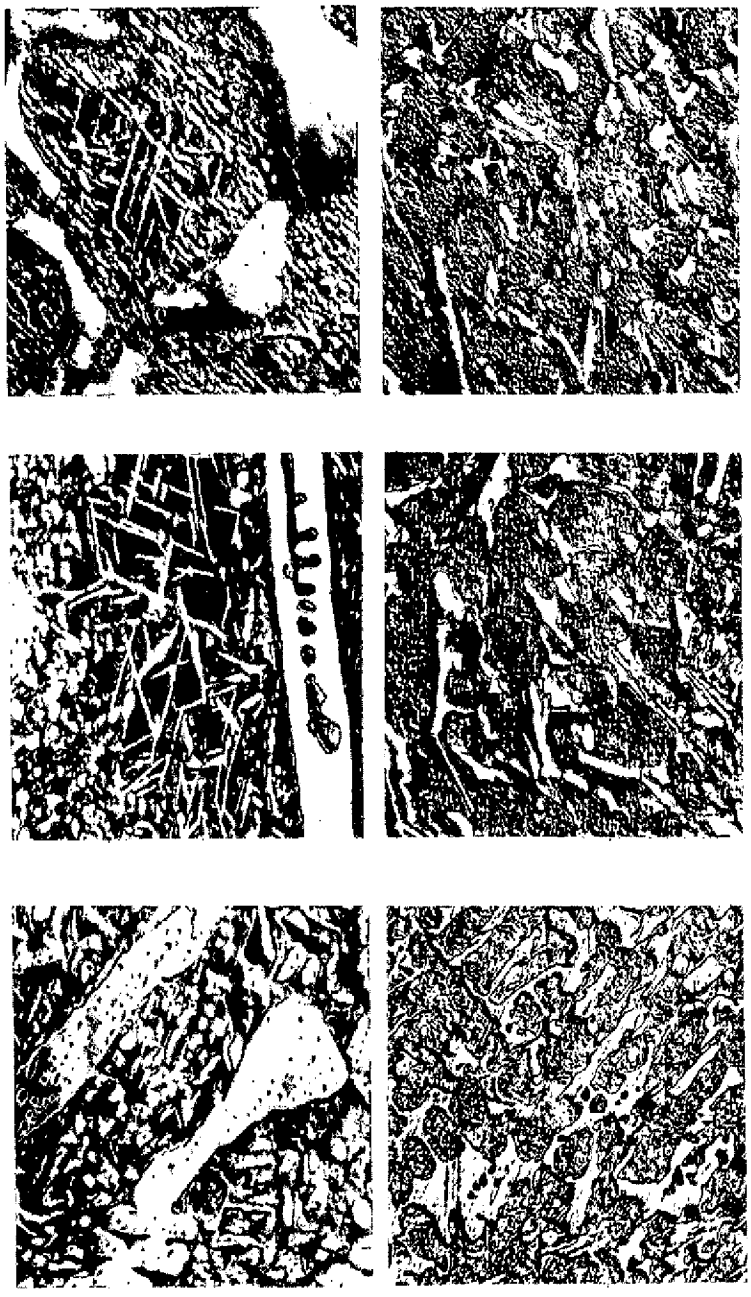

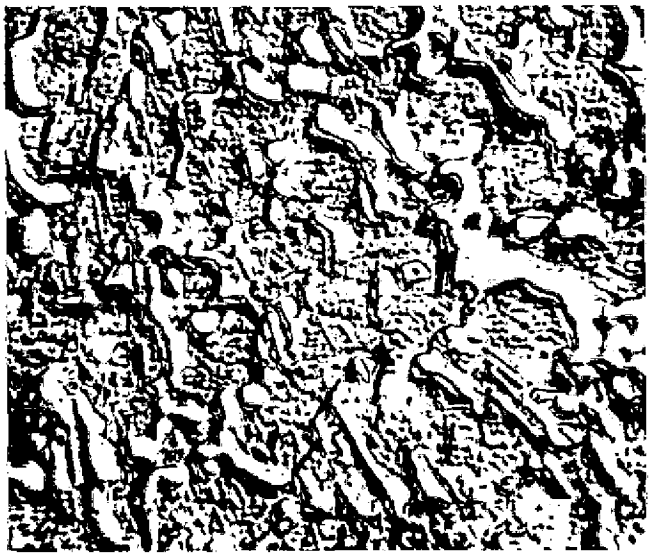

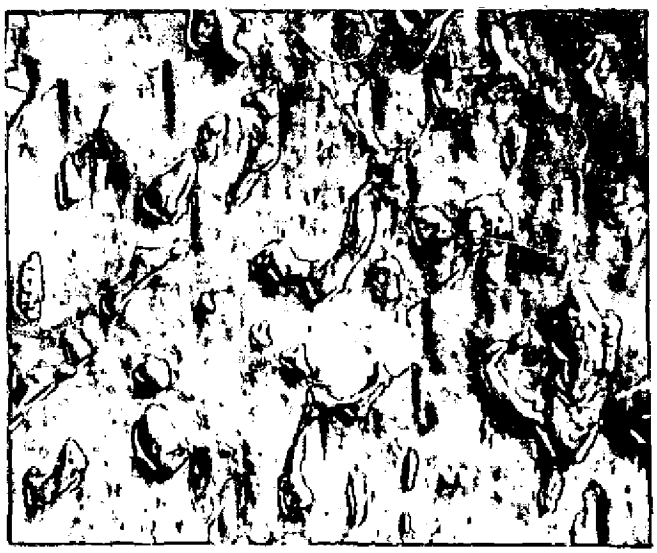

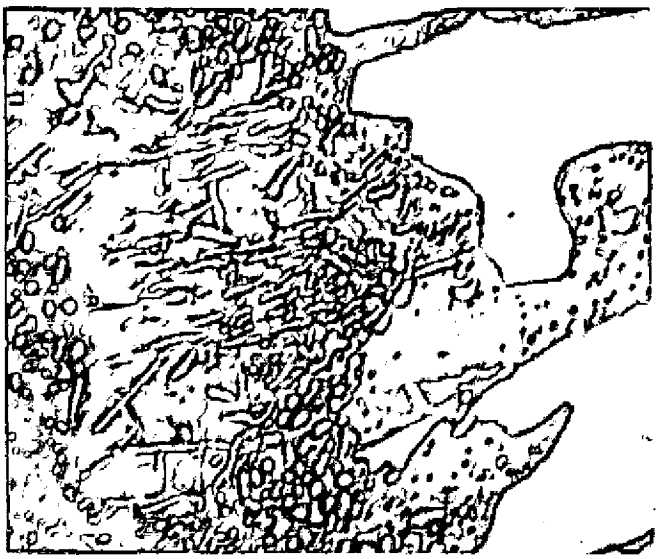

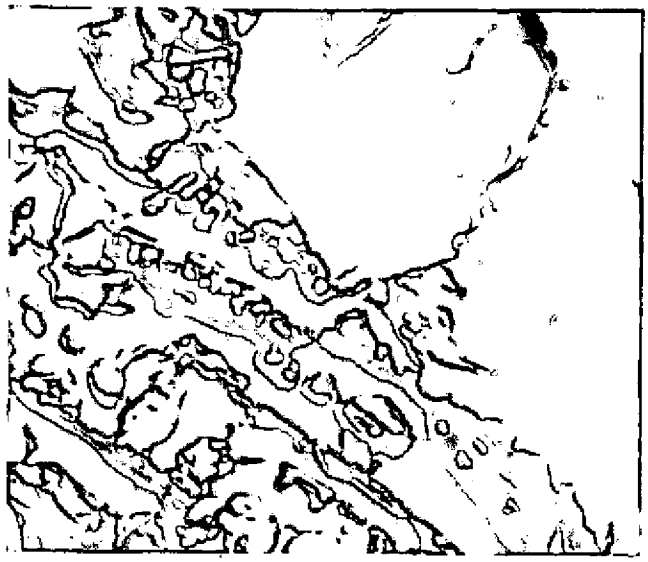

Fig. 4.34 Composite histograms depicting class-wise particle distribution at five different locations

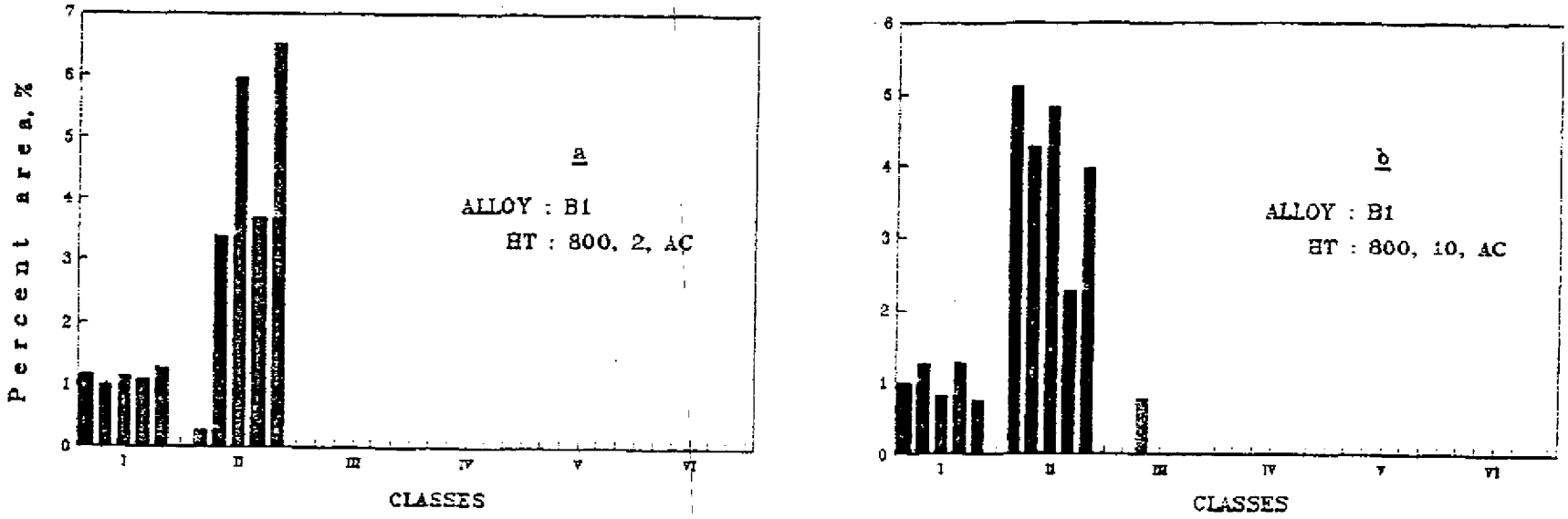

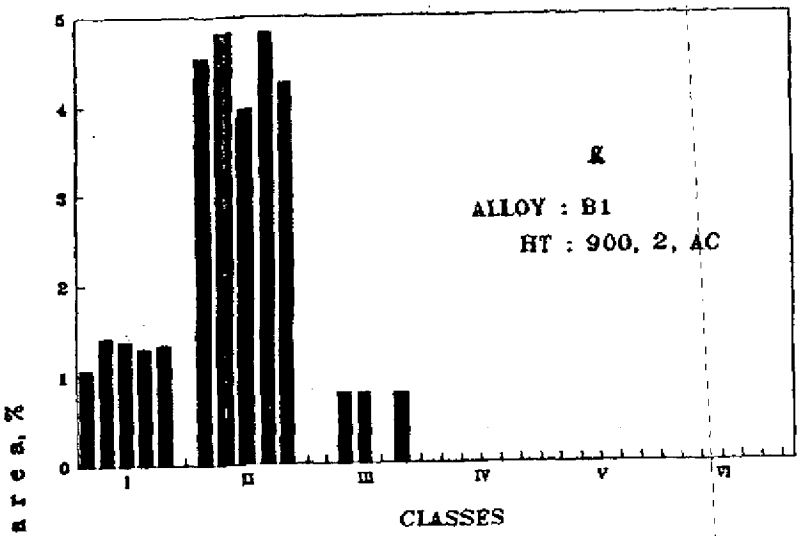
g
ALLOY : B1
HT : 900, 2, AC
Percent area, %
CLASSES

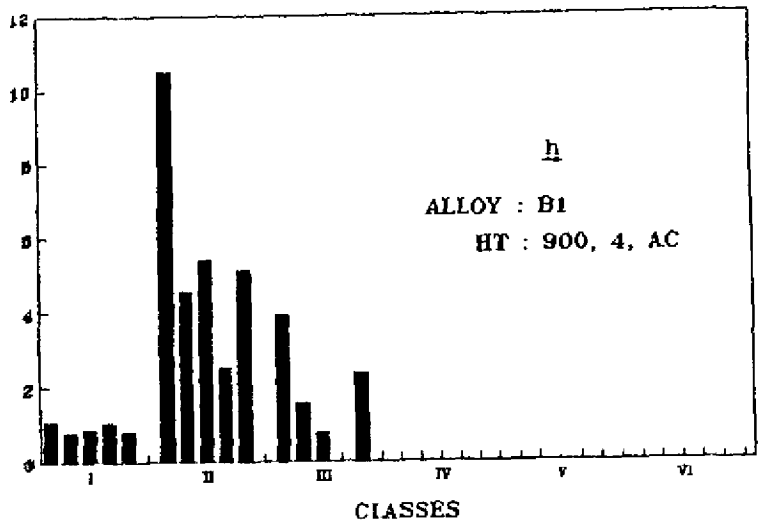
h
ALLOY : B1
HT : 900, 4, AC
CLASSES

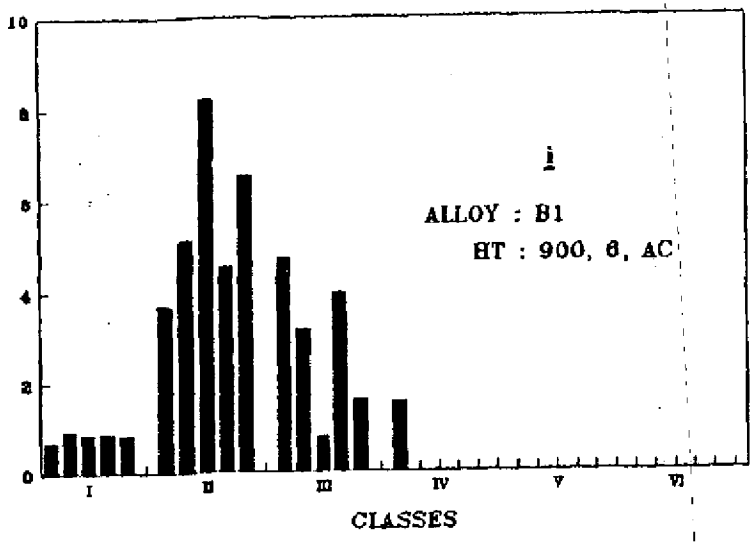
i
ALLOY : B1
HT : 900, 6, AC
CLASSES

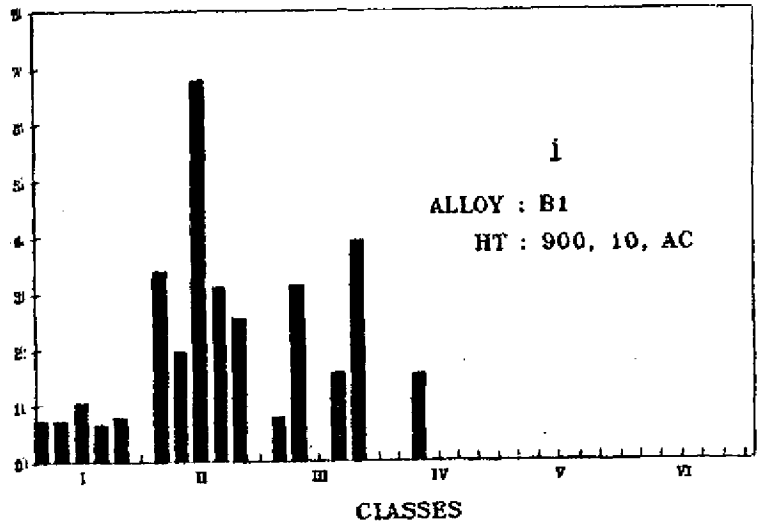
j
ALLOY : B1
HT : 900, 10, AC
CLASSES

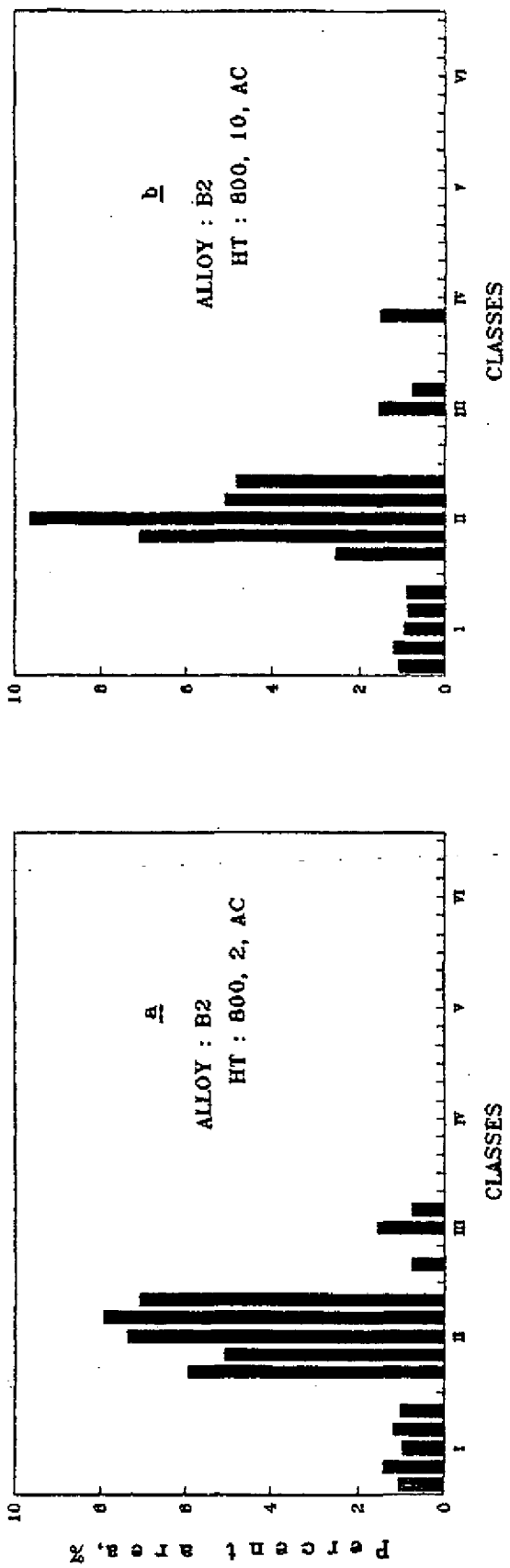

Fig. 4.35 Composite histograms depicting class-wise particle distribution at five different locations

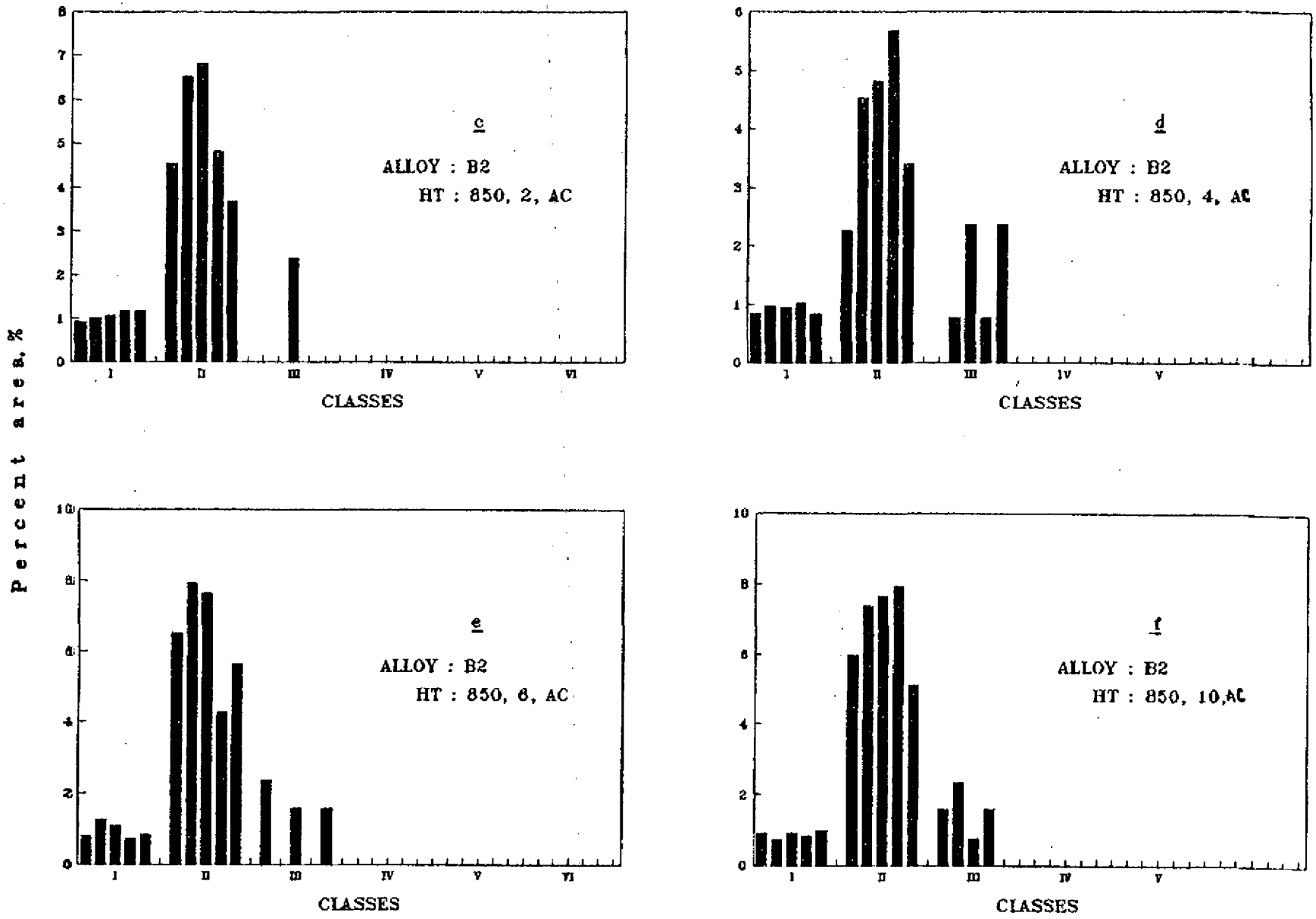
Percent area, %
c
ALLOY : B2
HT : 850, 2, AC
CLASSES
d
ALLOY : B2
HT : 850, 4, AC
CLASSES
e
ALLOY : B2
HT : 850, 6, AC
CLASSES
f
ALLOY : B2
HT : 850, 10, AC
CLASSES

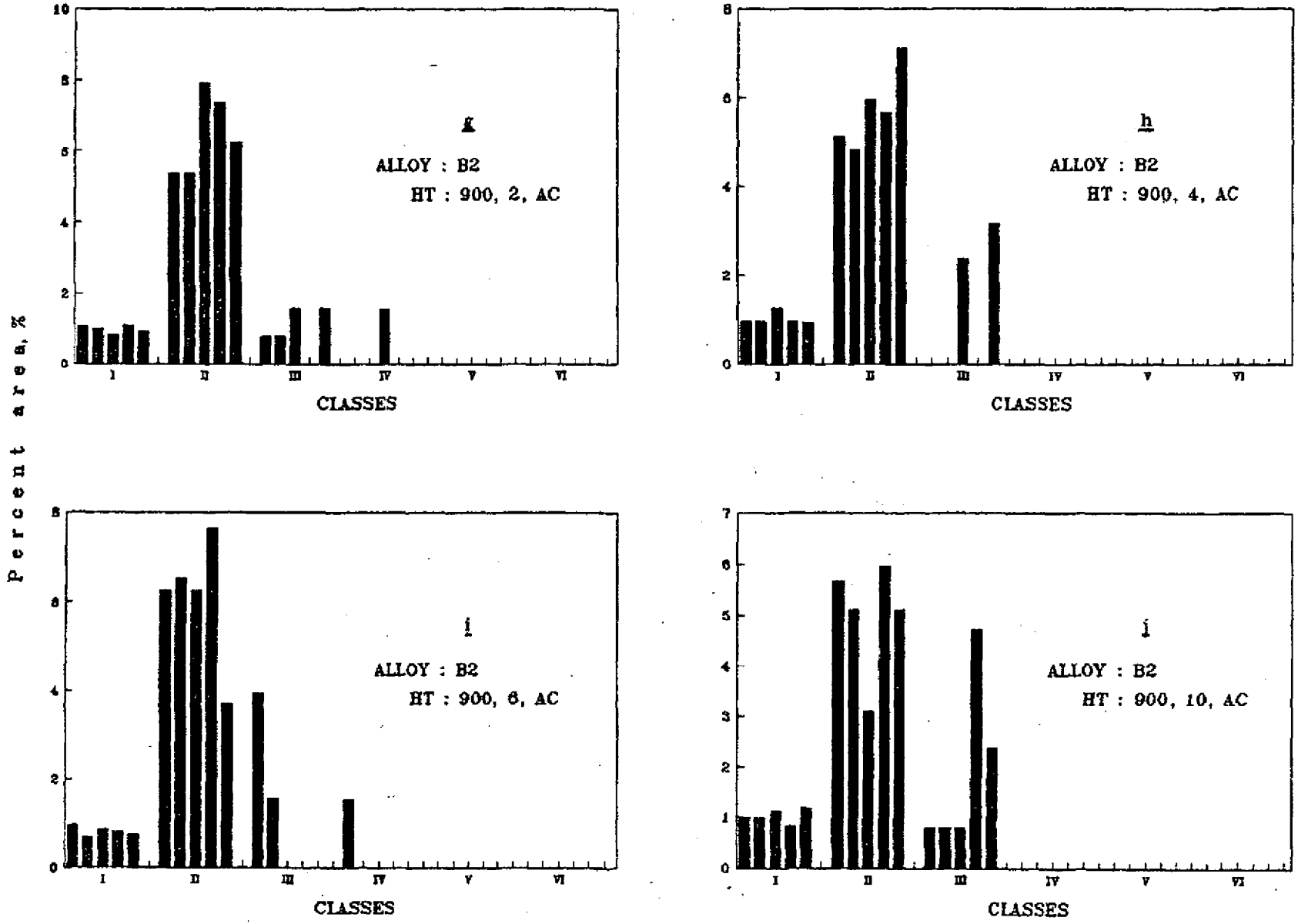
Percent area, %
g
ALLOY : B2
HT : 900, 2, AC
h
ALLOY : B2
HT : 900, 4, AC
i
ALLOY : B2
HT : 900, 6, AC
j
ALLOY : B2
HT : 900, 10, AC
CLASSES
CLASSES
CLASSES
CLASSES

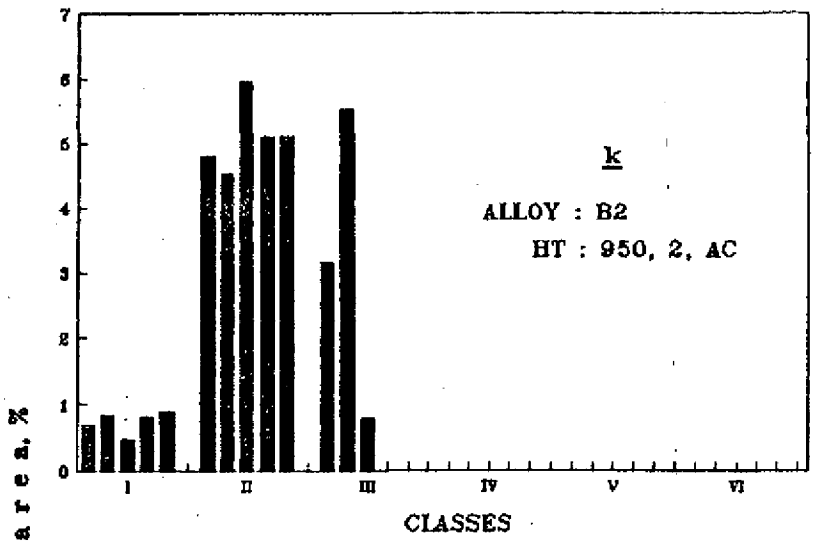
k
ALLOY : B2
HT : 950, 2, AC
Percent area, %
CLASSES
I
II
III
IV
V
VI

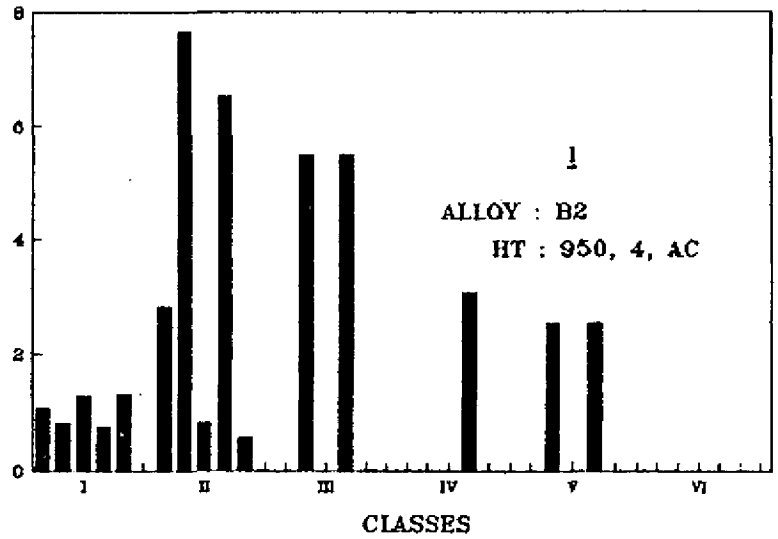
l
ALLOY : B2
HT : 950, 4, AC
CLASSES
I
II
III
IV
V
VI

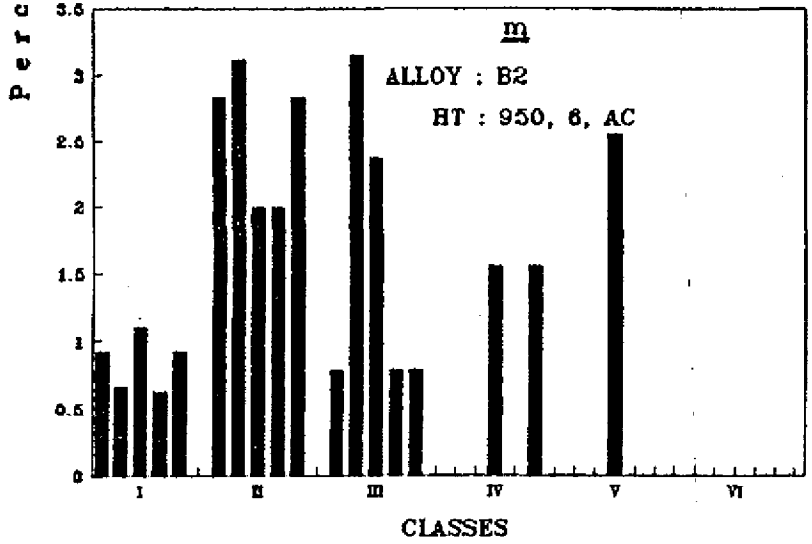
m
ALLOY : B2
HT : 950, 6, AC
CLASSES
I
II
III
IV
V
VI

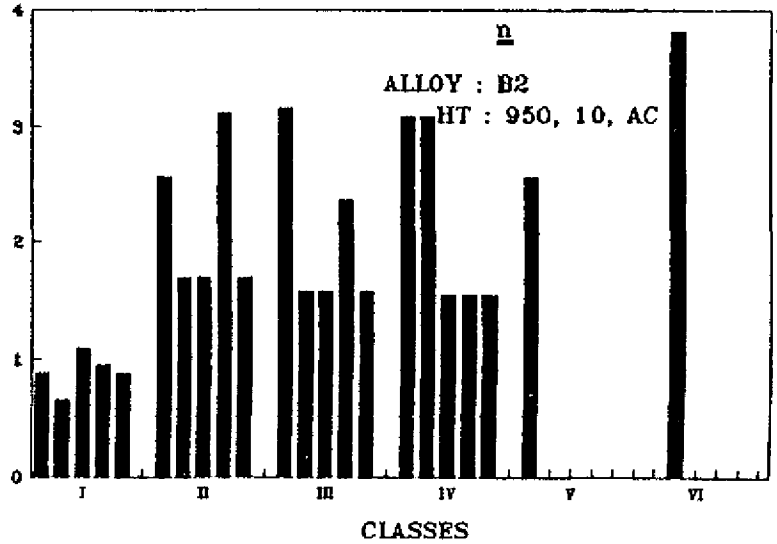
n
ALLOY : B2
HT : 950, 10, AC
CLASSES
I
II
III
IV
V
VI

Fig. 4.36 Composite histograms depicting class-wise particle distribution at five different locations

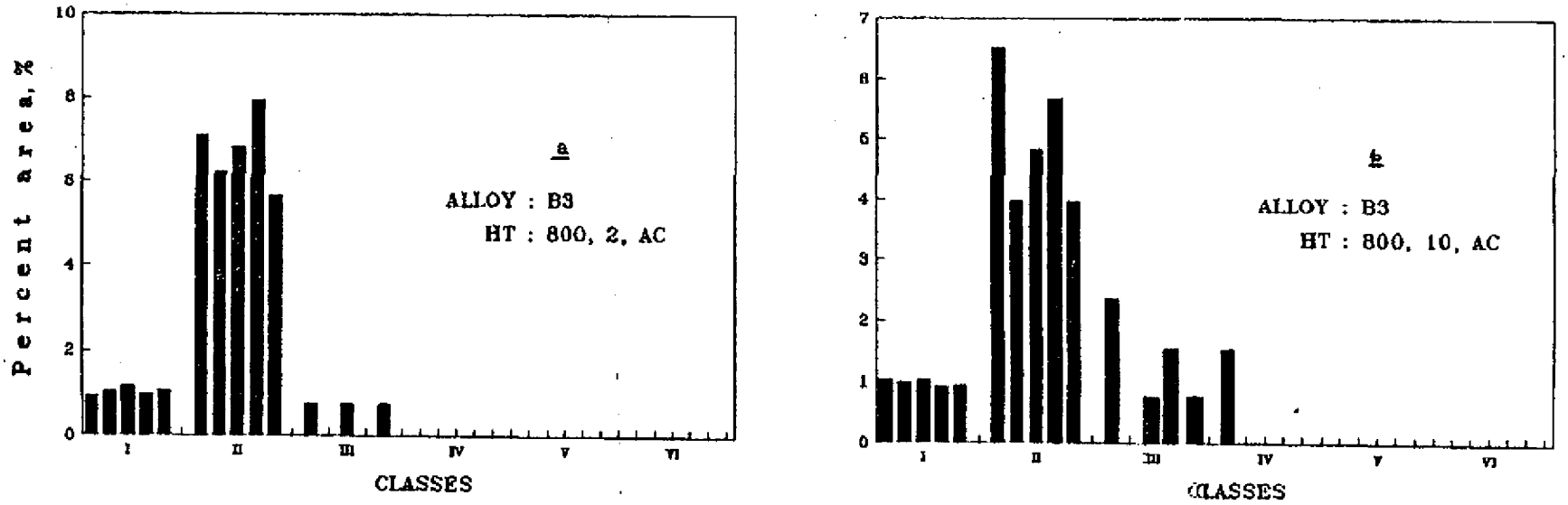

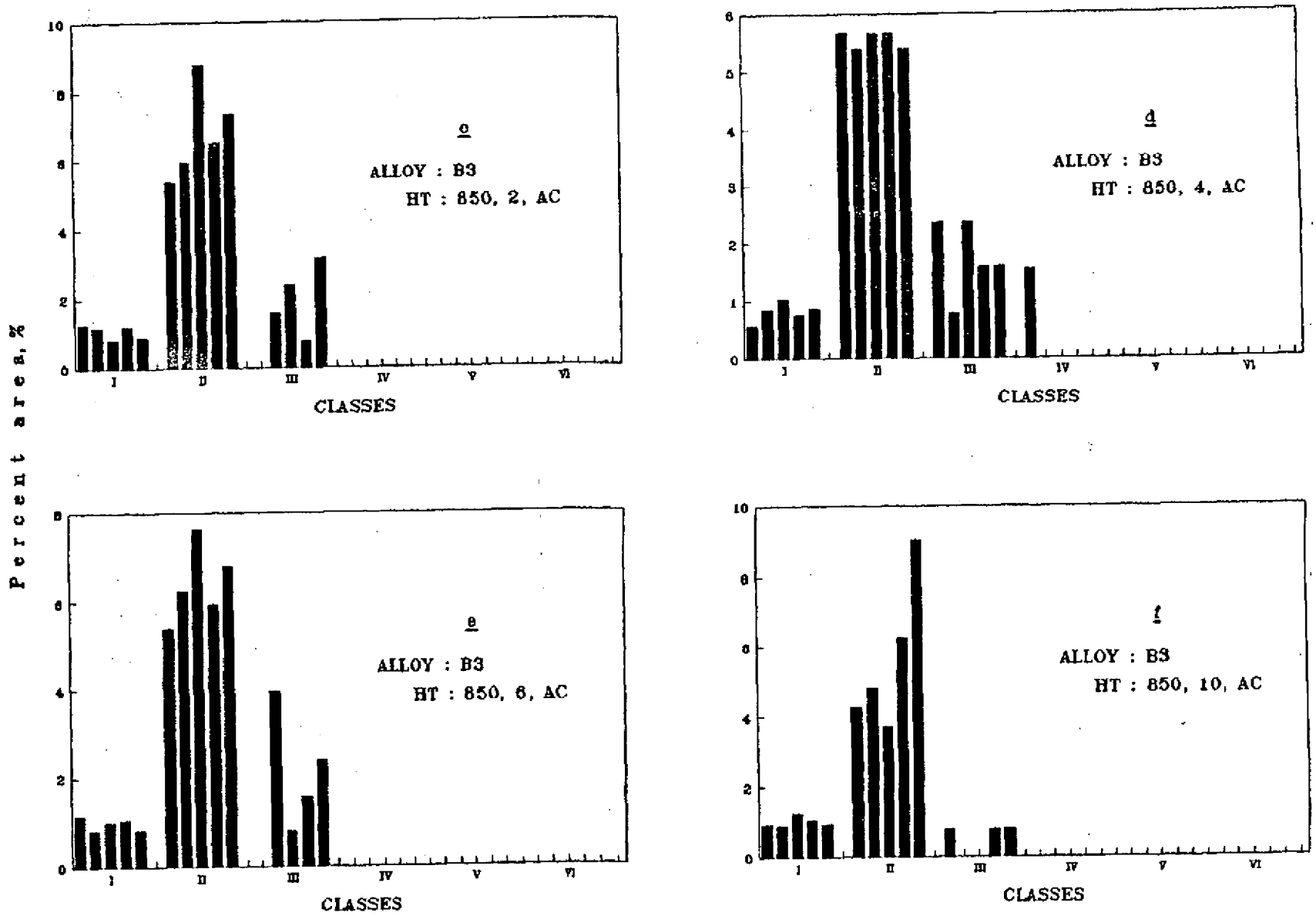
c
ALLOY : B3
HT : 850, 2, AC
d
ALLOY : B3
HT : 850, 4, AC
e
ALLOY : B3
HT : 850, 6, AC
f
ALLOY : B3
HT : 850, 10, AC
Percent area, %
CLASSES
I
II
III
IV
V
VI

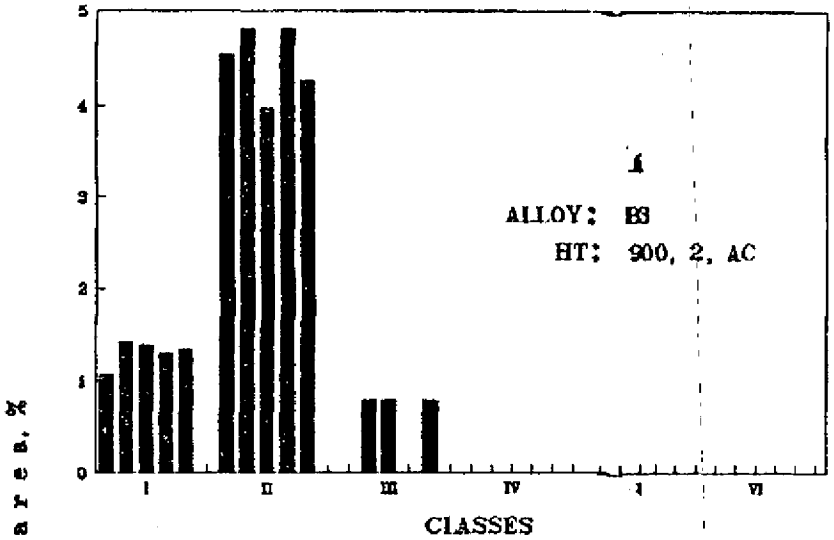

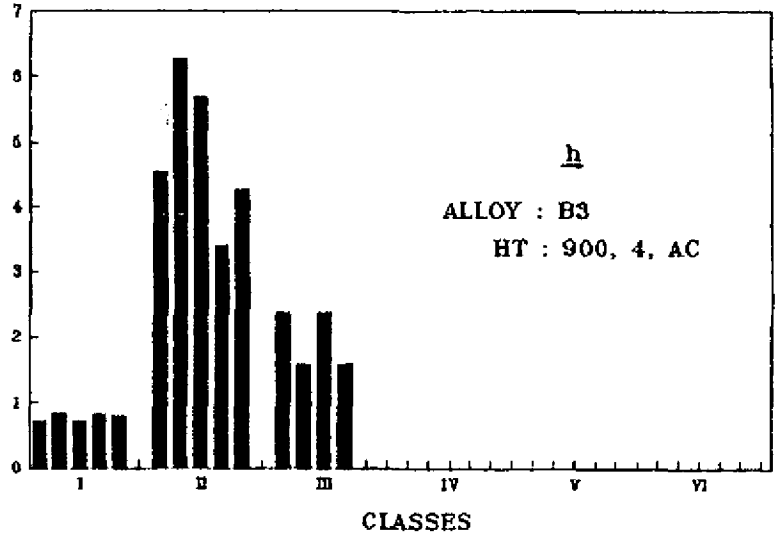

Percent area, %

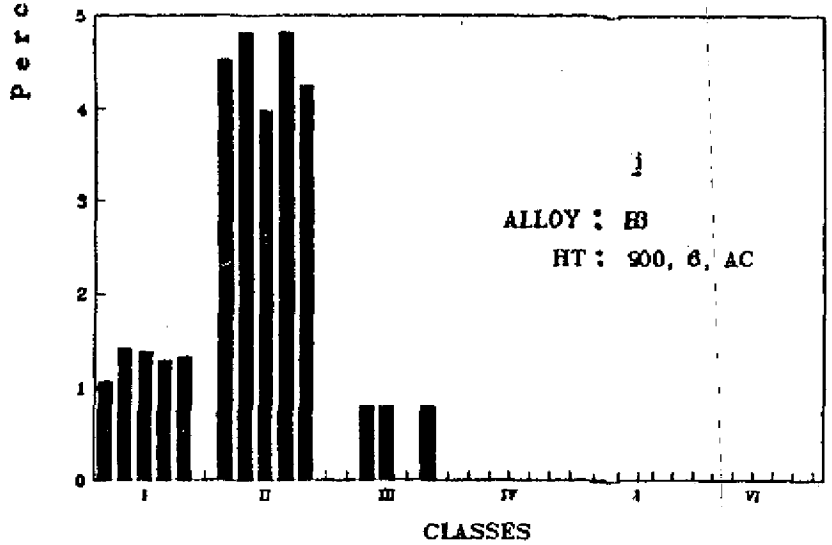

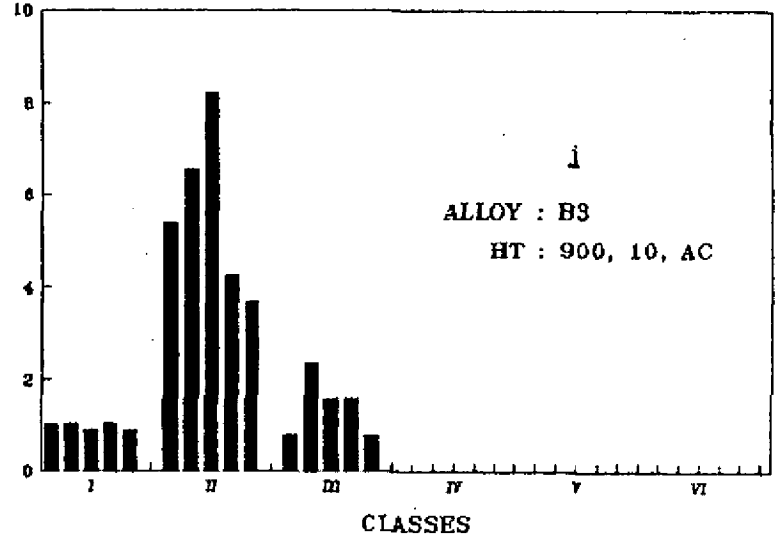

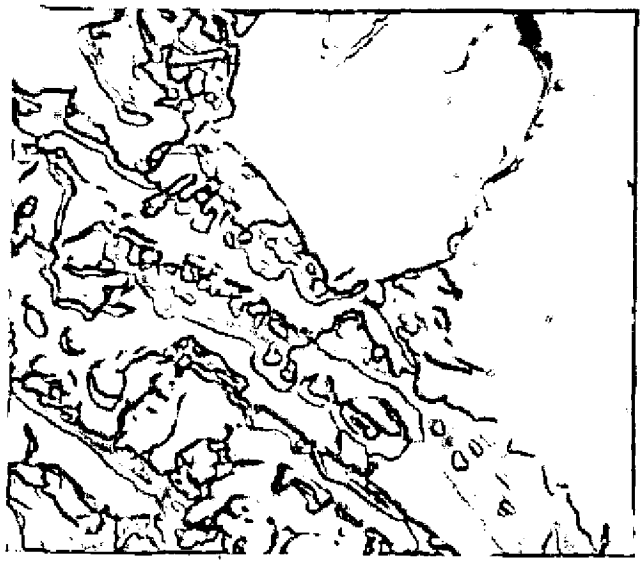

Fig. 4.34 Composite histograms depicting class-wise particle distribution at five different locations

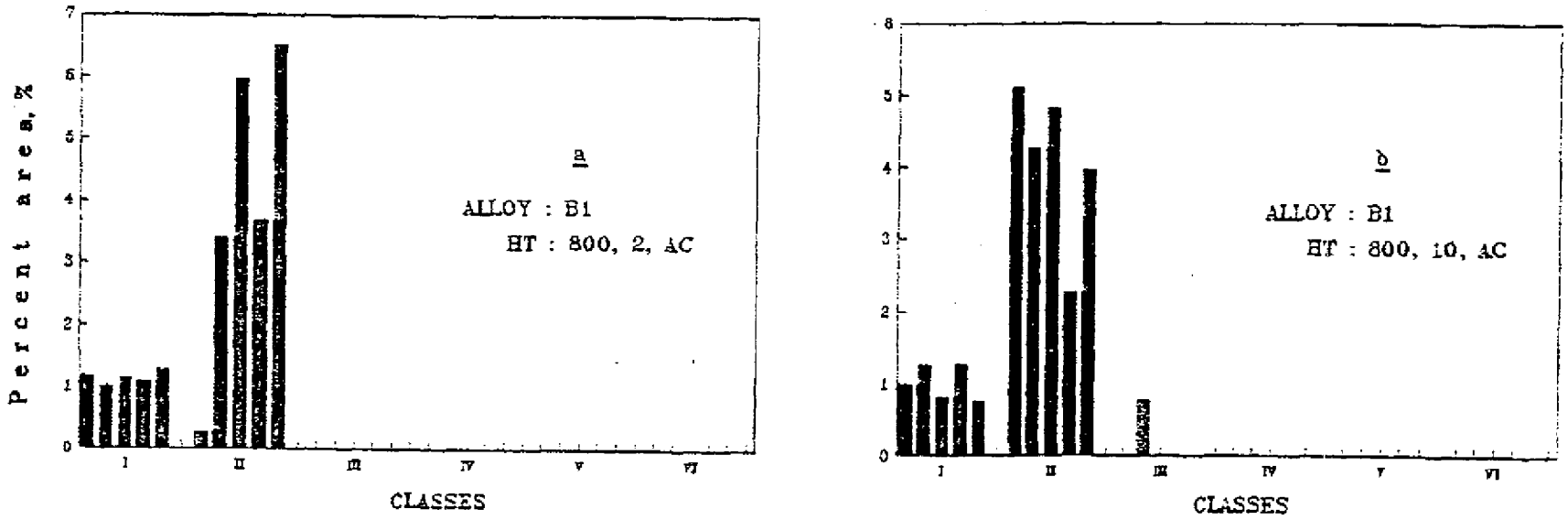

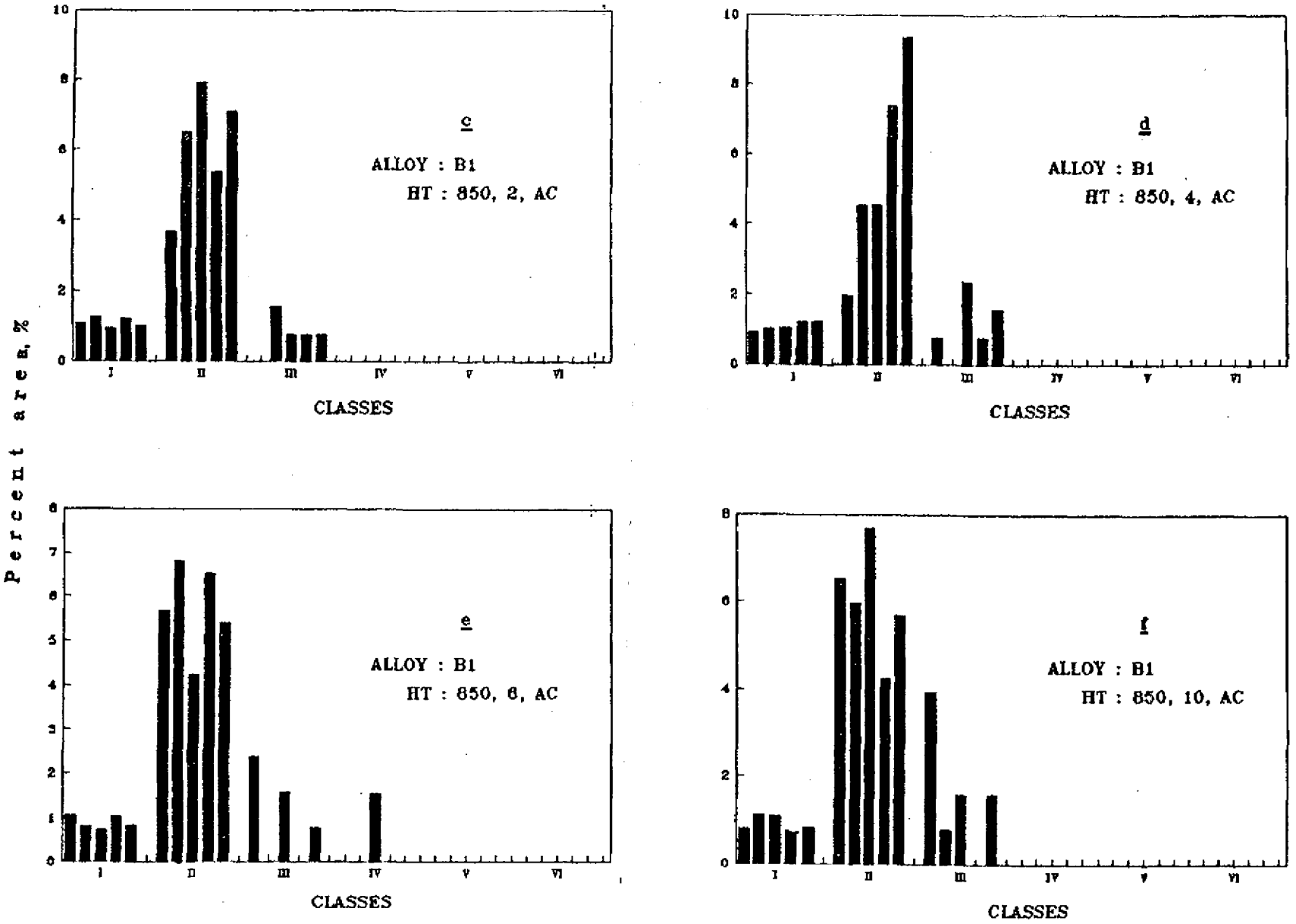
Percent area, %
c
ALLOY : B1
HT : 850, 2, AC
d
ALLOY : B1
HT : 850, 4, AC
e
ALLOY : B1
HT : 850, 6, AC
f
ALLOY : B1
HT : 850, 10, AC
CLASSES
CLASSES
CLASSES
CLASSES

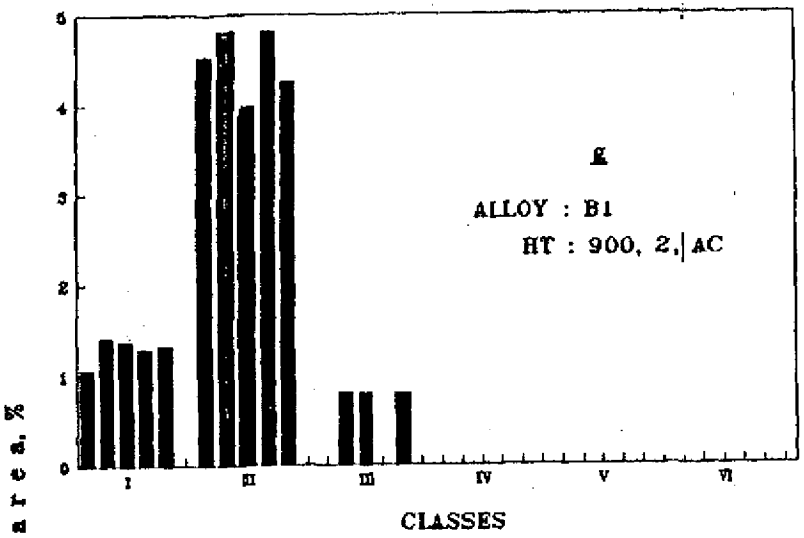
g
ALLOY : B1
HT : 900, 2, AC
Percent area, %
CLASSES

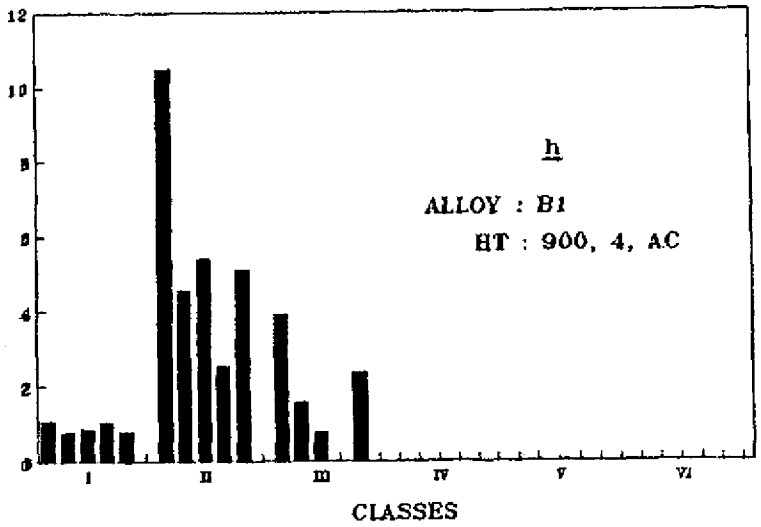
h
ALLOY : B1
HT : 900, 4, AC
CLASSES

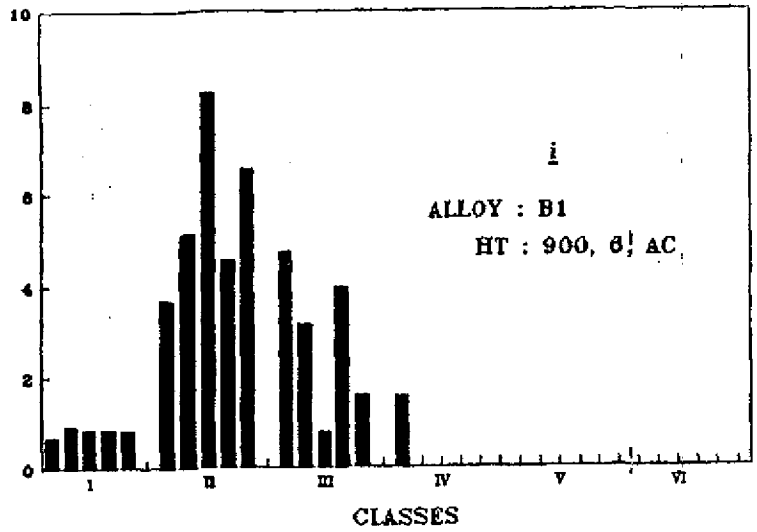
i
ALLOY : B1
HT : 900, 6, AC
CLASSES

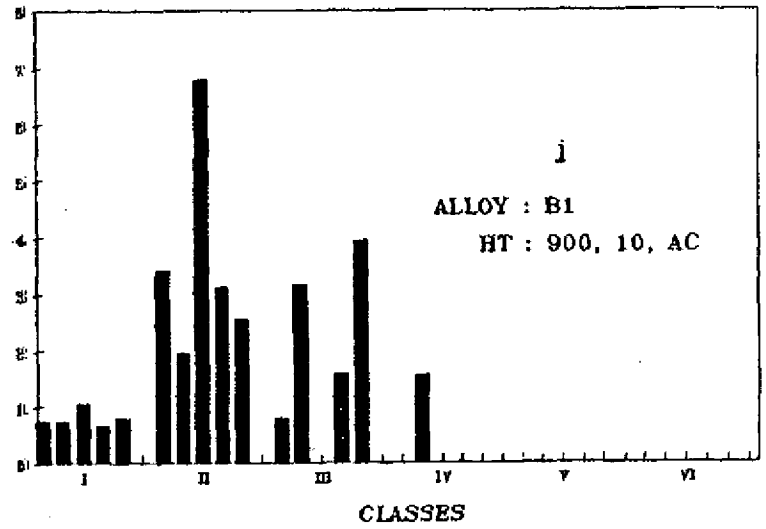
j
ALLOY : B1
HT : 900, 10, AC
CLASSES

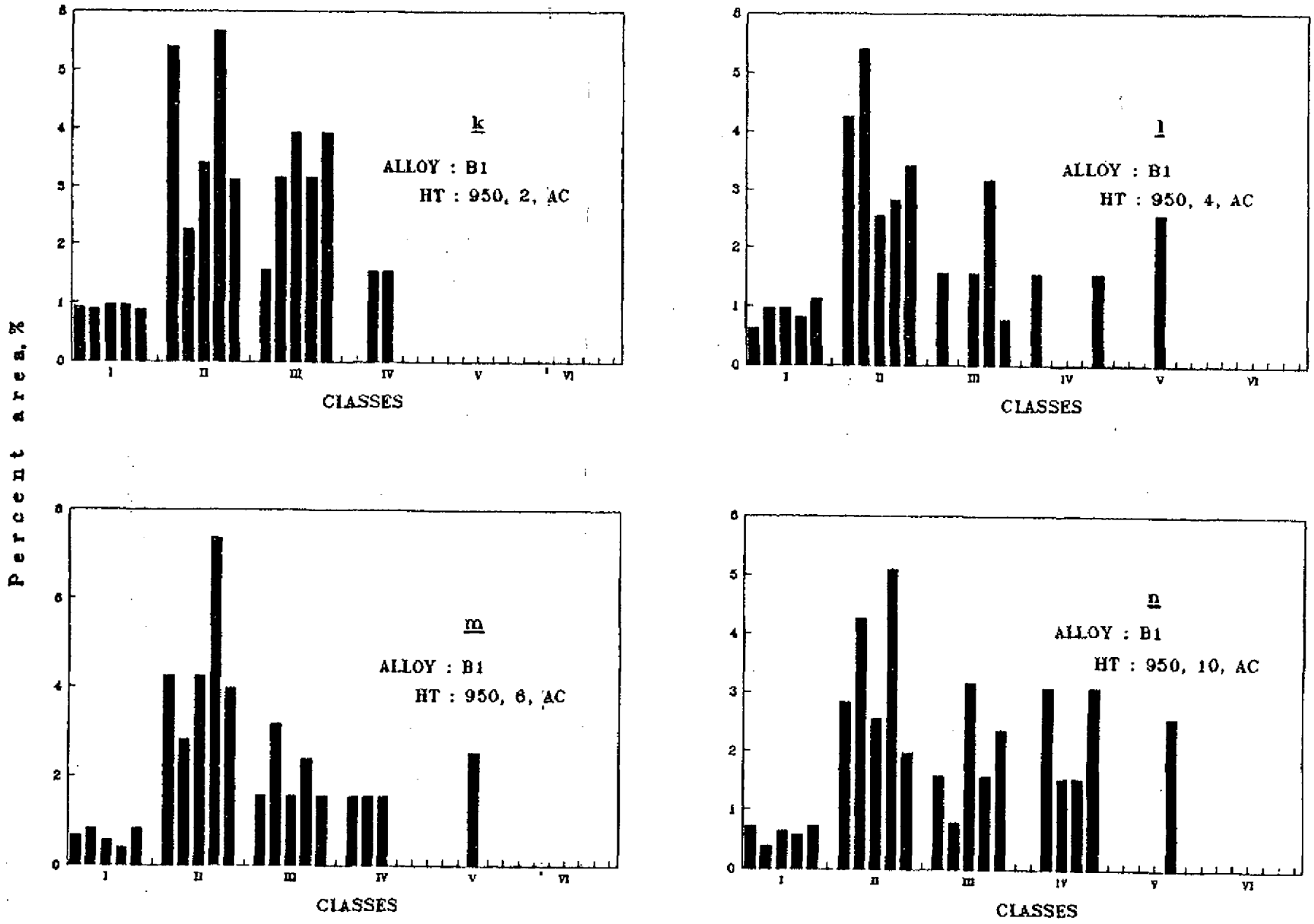
Percent area, %
k
ALLOY : B1
HT : 950, 2, AC
CLASSES
l
ALLOY : B1
HT : 950, 4, AC
CLASSES
m
ALLOY : B1
HT : 950, 6, AC
CLASSES
n
ALLOY : B1
HT : 950, 10, AC
CLASSES

Fig. 4.35 Composite histograms depicting class–wise particle distribution at five different locations

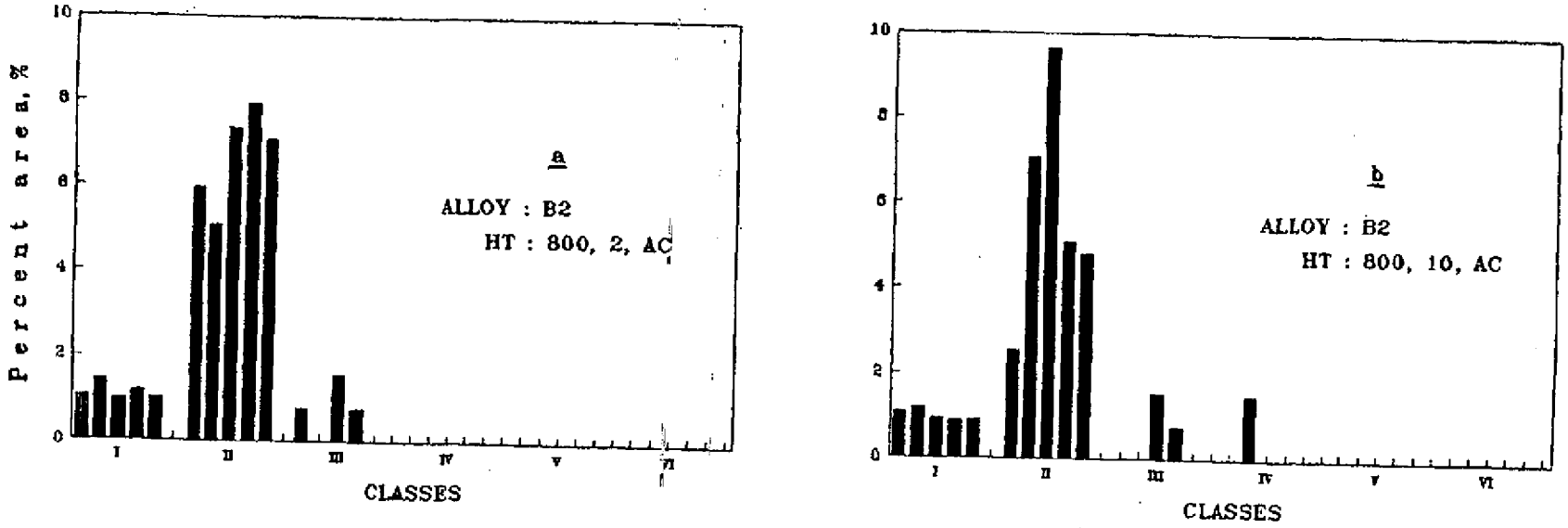

Fig. 4.37 Composite histograms depicting class-wise particle distribution at five different locations

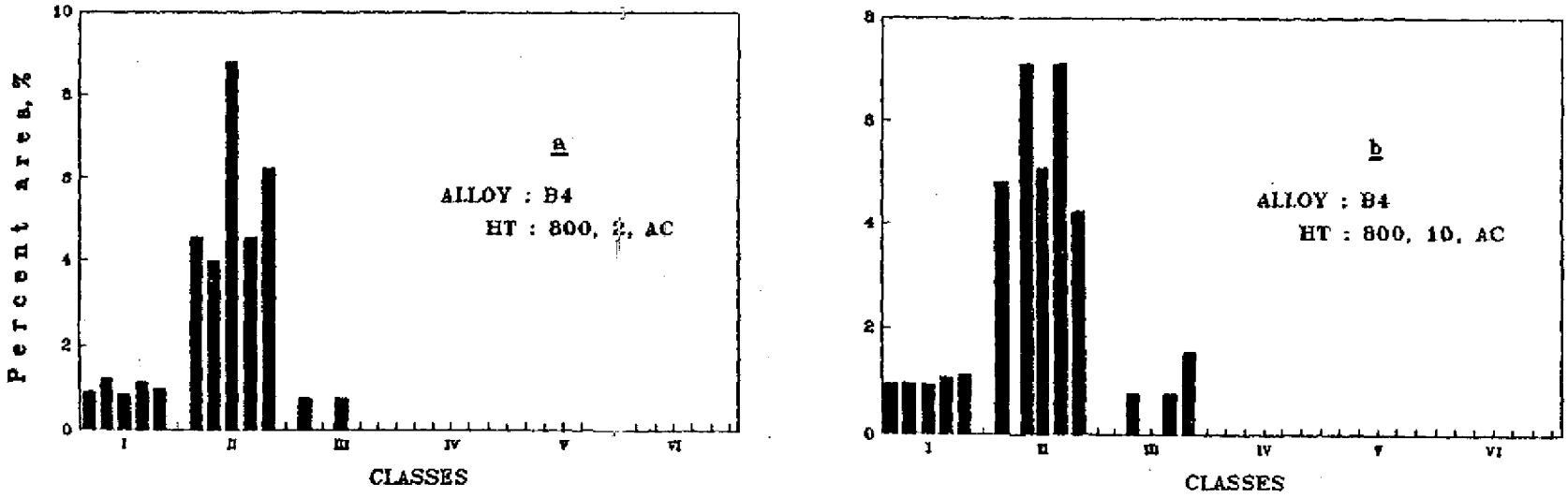

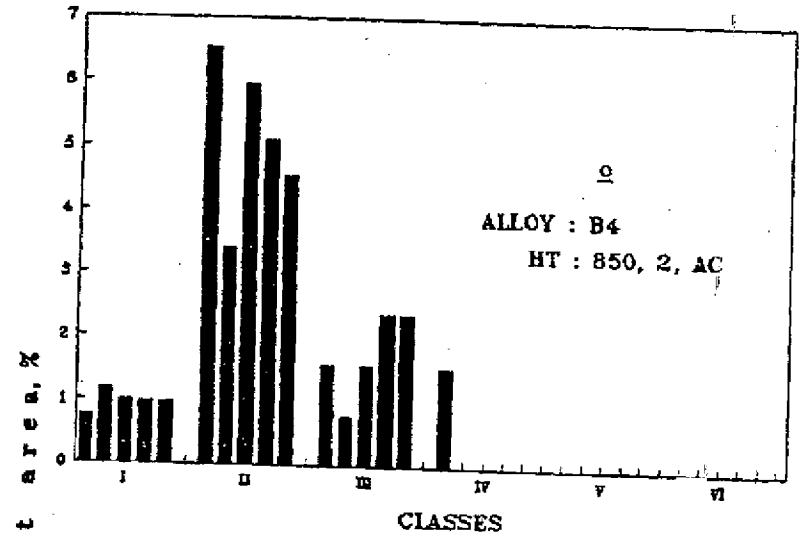
c
ALLOY : B4
HT : 850, 2, AC
Percent area, %
CLASSES

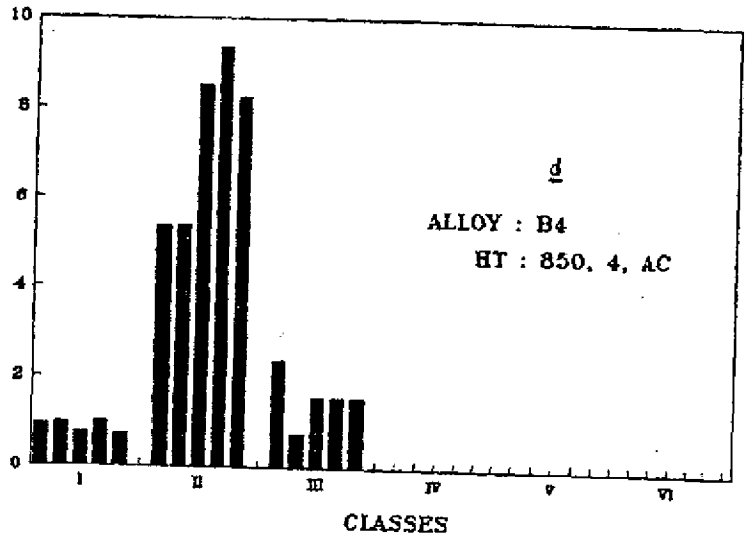
d
ALLOY : B4
HT : 850, 4, AC
CLASSES

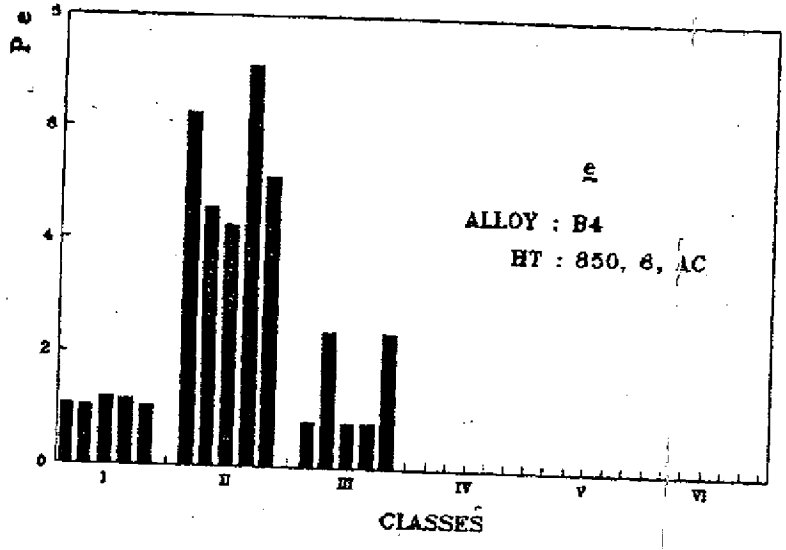
e
ALLOY : B4
HT : 850, 6, AC
CLASSES

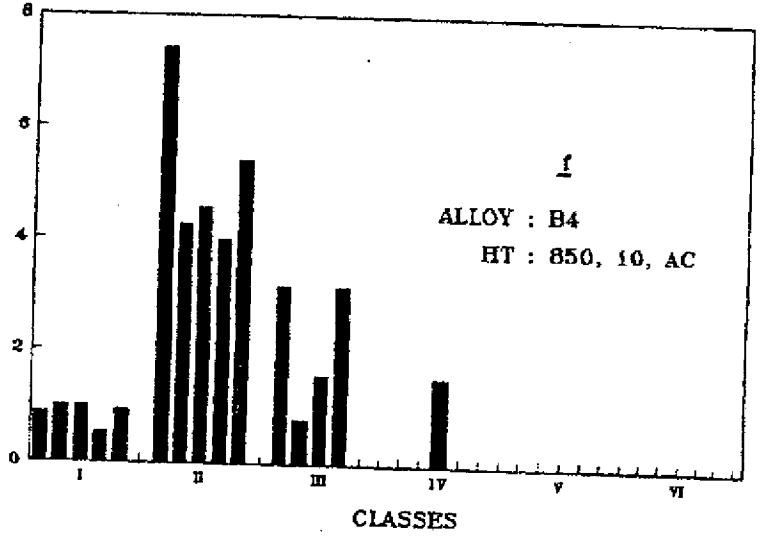
f
ALLOY : B4
HT : 850, 10, AC
CLASSES

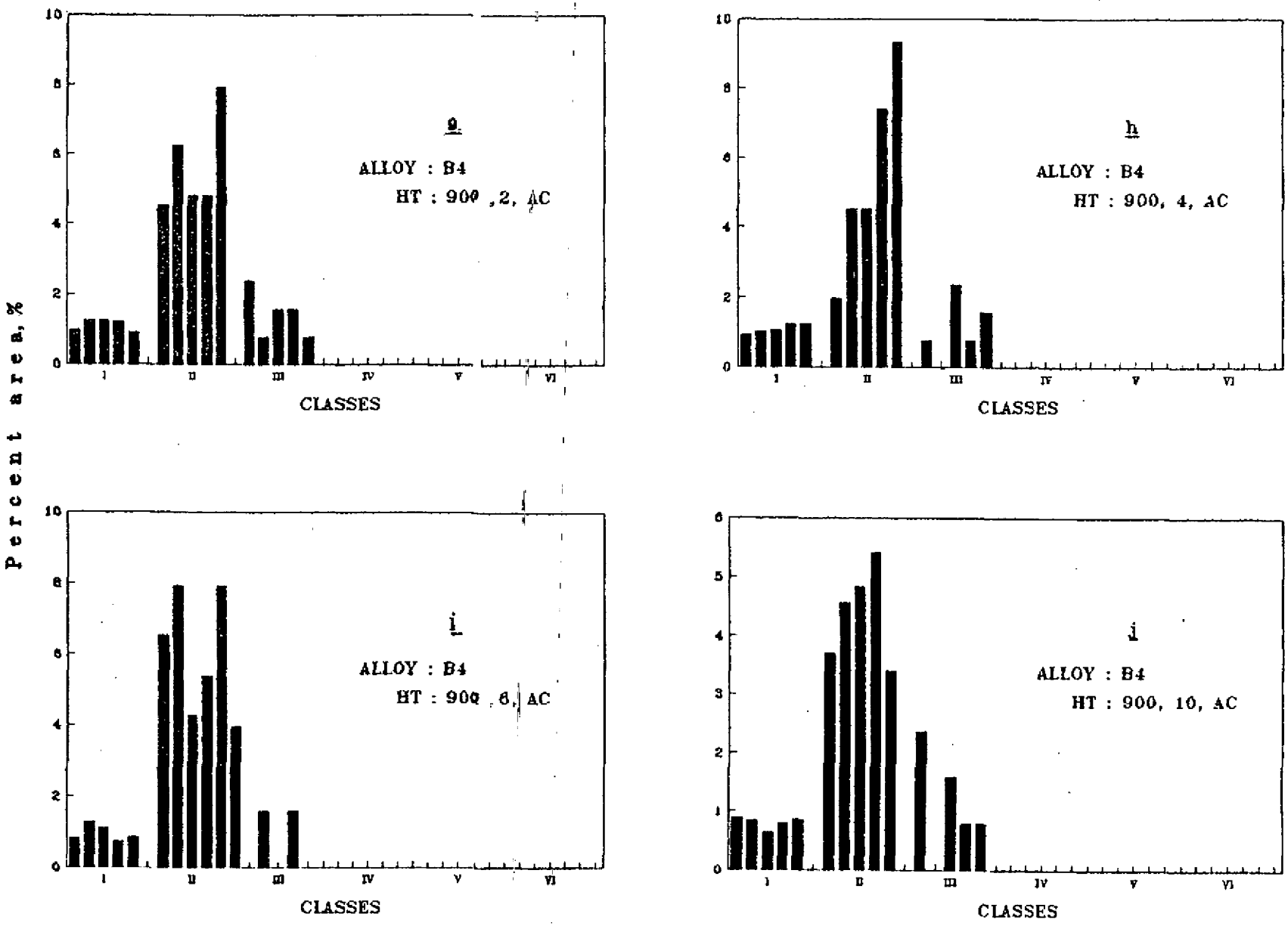
Percent area, %
g
ALLOY : B4
HT : 900 ,2, AC
h
ALLOY : B4
HT : 900, 4, AC
i
ALLOY : B4
HT : 900 , 6, AC
j
ALLOY : B4
HT : 900, 10, AC
CLASSES
CLASSES
CLASSES
CLASSES

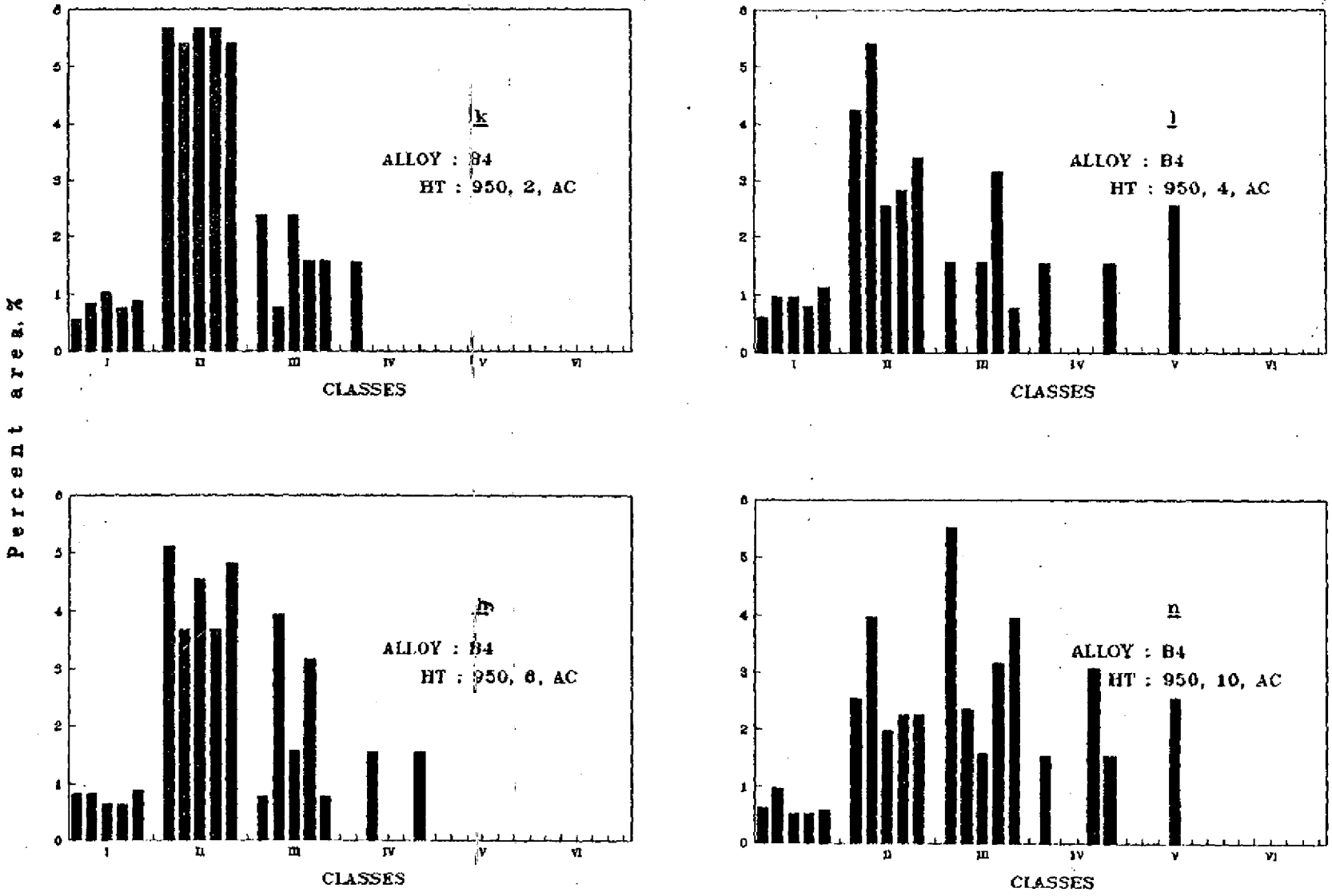
Percent area, %
k
ALLOY : B4
HT : 950, 2, AC
CLASSES
l
ALLOY : B4
HT : 950, 4, AC
CLASSES
m
ALLOY : B4
HT : 950, 6, AC
CLASSES
n
ALLOY : B4
HT : 950, 10, AC
CLASSES

Fig. 4.38 A plot of experimental vs predicted hardness values in the experimental alloys

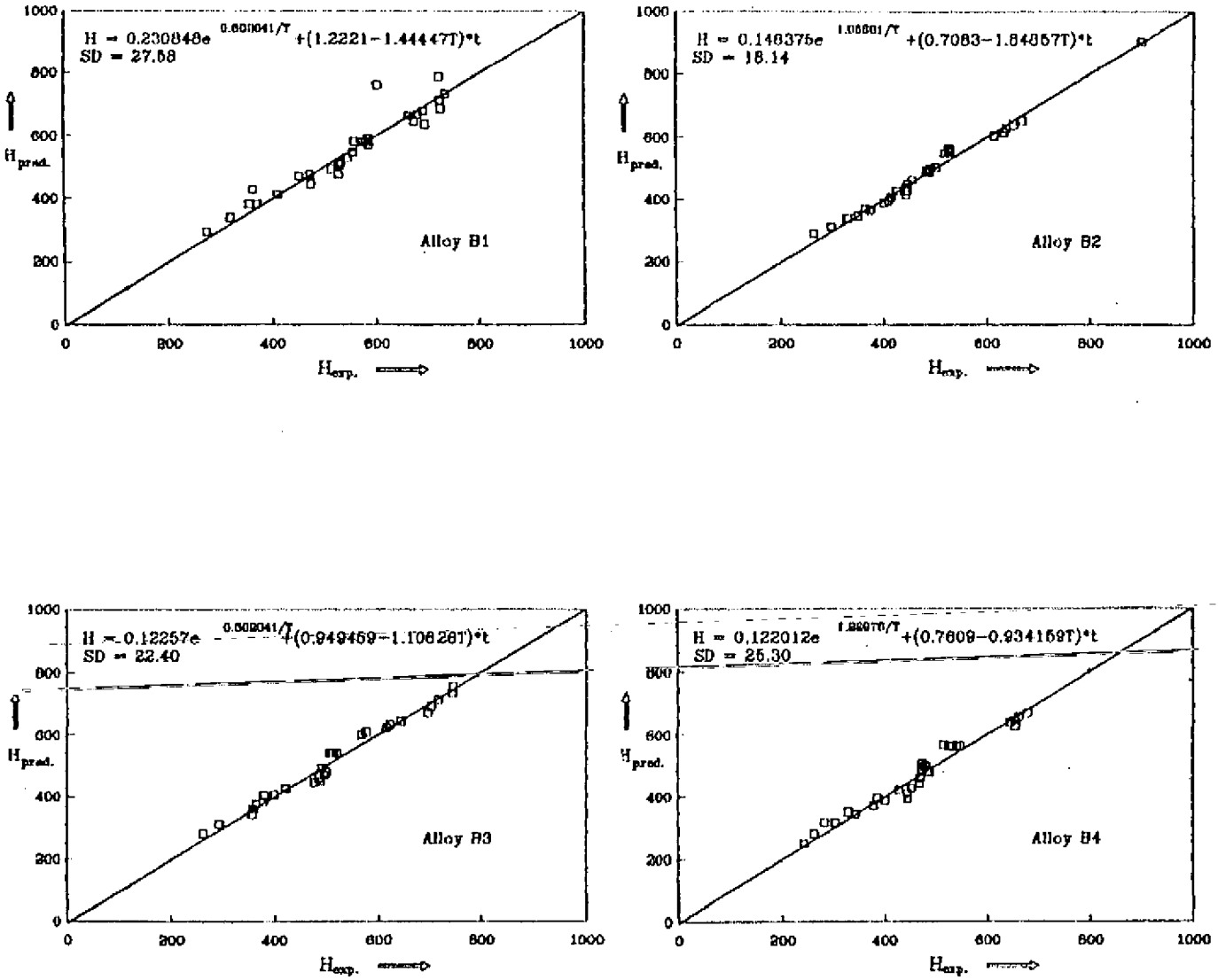

Fig. 4.40 3D plot depicting the effect of h/t parameters on hardness

Alloy B2

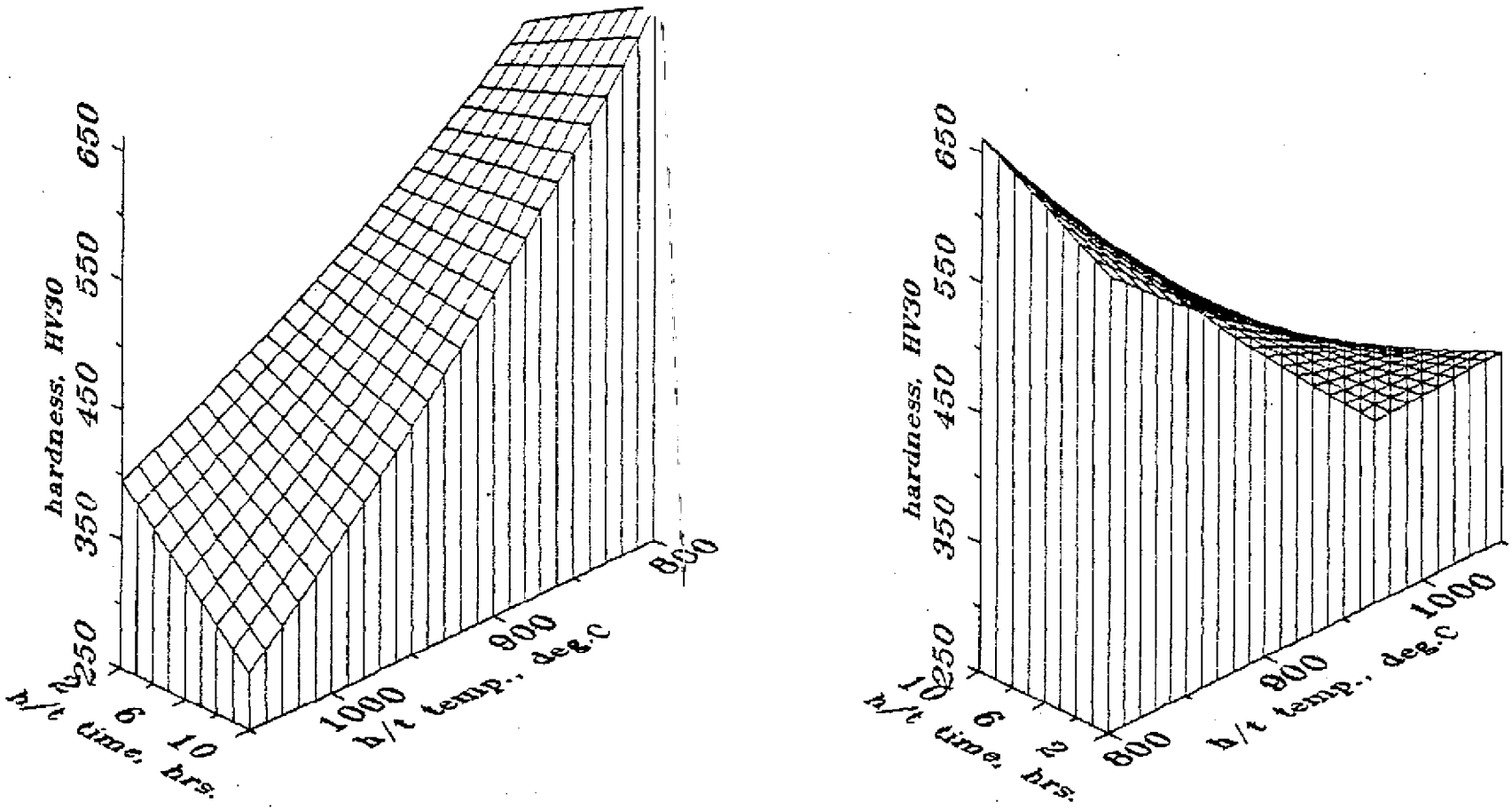

Fig. 4.41 3D plot depicting the effect of h/t parameters on hardness

Alloy B3

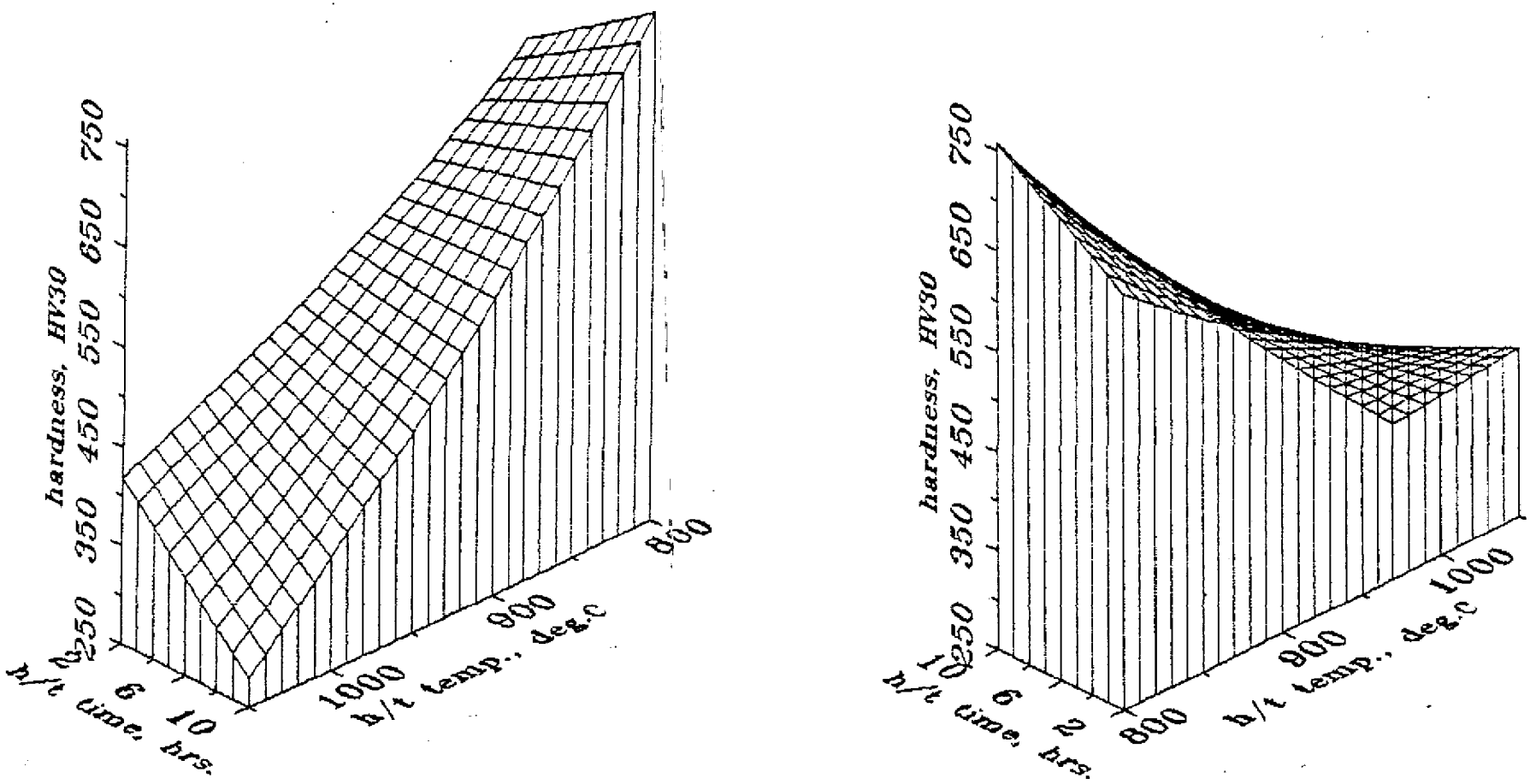

Fig. 4.42 3D plot depicting the effect of h/t parameters on hardness

Alloy B4

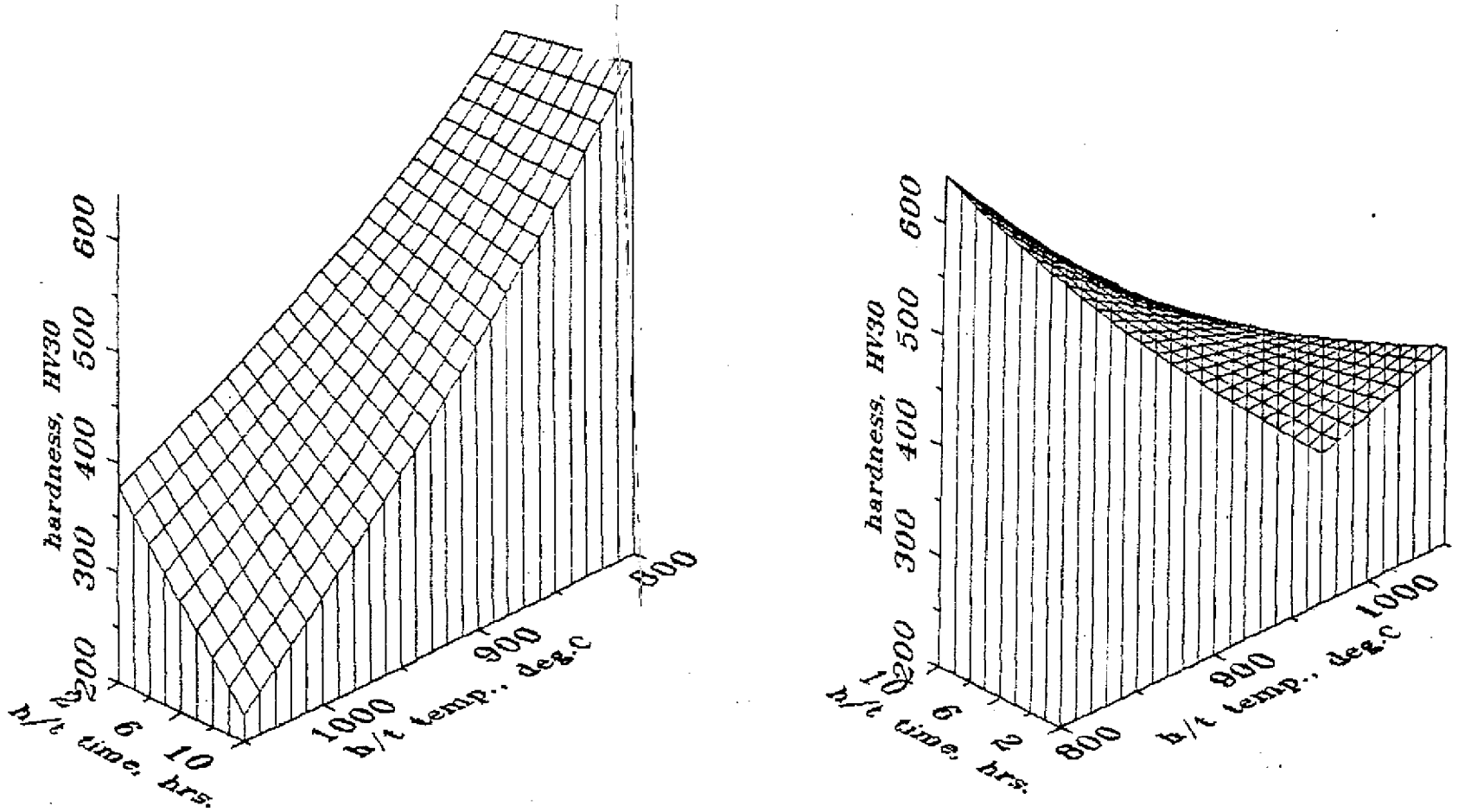

FIG. 4.43 ISO-HARDNESS PLOT OF ALLOY B1

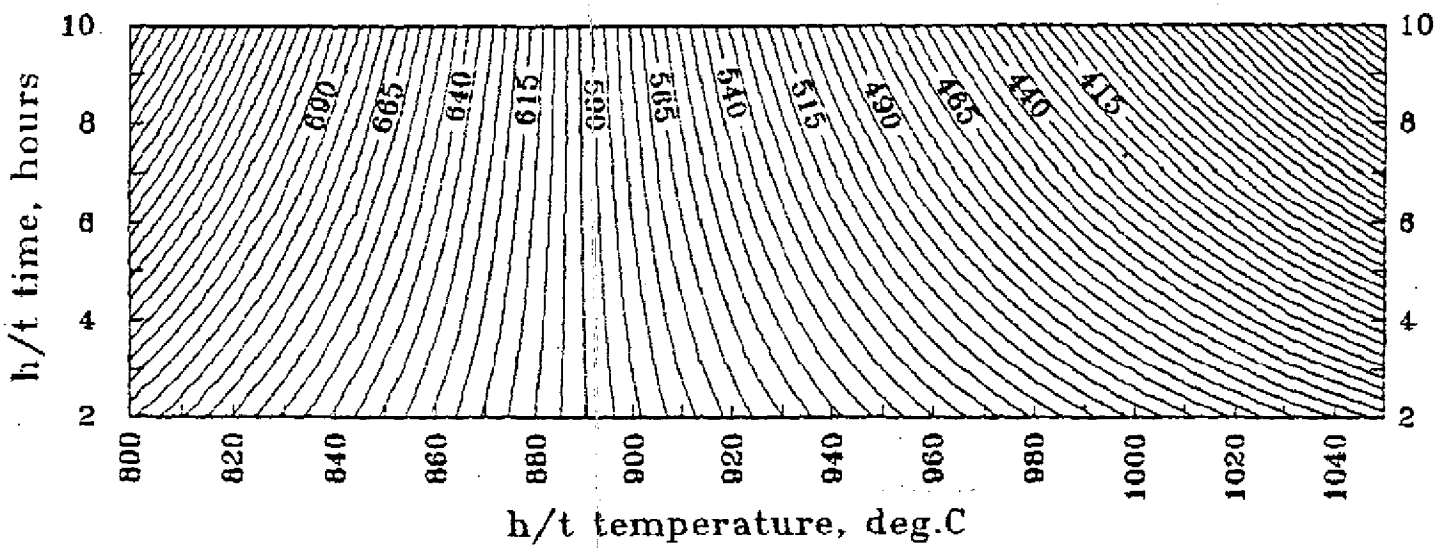

FIG. 4.44 ISO-HARDNESS PLOT OF ALLOY B2

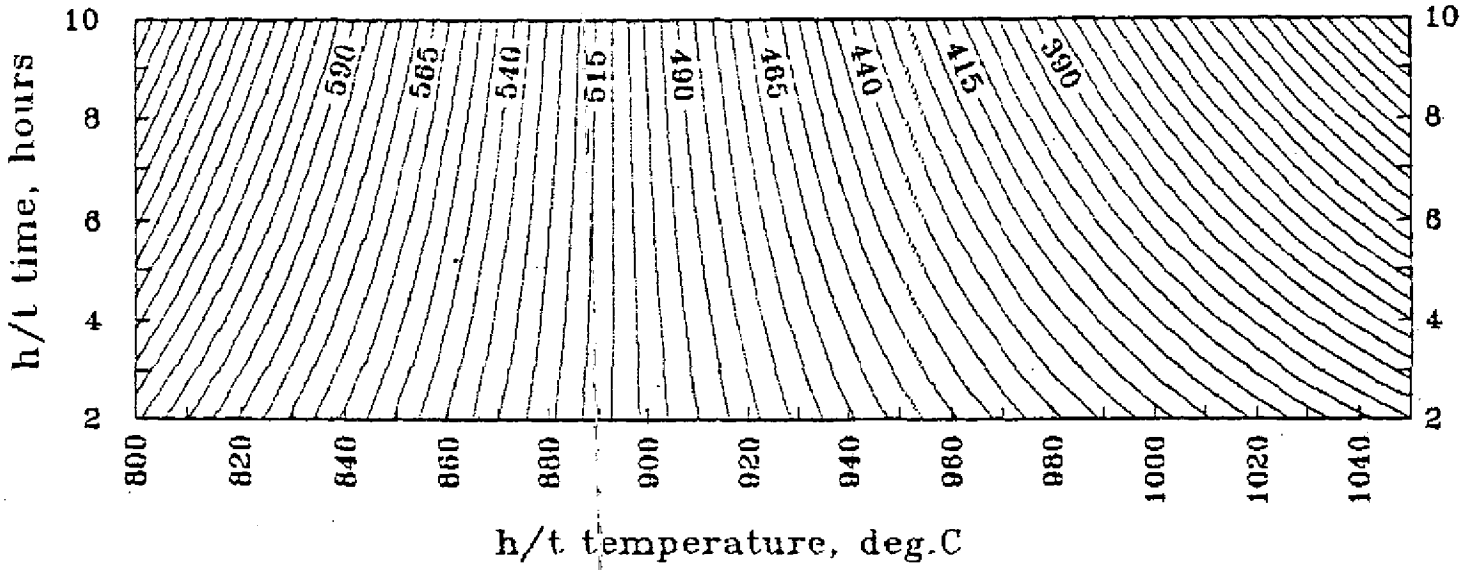

FIG. 4.45 ISO-HARDNESS PLOT OF ALLOY B3

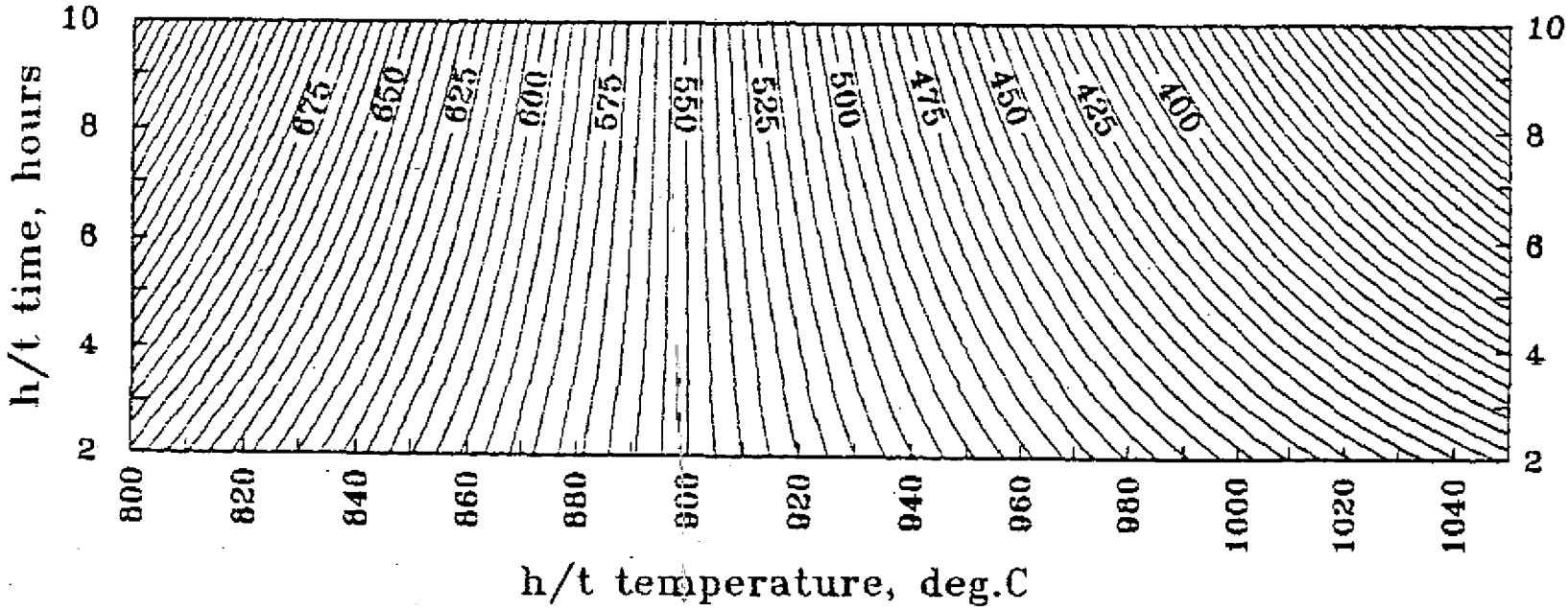

FIG. 4.46 ISO-HARDNESS PLOT OF ALLOY B4

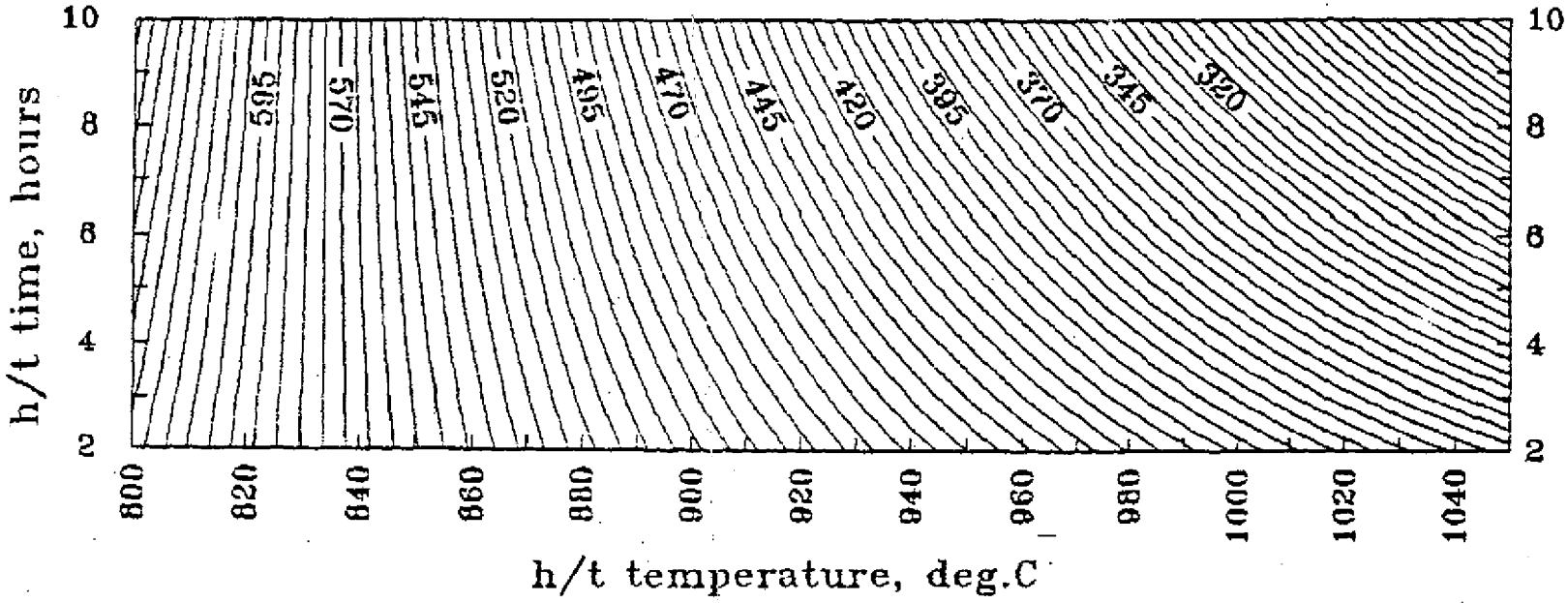

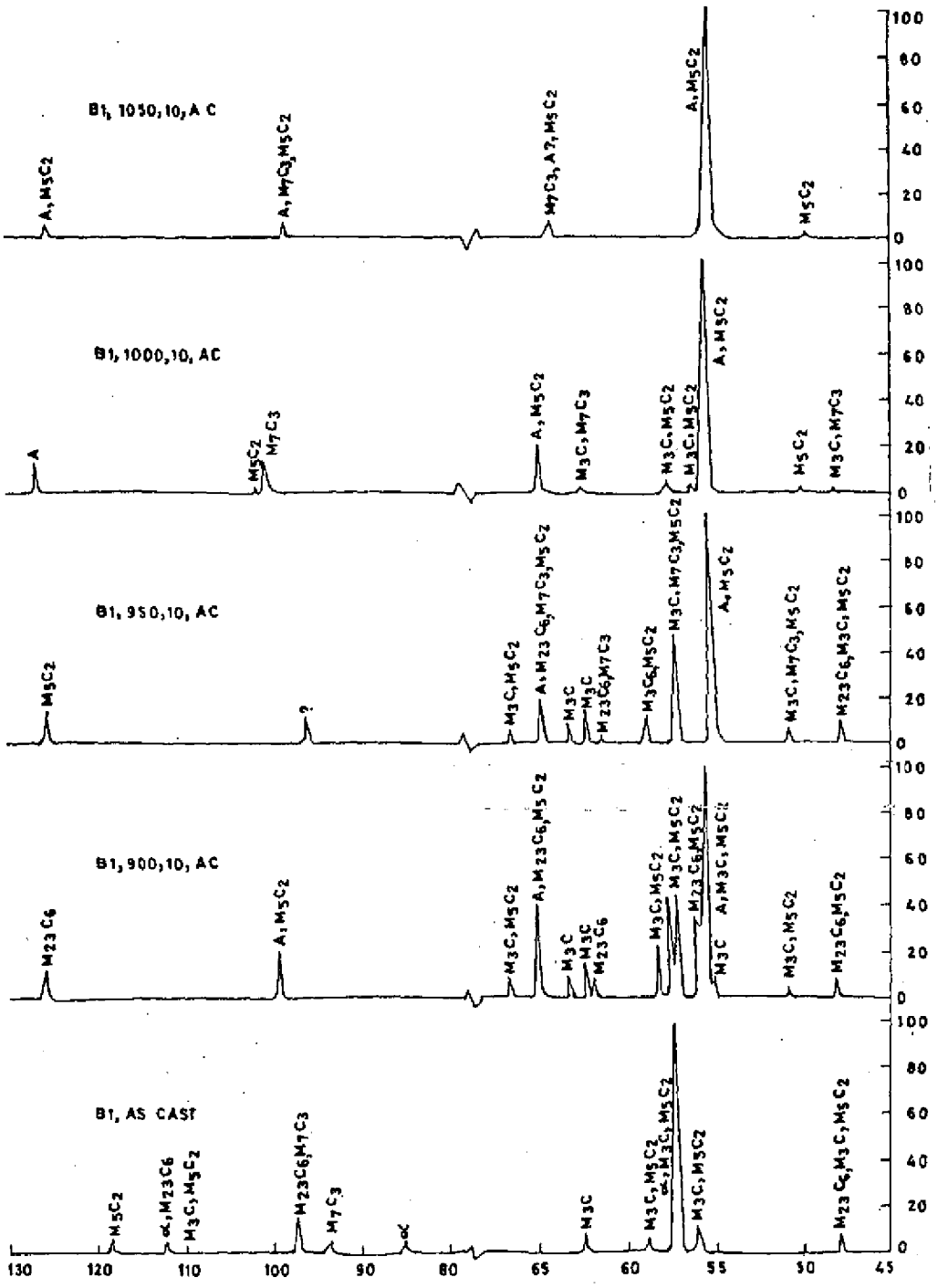

FIC. 5.1- COMPARATIVE X-RAY DIFFRACTOGRAMS OF ALLOY B1

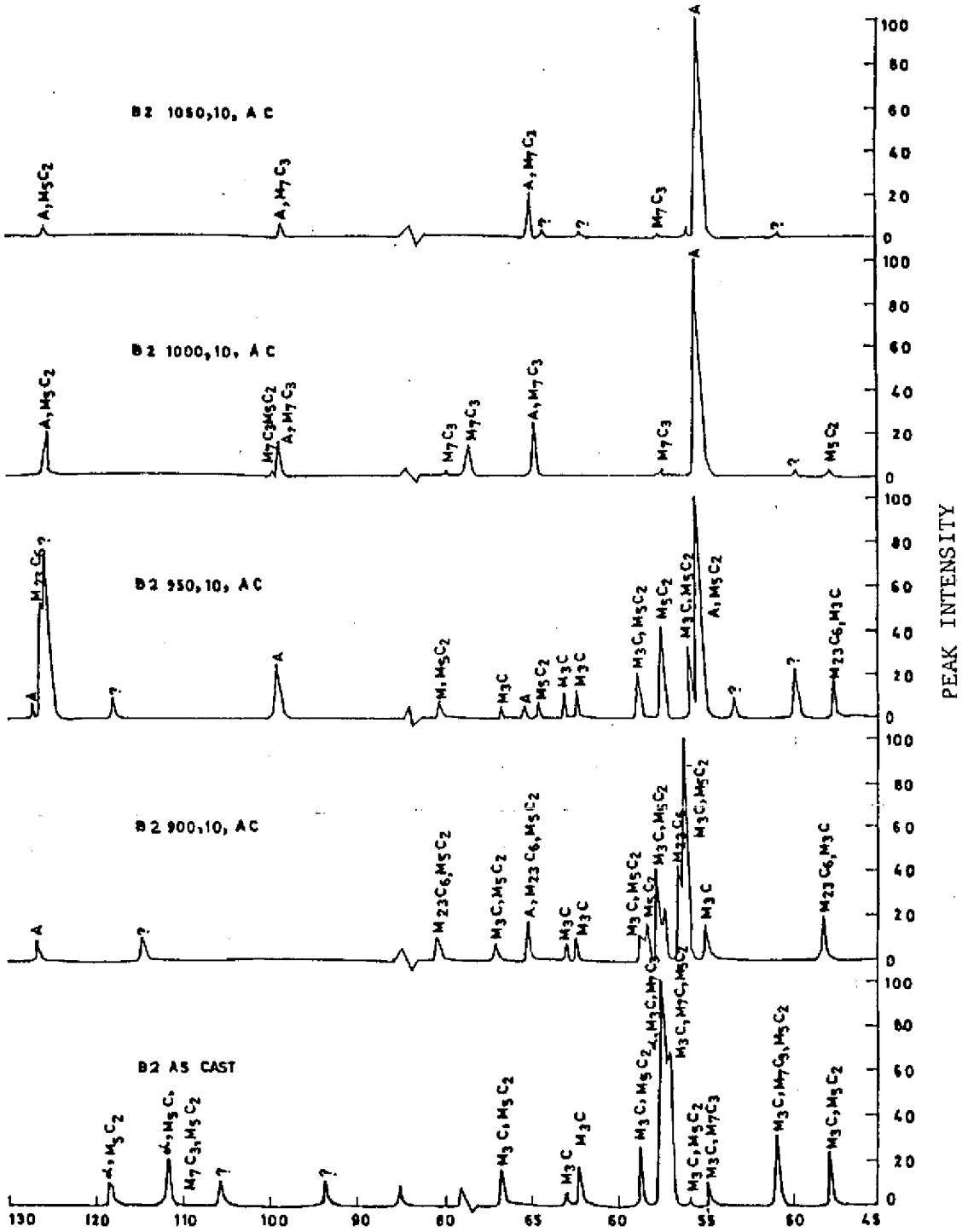

FIG. 5.2- COMPARATIVE X-RAY DIFFRACTOGRAMS OF ALLOY B2

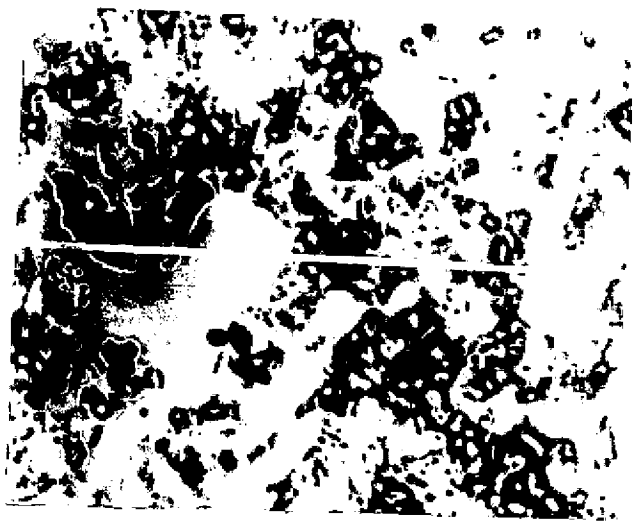

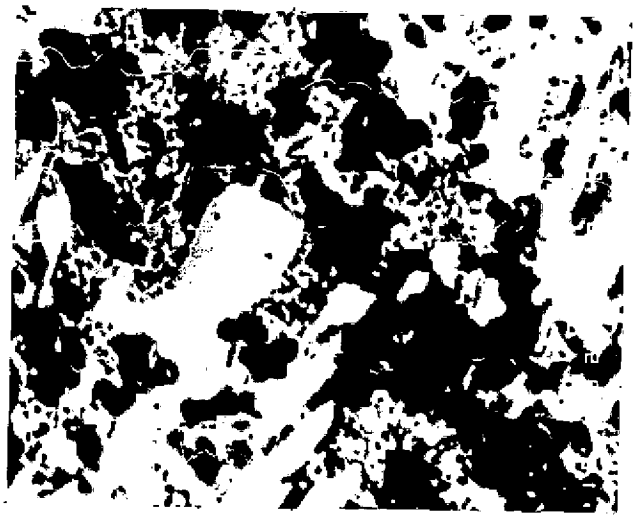

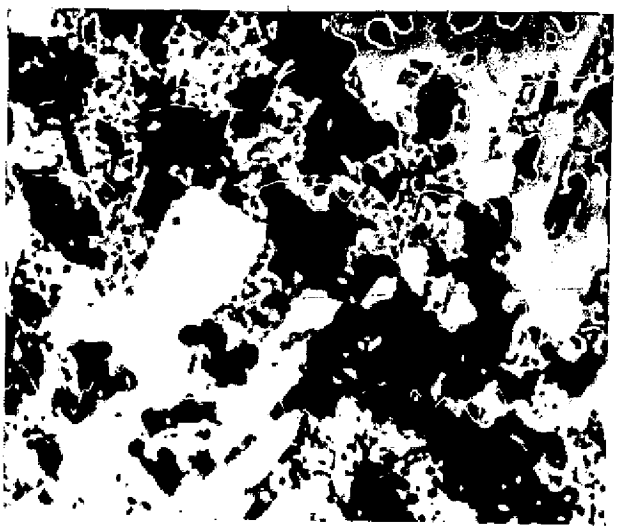

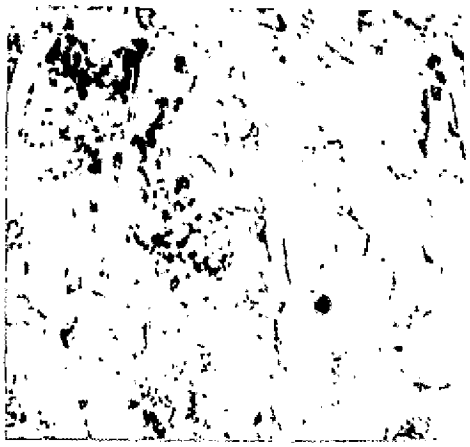

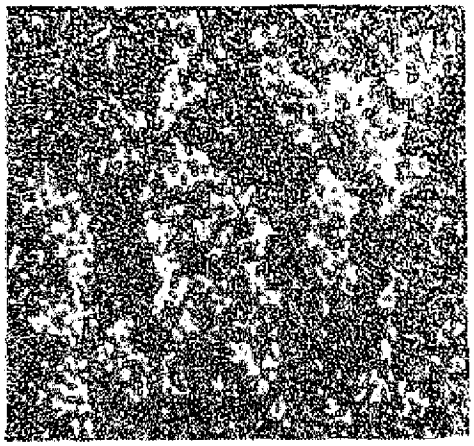

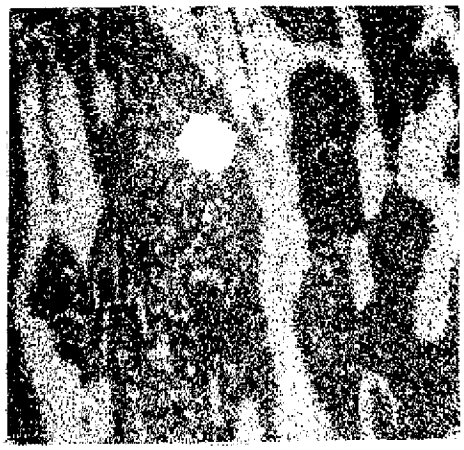

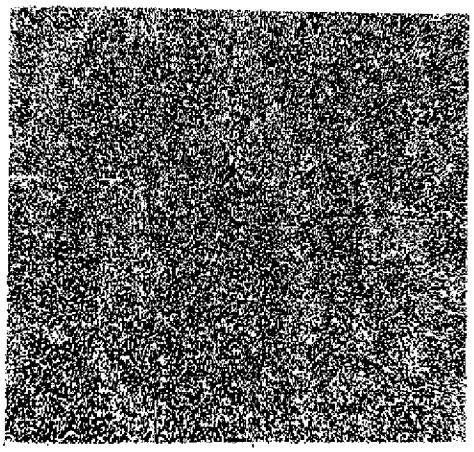

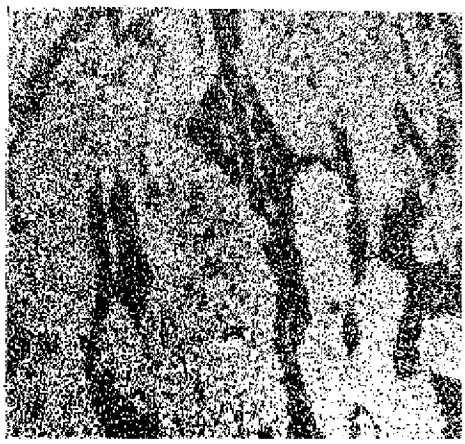

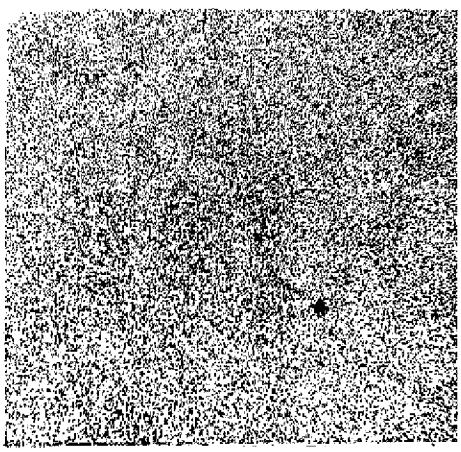

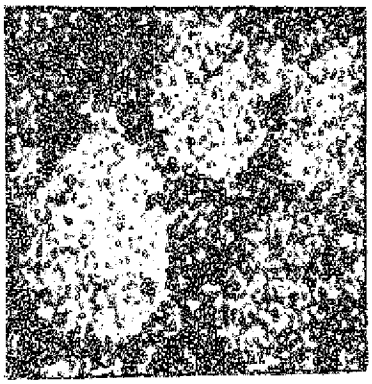

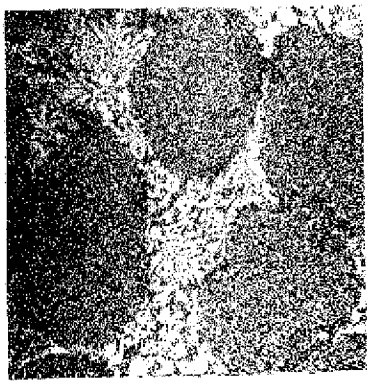

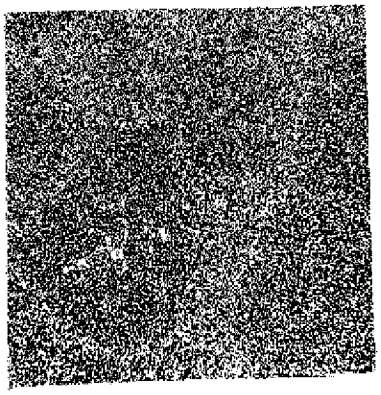

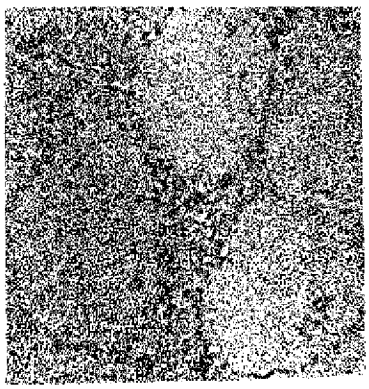

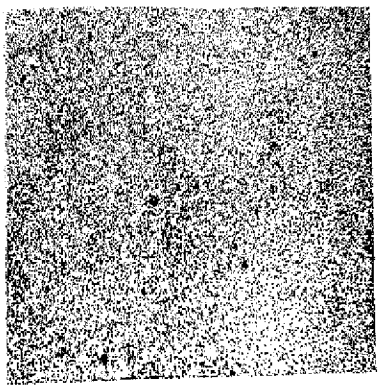

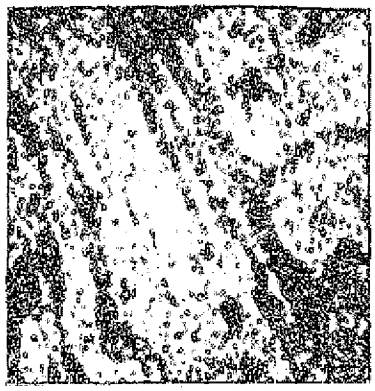

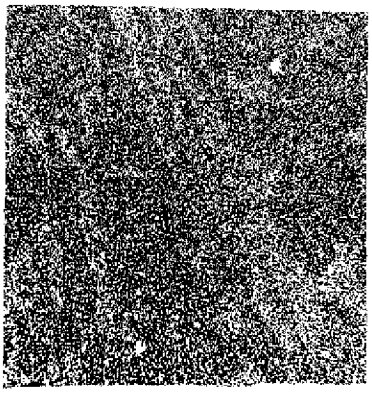

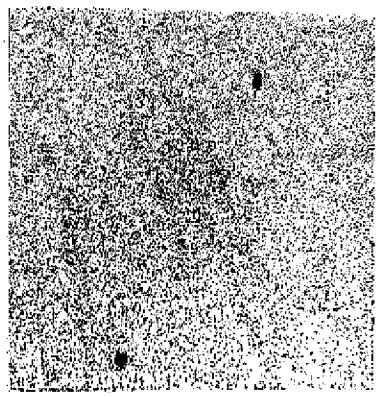

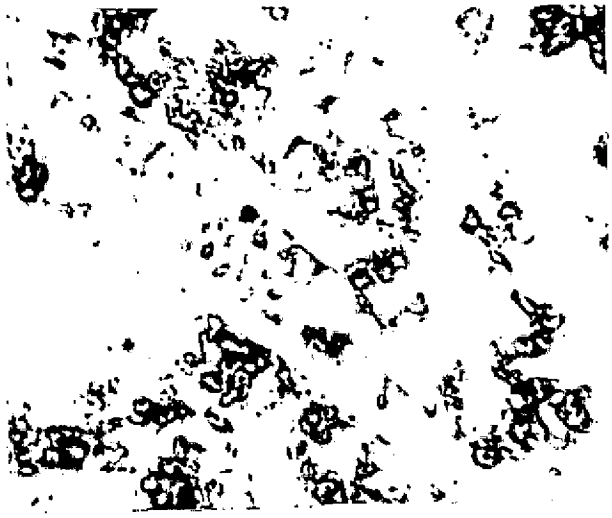

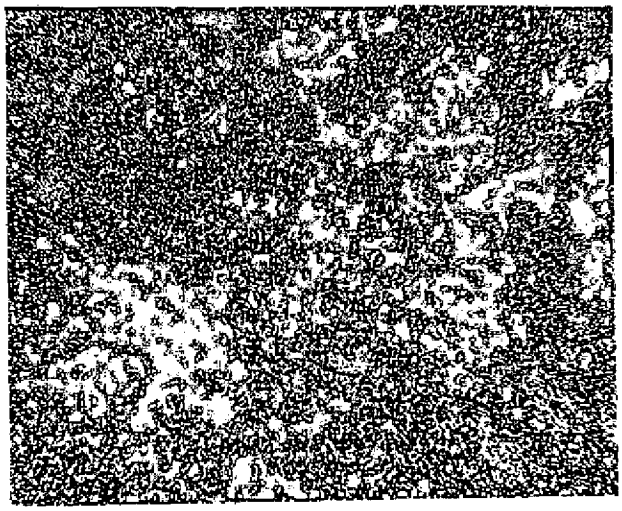

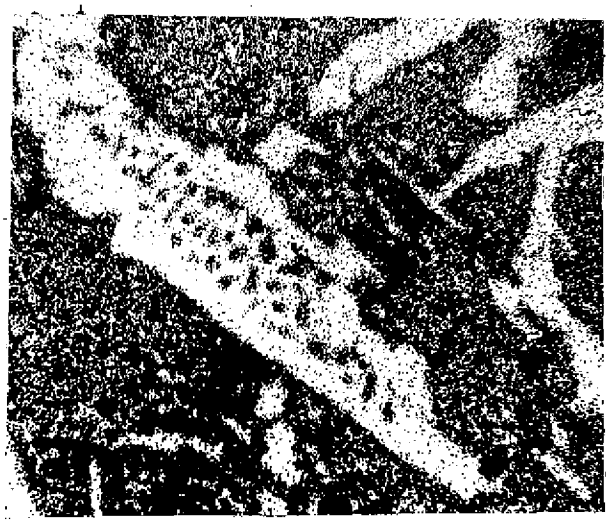

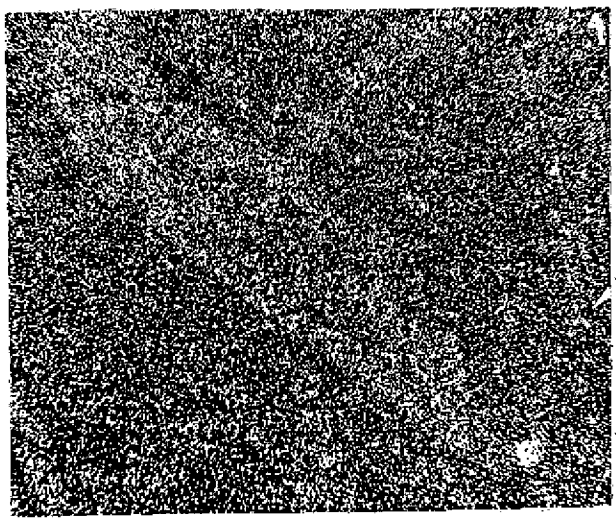

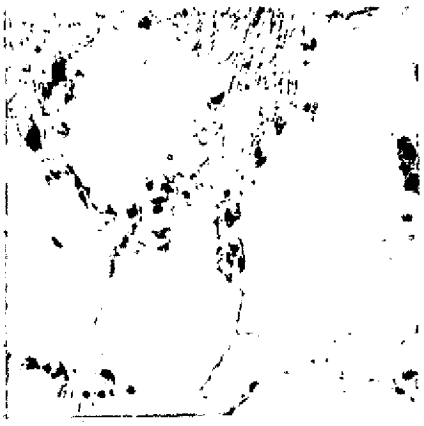

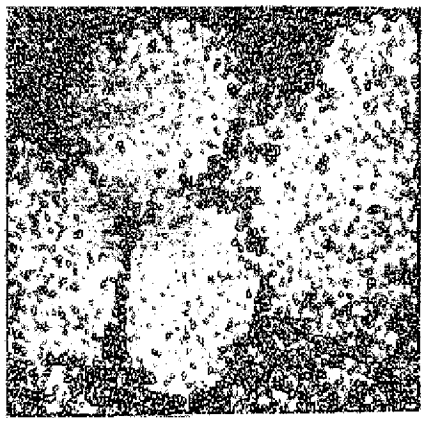

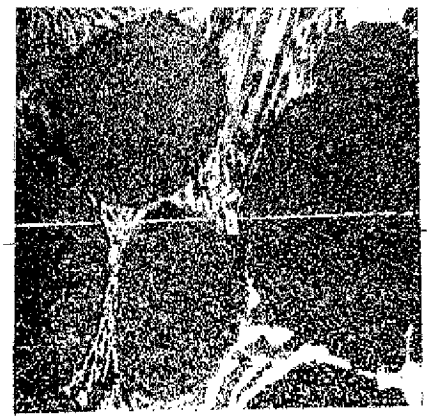

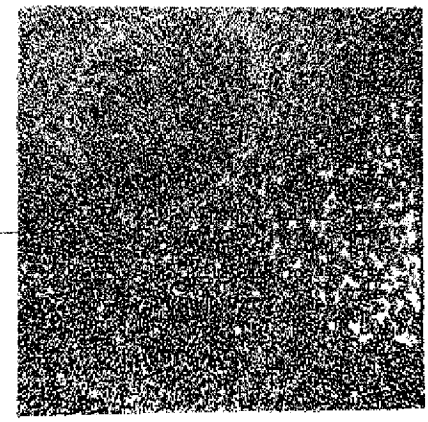

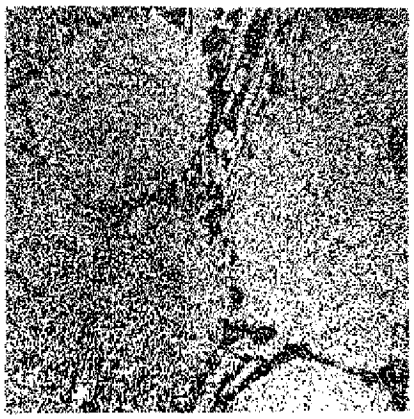

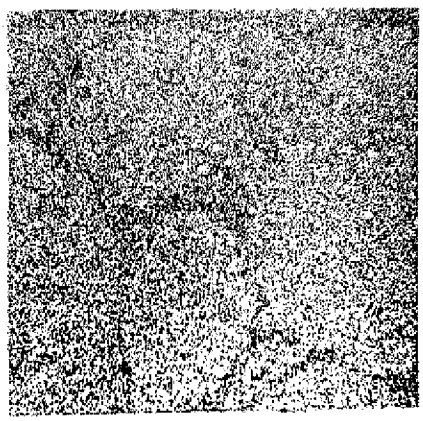

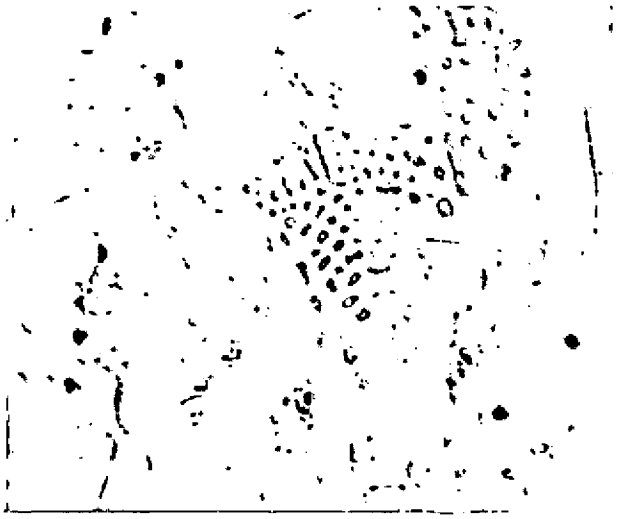

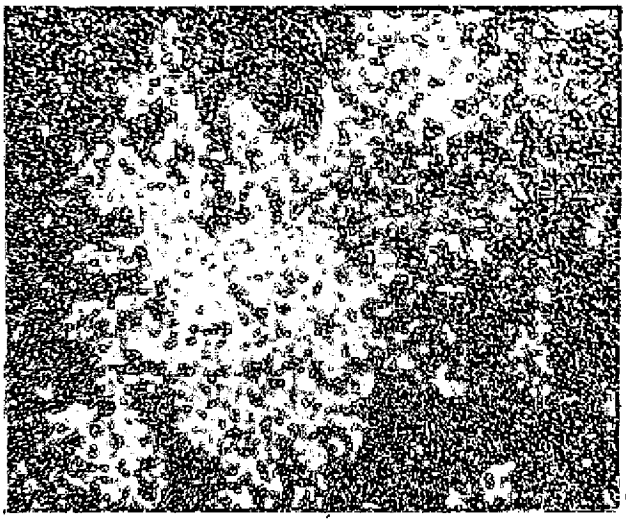

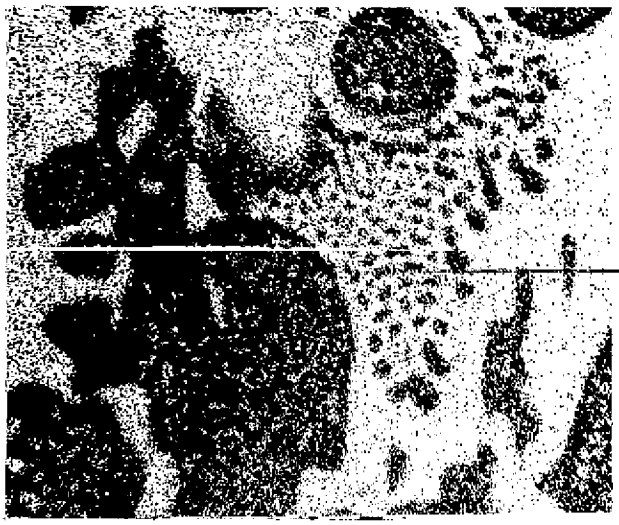

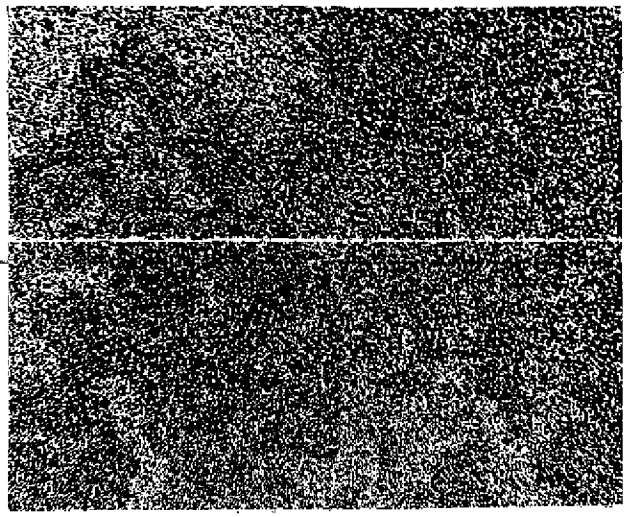

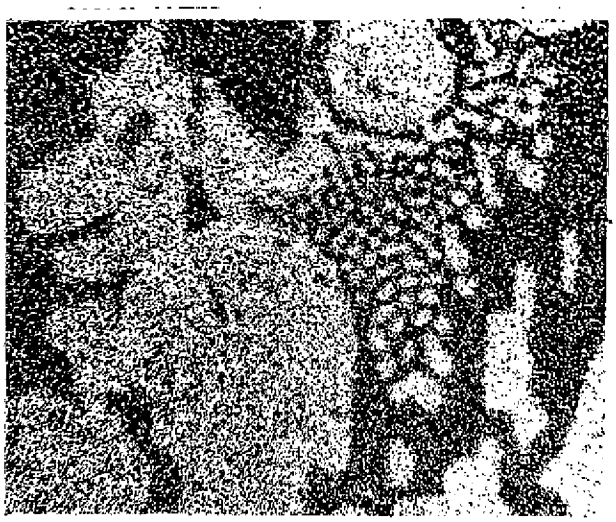

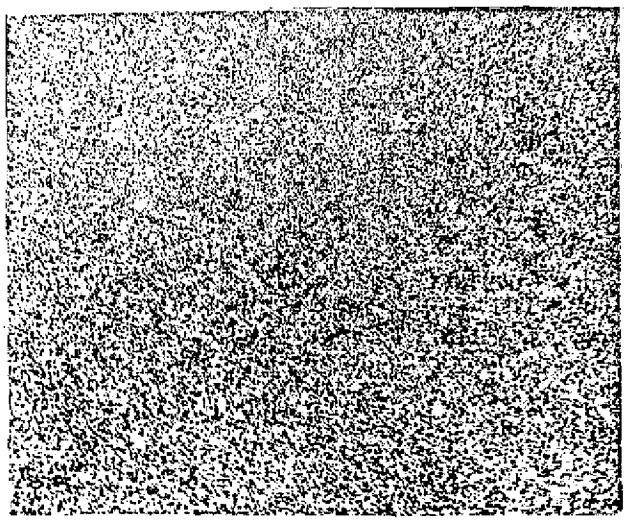

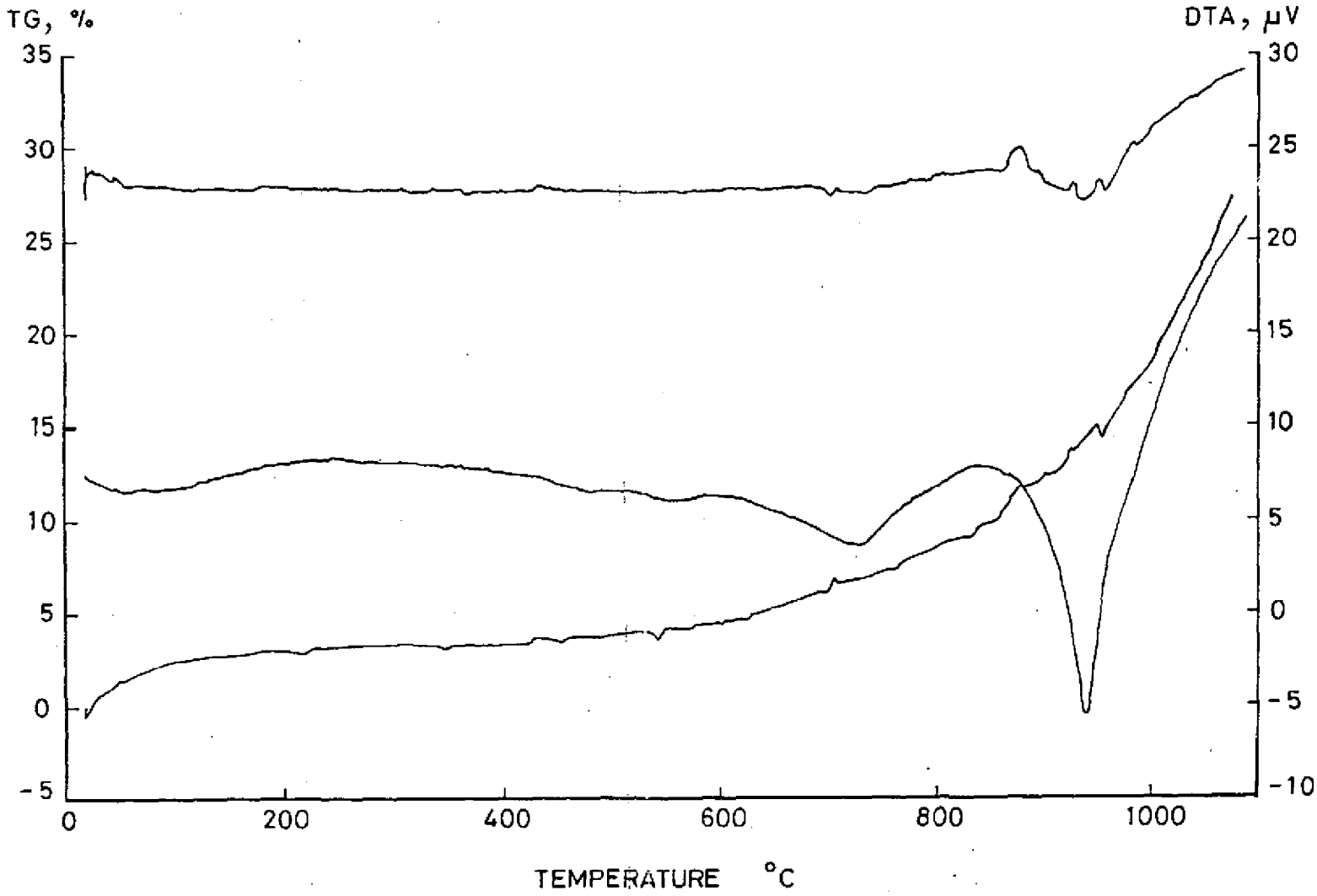

FIG. 5.12 DIFFERENTIAL THERMAL ANALYSIS PLOT OF ALLOY B_1

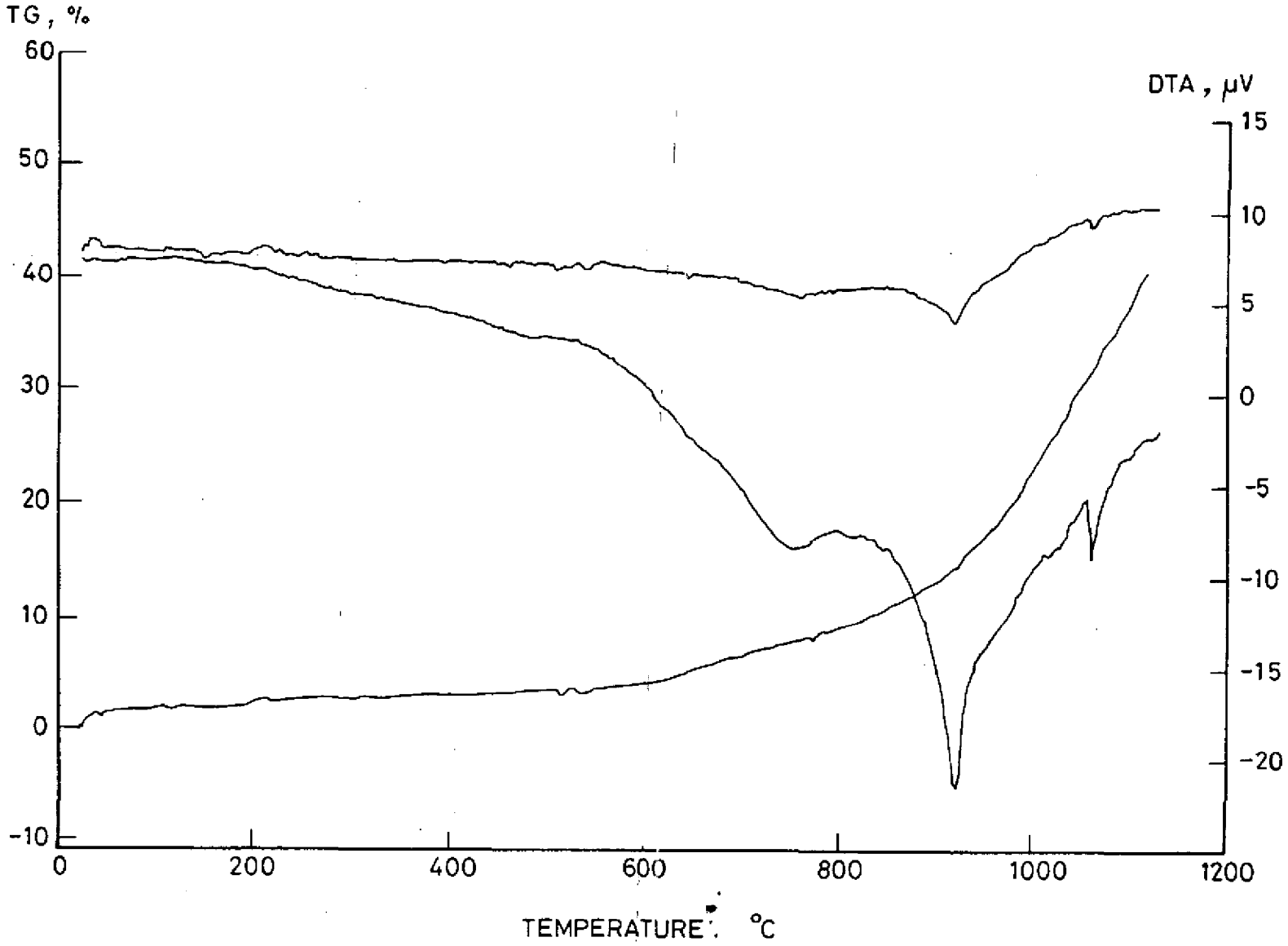

FIG.5.13 DIFFERENTIAL THERMAL ANALYSIS PLOT OF ALLOY B_2

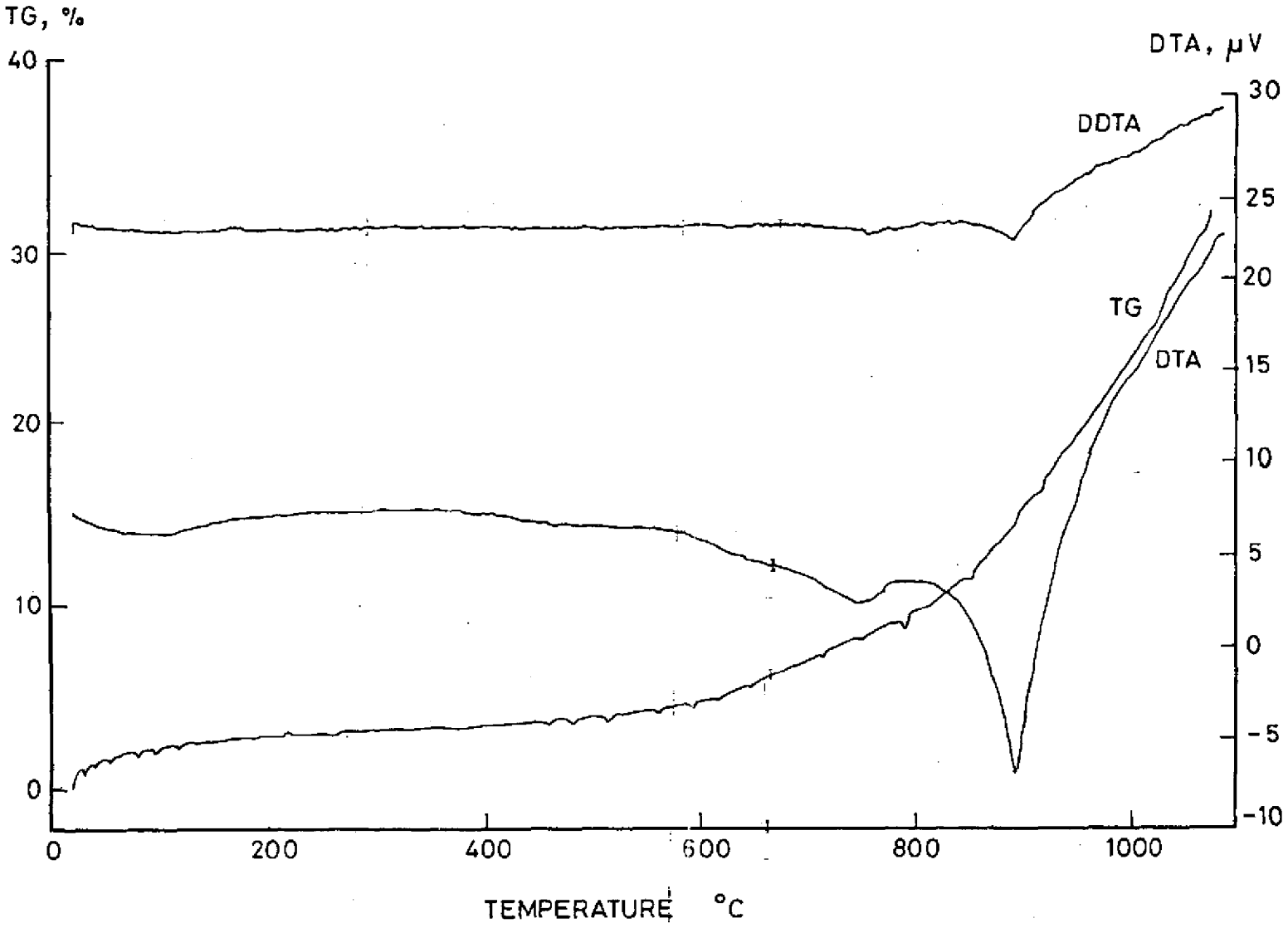

FIG.5.14 DIFFERENTIAL THERMAL ANALYSIS PLOT OF ALLOY B_3

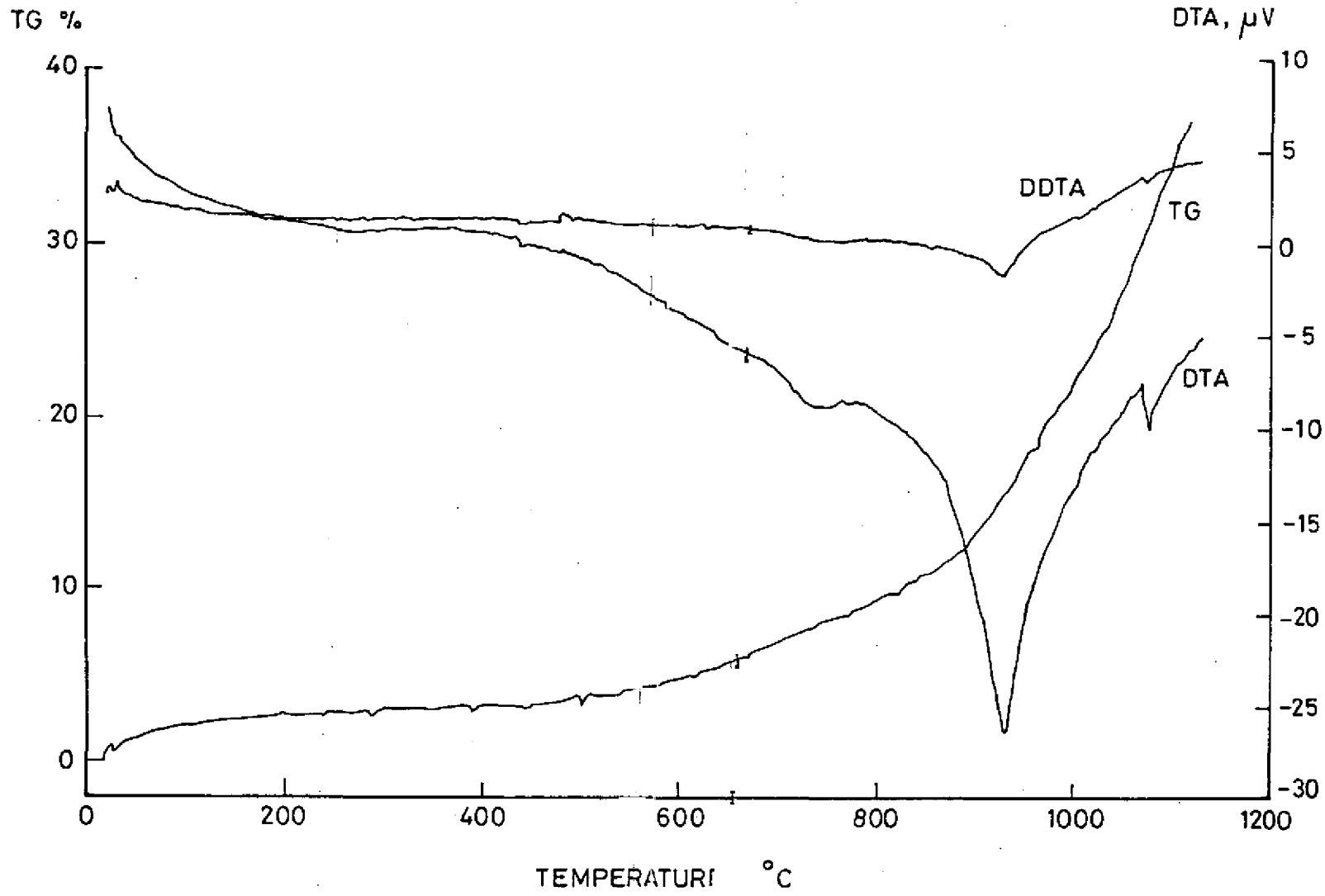

FIG.5.15 DIFFERENTIAL THERMAL ANALYSIS PLOT OF ALLOY B_4

Fig. 5.16 A summary plot of differential thermal analysis of experimental alloys

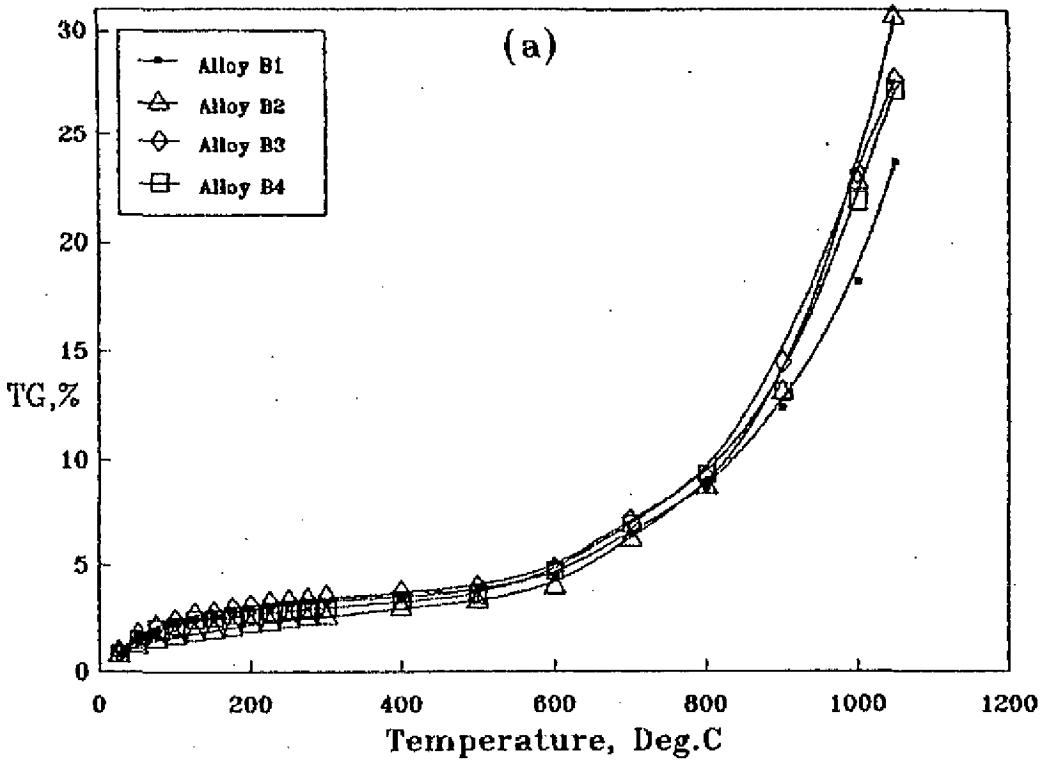

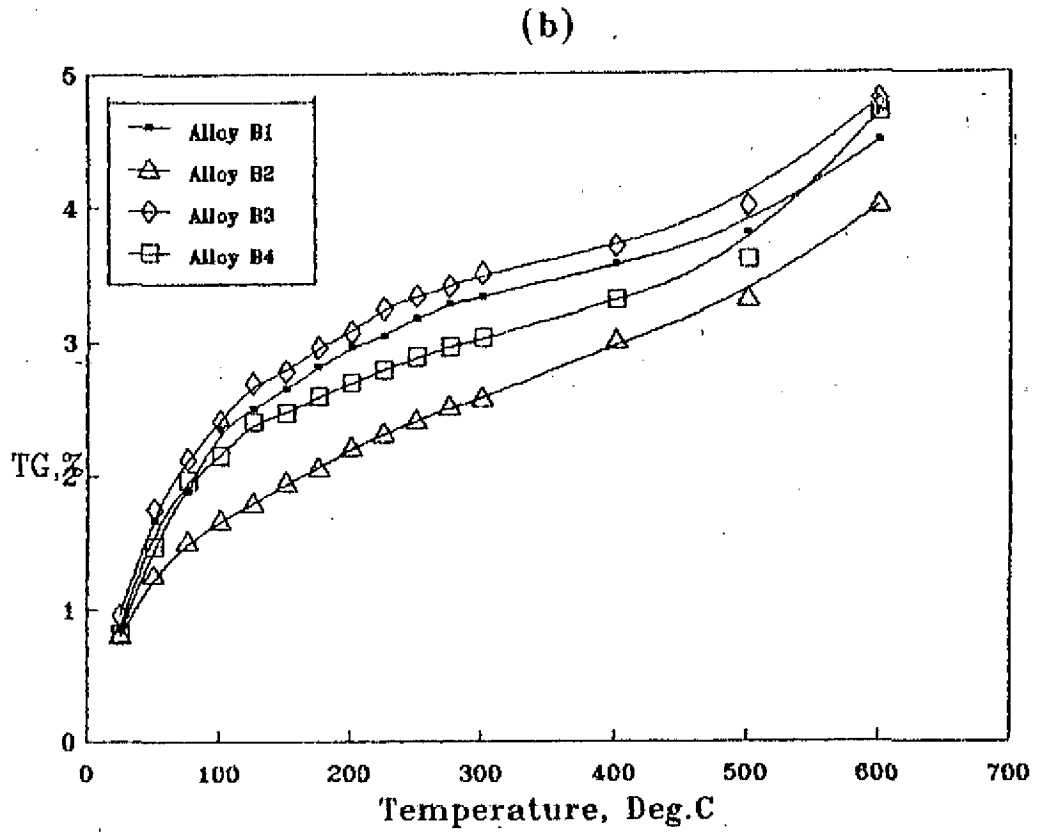

Fig. 5.17 Differential thermal analysis plot at 950 deg.C

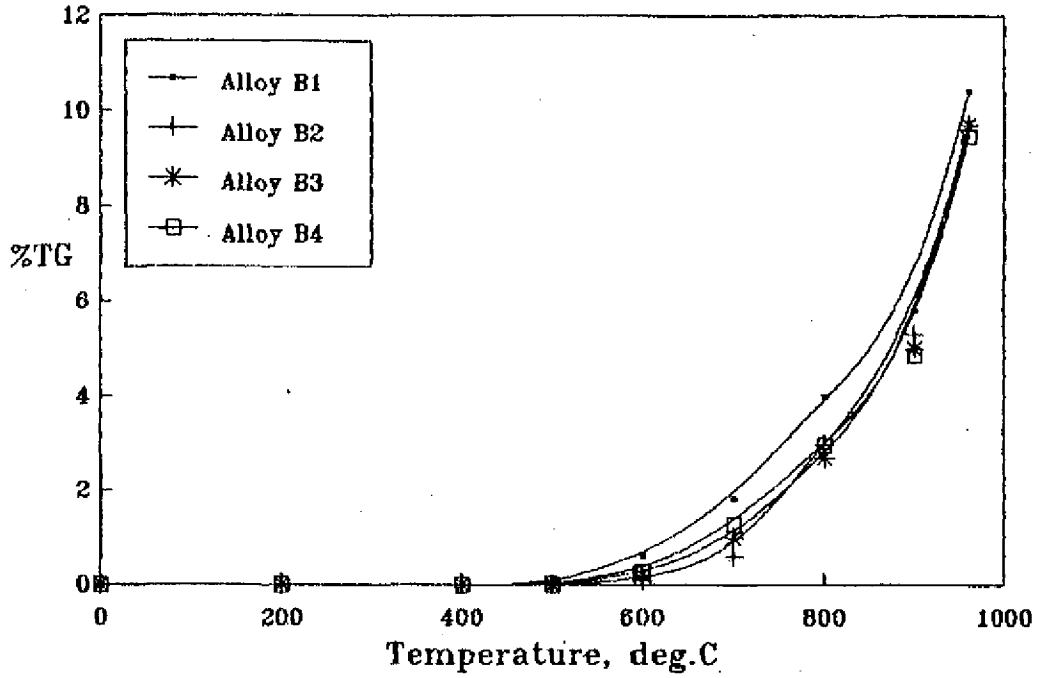

Fig. 5.18 Differential thermal analysis plot at 1050 deg.C

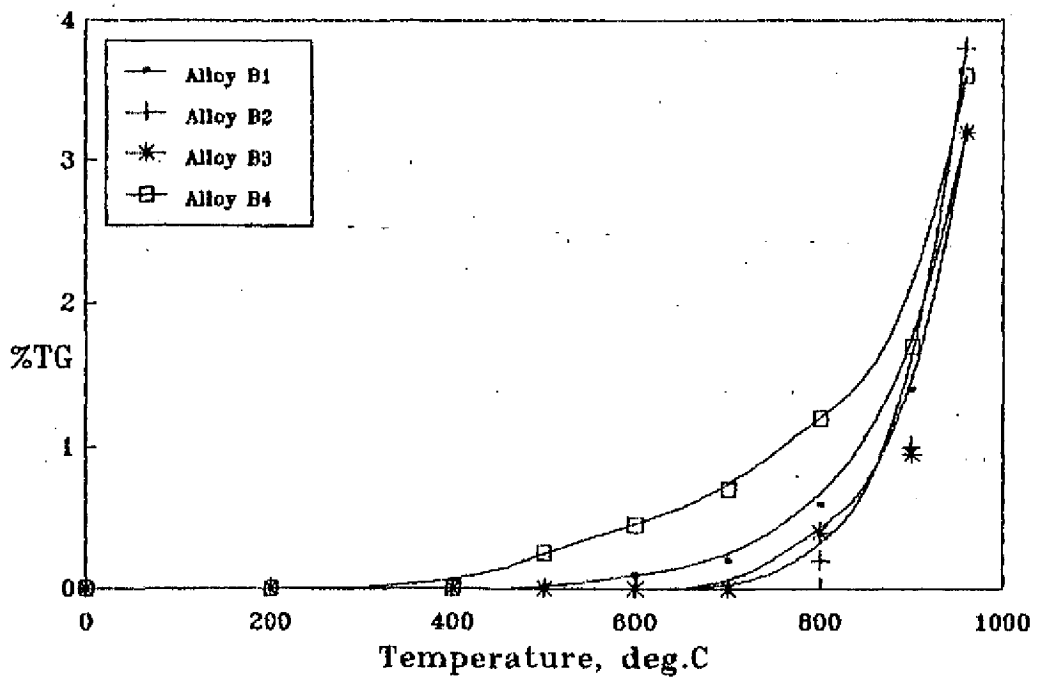

Fig. 5.19 A plot of experimental vs predicted %TG in the experimental alloys

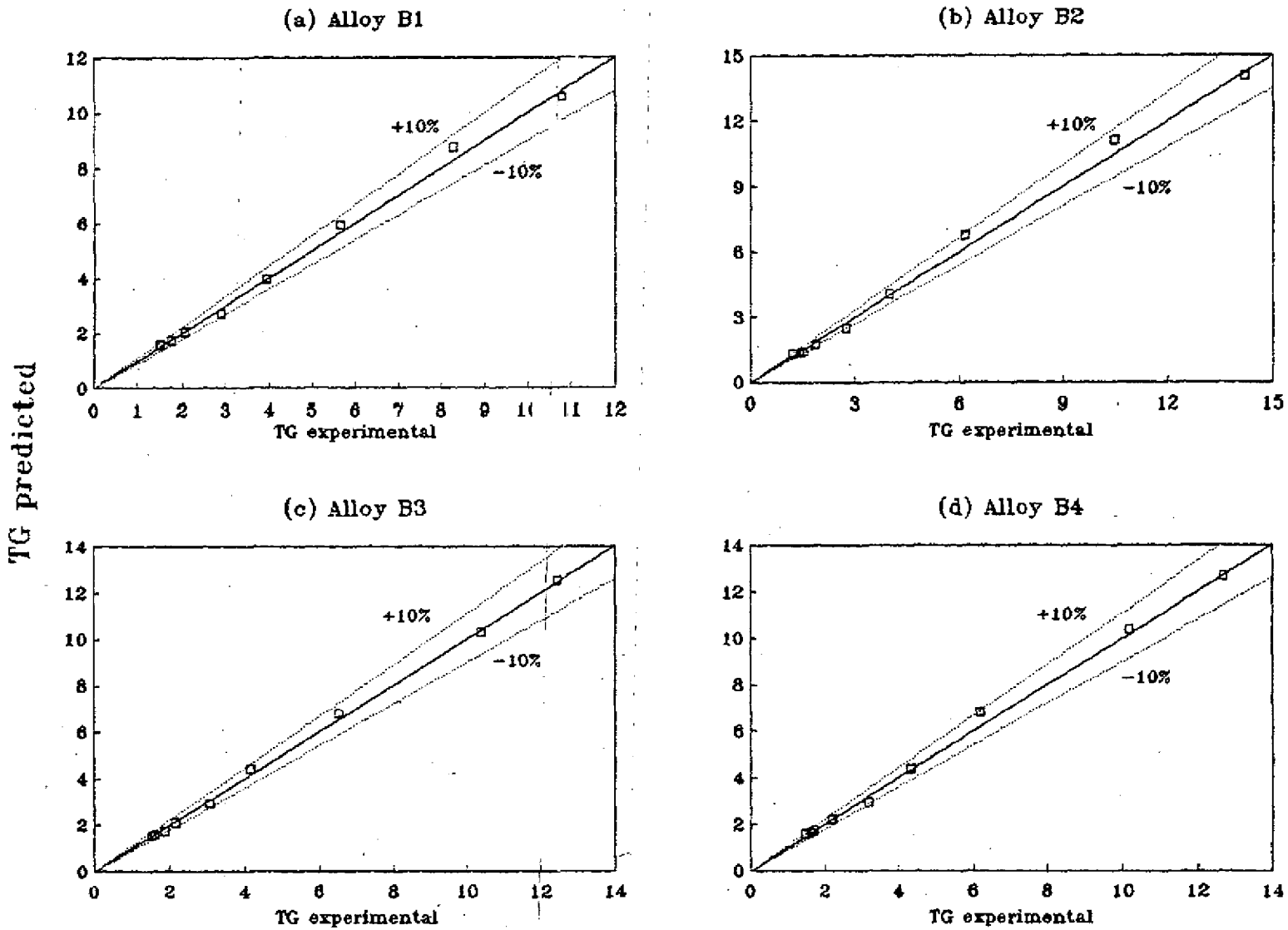

Fig. 6.1 Tafel plot of Alloy B1 in 5% NaCl solution

(a) B1,950,10,AC

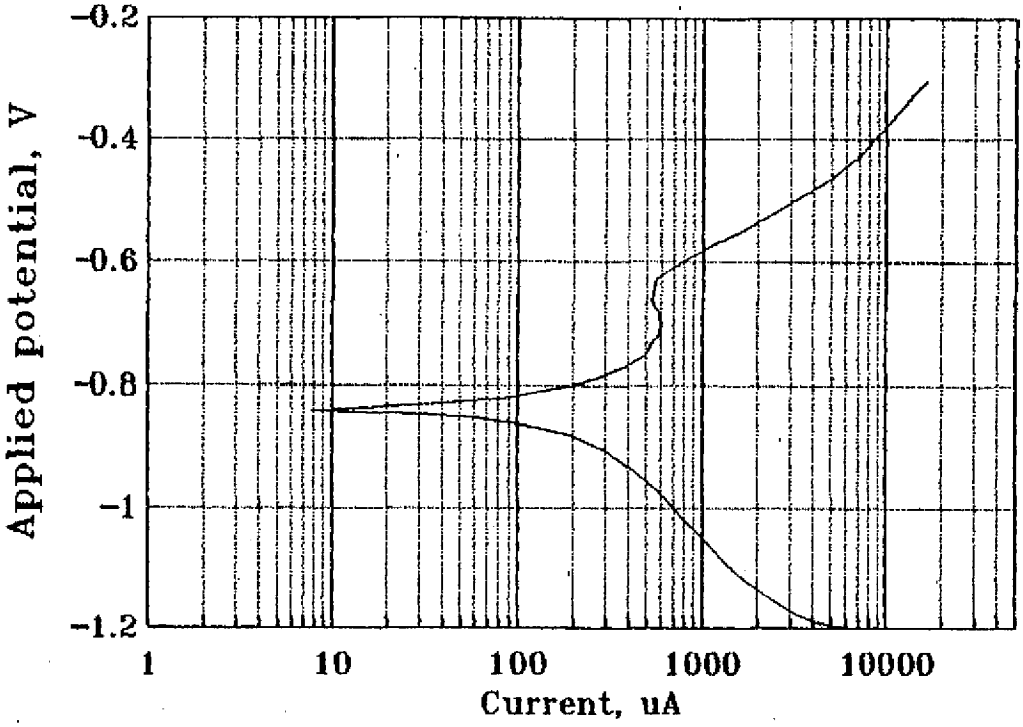

(b) B1,1050,10,AC

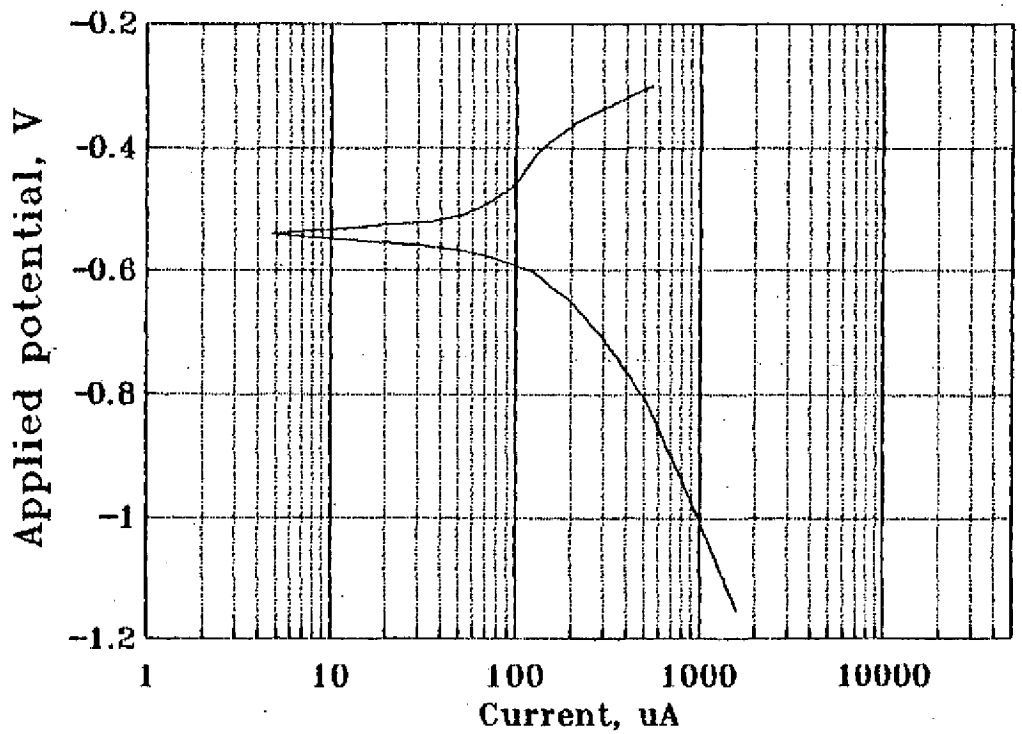

Fig. 6.2 Tafel plot of Alloy B2 in 5% NaCl solution

(a) B2,900,10,AC

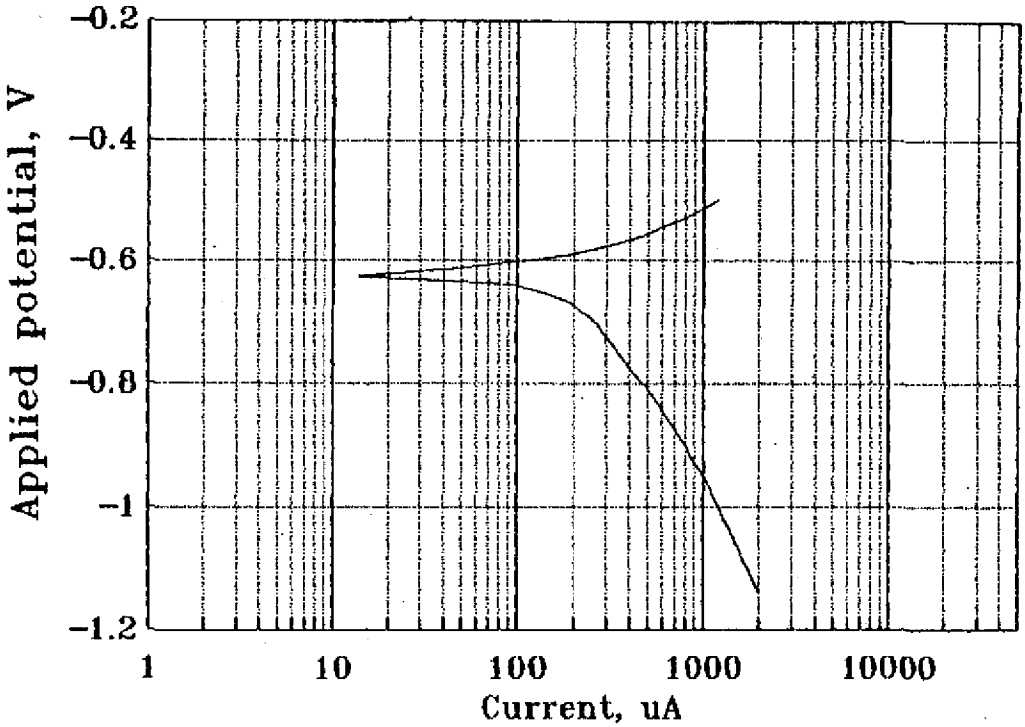

(b) B2,950,10 AC

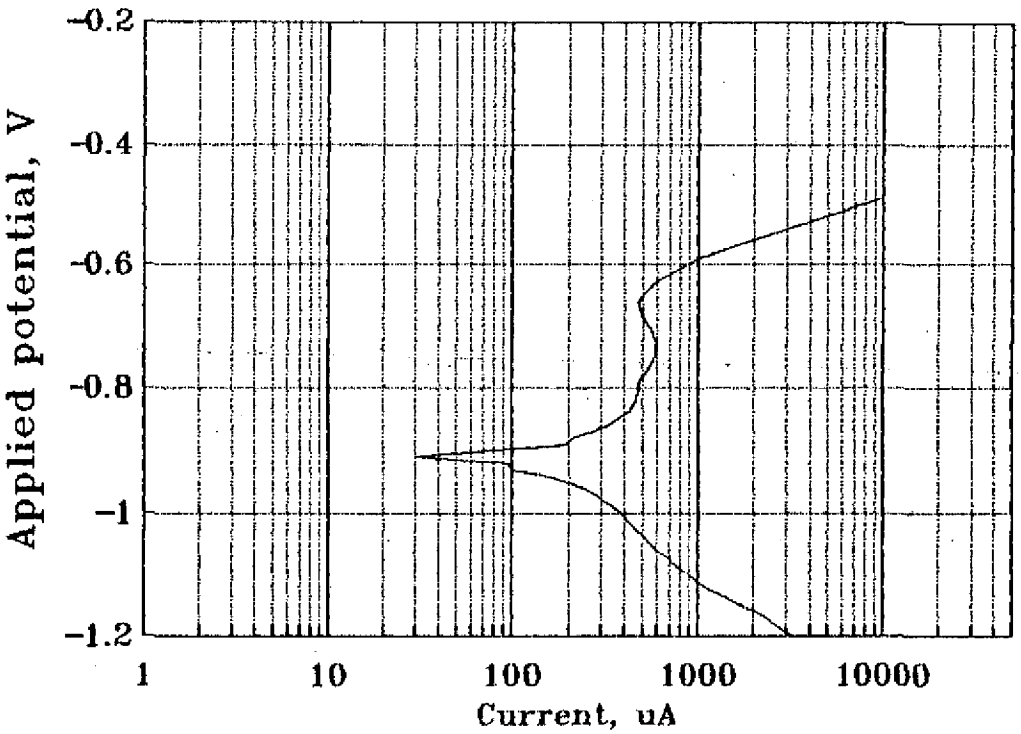

(c) B2,1000,10,AC

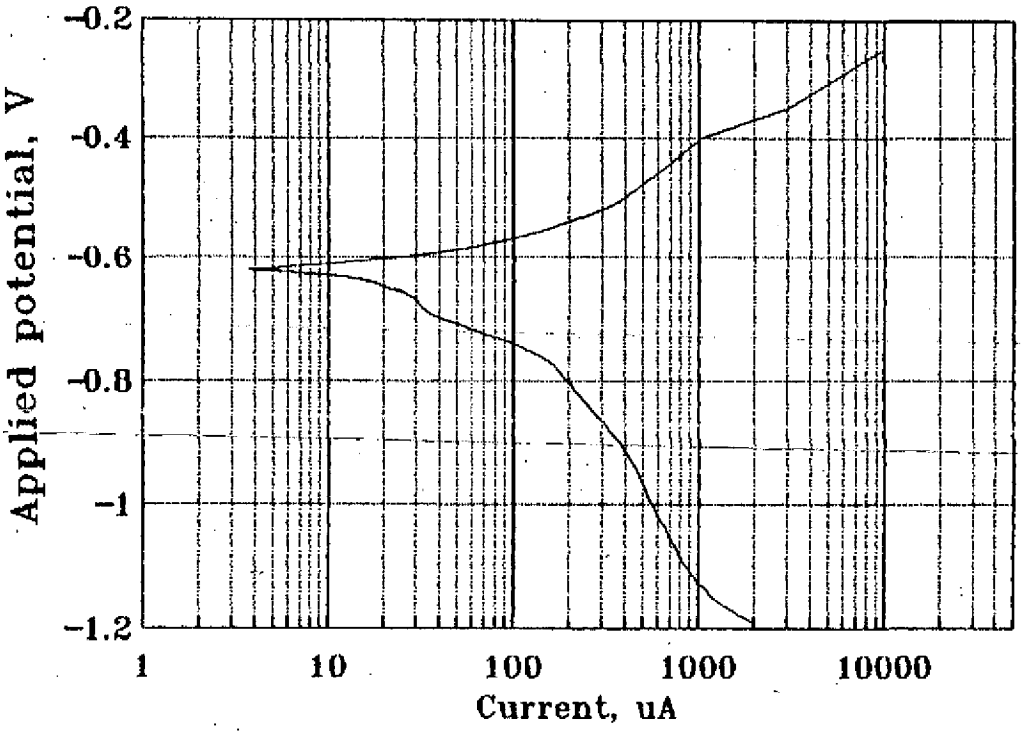

(d) B2,1050,4,AC

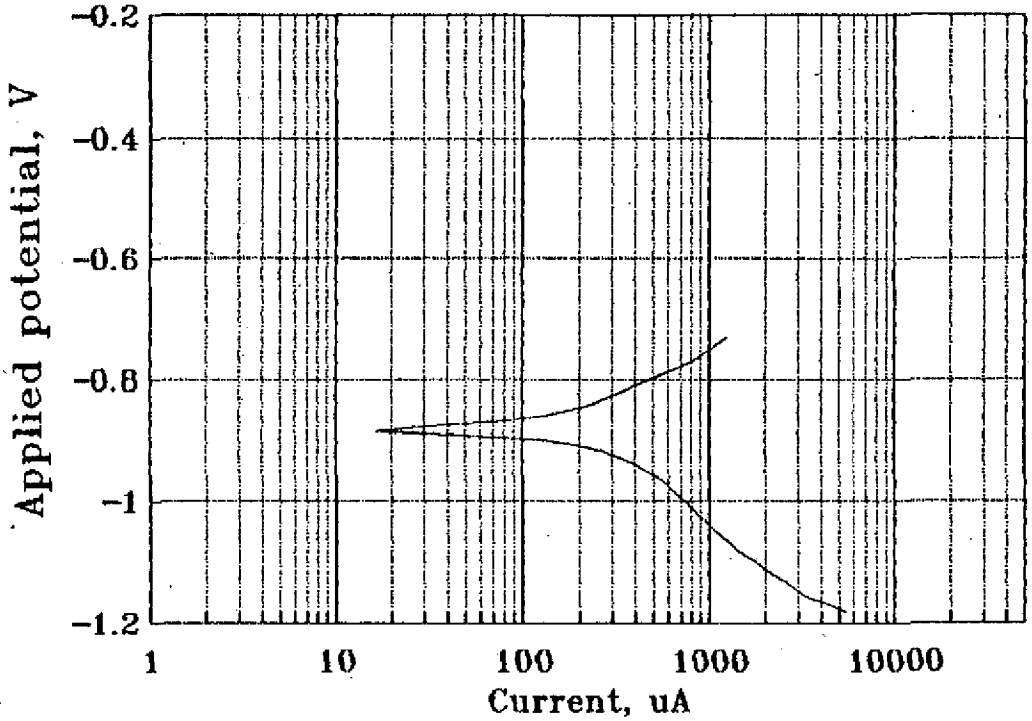

(e) B2,1050,10,AC

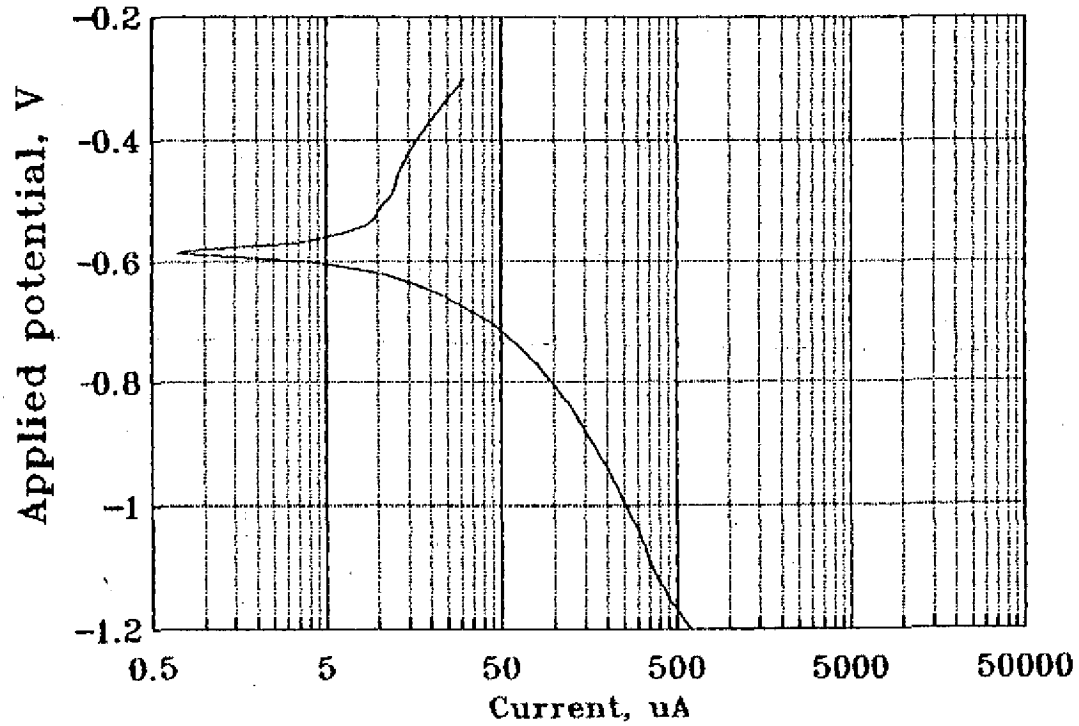

Fig. 6.3 Tafel plot of Alloy B3 in 5% NaCl solution

(a) B3,950,10,AC

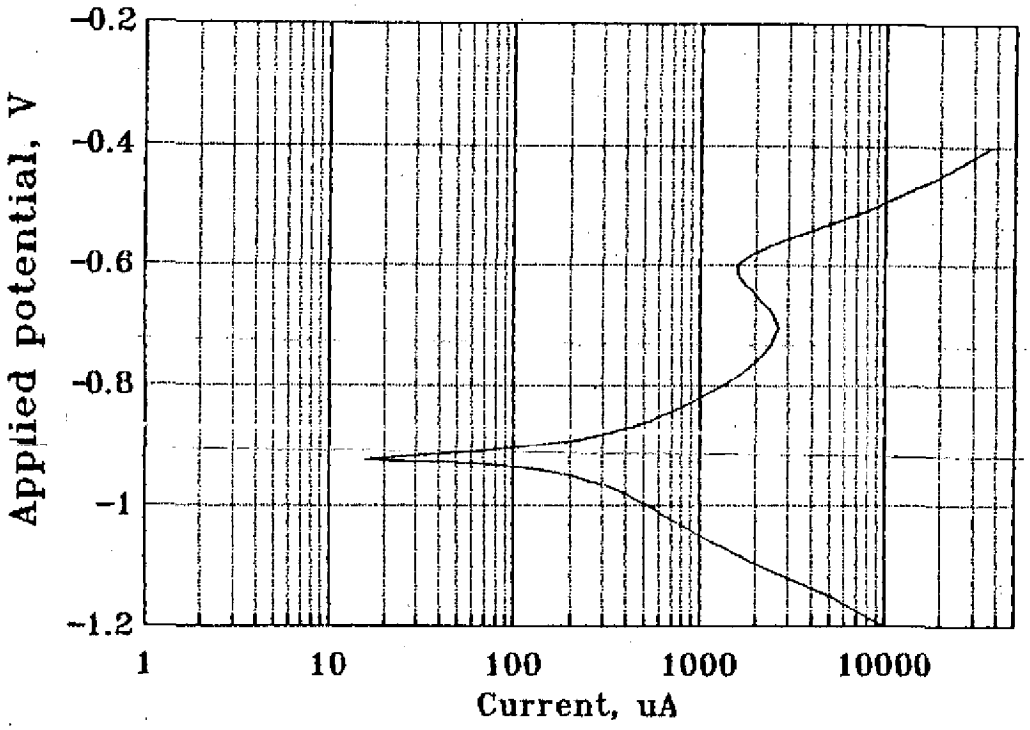

(b) B3,1050,4,AC

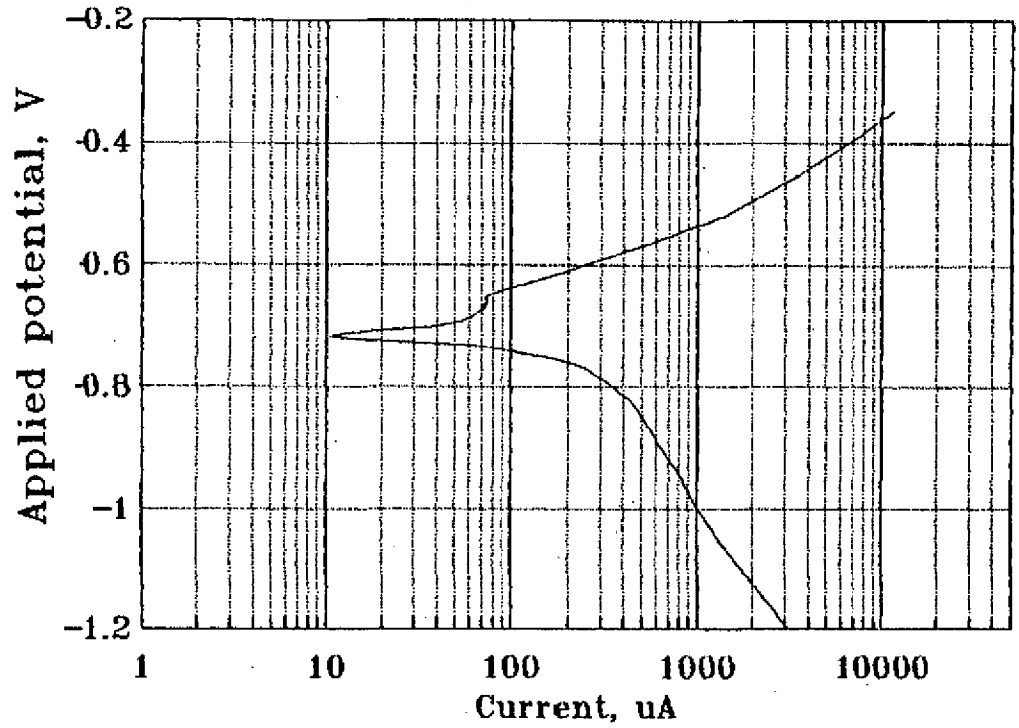

(c) B3,1050,10,AC

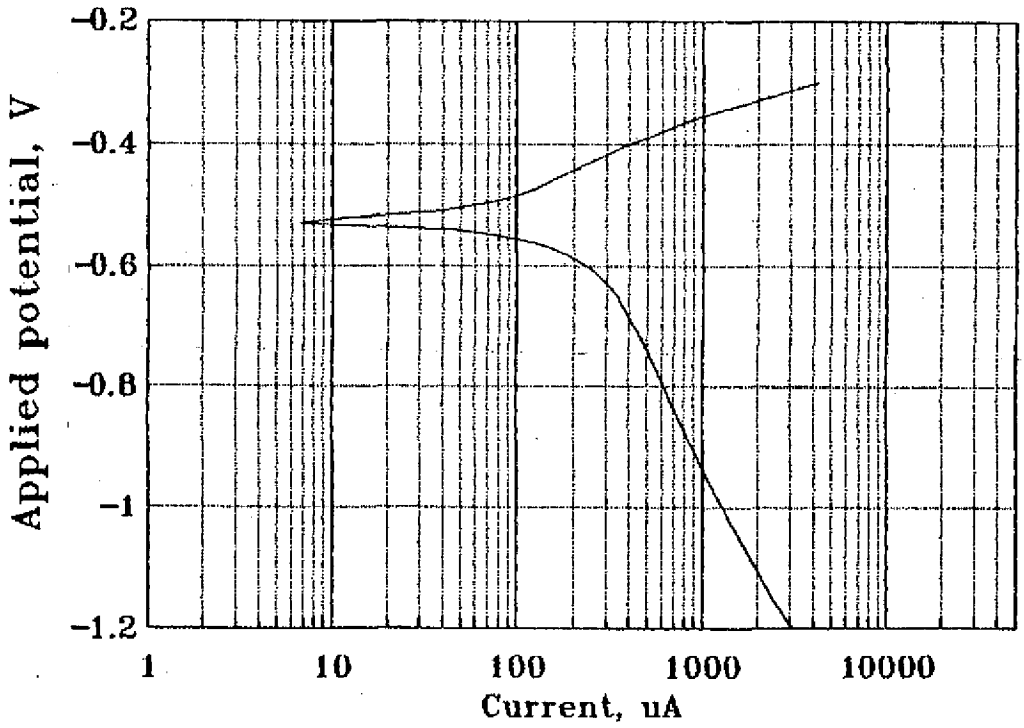

Fig. 6.4 Tafel plot of Alloy B4 in 5% NaCl solution

(a) B4,900,10,AC

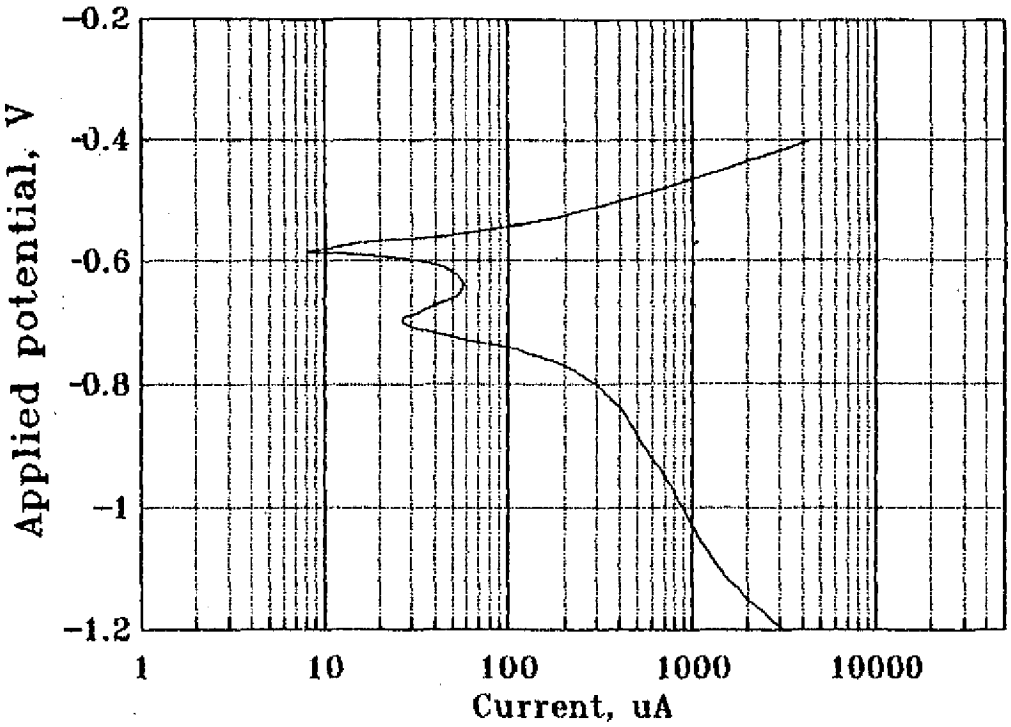

(b) B4,950,10,AC

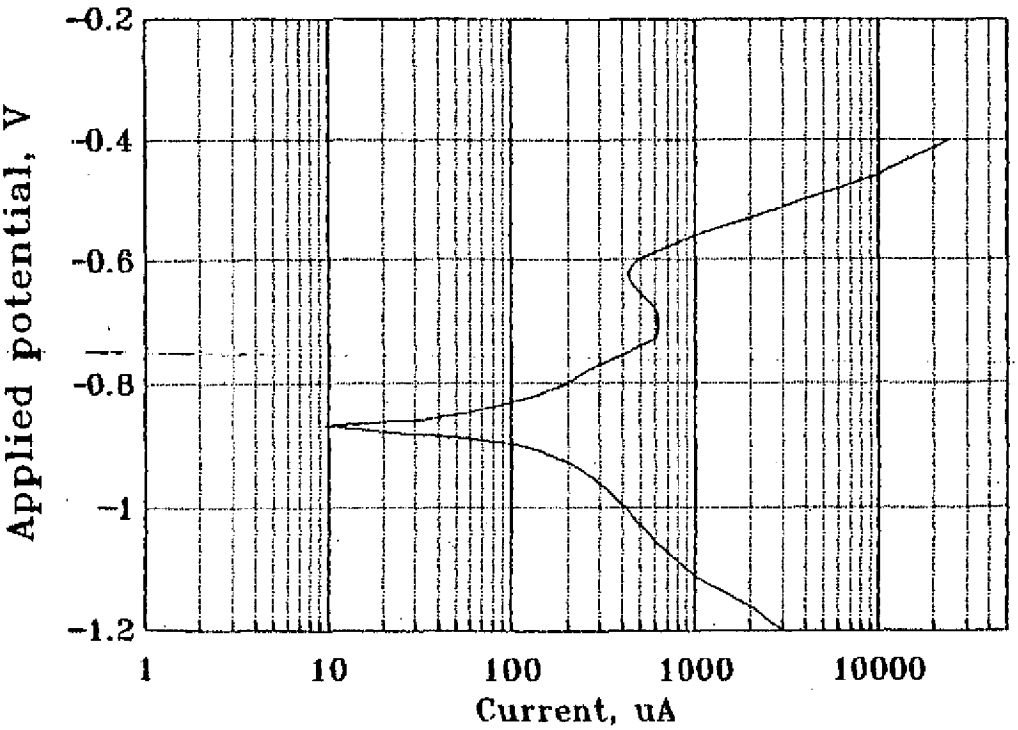

(c) B4,1000,10,AC

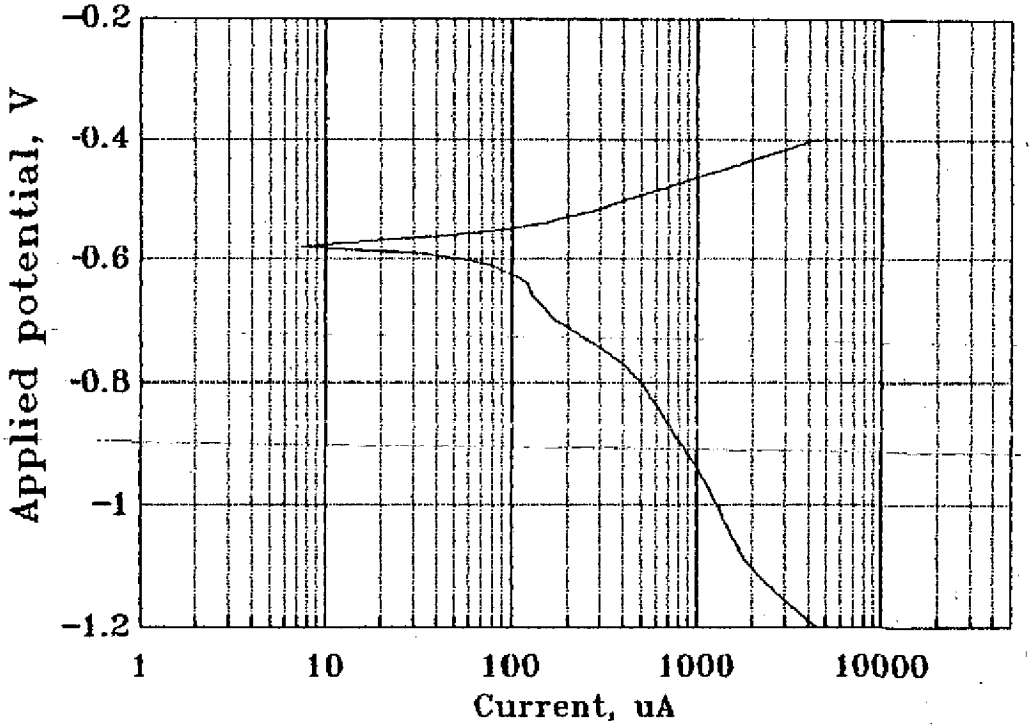

(d) B4,1050,4,AC

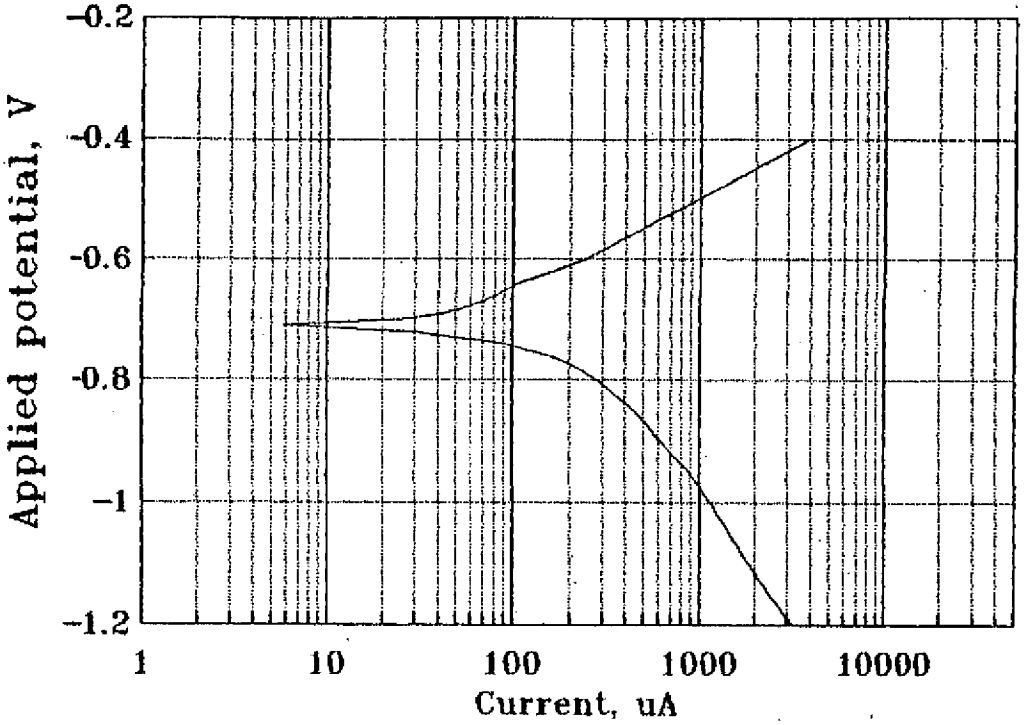

(e) B4,1050,10,AC

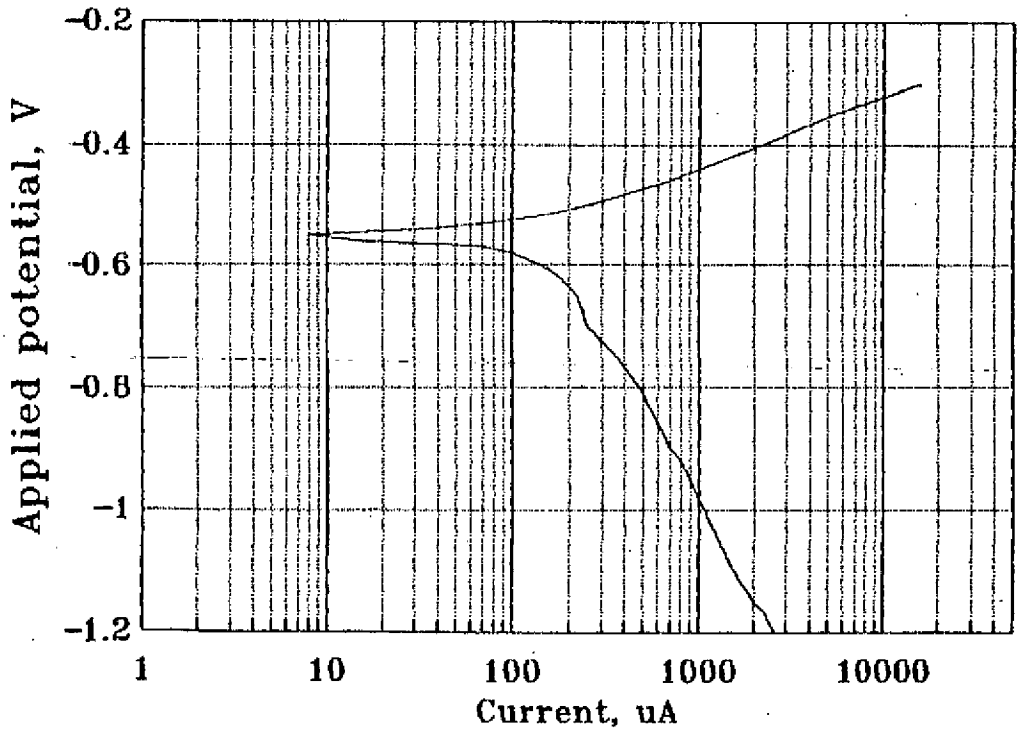

Fig. 6.5 Tafel plot of Ni-resist irons in 5% NaCl Solution

(a) KC

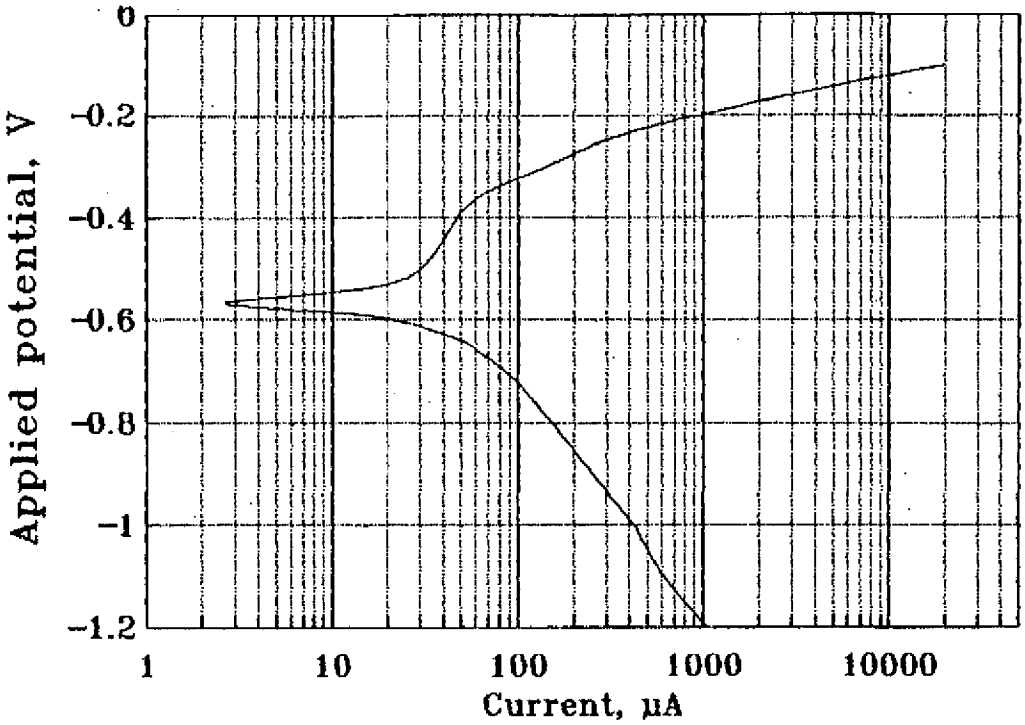

(b) KC1

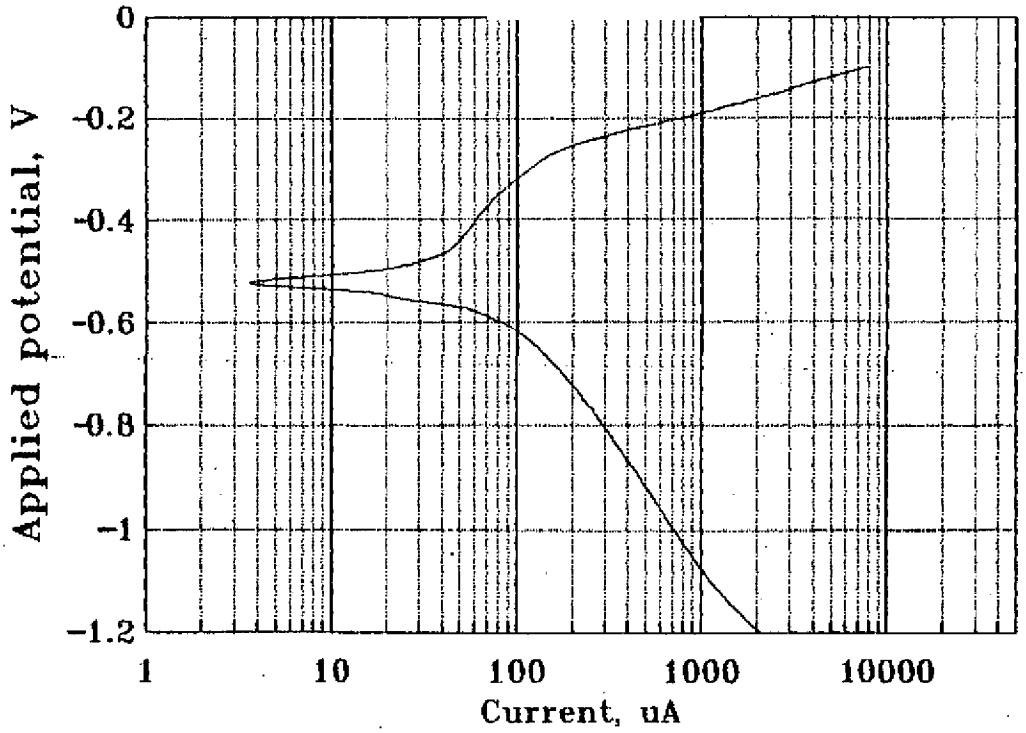

Fig. 6.6 3D plot depicting the effect of VCb & NOP on corrosion rate (168 hours)

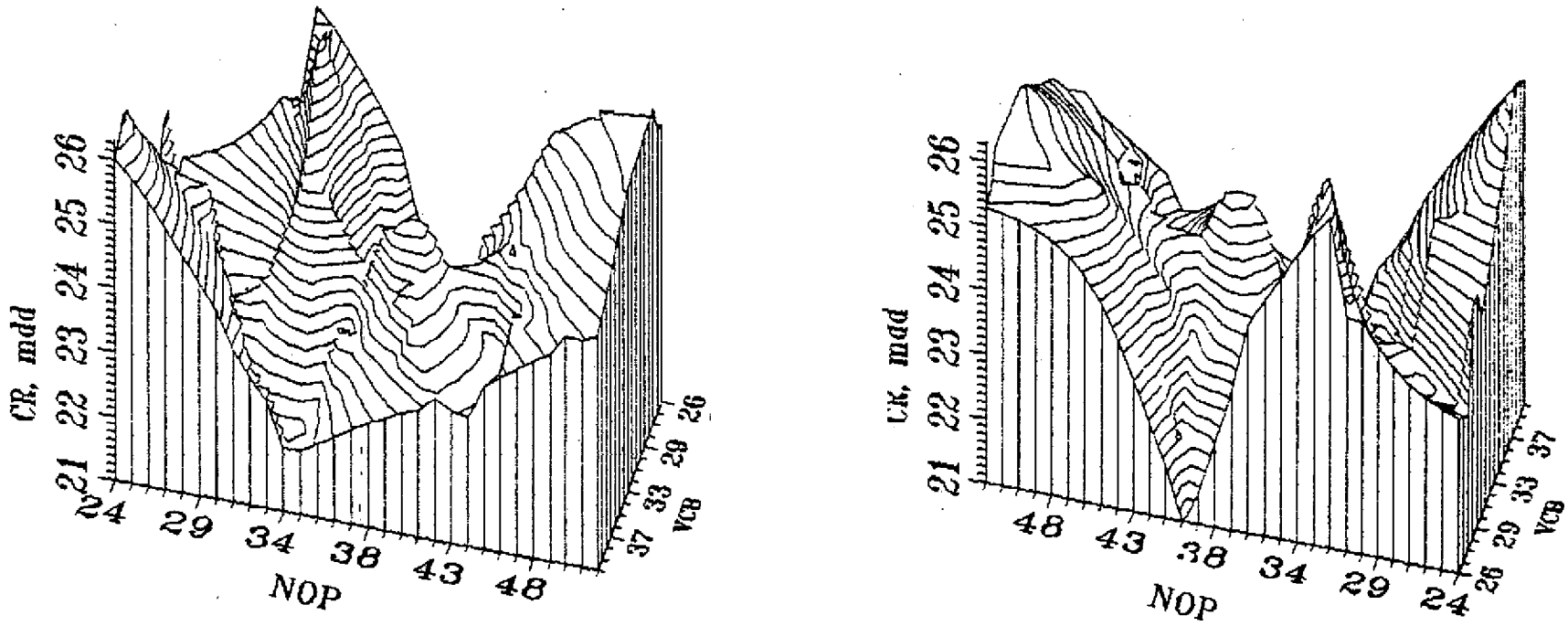

Fig. 6.7 3D plot depicting the effect of VCb & NOP on corrosion rate (720 hours)

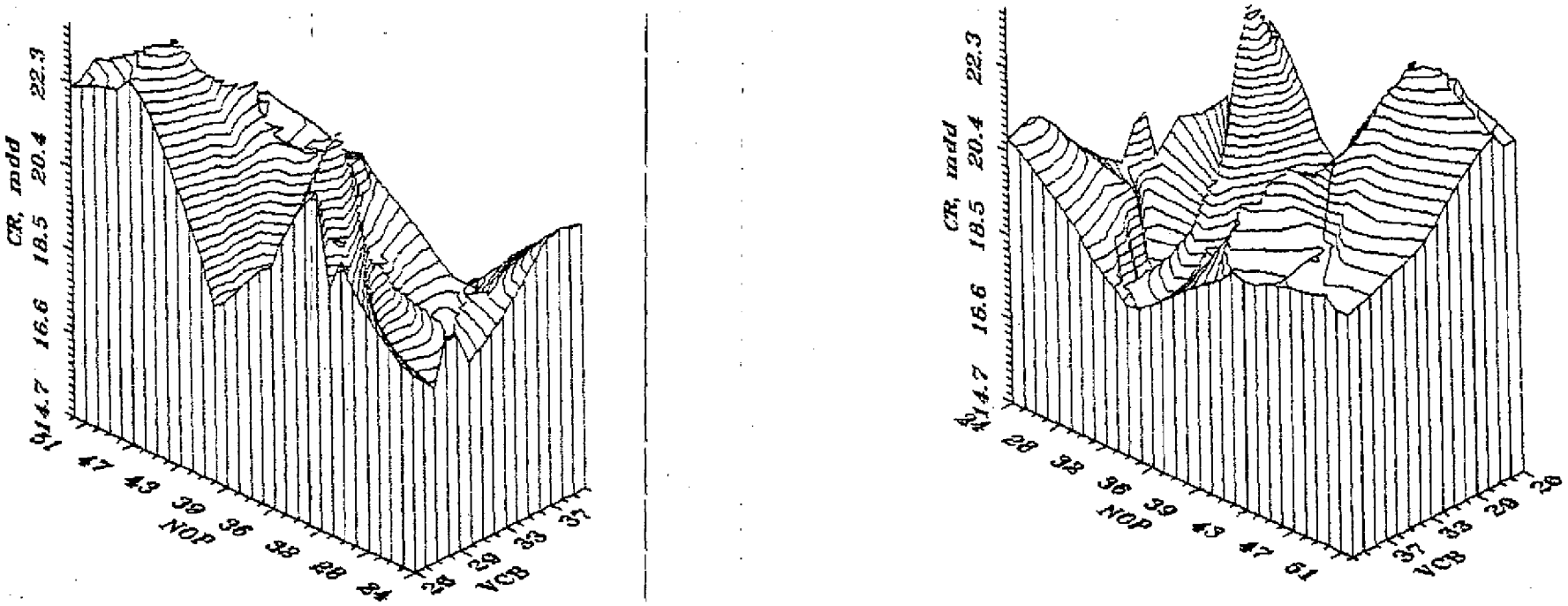

Fig. 6.8 3D plot depicting the effect of VMC & NOP on corrosion rate (168 hours)

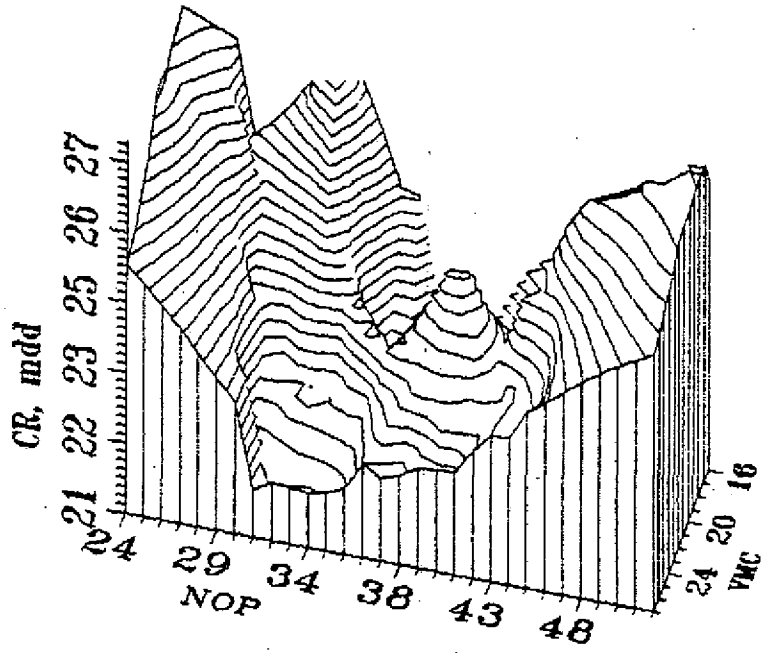

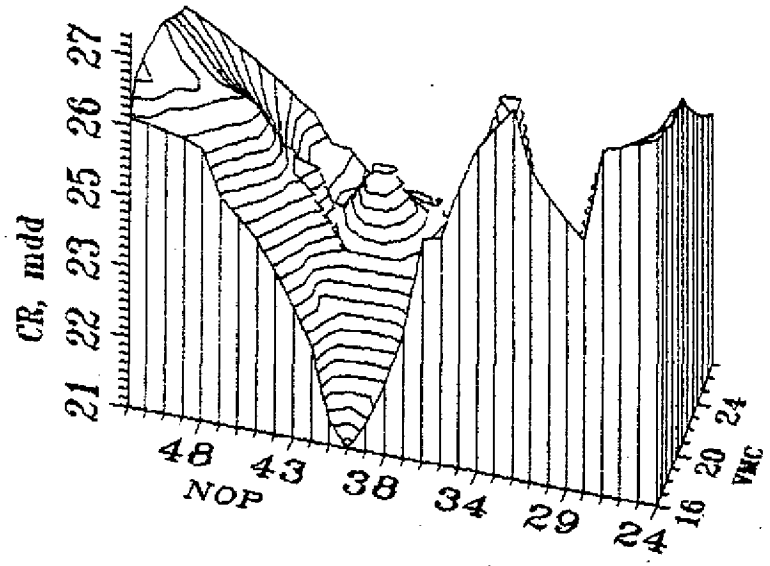

Fig. 6.9 3D plot depicting the effect of VMC & NOP on corrosion rate (720 hours)

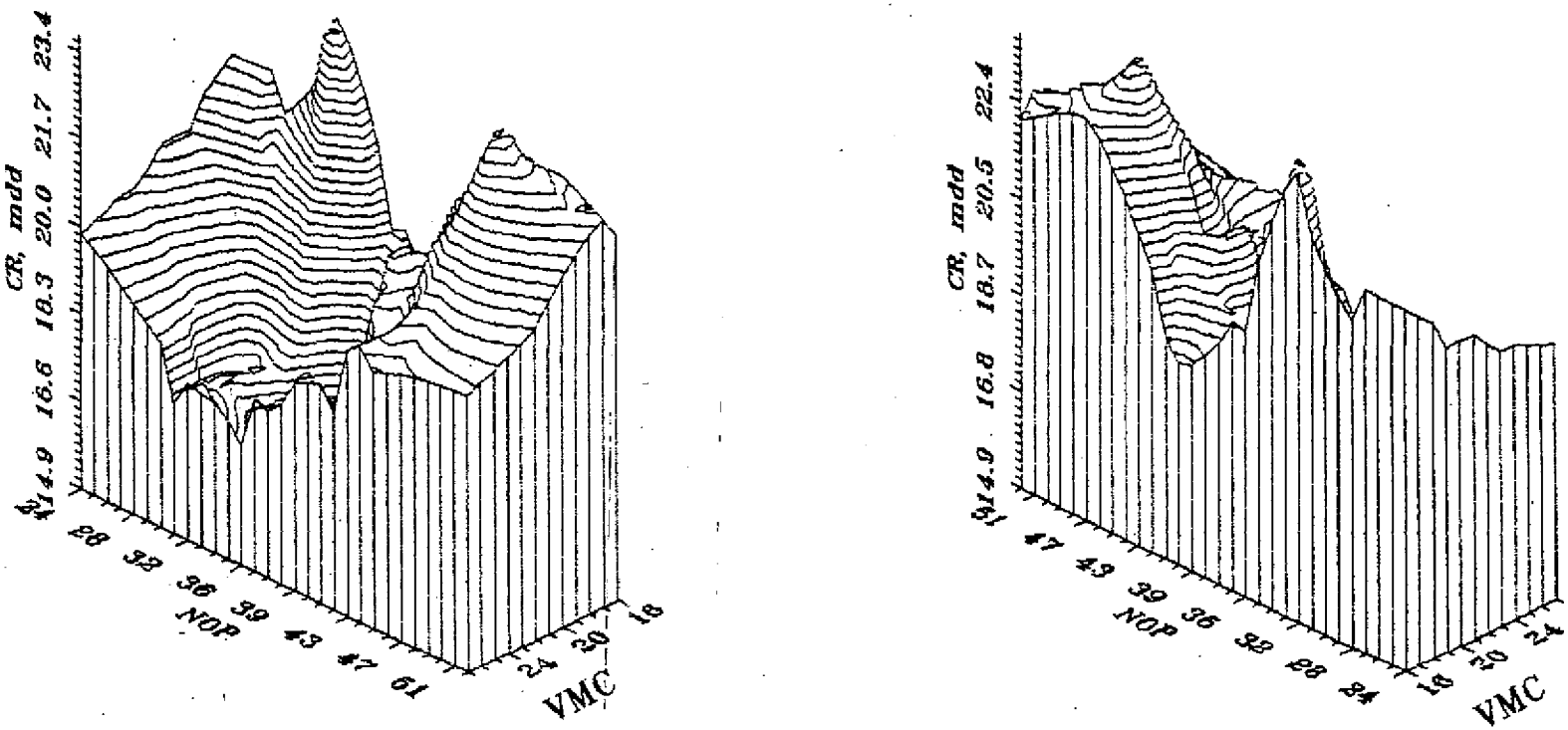

Fig. 6.10 3D plot depicting the effect of VMC & DF on corrosion rate (168 hours)

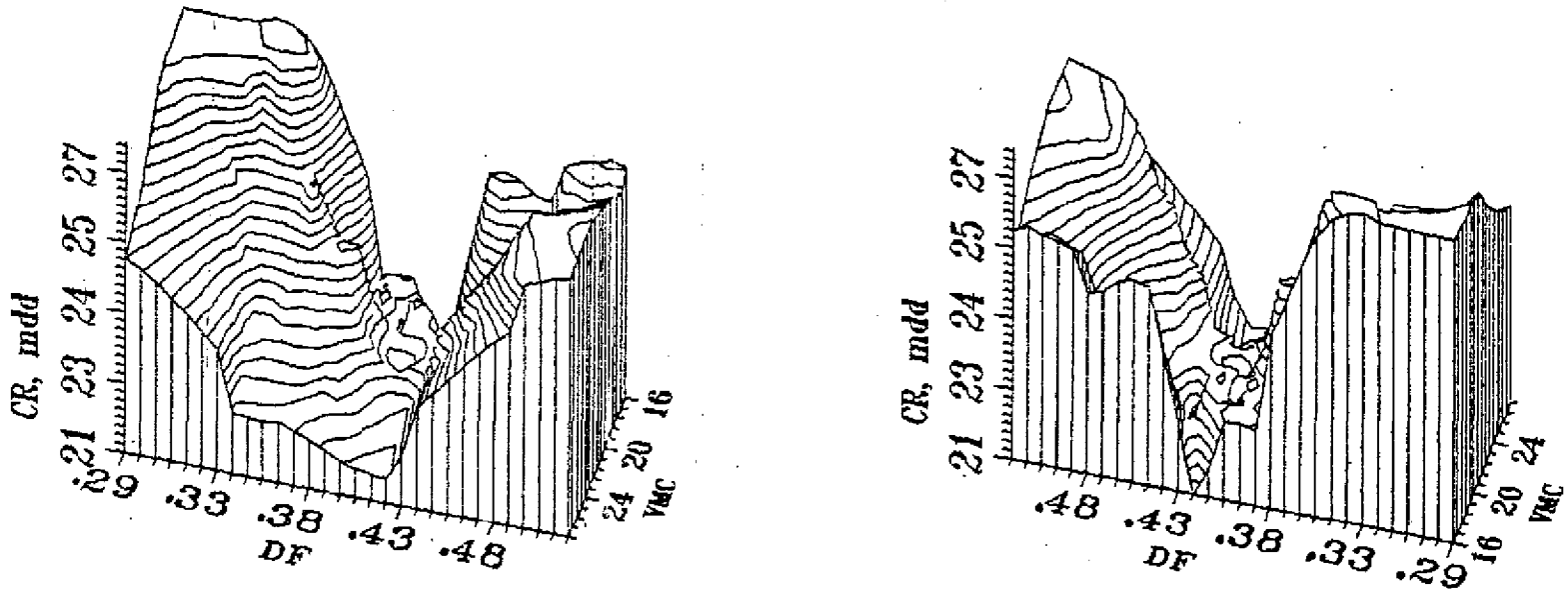

Fig. 6.11 3D plot depicting the effect of VMC & DF on corrosion rate (720 hours)

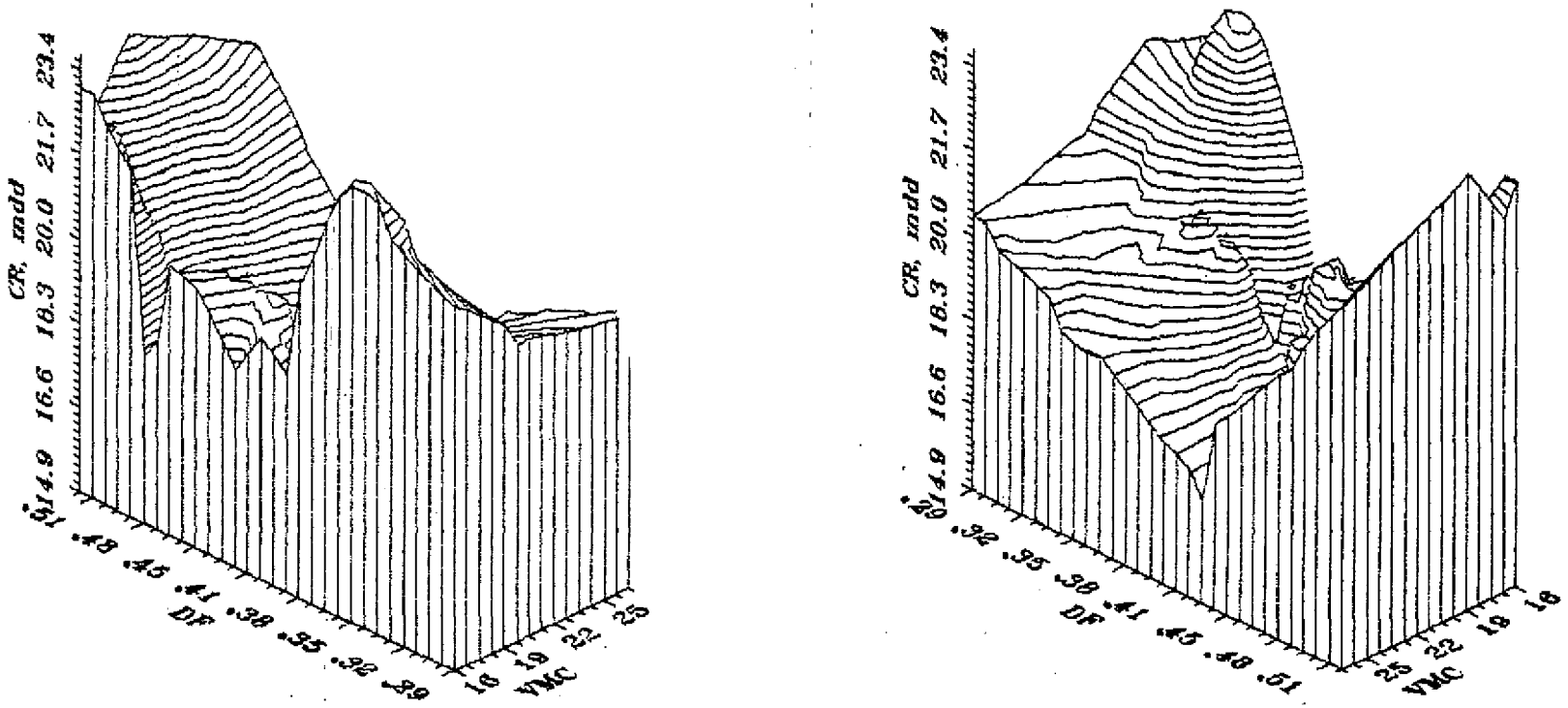

Fig. 6.12 3D plot depicting the effect of VMC & NOP on minimal corrosion rates

(a) 168 hours

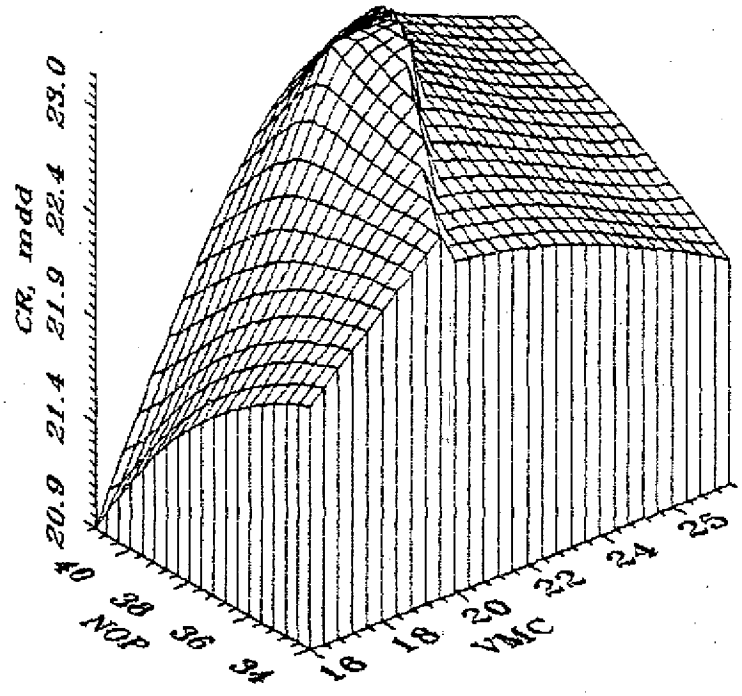

(b) 720 hours

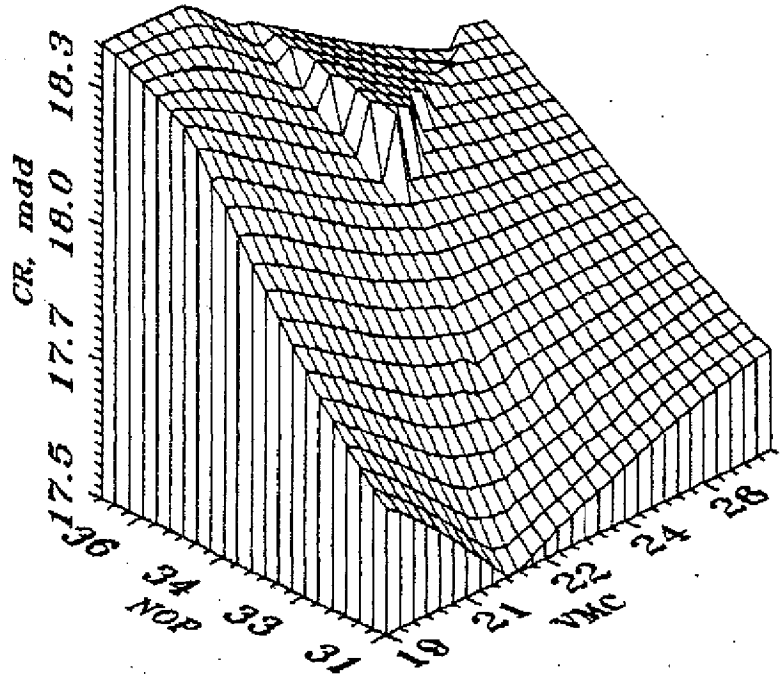

Fig. 6.13 3D plot depicting the effect of VMC & DF on minimal corrosion rates

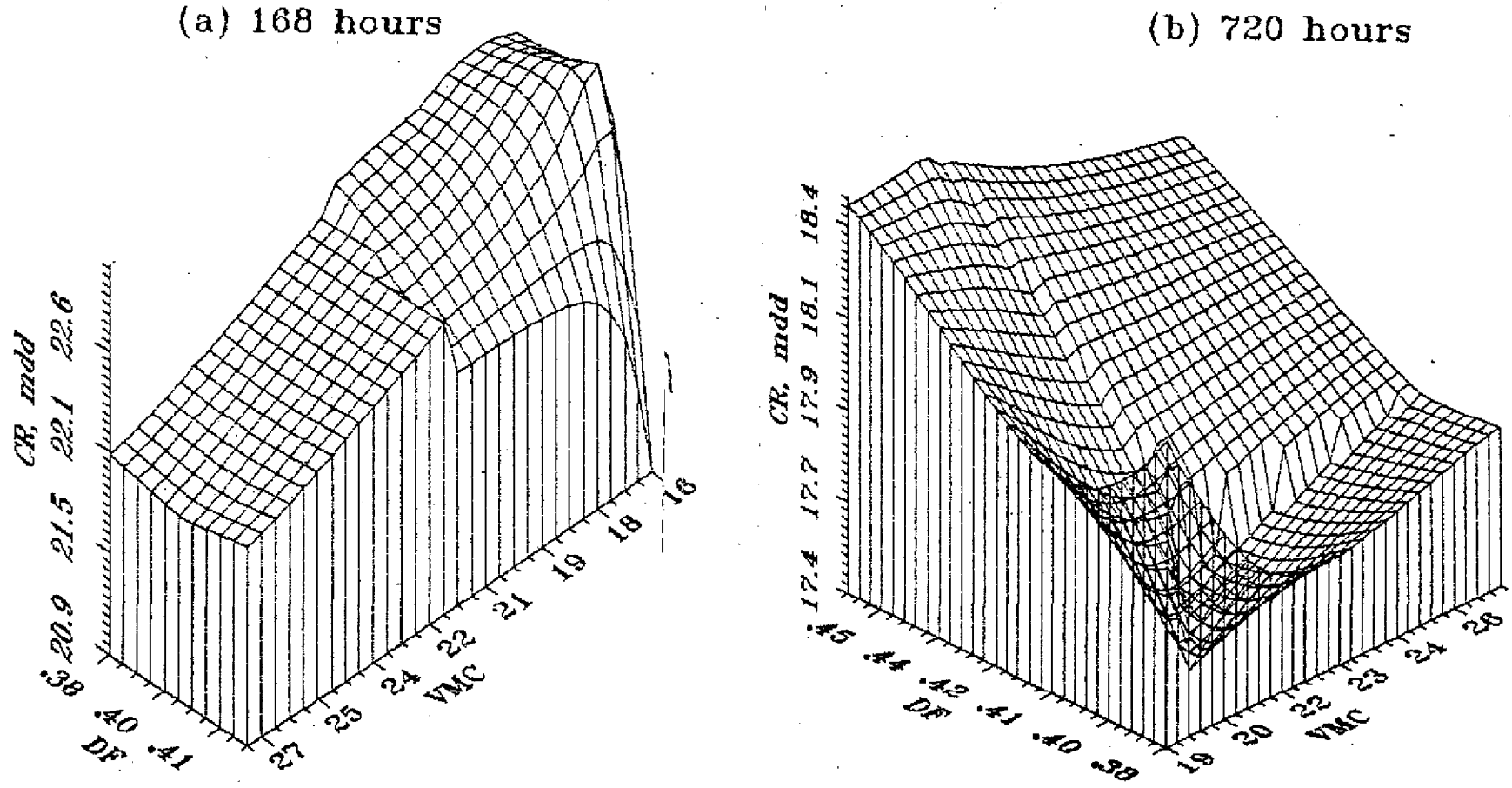

Fig. 6.14 Contour plot depicting the combined effect of VMC & NOP on corrosion rate (168 hours) based on unified model (Eq. 6.45)

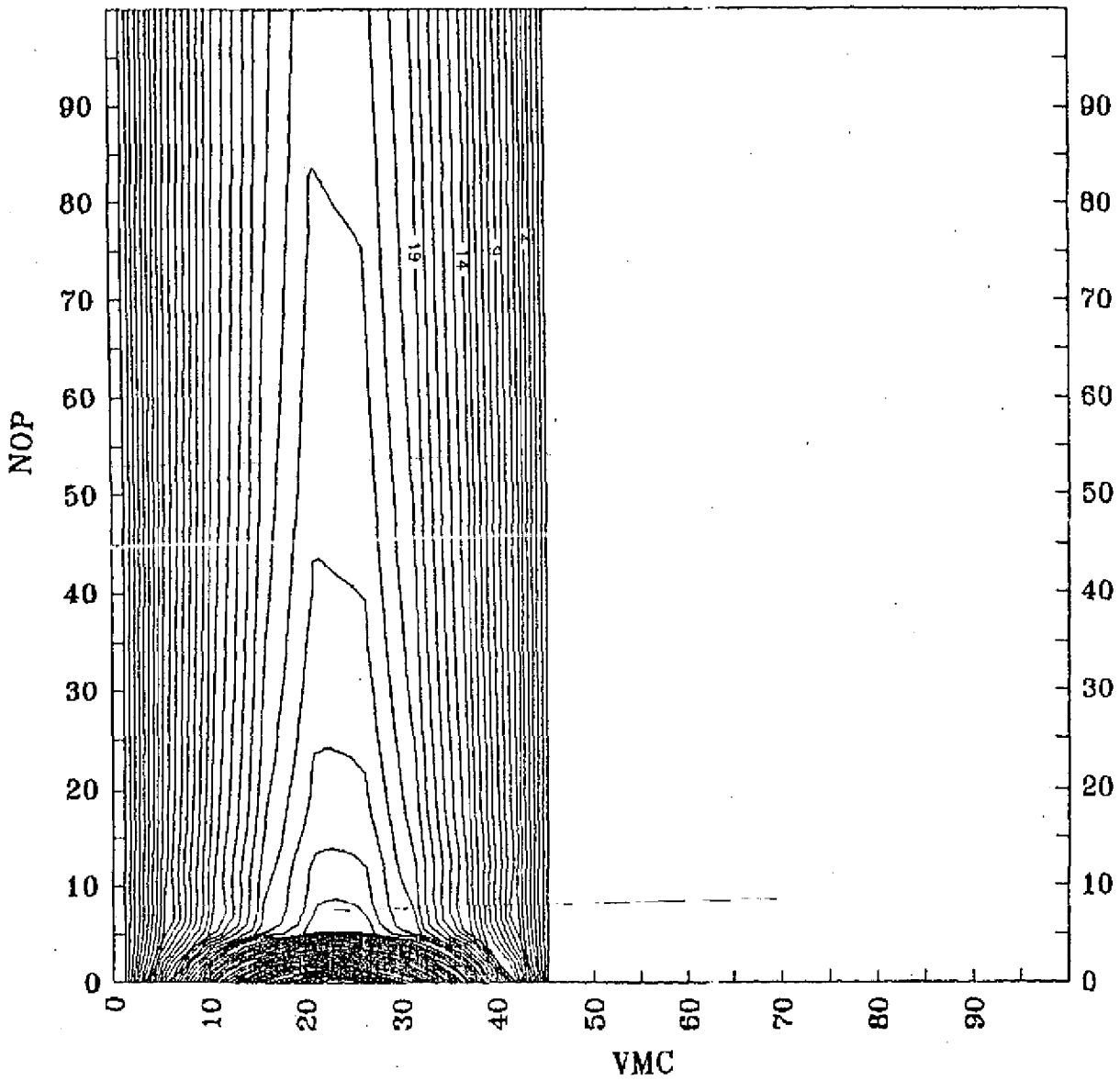

Fig. 6.15 Contour plot depicting the combined effect of VMC & NOP on corrosion rate (720 hours) based on unified model (Eq. 6.46)

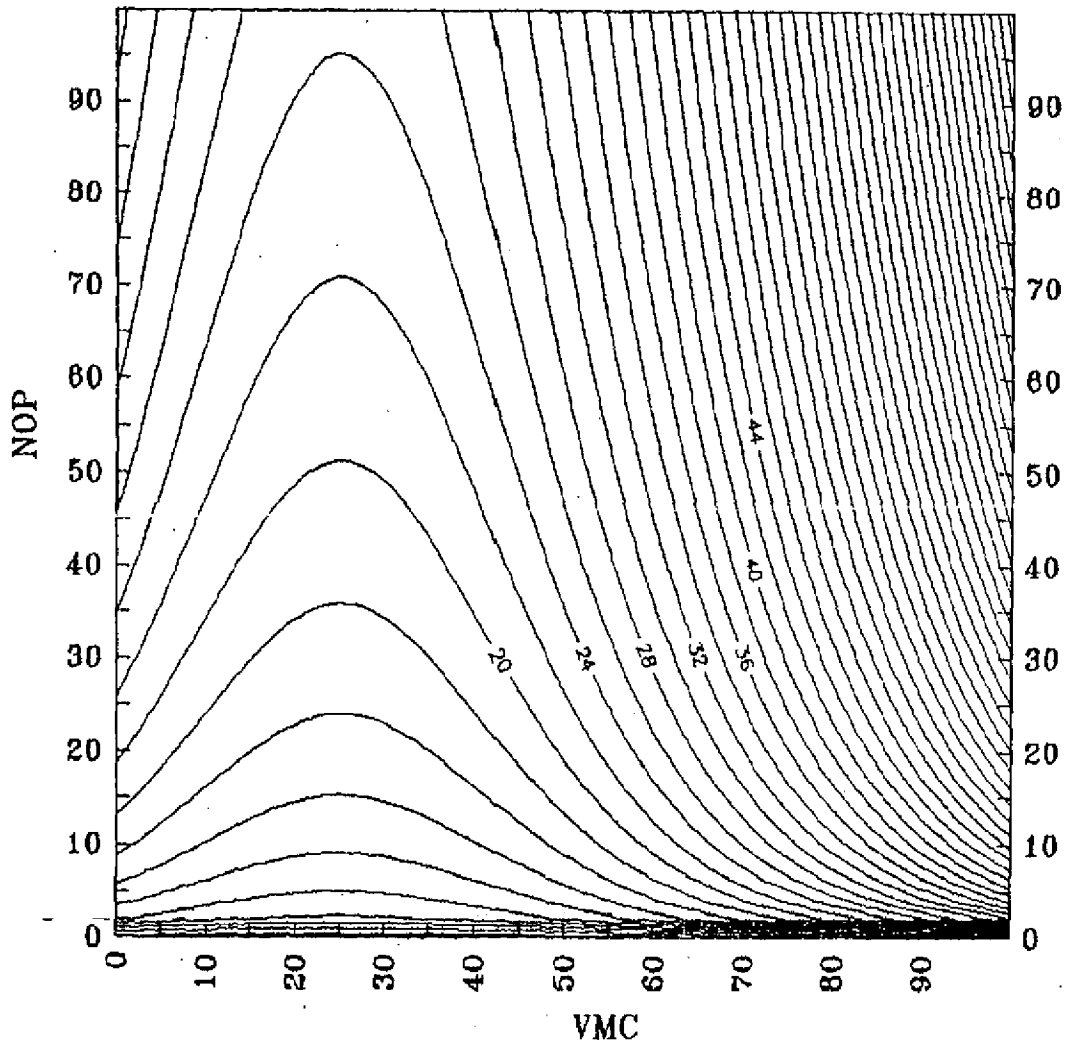

Fig. 6.16 Contour plot depicting the combined effect of VMC & DF on corrosion rate (168 hours) based on unified model (Eq. 6.47)

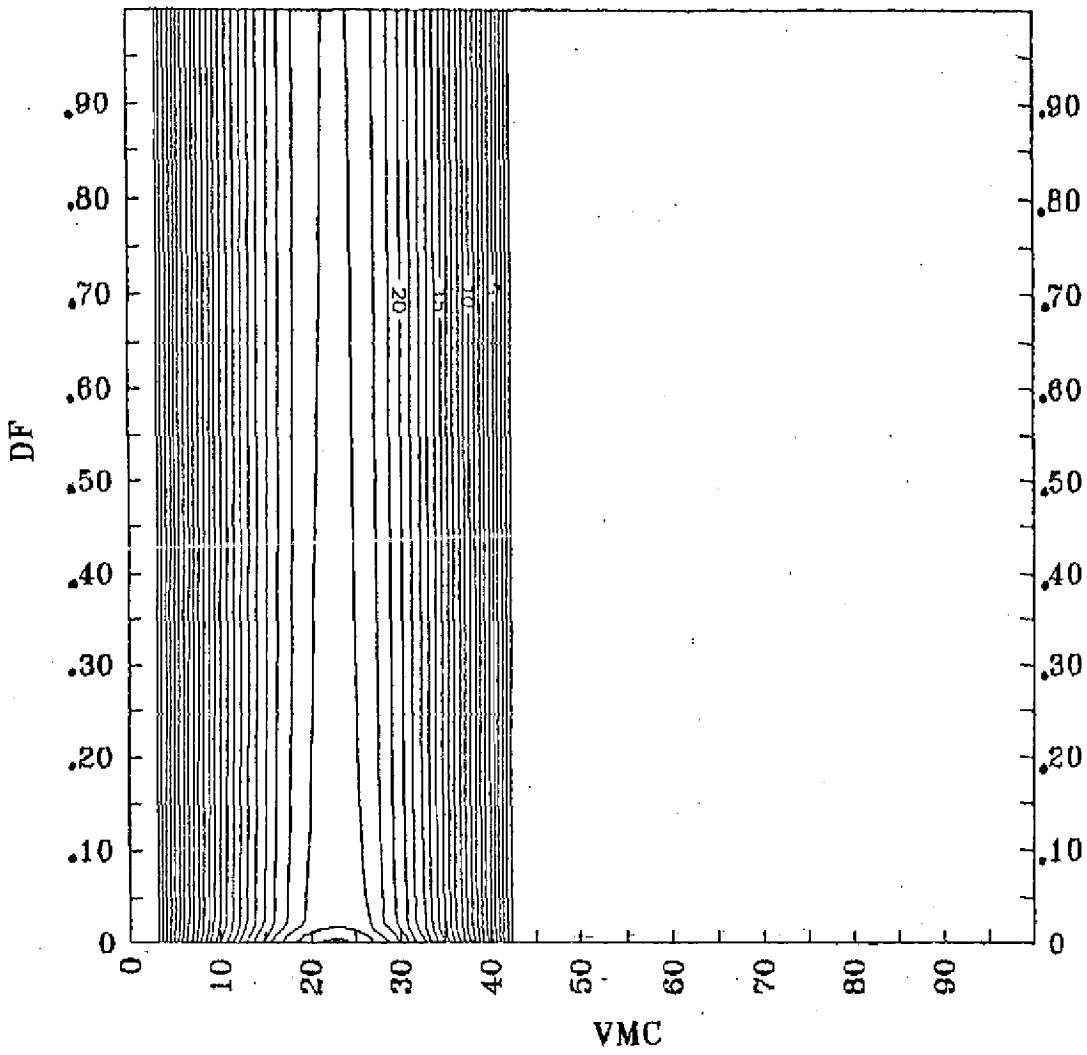

Fig. 6.17 Contour plot depicting the combined effect of VMC & DF on corrosion rate (720 hours) based on unified model (Eq. 6.48)

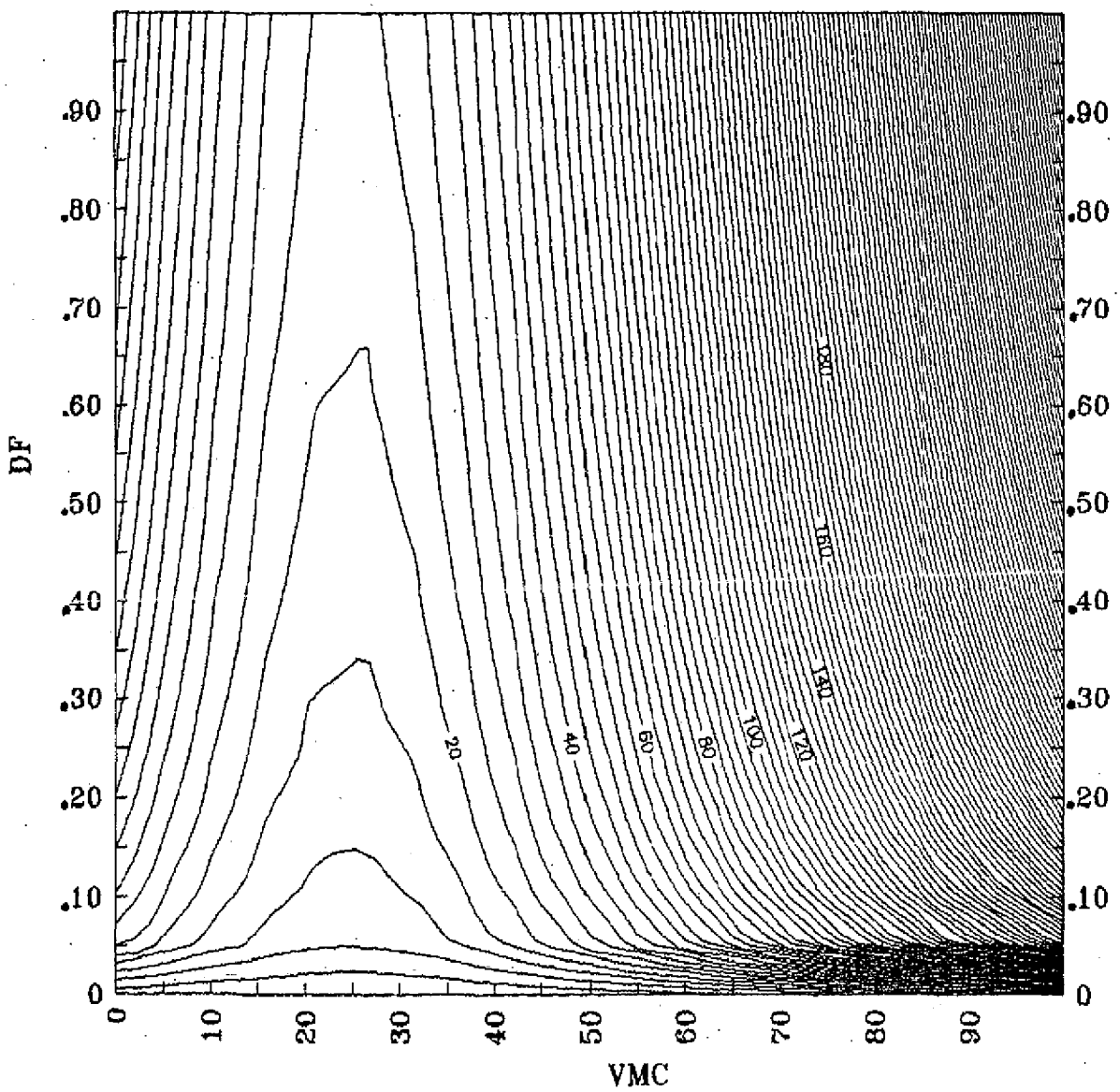

Fig. 6.18 A plot of experimental vs predicted CR based on unified model

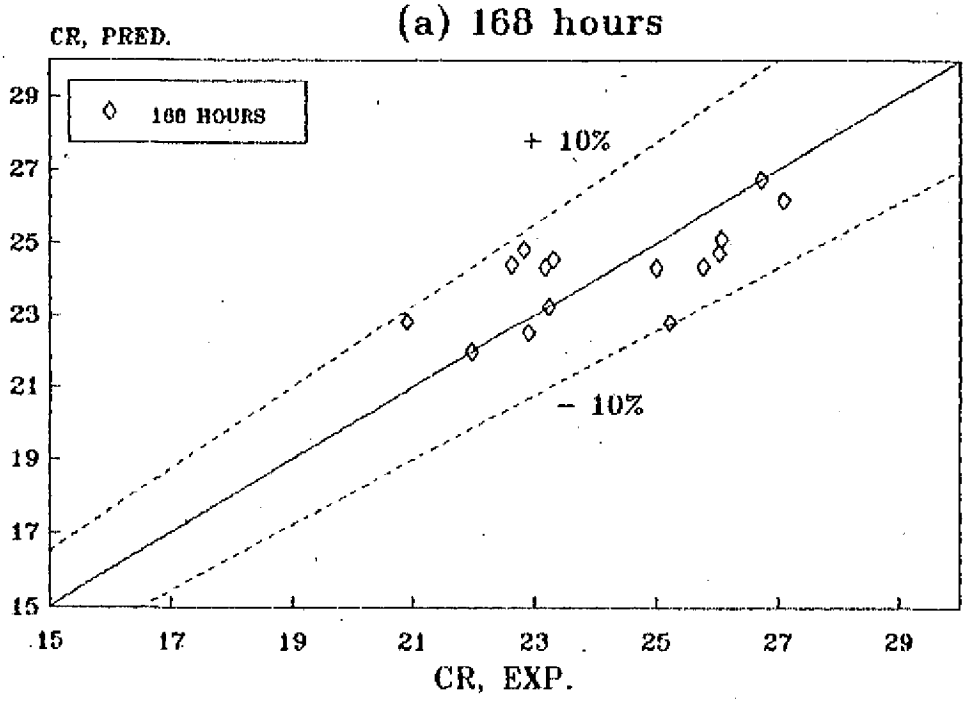

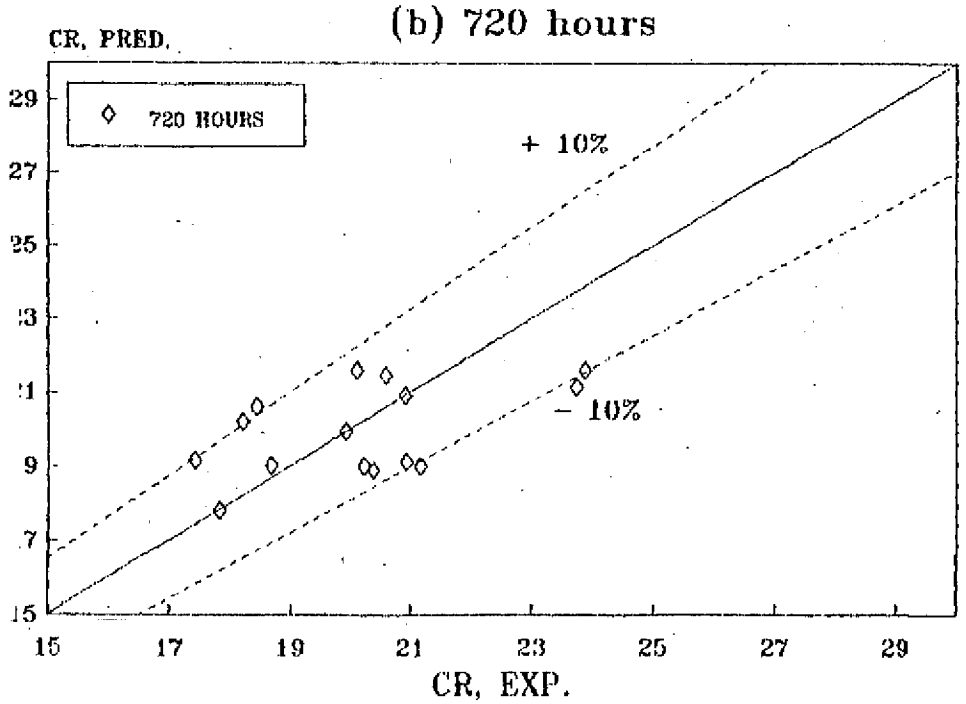

Fig. 6.19 Compressive strength–hardness interrelation

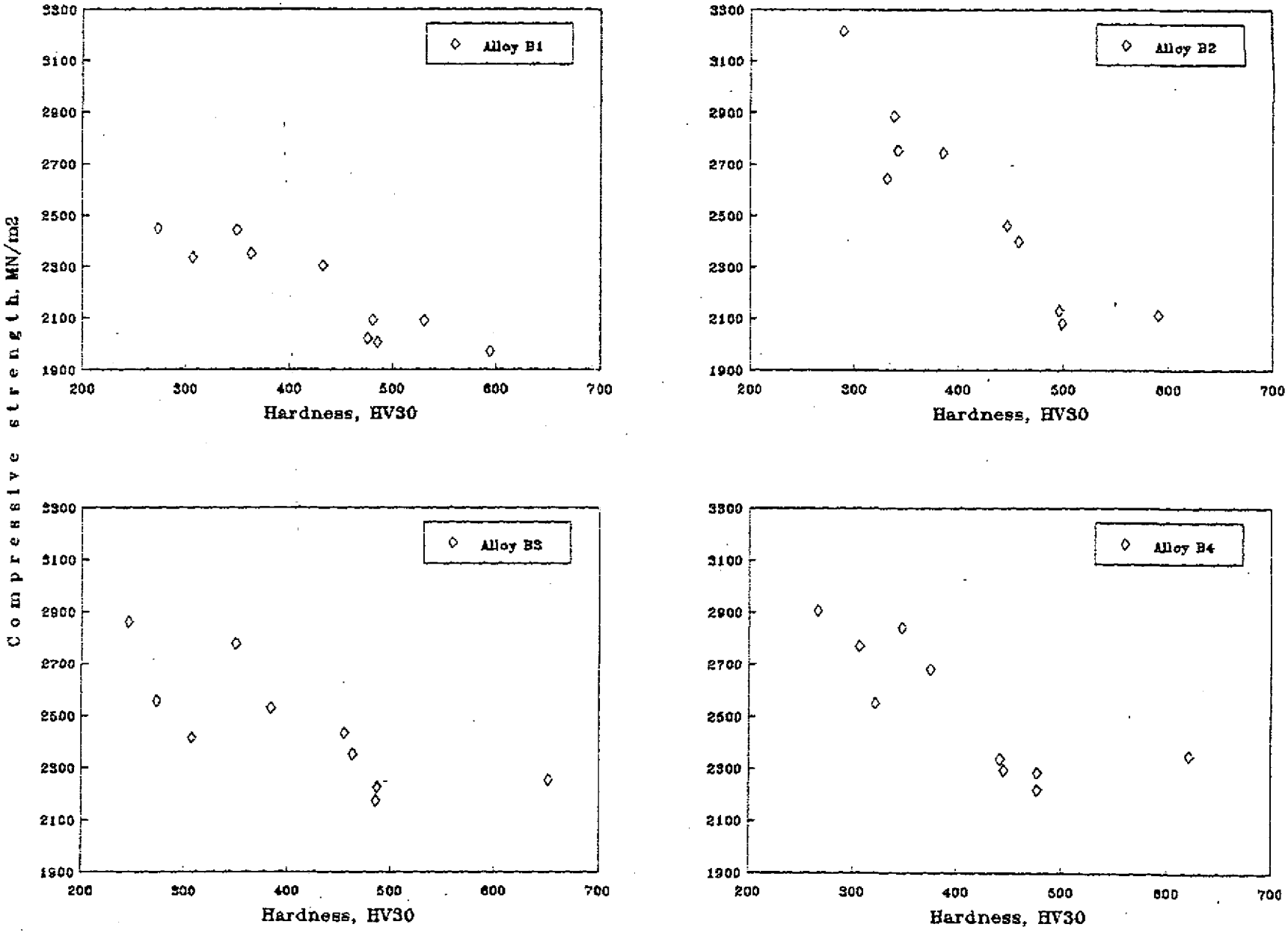

Fig. 6.20 R (CS/H) – hardness interrelation

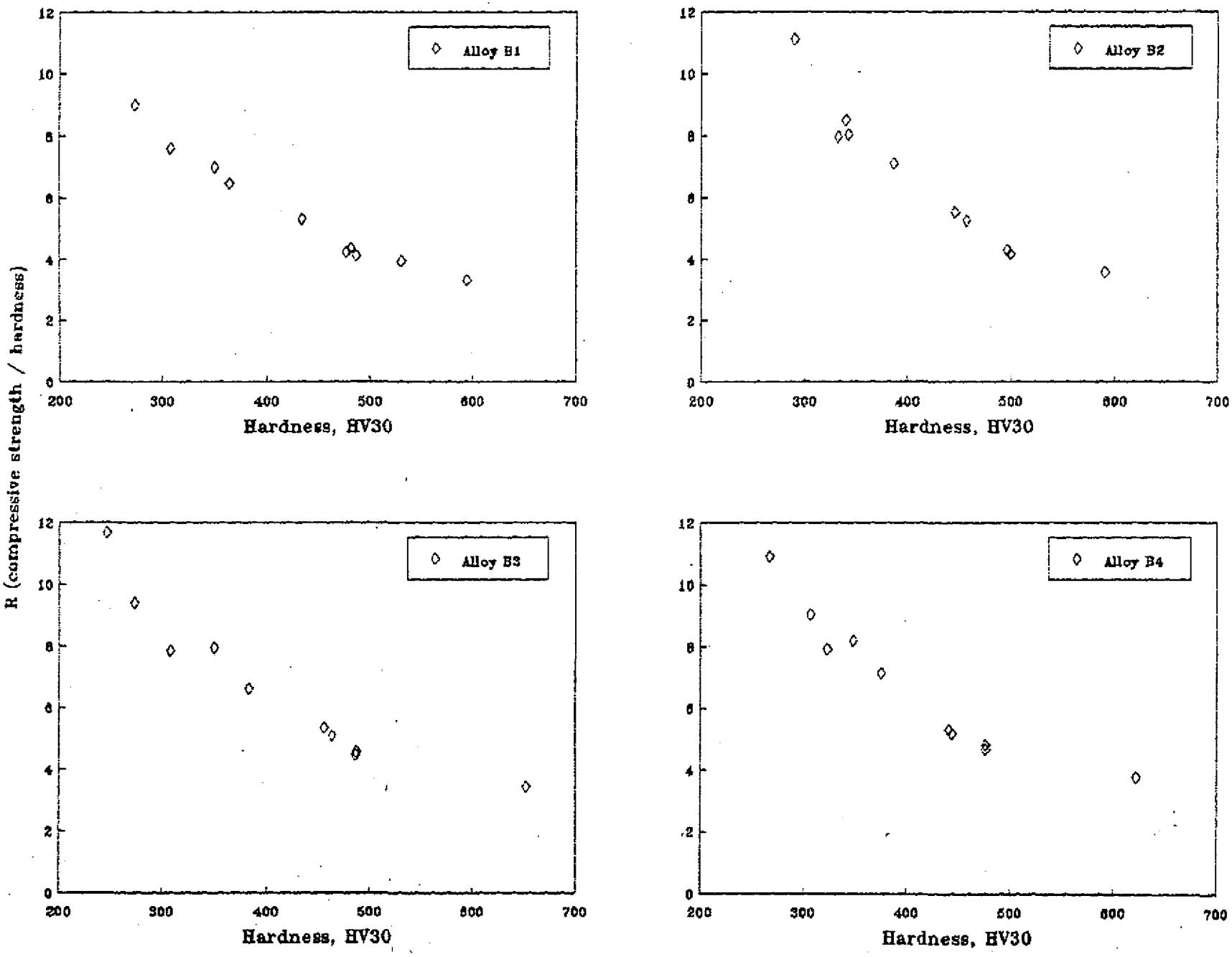

Fig. 6.21 A plot of experimental vs predicted CS

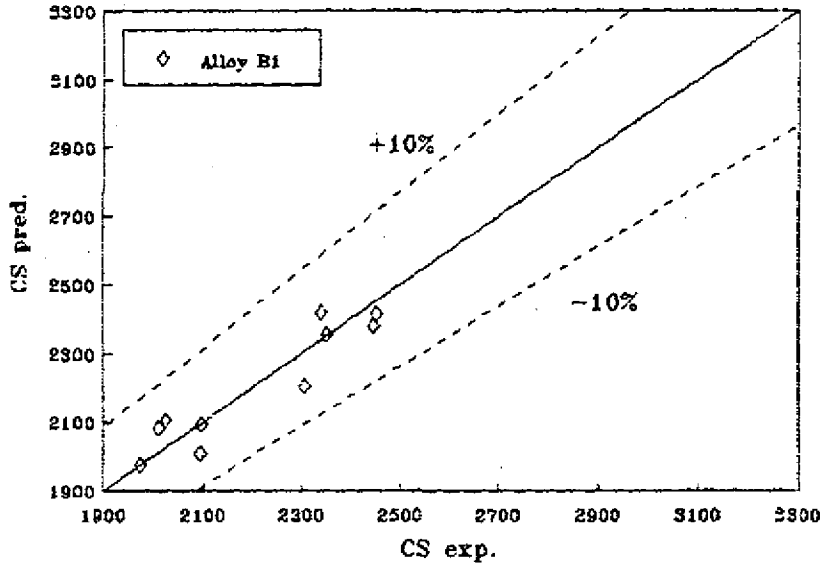

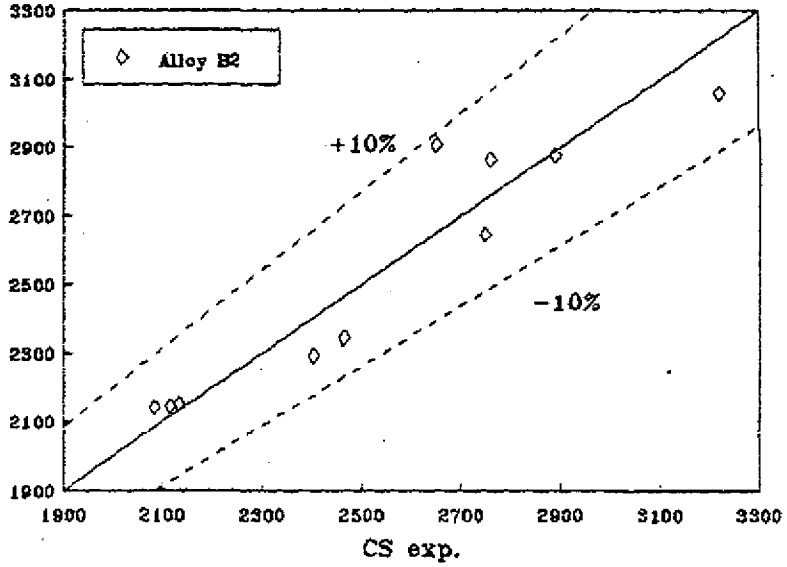

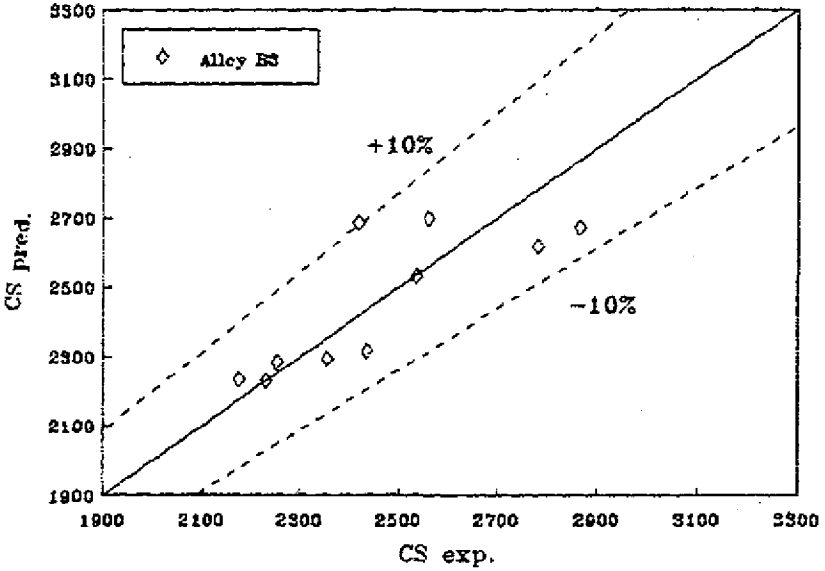

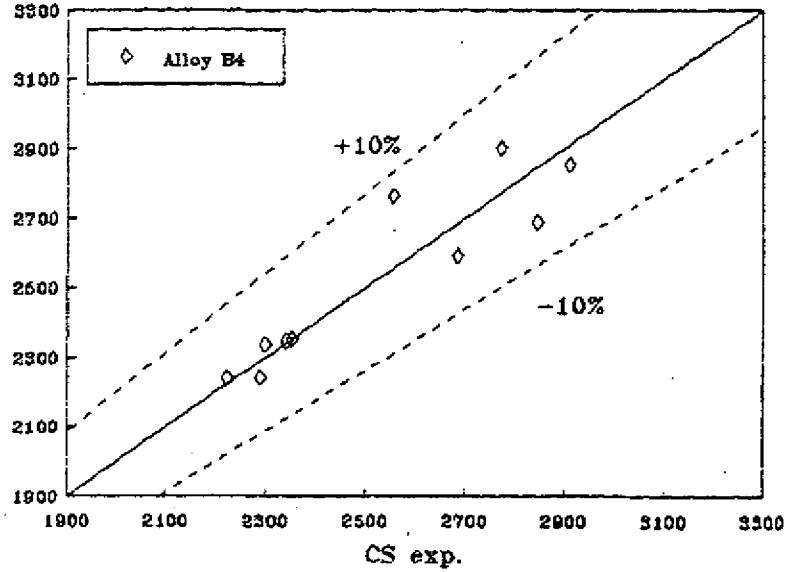

Fig. 6.22 %strain – hardness interrelation

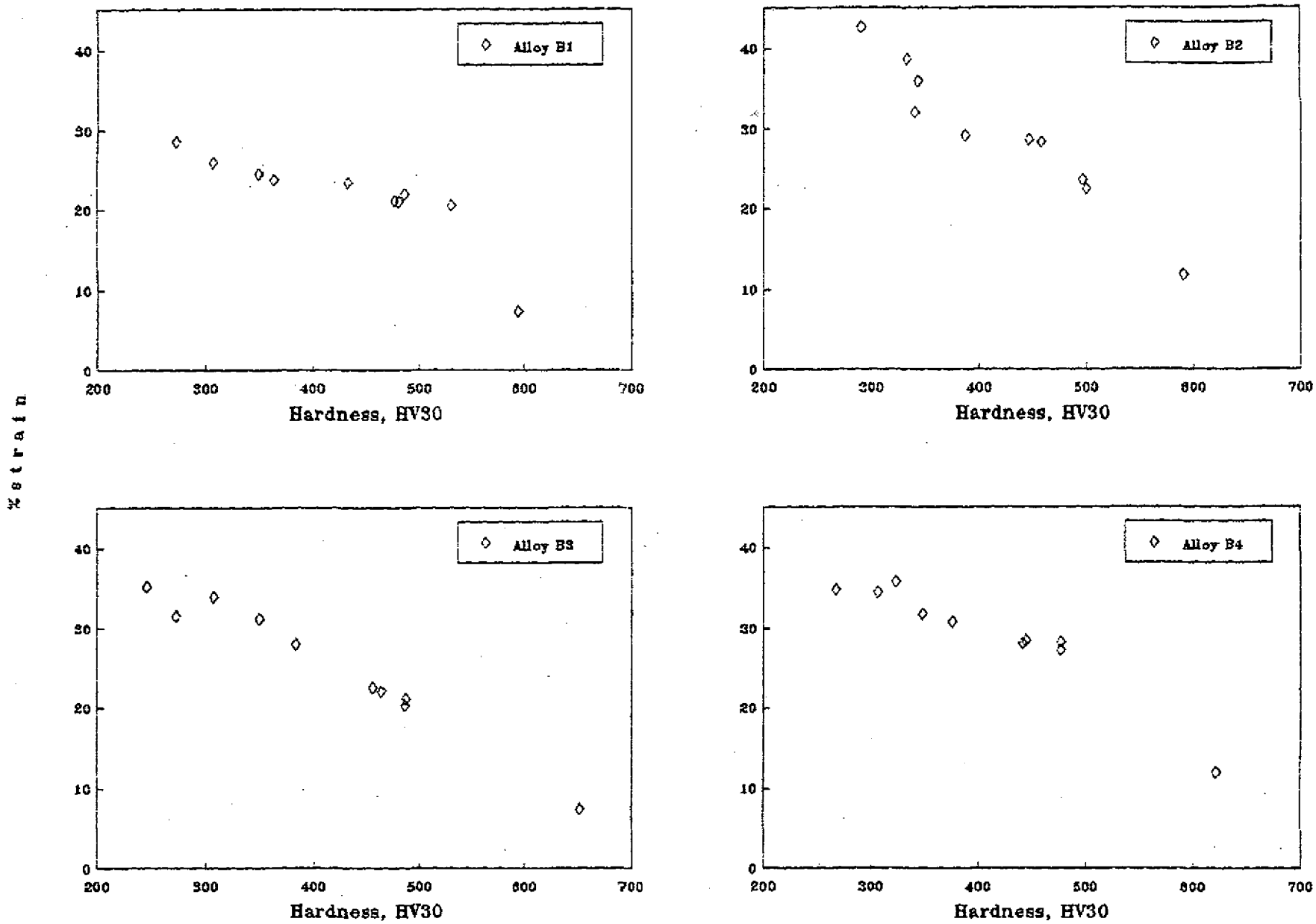

Fig. 6.23 R' (%strain/H) – hardness interrelation

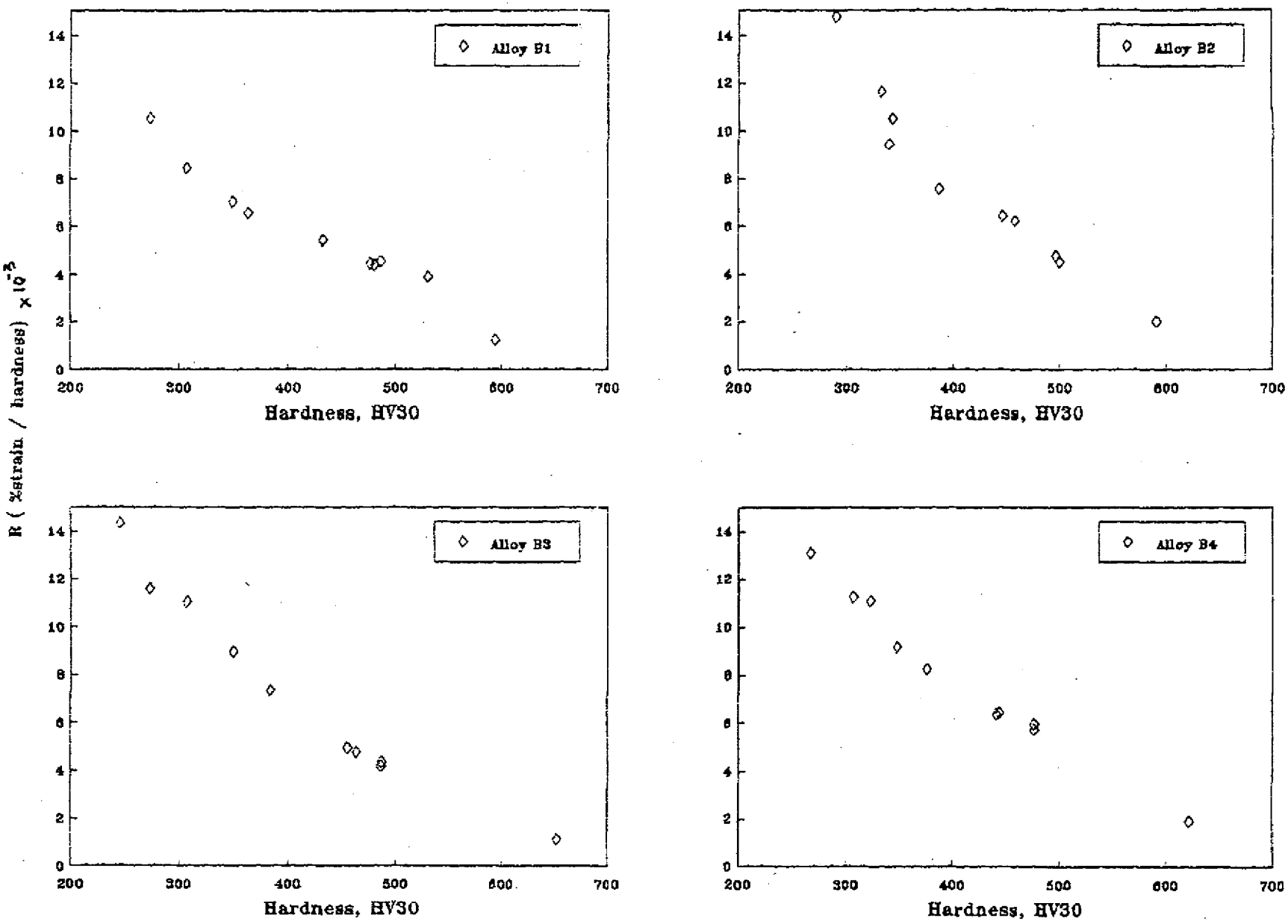

Fig. 6.24 A plot of experimental vs predicted % strain

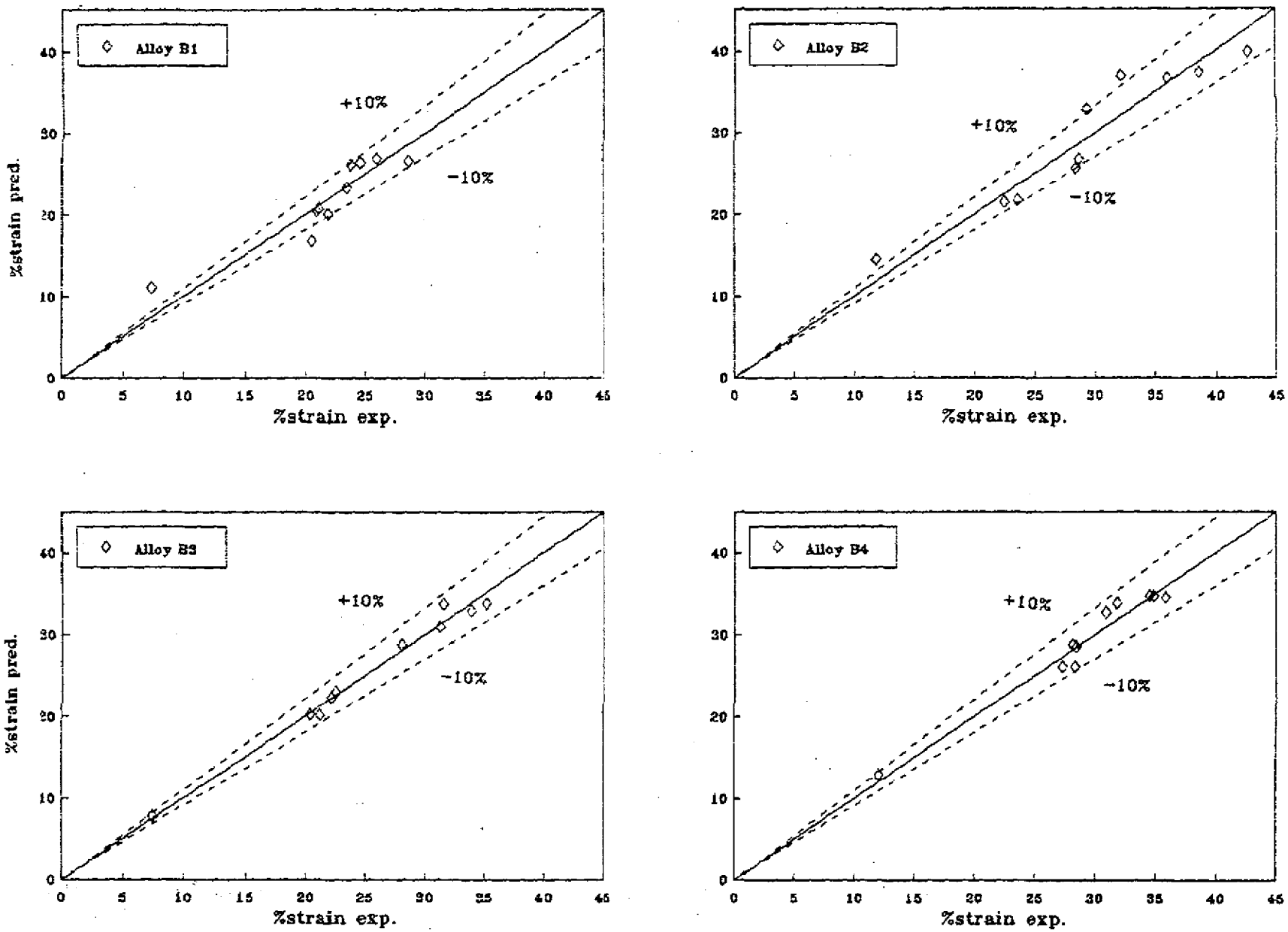

Fig. 6.25 Effect of heat-treatment on deformation behaviour under compression

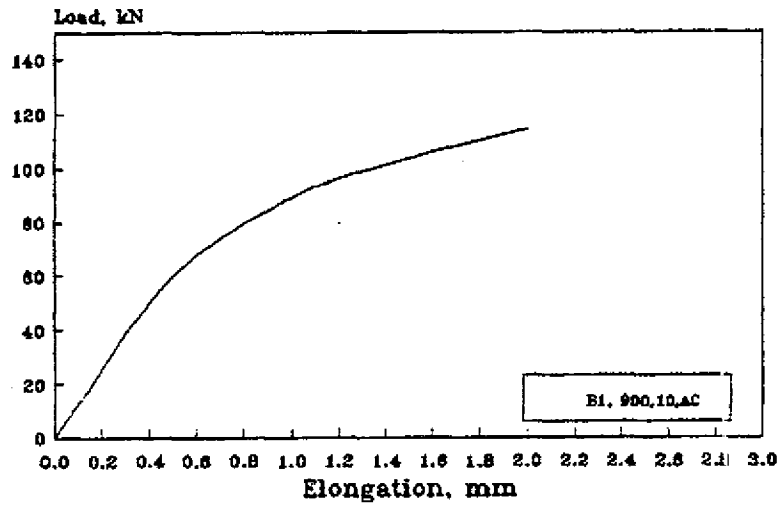

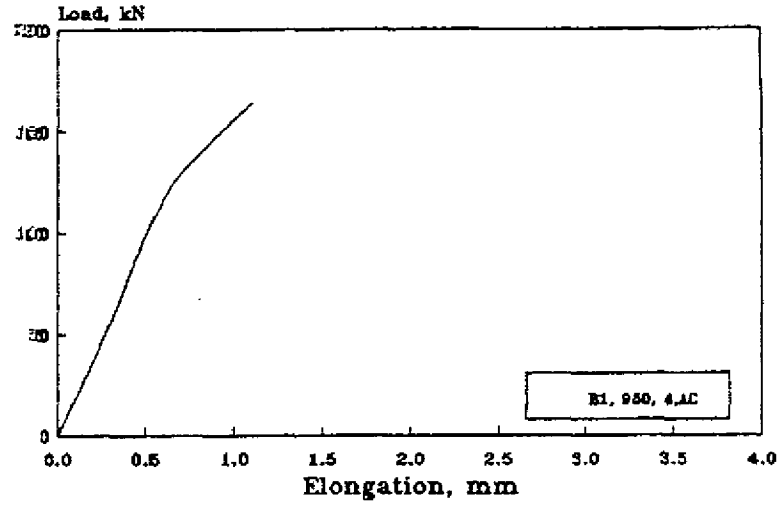

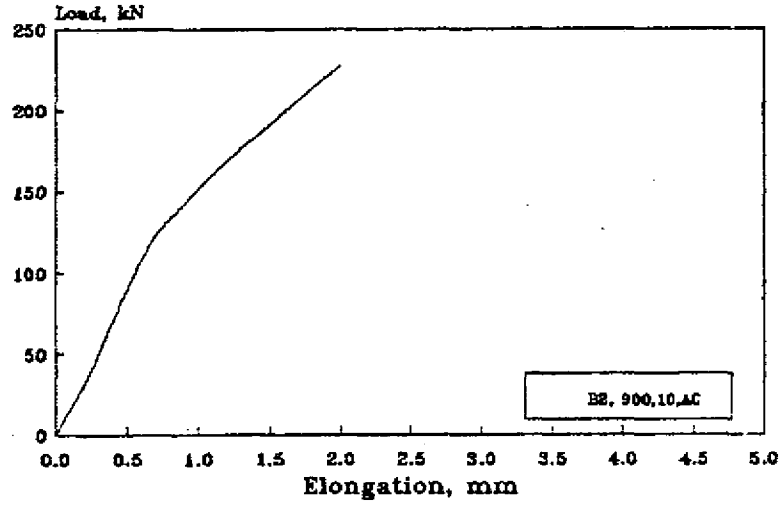

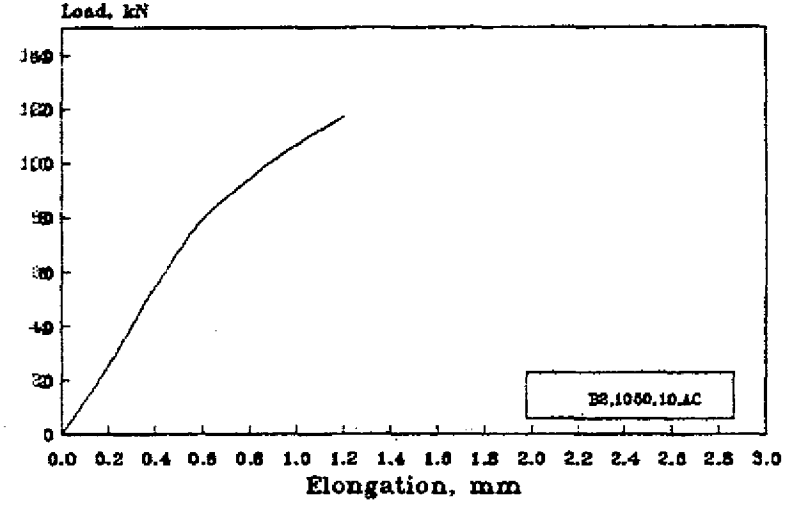

Fig. 6.26 Effect of heat-treatment on deformation behaviour under compression

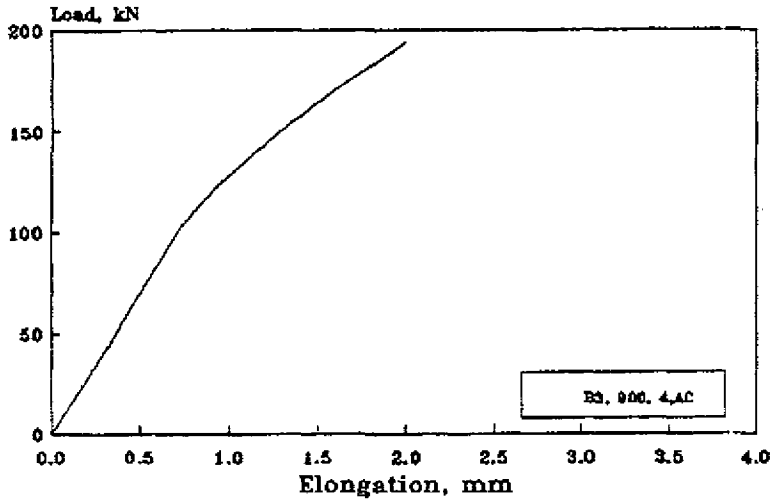

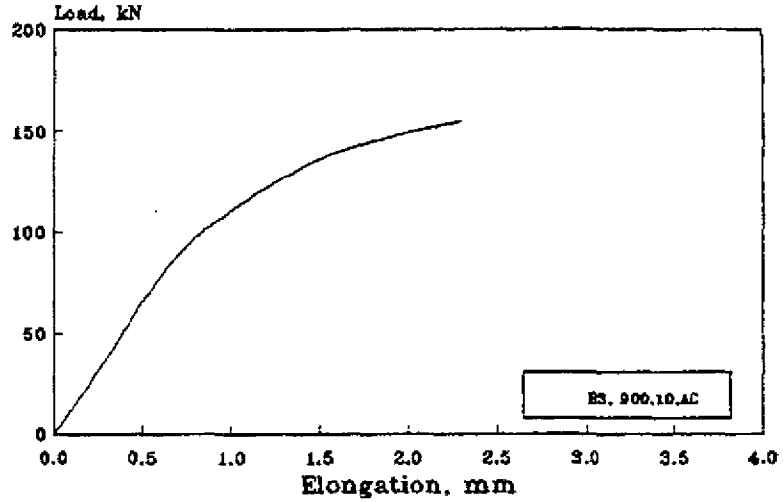

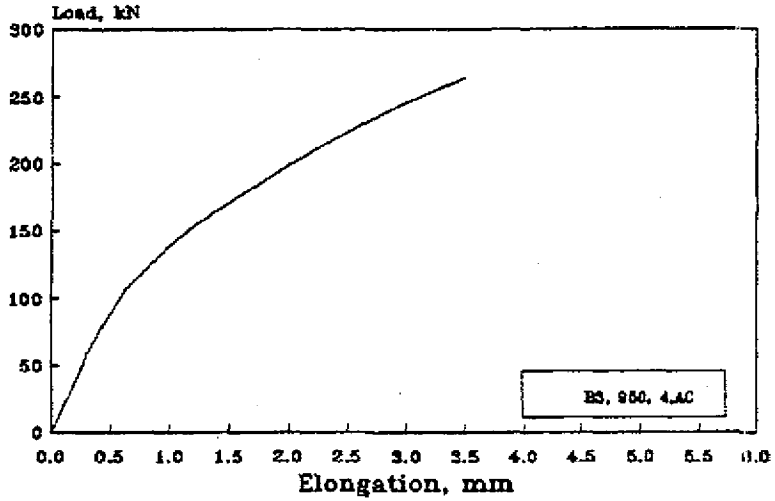

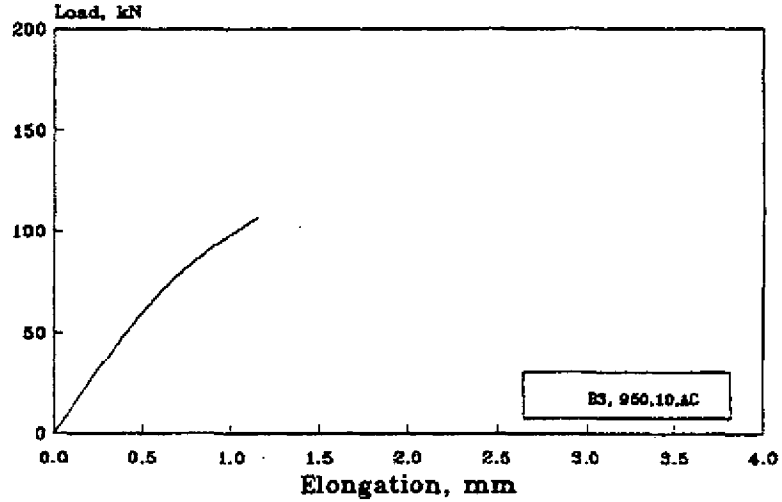

Fig. 6.27 Effect of heat-treatment on deformation behaviour under compression

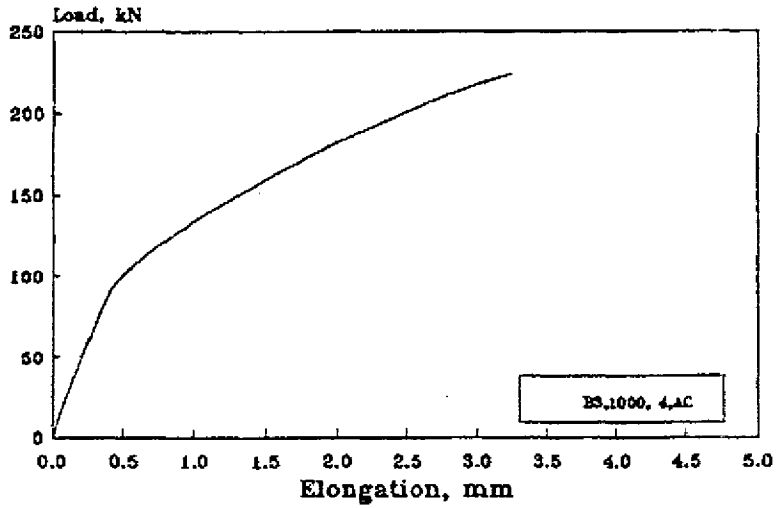

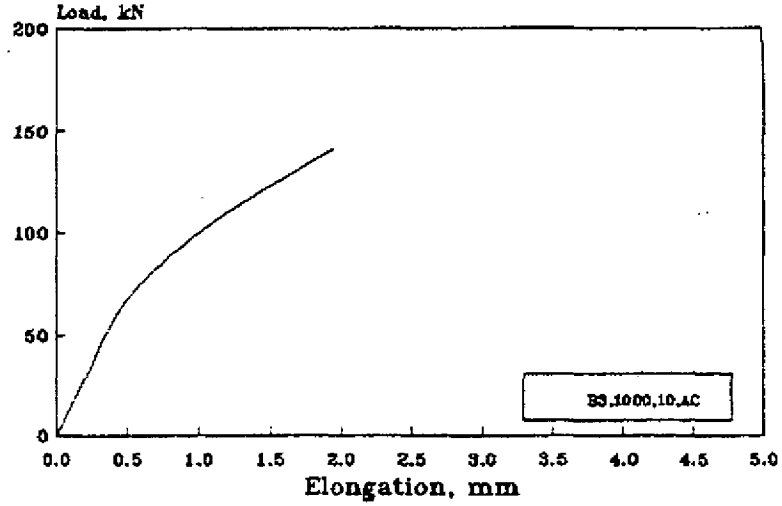

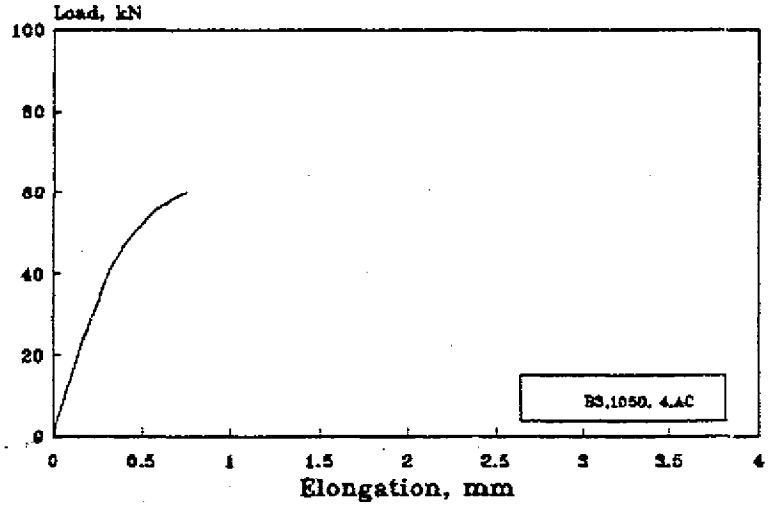

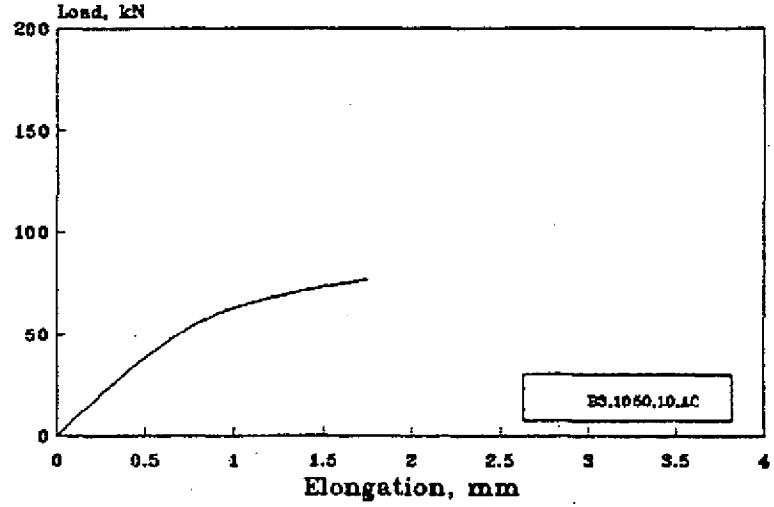

Fig. 6.28 Effect of heat-treatment on deformation behaviour under compression